Oxygen Dynamics in Algal Based Wastewater Treatment Systems

Richard Andrew Evans B.Sc.(Hons.)

School of the Environment.

Faculty of Science and Engineering.

Flinders University

Submitted as a PhD thesis at Flinders University of South Australia.
March 2012.

Declaration

I certify that this thesis does not incorporate without acknowledgment any material previously submitted for a degree or diploma in any university; and that to the best of my knowledge and belief it does not contain any material previously published or written by another person except where due reference is made in the text.

Acknowledgments

I would like to thank all of my colleagues from the former Department of Environmental Health and Biomedical Engineering at Flinders Medical Centre; Given my long tenure in EH during my research it may be best to do this in order of appearance (as best as my memory can now provide); Duncan Craig, Alana Hansen, Peter Hobson, Michelle Critchley, Megge Miller, Briony Vickery, Maria Wilson, Ben Pol, Linda Health, Julanta Ciuk, John Edwards, Richard Bentham, Emily Fearnley, Brian Bridger, Jack Beasly, Darcy Schultz, Robin Woolford, Kateryna Babina, David Sweeney, Eddie Herdianto, Michael Short, Ben Vandenakker, 'the evil third twin', Louis Bradbury, Akio Yamamoto, Kirstin Ross, Sharyn Gaskin, Iryanti Suprihatin, Cheryl Caldwell, Neil Buchanan, Mark Disher, Team Honda, Captain Beefheart, Magnus Fairweather Peabody, Monte Zuma, Peke Deboo, Snoop Dog and of course Mrs Lincoln; to those many I have not mentioned I thank you also. Huge huge thanks go to Monika, Ian and Kateryna, Catherine and David and other colleagues and friends in the Department of Health without whom I would surely have lost my way.

Of course great thanks are offered to my supervisors Nancy Cromar and in particular Howard Fallowfield for his notably notable patience and support, and enthusiasm for science without which I would not have finished.

Lastly and certainly not leastly I offer my deepest thanks to Roma and Dylan for all the encouragement and patience they have shown over the years and of course my wonderful sister Jane, Mum and Mike for all their kind words and support.

Table of Contents

Chapter 4
Materials and Methods

Chapter 6
Oxygen and Temperature Dynamics Bolivar WSP 1

Appendices

List of Tables

List of Figures

1. INTRODUCTION

Wastewater derived from domestic or industrial sources can contain a diverse range of dissolved and suspended chemical and/or biological contaminants (e.g. nutrients, heavy metals, pharmaceuticals, pathogens) and can present a serious risk to human health or ecosystems if not disposed of appropriately (Metcalf and Eddy 2004).

Such effluent if disposed of without appropriate treatment can cause illness to those who have primary or secondary contact with it. In an effort to protect human health, treated and untreated wastewaters from coastal cities worldwide have traditionally been disposed of via ocean and river outfalls. Unfortunately, an unintended side effect of such disposal methods has been the eutrophication (sometimes termed cultural eutrophication) of these receiving waters and ecosystems (Nixon 1995, 1998) in addition to contamination of recreational and groundwater resources.

In Australia as elsewhere such disposal methods have been shown to contribute to the intensity of some toxic algal blooms in receiving waters (Davis and Koop 2000). Similarly there is strong evidence that disposal of treated wastewater and untreated storm-water from the city of Adelaide to the adjacent coastal environments may have contributed to large declines in sea-grass cover in this area (Fox et al. 2007).

Various methods of wastewater treatment (Chapter 2) are employed to remove nutrients, pathogens, heavy metals, persistent organic pollutants; with the treatment type determined by factors such as effectiveness, cost (land, initial and maintenance) disposal and re-use options and community and government expectation.

An effective and commonly used method for treating organic or domestic wastewaters is to detain the effluent stream in large and shallow lined ponds or impoundments for a period of time. Such ponds are typically termed ‘waste stabilisation ponds’ (WSP) or ‘waste stabilisation lagoons’ or simply ‘ponds’ or ‘lagoons’. Ponds actively mixed using paddlewheels are typically termed ‘high rate algal ponds’ (HRAP) or ‘high rate oxidation ponds’ (HROP). Semantics and basic differences aside, such systems provide a contained environment that allows naturally occurring algae and photosynthetic bacteria to grow profusely in response to light from the sun. The abundant oxygen produced by this photosynthetic activity in a nutrient rich medium provides heterotrophic bacteria with an ideal environment in which to flourish and oxidise organic and inorganic nutrients. Such conditions can also result in dramatic declines in the concentration of viral and bacterial pathogens (Fallowfield et al. 1996, Bolton et al. 2010). Provided that conditions in a pond remain aerobic (an excess of dissolved oxygen in the water) the pond will be largely odour free due to the rapid oxidation of H_2S and other odour forming compounds by dissolved oxygen. The removal of planktonic biomass (algal, bacterial, fungal matter) via settlement, filtration or both can produce an effluent (after chlorination) of sufficient quality for crop irrigation or other non-potable uses (Chapter 2).

Whilst the systems described above are relatively simple from a construction and engineering perspective, the ecology of such systems is not. Design principles have traditionally relied on ‘rules of thumb’ based of hard won experience of what works and doesn’t in the field to determine functional pond depths, waste loading rates and retention times (Chapter 2).

A lesson from history may show how wastewater treatment plants (WWTP) operators and the community might benefit from improvements in the scientific understanding of ecological processes at work in algal based treatment systems. The Bolivar treatment system Adelaide, Australia was constructed during the mid-sixties in response to increased population size and ultimately removed the need for the disposal of screened raw sewage into the Port River and the Gulf St Vincent. The details of the system itself, including primary and secondary bio-filter components are described in Chapter 2.

Treatment failure was experienced at the Bolivar wastewater treatment lagoon during later part of the 1997 (Sheil 2000); organic content of the waste stabilisation pond influent was increased purposefully due to a managed reduction in the capacity of the primary treatment system until the pond 'mode' changed from aerobic to anaerobic, resulting in serious odour problems for the entire city of Adelaide. Prior to this incident the plant had operated to the satisfaction of the community for a period of over thirty years. It can be argued that this episode provides a useful case study where the wastewater treatment system, designed using 'rule of thumb' based approach with a large margin for error, was 'optimised' for the purposes of efficiency (cost saving) without understanding the consequences of these changes on algal productivity and oxygen production. The sulphurous odour that arose from the lagoons was ultimately suppressed when sufficient dissolved oxygen from algal photosynthesis was available in the ponds for oxidation of sulphides.

Photosynthesis drives treatment processes afforded by heterotrophic bacteria and ensures maintenance of aerobic conditions within pond, a great deal of research has

therefore been undertaken over the decades to better understand the factors that determine the oxygen dynamics, productivity and ecology of algal/bacterial assemblages present in these systems. Such research has also been undertaken in the area of algal biomass production of *Spirulina sp* for example.

The research presented in this thesis was undertaken with the goal of characterising relations between irradiance, algal oxygen dynamics and productivity. Such factors are basic to the cycling of energy in algal-based wastewater treatment systems as well as natural aquatic ecosystems. It is hoped that the findings of this research may contribute towards a greater understanding of the phytoecology of these systems.

2. ALGAL BASED WASTEWATER TREATMENT SYSTEMS

2.1. Introduction

Wastewater is a term commonly used, but infrequently defined in common language used in the media and non-scientific press. In the scientific press it is often defined in very specific terms of relevance for a specific waste stream; e.g. Werner et al. 2010. When defined for the purposes regulation by health departments or other relevant authority, the following type of definition is considered useful as it is general: *'The used-water arising from domestic activities in dwellings, institutions or commercial facilities consisting of all wastewater, grey-water or black-water or as approved by the relevant authority'* (Luke Seidel, SA Health: personal communication). Wastewater derived from domestic or industrial sources can contain a diverse range of dissolved and suspended chemical and/or biological contaminants (e.g. nutrients, heavy metals, pharmaceuticals, pathogens) and can present a serious risk to human health or ecosystems if not disposed of appropriately. Contaminants of concern to public health from typical domestic wastewater include nutrients and pathogens such as viruses and bacteria. Such effluent if disposed of without appropriate treatment can cause illness due to primary or secondary contact/use with the untreated effluent or water contaminated by effluent contaminants; SA Government (1966), Gloyna (1971) Dorsch et al. (1984).

2.2. Wastewater Treatment and Disposal

A number of approaches are available for the treatment of wastewater including physical, chemical and biological or combinations of all (Metcalf and Eddy 2003). In Australia as elsewhere inappropriate disposal methods have been shown to contribute

to the intensity of some toxic algal blooms in aquatic systems receiving the wastewater (Davis and Koop 2006); impacts upon primary production within natural ecosystems can be significant and have important implications for ecosystem functioning (Staehr et al. 2008, Conley et al. 2009). Algal based wastewater treatment systems (including high-rate algal ponds (HRAP) and waste stabilisation ponds (WSPs)) are typically large shallow impoundments used to detain nutrient rich wastewater. The propensity for algae and bacteria to grow in nutrient rich water is utilized to advantage within algal/bacterial wastewater systems (ABWWTS). These ponds therefore provide a contained environment in which dissolved organic and inorganic nutrients can be assimilated by bacterial and algal organisms (Chapter 3) prior to release of a less harmful effluent wastewater to receiving environments. Defined conditions of depth and retention time and mixing can be used to manage changes in wastewater strength or modify treatment goals (Oswald 2003). Both WSP and the HRAP systems are simple, cost effective technologies for reducing nutrient and contaminant concentrations in sewage and industrial wastewaters (e.g. Oswald 1995, Oron et al 1979, Fallowfield and Garret 1983, Fallowfield et al. 2001, Smith et al. 2004, Godos et al. 2009) and provided that sufficient land is available can be far more cost effective than high energy input systems such as the activated sludge process. However, the form of treatment system used must be carefully considered based on numerous factors such as wastewater composition, land cost, capital cost, operational cost, maintenance cost, and performance (Shilton and Walmsley 2005; in Pond Treatment Technology, p8).

HRAP systems are efficient actively mixed systems and can sustain very high areal biomass concentrations (Oswald 1995) thus reducing land requirements for treatment plant infrastructure. Active mixing, typically by paddlewheel, allows flocculent

particles to form in suspension; these so called ‘flocs’ are generally comprised of algal/bacterial/zooplankton biomass and detritus (ALBAZOD) (Soeder (1984), Cromar and Fallowfield (1992)). This is in contrast to WSP algal biomass which tends to be rather dispersed (consistency of green soup); active mixing in HRAP systems maintains these flocs in suspension and facilitates cycling of photosynthetic biomass through the underwater light field (Pearson 2005; in Pond Treatment Technology, p34 2005). WSP are, in biological terms, extremely complex systems that still require a great deal of research into microbiological processes to provide engineers with tools for improving WSP design (Pearson 2005; in Pond Treatment Technology, p40).

WSPs are a widespread and commonly used technology; for example at the time of writing there were 40 WSPs in South Australia used to treat human sewage (Farror pers.com. 2010); with thousands more being used through the developed and developing world (Shilton and Walmsley 2005; Pond Treatment Technology, p1)

At the time of writing, the strategic infrastructure plan for South Australia regional overview (SA Government 2006) encouraged proposals directed at reusing high-volume industrial sources of wastewater, e.g. Murray Bridge abattoir, for ‘higher value uses’ e.g. production of common-vetch as stock feed (Farror pers. com. 2010); such projects, if properly designed and regulated, should provide a long term, profitable and safe means of reducing nutrient loading on the lower reaches of the River Murray and thereby improve water use efficiency for the benefit of both the Murray River ecosystem and the communities that depend on it.

2.3. Bolivar WWTP and Wastewater Reuse in South Australia

Until recently the WSP system at Bolivar, Plate 2.1, was the major nutrient reduction stage of treatment provided to sewage from the north-western suburbs of Adelaide prior to effluent disposal at sea. The original design consisted of primary screening of the raw sewage followed by grit removal and a settling stage prior to partial nitrification and BOD removal through a series of trickling filters (Hodgson et al. 1966, Herdianto, 2003, Sweeney 2004, Short 2010). Trickling filter effluent was then divided between two, in series trains, each comprising three separate WSPs of nominal average depth 3'6" (1.065m) and a total area of approximately 850 acres (344 ha) (SA Government 1966) with a detention time in the lagoons of approximately 32 days. The design included the capacity to treat wastewater derived from the equivalent of 1.3 million people, with treatment optimised with respect to re-use of effluent from the WSPs for agricultural, horticultural and aesthetic purposes (SA Government 1966) with first flows being received by the system in June 1966. Prior to this time, a large proportion of sewage and industrial effluent from port Adelaide and the North of Adelaide was pumped for treatment at the Port Adelaide sewage farm prior to disposal into the Port River. Population increases following the end of WWII resulted in significant overloading of this system during the 1950s resulting in substantial quantities of trade-waste and sewage entering the Port River estuary with no or little treatment. After commissioning, the Bolivar treatment system operated in its original configuration until upgrade of the secondary treatment system from bio-filters to activated sludge in 2000. The authors of the report of the committee of enquiry into the utilisation of effluent from Bolivar sewage treatment works (SA Government 1966) provided extremely detailed information regarding the

potential for re-use of the treated wastewater from the system. This included assessments of likely pathogen and virus removal rates (and content), soil types and potential suitability of the water for irrigation; design effluent nutrient concentration based on a population of 1.3 million people and the likely returns from farming and horticulture upon recycling the wastewater.

The authors concluded with the following statement;

> *"Whatever the future holds, the committee does not believe that this valuable water can be thrown away by the driest State in the driest Continent of the world. The profitable reclamation and re-use of this water is therefore the challenge which will face South Australia's engineers, scientists and administrators in the future" (Hodgson et al 1966, p44, para.2).*

During the late 1990s the pre-treatment plant underwent a major upgrade to the activated sludge process (Sweeney et al. 2005a, Sweeney et al. 2005b); since this time there has been renewed recognition in the community of the potential benefits of wastewater reuse; no doubt due to the severe water restrictions imposed during the recent drought. A significant portion of this wastewater with some additional treatment (filtration and oxidative disinfection) is recycled for horticultural or non-potable domestic purposes. In Adelaide, at the time of writing, some 30% of wastewater from domestic sewage treatment processes was recycled for the watering of parks and gardens (SA Government 2009), with water recycling levels in South Australia far in excess of those reported interstate. Reuse is expected to increase substantially in the future; i.e. planning is underway for the installation of dual reticulation systems in a southern suburbs housing development of 8000 homes. Such developments may reflect community acceptance of the reuse of wastewater.

Plate 2-1 Satellite image of Bolivar waste stabilization lagoon system; circa 2007.

As discussed above, wastewater containing pathogens, hazardous compounds or elements requires sufficient treatment to remove or reduce the levels of these contaminants prior to re-use. As such, the consequences of treatment failure (or non-treatment) followed by reuse or release may be significant in terms of public health (Dorsch et al. 1984, Morris 1999) or ecosystem functioning (Westphalen et al. 2005). Whilst rule based approaches to design and management of these treatment systems has proven very effective in many instances; examples are to be found in the literature where limitations in knowledge with respect to system ecology, design,

functioning and requirements for preventative maintenance can lead to inappropriate management practices and treatment failure (Sheil 2000).

2.4. Biological Processes in Ponds

Oxygenic photosynthesis by microalgae is currently believed to provide at least 80% of dissolved oxygen in WSP systems (Pearson 2005; in Pond Treatment Technology, p18 2005) with the balance provided by atmospheric re-aeration (Gloyna 1971). Phytoplankton require carbon dioxide for photosynthesis and this is released in large quantities to the water column by respiration of fast growing heterotrophic bacteria that oxidise organic material for synthesis of cellular material and energy for growth. As such the relationship between algae and heterotrophic bacteria in these and other remediation systems has been considered to be functionally mutualistic, a form of symbiosis (Oswald et al. 1953, Borde et al. 2002, Danger et al. 2007) although this has yet to be experimentally confirmed in the field. Figure 2.2 shows a depiction of the proposed mutualistic relationship and the currently accepted functional links between the algal and bacterial components of the pond biomass (Oswald et al. 1953). Upon inspection of this figure the reader may note that an emphasis is placed on the link between solar energy input and algal photosynthesis; this reflects the critical importance of this relationship to the maintenance of aerobic conditions within these systems and also the relatively immature state of understanding with respect to factors that mediate this relationship in these systems. In addition, aerobic conditions, if allowed to prevail in a pond, or in the surface layer of a pond, can prevent or limit generation of odours from sulphides released from anaerobic or anoxic portions of the pond (Gloyna 1971) due to the fast reaction rates of dissolved oxygen with sulphides. The biological processes occurring within WSP systems are

of course considerably more complex than depicted in Figure 2.1. These include the cycling of nutrients due to grazing of algae and bacteria by zooplankton, populations of which can be substantial (Short 2010). Aerobic/anoxic/anaerobic nutrient conversion processes and exchanges with the sediment (Carmargo Valero and Mara 2007, Yamamoto et al 2010); are processes that can be strongly influenced by stratification and wind induced mixing (Meneses et al. 2005, Sweeney et al. 2007) and have importance in the effectiveness of pathogen removal (Shilton and Harrison 2003, Munoz and Guieysse 2006, Bolton et al. 2010).

For an extensive and thorough review of the ecological literature relating to WSP operation and function the reader is referred to Sweeney (2004), Yamamoto (2007) and in particular Short (2010). For the purposes of brevity, and to avoid duplication of the highly thorough review of Short (2010), this portion of the literature review (Chapter 2) focuses particularly on light and substrate (carbon) availability to algae, in addition to the influence of physical mediators (such as mixing).

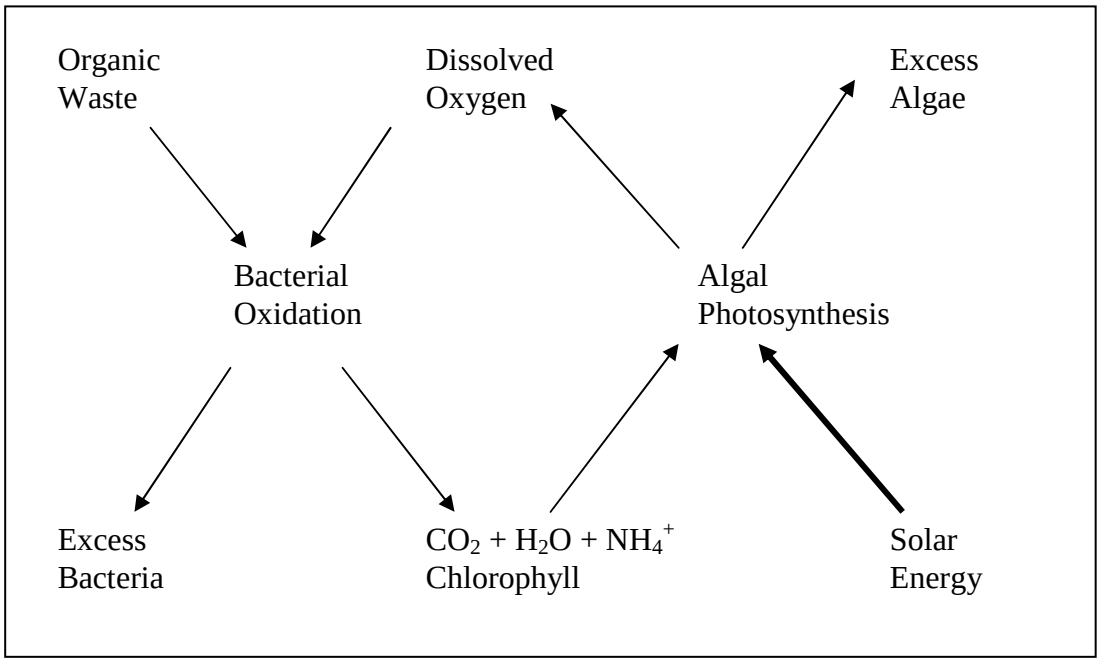

Figure 2-1 The Cycle of Oxygen and Algal Production as a function of Bacterial Oxidation of organic waste; Adapted from Oswald et al. (1955).

2.5. Photosynthesis in Algal Based Wastewater Treatment Systems

The net reaction summarizing photosynthesis, in plants and algae, as the production of carbohydrate and evolution of molecular oxygen as a by-product is shown in Equation 2.1 (modified from Falkowski and Raven 2007, p301).

$$CO_{2(g)} + H_2O_{(\ell)} + \geq 8 \text{ Photons (400 to 700 nm)} \longrightarrow$$
$$(CH_2O) + H_2O_{(\ell)} + O_{2(g)} \qquad \text{Eq. 2.1}$$

With reference to this equation it is noteworthy that, in general, photosynthetic bacteria, with the exceptions of cyanobacteria and prochlorophyta, do not evolve oxygen as a by-product and are capable of photosynthesis only under anaerobic conditions, and in addition rely on light capturing pigments other than chlorophyll_a (Falkowski and Raven 2007), such phytoplankton are not considered further in the following discussion.

Light within the wavelength band 400-700 nm is termed photosynthetically active radiation (PAR); SI derived units that can be used to quantify radiant flux/m^2 (Φ) are the 'watt' or equivalently Joules/s (NIST 2010). An empirical relationship (Eq 2.2) relates wavelength of light, energy and quanta(photons)/s to specific radiant intensity (Morel and Smith 1974, Kirk 1994).

$$\text{quanta/s} = 5.03\ \Phi\ \lambda \times 10^{15} \quad \text{(Kirk 1995)} \qquad \text{Eq. 2.2}$$

When integrated across the wavelength band most active in photosynthesis (nominally 400 – 700nm)[1] the familiar quantity of PAR with units of µmolquanta/m2/second can be derived; more correctly with respect to the above derivation the term 'photon flux density' (PFD) can be used. However both terms

[1] Introduces an error of approximately 5% due to the action spectra of photosynthesis being within the band of 350-700nm (Raven and Falkowski 2007, p341).

(PAR and PFD) are in common usage within the photosynthesis literature and are often used interchangeably.

The absorption of energy of photons for synthesis of carbohydrates by algae (and most other plants) is mediated by the photosynthetic pigments such as chlorophyll_*a*, b and c; the energy of the absorbed photons (PAR) is transferred through the 'antenna complex' by an electron transport chain in a series of oxidation/reduction reactions. Attenuation of light within the water column is a key factor that influences the spectral quality and PFD of light available to the photosynthetic pigments contained in the algal cell (Kirk 1994). The reductants generated in this reaction are used to assimilate inorganic carbon and to maintain metabolic activity of the algal cell (Falkowski and Raven 2007, p 118). The enzyme that ultimately catalyses the chemical reaction depicted in Equation 2.1 is ribulose-1,5,-bis-phosphate carboxylase/oxygenase (RuBisCO). This enzyme catalyses the fixation of carbon at an extremely slow rate in comparison to most other bio-catalysts (Gerritsen 2003); as such it is required in large quantities in the algal or plant cell and may constitute, dependant on algal species or growth conditions, 50% of the soluble protein in a cell. As such it has been speculated that it is the most abundant protein on earth (Ellis 1979, Gerritsen 2003, Feller et al. 2008); the enzyme is characterised by its extremely large size, slow reaction rates and its tendency to react with oxygen. As such it has also been described as a "fat lazy promiscuous enzyme" (pers. com. Professor. S. Tyerman 1995) and "the plant kingdom's sloth" (Gerritsen 2003). An additional benefit to algae from the presence of bacteria may be the removal of excess oxygen from the growth medium by bacterial respiration; some studies have indicated that high oxygen partial pressures may inhibit the activity of RuBisCO in algal cells (Mouget 1995, Danger et al. 2007b) and may result in a phenomenon

known as ‘photorespiration’. That is, the loss of fixed carbon resulting from the oxygenase activity of the RuBisCO enzyme which manifests as a light-dependent consumption of oxygen and reduction in photosynthetic efficiency (in terms of carbon fixation); typically these effects in algae culture are considered to be small except at extremely high DO concentration (Raven and Larkum 2007). Nevertheless, within highly productive systems such as WSPs and HRAPs, extremely high DO partial pressures are commonplace during the photoperiod and may therefore be a potentially significant factor in controlling algal productivity during these periods although it appears this has yet to be shown in the field. The potential for productivity losses due to photorespiration is believed to have driven the evolution of morphological and biochemical process in terrestrial C_4 plants; adaptations that facilitate the concentration of CO_2 within the chloroplast (Raven and Beardall 2006). Carbon concentrating mechanisms are very common in algae and may have evolved these features as adaptations to the oxygenase activity of RuBisCO (Giordano et al 2005).

The equation depicting standard mitochondrial respiration of the organic carbon produced during photosynthesis in order to provide energy (ATP) for processes such as algal cell maintenance, growth and division is shown in Equation 2.2 (modified from Falkowski and Raven 2007, p301).

$$(CH_2O) + O_{2(g)} + H_2O_{(\ell)} \longrightarrow CO_{2(g)} + 2H_2O_{(\ell)} \quad \text{Eq. 2.2}$$

The same basic stoichiometry can be used to depict respiration in heterotrophic bacteria (Metcalf and Eddy 2003) where stored carbohydrates are oxidised to release energy for cell maintanence and growth.

Ultimately, primary producers such as autotrophic algae provide organisms at the lower trophic levels with energy they require for processes such as growth and reproduction (Lindeman 1942). In addition the waste oxygen derived from algal photosynthesis is ultimately used by aerobic bacteria that have evolved to exploit the resources available within aerobic waters and sediments. With reference to algal and bacterial based wastewater treatment systems, aerobic bacteria and other aerobic organisms exploit the nutrient rich wastewater, remove nutrients via sedimentation or nutrient conversion, and do so at significantly higher reaction rates and with reduced odour emissions than anaerobic bacteria. Despite the high inorganic and organic nutrient loading (compared to natural systems such as many lakes, rivers and oceans) in wastewaters, algae can provide the majority of the oxygen required to maintain a pond in an aerobic state (Oswald 2003) despite the high concentrations of heterotrophic bacteria. In fact the mass of bacteria per unit volume of pond supported by the activity of the algae can be significantly greater than the biomass of algae (Cromar 1996).

2.6. Dissolved Inorganic and Organic Carbon

Inorganic carbon (carbon dioxide) as shown in Equation 2.1 and 2.2 is the substrate required by RuBisCO (Giordano et al. 2005) and the waste product produced by respiration. However, in the aquatic medium the carbon ultimately fixed by cell biochemistry in the Calvin cycle is more correctly characterized by the carbon store (CS) equilibrium shown in Equation 2.3 (Modified from Mukherjee et al. 2002).

$$CO_{2(g)} + H_2O_{(\ell)} \leftrightarrows H_2CO_{3(aq)} \leftrightarrows H^+_{(aq)} + HCO_3^-{}_{(aq)} \leftrightarrows H^+_{(aq)} + CO_3^{2-}{}_{(aq)} \qquad \text{Eq.2.3}$$

This equilibrium is, as suggested by the presence of hydrogen ions on the products side of the equation, pH dependent. Algae have evolved various mechanisms for

concentrating carbon across the cell membrane and into the cell that include both passive and/or active transport of bicarbonates or CO_2 (Giordano et al. 2005, Falkowski and Raven 2007). As algae remove CO_2 or bicarbonate from the aquatic medium, be it a wastewater or culture medium, the equilibrium shown in Eq. 2.3 will shift away from products and toward reactants, removing hydrogen ions from solution and increasing the pH of the culture. It is worth noting that the carbonate ion (CO_3^{2-}) is a low efficiency carbon source for photosynthesis (Beardall et al. 1998) and that characteristically, algal cultures tend to increase the pH of the culture medium during photosynthesis unless it is well buffered. Therefore the degree of pH shift due to algal carbon uptake during photosynthesis, under given conditions, will reflect the degree of buffering afforded by the wastewater or the culture medium. Typically, domestic wastewater is alkaline due to the presence of chemical species such as hydroxides, carbonates (as specified in Eq. 2.3), phosphates, borates and silicates in electrochemical balance with ions such as calcium, magnesium, potassium, sodium and ammonia, all derived from domestic, industrial or natural sources (Metcalf and Eddy 2003). Importantly, the CS equilibrium as shown in Eq. 2.3 and to lesser extent (based on concentration) components such as phosphates, borates and silicates and ammonium can act as a buffer system. As such, the wastewater acts as a chemical system that tends to resists changes to pH. Nevertheless biological processes such as nitrification/dentrification and particularly photosynthesis can and often do radically alter pH during the day.

The pH level (and alkalinity) has therefore been used in the development of some models of phytoplankton productivity, nutrient and carbon budgets (e.g. Mukherjee et al. 2002, Mukherjee et al. 2007, Mukherjee et al. 2008). A cyclic pattern of pH (and by inference DIC speciation) change is commonly observed in algal ponds but it

appears that in the field ('in-vivo') the relative importance to photosynthesis from changes in CS equilibrium and/or pH are yet to be clearly elucidated in the literature. For example Beran and Kargi (2005) constructed a mathematical model of WSP productivity where DIC concentrations were considered to be sufficient for photosynthesis at all times; whereas the influence of pH upon algal activity was considered inhibitory at high levels and described by Monod type kinetics: the authors suggested that high pH is due to removal of CO_2 at high rates of photosynthesis. Conversely a model described in Kayombo et al. (2000) assumed that the rate of photosynthesis, at optimal light intensity and temperature, was determined by the CO_2 concentration in the WSP water column; impact of pH was included as a parameter and it was assumed by the authors that algae are able to grow only within a specific optimal range. Surprisingly neither of the authors explicitly raised the issue of the inhibitory activity of free ammonia (or free sulphide) to photosynthesis (Abeliovich and Azov 1976, Azov and Goldman 1982, Veenstra et al 1995), such relationships are pH dependant and of potential importance in most WSP systems.

Klug (2005) points to a study of Cole et al. (2000) who showed that some lakes displaying high levels of dissolved organic matter (DOM) may also be supersaturated with dissolved inorganic carbon (DIC) and can remain supersaturated even during periods of high algal growth. A significant portion of this pool of inorganic carbon is considered likely to be the product of bacterial respiration (Moran and Hodson 1990, Karlsson et al. 2008) and also derived from photochemical oxidation (Vahatalo et al. 2003) of allochthonous DOM. Recent studies of oligo and mesotrophic water bodies indicate that the result of this bacterial respiration can be a net contribution of CO_2 to the atmosphere despite the presence of

actively growing autotrophic phytoplankton (Duarte and Prairie 2008). Recent research by Short (2010) confirmed that DIC can be a limiting nutrient for photosynthesis and lead to algal cell death in the dark (in vitro), however despite this finding the author stated that this result was unlikely to have application in-vivo (in WSPs) due to the low concentrations of DIC required to inhibit algal growth (<0.2 – 0.3 mg/L). As simplistically depicted in Figure 2.1, phytoplankton; the primary producers at the base of the trophic food web, are in principle complemented by the activity of heterotrophic bacteria (decomposers). The combined activity of phytoplankton and heterotrophic bacteria has been described as the basis of aquatic ecosystems (Loreau 2001, Danger et al 2007a). Both groups of organisms appear to benefit from the presence of the other; for example bacteria may provide an inorganic carbon source that is potentially depleted during periods of high photosynthetic activity (Klug 2005), while converting allochthonous DOM sources containing Gilvin and other coloured dissolved organic matter (thus potentially improving light penetration) and release nutrients including N, P and C into solution. It is noteworthy that the bioavailability of DOM (to bacterial oxidation) may differ based on its source, for example, Moran and Hodson (1990) showed that DOM extracted from a lake was more available to bacteria that DOM extracted from a black-water marsh. In aerobic algal-based wastewater treatment systems the solubilisation of BOD/DOM by heterotrophic bacteria performs a wastewater treatment function while generating DIC for algal photo oxygen production. With respect to the Bolivar WSP system, Sweeney et al. (2005b) showed that the installation of activated sludge (AS) treatment of the Bolivar wastewater as pre-treatment for the WSP in February 2005 resulted in a 55% decrease in average loading of total biochemical oxygen demand (BOD_{tot}) and a 94% reduction in

average loading of soluble biochemical oxygen demand (BOD_{sol}) to the ponds. It should be noted that whilst average BOD loadings to the Bolivar WSP such as those quoted above can be calculated the volume of effluent from the AS system wastewater treatment processes is subject to regular diurnal variations due to the daily pattern of sewage effluent production by the community (Sweeney 2004).

An investigation of the effluent DOC from seven AS systems (Amai et al. 2005), with similar BOD_{sol} to that displayed by Bolivar AS effluent, showed that a significant concentration of BOD was 'recalcitrant' DOC (2.6 – 31.6 mg/L), with the majority of this recalcitrant DOC composed of organic acids. In a complementary study Katsoyiannis and Samara (2007) showed that approximately 40% of the DOC present in the raw influent to a conventional treatment plant (of similar configuration to the Bolivar AS system) was present in the effluent, i.e. a significant portion was not readily biodegradable in the AS system.

2.7. Productivity in Algal Pond Systems

Algal ponds provide a contained environment in which waste organic matter can be chemically altered by 'beneficial' (in a utilitarian sense) biological reactions; these reactions are able to occur prior to release of the wastewater to natural ecosystems and/or prior to re-use.

Algal productivity in pond systems is fundamentally limited by the efficiency with which incident light energy can be converted into chemical energy (Kirk 1994); therefore for a given non-nutrient limited algal assemblage system and at a given temperature, photosynthetic rate is strongly driven by light availability, i.e. factors such as the intensity of sunlight incident on the pond surface, water depth and water transparency (Kirk 2003, Davies-Colley et al. 2005, Reynolds 2006, Pearson 2005;

in Pond Treatment Technology (Shilton, A. Ed. p20), Falkowski and Raven 2007 p3). With reference to Equation 2.1, gross photosynthesis (GP) can be defined as the light dependent rate of electron transport to a terminal electron acceptor, e.g. CO_2, in the absence of respiratory losses (Kirk 94, Reynolds 2006, Falkowski and Raven 2007). The captured carbon may be respired, incorporated into the structure of the algal cell e.g. protein, or be excreted (or diffuse) from the cell as DOC (Reynolds 2006, Falkowski and Raven 2007). It is noteworthy in the context of this discussion that gross photosynthesis is also directly proportional to oxygen evolution. As a consequence, measurements of oxygen evolution, at a given temperature, algal concentration and at a series of light intensities, when corrected for oxygen loss due to respiration (R), can provide a measure of 'net photosynthesis' (Pnet) which is directly proportional to net organic carbon production (Harris 1984, Kirk 1994, Reynolds 2006, Falkowski and Raven 2007). On this basis an equation relating net to gross photosynthesis and respiratory oxygen losses can be represented as Equation 2.3 (adapted from Falkowski and Raven 2007).

Pnet (mgO2/L/unit time) = GP (light) – R (dark) Equation 2.3

This approach has been widely used since the time of Emmerson and Green (1934) Examples of research in the literature based on this methodology are too numerous to list, however some representative examples are Manning et al 1938, Myers and Cramer 1948, Odum 1956, Talling 1956, Falkowski 1981, Neale and Marra 1985, Bender et al. 1987, Aalderink and Jovin 1997, and Gruber et al. 2007.

Quotients of Production

The stoichiometry of photosynthesis, for the production of carbohydrate, as summarised in Equation 2.1, can be expressed as moles of O_2 produced per moles of

CO_2 assimilated by the cell; this ratio is termed the 'photosynthetic quotient' (PQ) (Emmerson and Green 1934, Manning et al. 1938, Sargent 1940, Odum 1956, Harris 1984, Kirk 1994, Falkowski and Raven 2007), 1.0 from Equation 2.1. Similarly, the directly complementary parameter, 'respiratory quotient' (RQ) can be expressed as the number of CO_2 produced per moles of O_2 consumed, upon complete oxidation of carbohydrate in this case, and therefore 1.0 for respiration; Equation 2.2. The PQ and RQ quotients are termed assimilation numbers (Ryther and Yentsch 1957, Falkowski 1981, Platt and Gallegos 1980, Cullen 1990, Kirk 1994).

Deviations from *a priori* stoichiometric related PQ and RQ values can provide valuable insights into the causes of photosynthetic yield variation and the energetic efficiency of algal growth (Reynolds 2006). In particular, comparison of stoichiometric PQ and RQ values from both culture and field studies have provided a means of understanding how differing costs for respiration, synthesis and the corresponding photosynthetic efficiency as determined by photosynthetic rate depend on substrate type (Emmerson and Green 1934, Odum 1956, Falkowski 1981, Neale and Marra 1985, Bender et al. 1987, Laws 1991, Morris and Kromkamp 2003, Eriksen et al. 2007, Jakob et al. 2007, Hancke et al. 2008).

An important caveat that must be placed upon interpretation of measurements of net primary production in natural ecosystems is the contribution to respiratory losses by heterotrophs (Li and Maestrini 1993; secondary citation from Falkowski and Raven 2007). Measurements of net algal productivity in mixed cultures (autotrophic algal and non-autotrophic organisms) are more uncertain than measurements of gross photosynthesis (Falkowski and Raven 2007); where measurements of gross photosynthesis can rely specifically upon measurements of oxygen production per unit algal biomass (chlorophyll_a). Cromar and Fallowfield (1992) in a seminal

paper used Percoll^{R}/sucrose density gradients to establish the relative contribution of algal and bacterial biomass to productivity within a HRAP and showed that on average algal biomass within these highly productive systems contributed only 40% of the dry matter (suspended solids) biomass. Thus productivity measurements derived from dry matter are considered likely to overestimate productivity; consequently algal productivity measurements are typically normalised to chlorophyll_a as a proxy for algal biomass independent of bacterial biomass; nevertheless the error introduced by the respiration of non-algal biomass upon estimates of 'algal' respiration used subsequently to derive estimates of net photosynthesis must be noted. Unfortunately the Percoll^{R} density gradient method is technically challenging and therefore requires calibration against other more straightforward measures for widespread application in field studies that require equally accurate estimates of net algal productivity.

On the basis of the above and with reference to the observation that the surface of the earth (in mid latitudes) receives an average of 240 Wm^{-2} (240 J/m^2/second), (1104 umolquanta/m2/sec) an upper limit in terms of productivity in a 12 hour diurnal cycle in algal ponds can be calculated for photosynthesis (Grobbelaar 2010). That is:

$$\text{Productivity} = \%\text{Photosynthetic Efficiency} \times [3.97 g(dw)/m^2/day] \qquad \text{Equation 2.4}$$

i.e. 5.7gC/m^2/day for high rate algal ponds based on 40% algal mass as C (Cromar and Fallowfield 1992) (≈ 14 gdw/m2/day). Photosynthetic efficiencies in the literature were reported by Grobbelaar (2010) to range from 0.1-8% for total irradiance (0.05 – 3.5% PAR; Morel 1991). The above calculation is based on the theoretical maximum value of 8% (3.5% PAR); another example is provided by a HRAP system treating abattoir wastewater (Fallowfield et al. 2001) where a

maximum productivity of ≈ 38 gdw/m^2/day was observed; implying an efficiency of ≈ 4% PAR, when corrected for the 40% algal biomass factor discussed above. Grobbelaar (2010) has reported substantially higher productivity measurements in HRAP systems and attributed this to the enhanced light/dark cycle that occurs in these systems. In laboratory based bioreactors with defined light/dark cycles Grobbelaar (1989), Grobbelaar et al. (1996) have observed productivities of close to an order of magnitude higher and attributed the observation to the advantages of active mixing. Mechanistic explanations for these differences include reduced potential for photo-inhibition in non-stratified (mixed) HRAP systems and improved light climate due to cycling of the algal culture within the photic zone (Ratchford and Fallowfield 2003).

Rates of productivity in WSPs (unmixed) are therefore reported to be lower than those of HRAPs; it is however noteworthy that the literature reporting algal productivity in field experiments of WSPs is generally sparse (Weatherall 2001, Mashauri and Kayombo 2001, Kayombo et al 2002, Beran and Kargi 2005, Bonachella et al 2007, Fyfe et al 2007, Weatherall 2007, Bernal et al 2008). However, recent direct comparisons of a HRAP system and WSP used to treat domestic wastewater in rural South Australia have shown that productivity may be enhanced by up to 2 orders of magnitude in the HRAP system (Fallowfield pers. com. 2011).

Mixing and Productivity

Mixing may modulate photosynthetic rates in systems with high productivity and attenuation of light such as WSPs and HRAPs. Hydrodynamic transport processes determine how phytoplankton, suspended heterotrophic organisms and nutrients are distributed within a pond system and therefore the extent of light penetration and

cycling within the algal pond (Sweeney 2004, Zhen-Gang 2007). HRAP systems being subject to active mixing are less prone to sedimentation or short-circuiting (El Ouarghi et al 2000, Pearson 2005). WSP systems such as Bolivar have been shown to be prone to frequent stratification during the summer period (Sweeney 2004); this layering of the water column may play a role in maintaining phytoplankton within undesirable zones of the light gradient, whilst active mixing in HRAP systems allows the circulation of phytoplankton through the light gradient. WSP systems are subject to passive mixing from wind, influent flow and the breakdown of thermal stratification gradients. They are therefore less likely to be stable and/or predictable in comparison to well mixed unstratified systems (Sweeney 2004, Beran and Kargi 2005, Pearson 2005).

The elucidation of hydraulic flow patterns within HRAP systems and WSPs in particular provides a means of better characterising patterns of change in availability of potentially limiting resources, whether they be light or nutrient (nitrogen, phosphorus or trace element) or substrate (carbon) (El Ourghi et al. 2000, Weatherall 2001, Sweeney 2004, Shilton 2005, Zhen-Gang 2007).

Measuring Productivity

As discussed above the measurement of productivity in large natural or field based systems is a challenging enterprise. A commonly used approach developed by early pioneers in the field is the use of transparent glass bottles containing algal material that are subject to differing nutrient conditions or light intensity, temperature, pH and so on. The application of this methodology or modifications of it (Hobson and Fallowfield 2003) in the field has provided extensive insights into algal ecophysiology (Harris 1984, Kirk 1994, Reynolds 2006, Pearson 2005, Falkowski and Raven 2007). Nevertheless ‘bottle effects’ are well recognized in the literature as

problematic due to the potential for non-representative (compared to open culture) conditions to prevail (Emerson and Greene 1934, Steemann Nielsen 1952, Odum 1956, Eppley 1980, Falkowski and Raven 2007). This is believed to include the impact of stirring on gas exchange within a cuvette for example as used for measurement of oxygen production in response to light intensity; specifically the diffusion of gasses such as oxygen from algal cells and carbon dioxide to algal cells is enhanced at higher levels of turbulence (Geider and Osborne 1992). These difficulties using direct methods (e.g. bottle incubations) have for a long period encouraged researchers to attempt to perfect measurement techniques using online high resolution data (typically semi-continuous) for estimating oxygenic productivity (e.g. Odum 1956, Kelly et al. 1974, Fisher and Carpenter 1976, Edwards et al. 1978, Marshall 1981, Thyssen and Kelly 1985, Markager and Sand-Jensen 1989, Fee 1990, Portielje et al. 1996, Aalderink and Jovin 1997, Uehlinger et al. 2000, Evans et al. 2003, Lopez-Arcilla et al. 2004, Ciavatta et al. 2008) and to determine its relationship to incident light intensity and other parameters such as BOD loading (Kelly et al. 1974). The method of Dubinksy et al. (1987) for measuring photosynthetic rates in controlled conditions of mixing and defined light field using an oxygen electrode has provided an essentially standard method with which to compare photosynthesis under highly controlled conditions (Ratchford and Fallowfield 1992, Hobson and Fallowfield 2005, Reynolds 2006, Patterson and Curtis 2007, Falkowski and Raven 2007, Sukenik et al. 2009, Halsey et al 2010). However due to the requirement for a laboratory to provide controlled conditions to successfully use this methodology the use of this approach in the field is typically limited to oceanic productivity measurements within ship-board laboratories (Falkowski and Raven 2007). This has stimulated sustained efforts to obtain practical

methods for in-situ measurement of photosynthetic rate (Kirk 1994). This has included measurement of light curves using fluorescence of algal cultures *in-situ* (Genty et al. 1989, Horton et al. 1994, Govindjee 1995, Kromkamp and Forster 2003, Falkowski and Raven 2007, Krustopf and Flynn 2006, Raven and Beardall 2006). The work of Odum (1956) established the standard methodology for in-situ measurements of photosynthesis in rivers (Standard Methods 1994); this methodology when applied using modern dissolved oxygen monitoring systems may allow precise and accurate estimates of photosynthesis in systems such as HRAPs (Portielje et al 1996, Fallowfield et al 2001, Evans et al 2003) and WSPs (Kayombo et al 2003).

The following portion of the literature review assesses relevant literature relating studies of algal photosynthesis to wastewater treatment and algal biomass production and reveals challenges that still exist for scientists attempting to understand the dynamics of photosynthesis in highly productive and biologically complex artificial and natural systems and provides context for the experimental work reported in later chapters.

3. MEASURES OF PHOTOSYNTHESIS

3.1. Introduction

Algal ponds have been used extensively for many decades throughout the world to treat domestic sewage (Oswald et al. 1953) and an increasing number of industrial wastes (Oswald 2003). There is however an ongoing need for improved understandings of the ecological processes occurring within these artificial algal ponds. This need can be justified from a largely utilitarian perspective; where identification and possibly manipulation of system 'control' parameters can provide information for improved operation, performance or design functions; some pertinent examples are provided in Oswald et al. (1953, 1955), Gloyna (1971), Dugan et al. (1972), Benemann et al. (1977), Buhr and Miller (1983), Berner et al. (1986), Hartig et al. (1988), Fallowfield et al. (1992), Cromar et al. (1996), Mihalyfalvy et al. (1998), Lee (1999), Grobbelaar (2000), El Ouarghi et al. (2000), Cromar and Fallowfield (2003), Ratchford and Fallowfield (2003), Sweeney et al. (2005b), Evans et al. (2005), Sweeney et al. (2005), Fyfe et al. (2007), Perner-Nochta and Posten (2007), Short et al. (2007), Sweeney et al. (2007), Silva-Aciares and Riquelme (2008), Yamamoto et al. (2010).

At a more fundamental level, an improved understanding of the phytoecology of these systems can provide the informational basis for the development of models used to assess understanding and functioning of both artificial and natural aquatic ecosystems; some pertinent examples are provided in Emerson and Green (1934), Smith (1936), Manning et al. (1938a and b), Emerson and Lewis (1942), French and Rabideau (1945), Myers and Cramer et al. (1948), Haxo and Blinks (1950), Arnold and Oppenheimer (1949), Talling (1956 and 1957), Oswald et al. (1965), Gavis and Ferguson (1975), Kroon et al. 1989, Kroon and Dijkman (1996), Simon et al (1998),

Huisman et al. (2002), Evans et al. 2003, Kroon and Thoms (2006), Mukherjee et al. 2007, Grobbelaar (2007), Weatherall et al. (2007), Coates and Mondon (2009), Robson and Mitchel (2010).

This chapter summarises relevant literature relating studies of algal photosynthesis, wastewater treatment and algal biomass production and reveals challenges that exist for scientists attempting to understand the dynamics of photosynthesis in highly productive and biologically complex artificial and natural systems.

3.2. Complexity in ecological systems and models of algal photosynthesis

An enormous literature is devoted to model theory and the specific techniques and approaches used for developing and assessing formal (mathematical or symbolic representation) and informal (conceptual) models; the following discussion is therefore, for the purposes of brevity and relevance, focussed specifically on issues surrounding the use of models as representations of scientific knowledge with respect to patterns and process in studies of algal photosynthesis. The reader desiring deep insights into the development and use and misuse of models in science and engineering more generally is referred to texts such as the Stanford Encyclopaedia of Philosophy (2009) http://stanford.library.usyd.edu.au/entries/models-science).

Whether such models are empirical and developed by experimentation or developed from first principles as is sometimes the case in physics, such formulations can be used to conduct numerical experiments, develop testable hypotheses or attempt to forecast the behaviour of the modelled system (Stow et al. 2009).

The mass of oxygen produced per unit time from algal photosynthesis is a key parameter used for determining the ‘capacity’ of an algal-based wastewater treatment

process (Chapter 2), i.e. sufficient oxygen must be produced by phytoplankton to meet respiratory requirements of an aerobic heterotrophic biomass in order to stabilise the nutrient load applied to the pond via the addition of wastewater (Oswald 2003, Davies-Colley et al. 2005). With reference to the stoichiometric equation of photosynthesis shown in Equation 2.1 (Chapter 2) and the definition of gross photosynthesis, it is apparent that changes in gross photosynthesis are directly proportional to oxygen evolution. The complementary stoichiometry of Equation 2.2 (Chapter 2) for respiration shows that oxygen use is also directly proportional to carbohydrate (fixed carbon) oxidised. As discussed in Chapter 2, it follows that measurements of oxygen evolution per unit algal biomass, conducted at a series of light intensities and corrected for oxygen loss due to algal respiration, can provide a measure of 'net photosynthesis'. Figure 3.1 shows one of the first detailed assessments of this type as carried out by Emmerson and Green (1934). These authors used bottles to incubate the algal material at a series of increasing light intensities at constant temperature in the laboratory; with rate of increase in dissolved oxygen production showing the characteristic Michaelis-Menten type enzyme kinetics that relate reaction rate to the concentration of the substrate (light in this case).

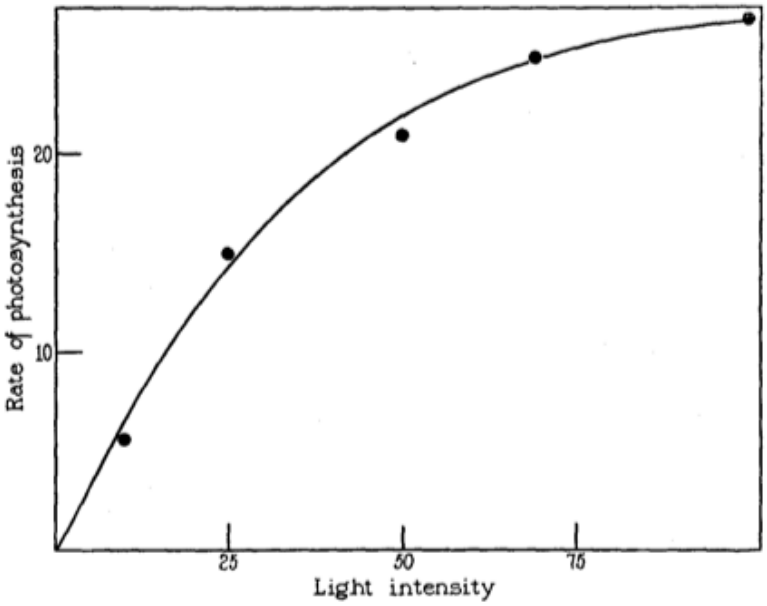

Rate of *Gigartina* photosynthesis as a function of light intensity. The unit of intensity is arbitrary. Temperature = 15°C. Rate of photosynthesis is in mm.³ O_2 per 15 minutes per cm.² of material.

TABLE II

Photosynthesis at Different Light Intensities. Detailed Data for Fig. 3

Area of algal material in each vessel = 2.1 cm.² Material suspended in ordinary sea water in equilibrium with air. Light from six 60 watt lamps close together, 8 cm. below vessels.

Temperature = 15.0°C.

Relative intensity (per cent transmission of filter)	Volume of gas space	Volume of fluid, including material	Vessel constants K_{O_2}	Δh change of pressure in 15 min.	x_{O_2} volume of oxygen evolved in 15 min. = $\Delta h \cdot K_{O_2}$	x_{O_2} with uniform correction for respiration, 1 mm.³ in 15 min.
	cc.	cc.		mm.	mm.³	mm.³
10	4.16	7.15	0.41	11.1	4.6	5.6
25	4.13	7.15	0.41	33.6	14	15
50	5.26	8.15	0.52	37.6	20	21
75	5.08	8.15	0.51	47.2	24	25
100	5.33	8.15	0.53	48.9	26	27

Figure 3-1. Reproduction of figure from the paper of Emmerson and Green 1934, showing the oxygen production rate of the alga *Gigartina* as a function of light intensity.

As discussed in Chapter 2 the bottle incubation approach (with suitable modifications) has and continues to provide useful information relating rates of photosynthesis to irradiance in natural systems. Nevertheless techniques such as the standard photosynthesis/irradiance (PI) apparatus that allow measurements of

photosynthesis to be undertaken using an oxygen electrode (Dubinsky et al 1987, Ratchford Fallowfield 1992) have provided researchers with the means of conducting such experiments at high resolution within a well defined light field. Such measurements are technically challenging in the field (Weatherell 2001) and the need for robust field systems capable of providing accurate measurements of photosynthesis has been recognised in the literature (Kirk 1994, Reynolds 2006, Falkowski and Raven 2007).

Algal Fluorescence

Other techniques have been trialled extensively in the field with some success using measurements of algal chlorophyll fluorescence in response to changing light; such techniques appear relatively mature in the study of ecophysiology of land plants but may require further validation when applied in aquatic systems (Kruskopf and Flynn 2006, Raven and Beardall 2006). Such approaches were briefly trialled in the Bolivar WSP system but were considered to require substantial and detailed research for the purpose of validation in these systems and are considered a potential focus for future research.

Oxygen Dynamics in Natural and Laboratory Based Systems

The concept of using measured changes in oxygen concentration in natural systems in order to reveal changes in primary production in flowing water bodies was pioneered by Odum (1956). In simplistic terms such measurements relied on the premise that flowing systems could be considered continually mixed and allow comparison of average oxygenic production from algal biomass during the day in comparison to night time oxygen use and theoretical estimates of re-aeration based

on stream flow velocity. By measuring parameters such as oxygen concentration directly *in-situ* the approach allowed, in principle, for measurements of gross photosynthetic rates in natural water bodies to be undertaken without the necessity to extrapolate from laboratory based studies or from bottles to the ecosystem of interest (McIntire et al. 1964). These authors developed what they termed a lab based 'photosynthesis/respiration chamber' that was effectively an early version of the standard PI apparatus and trialled it to determine photosynthetic rates in flowing 'laboratory streams'.

This enabled the authors to measure the light field and assess rates of oxygenic production of benthic biomass as a function of illumination, corrected for atmospheric oxygen diffusion (re-aeration) and respiration and to replicate it under defined physical conditions. The design of a separate part of the system was such that it was effectively a lab-scale high rate algal pond, a paddlewheel mixed raceway system (Chapter 5), operating with a depth of 20cm, with a non-planktonic algal and bacterial biomass. Subsequently, chamber studies based in the field have provided an effective tool for measurement of benthic biomass production in natural systems but the data obtained is subject to 'enclosure effects' as with bottle experiments (Uehlinger et al. 2000). An interesting method for determination of re-aeration rate in a HRAP system was presented by El Ouarghi et al. 2000, by dissolving a tracer gas (propane) into the pond the authors were able to calculate re-aeration transfer coefficient in-situ in the presence of pollution and photosynthesis rather than in potable water. Such an approach enables repeated measurements of this parameter as influent or effluent characteristics change over time.

Relatively recently, high quality dissolved oxygen monitoring units have become available that are robust and reliable for installation in field systems (Portielje et al.

1996, Kayombo et al. 2000, Uehlinger et al. 2000, Evans et al. 2003). These systems provide the opportunity to obtain *in-situ* measurement of dissolved oxygen with a degree of accuracy and frequency that was not possible prior to the development of these systems. Such systems were originally developed for the measurement of oxygen tension in blood (Clarke et al. 1953). Online DO monitoring systems have been perfected for use in activated sludge wastewater treatment systems; and have been effectively applied over periods of years in systems treating wastewater of variable composition, e.g. Fallowfield et al. 2001. One of the major challenges facing researchers in this area of ecology has been to extrapolate and compare results from controlled laboratory studies with those obtained in the field (Vollenweider 1974, Harris 1984, Kirk 1994, Evans et al. 2003, Reynolds 2006, Raven 2006, Falkowski and Raven 2007). As such there is a need to ground-truth or validate laboratory based techniques for measuring productivity (e.g. the standard PI approach) against robust and straightforward methods more suitable for routine use in the field without the need for extensive infrastructure (Kirk 1994, Evans et al. 2003). One of the features of measurements of oxygenic production by algae in relation to light intensity, whether obtained in the laboratory using the PI apparatus (Dubinsky et al 1987, Garret and Fallowfield 1992) or bottles (Emmerson and Green 1934) or directly using titration (Odum 1956) or using online data, (Uehlinger et al. 2000) is the generally characteristic shape of the photosynthesis-irradiance curve. The relationship between photosynthesis and irradiance has been extensively studied, and in a raw data form is form is shown in Figure 3.2. This plot shows data obtained from an experiment conducted in a laboratory based PI apparatus of the form of Dubinsky et al. (1987) and can be considered representative of that obtained using this basic approach.

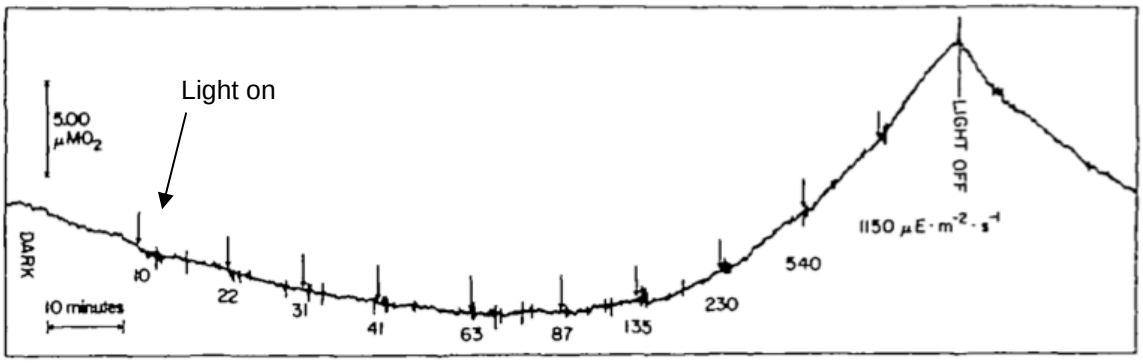

Figure 3-2. Representative PI trace showing photosynthetic O_2 evolution on the y axis and time on the x axis at increasing levels of irradiance (adapted from Dubinsky et al. 1987).

The initial portion of this plot showing the decrease in oxygen concentration during the dark, prior to illumination of the culture at a nominal light intensity of 10µmolquanta/m2/sec, can be used to calculate respiration rate. A slow reversal in rate of decline in DO is observed as light intensity is increased at each of the nominal increments shown in the Figure 3.2. The rate of decline in DO concentration stabilises at the nominal light intensity of 63µmolquanta/m^2/sec in this case; this point on the graph is termed the *light compensation point* (Kirk 1994) i.e. the location on the plot where oxygen loses from algal respiration are equalled by oxygen production from photosynthesis. The rate of oxygen production is observed to increase as light intensity is increased until the light source is turned off. Following cessation of illumination, production of oxygen from the culture ceases and a subsequent decline in DO concentration of the culture is observed. It is noteworthy that respiration rate following cessation of illumination is typically higher than prior to illumination; as a simplification it is generally assumed however that respiration is constant during illumination and equal to that observed prior to illumination (Falkowski and Raven 2007). Nevertheless this observation, termed light enhanced respiration has been attributed to metabolic effects on the

photosynthetic apparatus during high irradiances (Bender 1987, Graham et al, 1995, Jakob et al 2007, Dhiab et al 2007).

Photoinhibition, Pmax and Alpha

A corresponding, but possibly mutually exclusive effect, photoinhibition (Goldman 1979, Platt et al. 1980, Falkowski 1981, Vincent et al. 1984, Kroon and Dijkman 1996, Grobbelaar 2000, Hobson and Fallowfield 2001, Ratchford and Fallowfield 2003, Richmond 2004, Raven and Larkum 2007, Staehr et al 2009) is apparent in standard plots of the PI curve as shown in Figure 3.3. Specifically a decline in photosynthetic rates from Pmax at high irradiances; and this is apparent from inspection of hypothetical PI curves: a, b and c in the two plots. The initial light limited rate of photosynthesis (alpha) is also apparent from inspection of the two plots as the initial increase in photosynthetic rate prior to reaching Pmax.

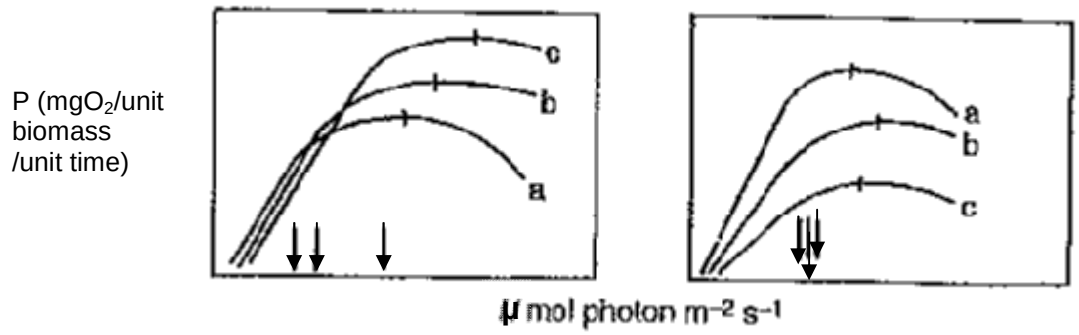

Figure 3-3. Hypothetical photosynthesis-irradiance plots (adapted from Reynolds 2006); showing rate of oxygenic photosynthesis per unit biomass as a function of irradiance at three different temperatures (a, b, c). In this case, in both plots, the sequence a, b, c is one of increasing temperature. In the left-hand plot, dependence of P upon light at sub-saturating light intensities was constant; in the right-hand plot, P vs. I varied but Ik (saturating light intensity, arrowed) was relatively constant. Pmax (maximum rate of oxygen production per unit biomass) for each experimental treatment was marked with a dash.

The PI curve is used to connect or link measures of phytoplankton biomass (e.g. chlorophyll_a, suspended solids) to rates of primary production, in this case when normalised to rate of change in oxygen concentration. It should be noted that data relating carbon-chlorophyll_a ratio in a cell or biomass (Cromar and Fallowfield 2003) is not critical to derivation of photosynthetic rates unless it is desired to derive specific growth rates of cells (Falkowski and Raven 2007, p 336). Interpretation of variations in PI curve attributes determined in the laboratory has allowed researchers to assess if some natural algal communities may be subject to depression of photosynthetic rates at high irradiance; or if not are protected as a result of self shading (light attenuation), light-dark cycling due to mixing in flowing systems or changes in the photosynthetic apparatus; e.g. increased chlorophyll_*a* concentration per cell (Falkowski et al. 1994, Uehlinger et al 2000, Ratchford and Fallowfield 2003). Another example is provided by research into the effects of changes in PI curves correlated with stratification and mixing; (Behrenfeld et al. 1998, Behrenfeld et al. 2002, Grobbelaar 2007, Kaiblinger et al. 2007). Such observations when conducted in the laboratory may, however, be subject to systematic errors resulting from nutrient depletion in PI chambers lacking a continuous supply of nutrients (Hornberger et al. 1976) and as such it can be difficult to definitively translate such results from the laboratory to natural systems (Kirk 1994). As such other methodologies such as algal fluorescence have been applied in order to provide an independent methodology without the same potential limitations; such assessments have shown, for example, depression in photosynthetic activity consistent with photoinhibition during high irradiance in dense cultures, an effect that may decrease areal productivities by 30% or more (Grobbelaar 2007). Improved mixing of dense cultures has therefore been consistently proposed as a means of improving

productivity in algal based wastewater treatment or biomass production systems (Ratchford and Fallowfield 2003, Sweeney et al 2003, Grobbelaar 2010), and may be of some importance in studies of natural systems (Zohary et al. 2010, Weber and Deutsch 2010).

It is therefore the case that empirical models such as the PI curve can be used to reveal functional relationships of relevance for understanding the ecology of these systems. In fact it can be argued that all models of photosynthesis used in ecology are ultimately empirically derived (Falkowski and Raven 2007), i.e. rates of reaction are measured rather than being derivable from first principles. This contrasts with models used to describe the physics of light transmission, energy budgets and the fluid dynamics of liquid flow; these can be (in principle) well defined by the use of physical constants, e.g. the Stokes equations of fluid dynamics (Sweeney 2004). The physical aspects of the pond environment can be precisely defined from careful measurement of flow rate, irradiance, light attenuation, temperature and density to calibrate a physical model of a pond system. Despite this, model outputs, regardless of formulation, require close scrutiny and analysis as slight errors in defining the state of a system propagate through each iteration, typically resulting, in non-trivial systems, to increasing deviation between observed and model predicted values over time (Lorenz 1963, May 1974, Lorenz 1989, Boffetta et al. 1998). Weather predictions provide a familiar example, with predictions, typically of greater than 3 days (72 Hours) becoming increasingly error prone; at a certain distance, x from the calibration point, t, (time = 0 at which parameters levels are set) weather models become less reliable than predictions simply based on the previous days weather. The most famous example of this fundamental limitation is well known as the ‘Butterfly Effect’ (Mazzocchi 2008).

Only perhaps in exceptionally simple and deterministic systems will a model provide consistent correspondence with the observed state. Empirical measurements (input data) therefore provide (in principle) not only the means of ensuring that model parameters are calibrated to simulate a particular scenario (=> output) but because of the limitations inherent in any particular model formulation, empirical data provides the means by which the failure or success of a model is usually assessed. This process is, for the assessment of ecological or other complex systems, generally an iterative one. Model formulations may range from the very simple to the complex but despite this may differ little in efficacy (observed/predicted) despite the great intellectual investment in a more complex model. Apparent 'failure' of a model is however from the perspective of those wishing to understand a particular system (e.g. algal productivity) a 'window' that allows the modeller to assess the relative importance of parameters used in a model formulation and thus focus resources on the measurement of parameters of particular importance to understanding the system or subsystem of interest. This highlights the important and often ignored fact that models of physical and biological systems are, more often than not, useful for understanding why our understandings of complex systems are incomplete. A sophisticated understanding of the modelling process and the limitations inherent must therefore be combined with validation data and 'ground truthing to test the hypotheses developed. A critical and careful regard for the many limitations inherent in the model formulations used to describe an aspect of the physical world is perhaps a necessary trait for the scientist wishing to understand a small portion of the physical world. The classic '3 body problem' in physics, is an instructive example; with the modelled behaviour of these systems indicating that three or more bodies in

orbit have the potential to display chaotic states. The example provided by May (1974) may be instructive in this regard; this author found that many of the early 'linear' models of population dynamics in fact revealed dynamics that were observed but largely ignored in previous studies.

These examples are intended to highlight the purpose of comparison of model outputs with empirical measurements. Limitations and uncertainties inherent in a model formulation or parameterisation are unavoidable in such descriptions of real-world and complex systems (Lynch and McGillicuddy 2009). The development of models is therefore typically a process where understanding the cause of model failure and/or deviation from empirical derived data facilitates further iterations in the development process and provides insights regarding the general and specific applicability of a particular model formulation and hopefully the system it is used to represent.

The Primary Productivity Algorithm Round Robin (PPARR)

During the past decade or so the United States National Aeronautics and Space Administration (NASA) has instigated and supported an international cooperative research project tasked with improving estimates of marine photosynthesis by means of remote sensing. An intensive series of reviews and model 'skill assessments' (Jolliff et al. 2009) known as Primary Productivity Algorithm Round Robins (PPARR) have been completed on aquatic productivity models e.g. Carr et al. (2006), Friedrich et al. (2009). The most recent and extensive of these PPARR's (Freidrich et al. 2009) assessed a total of 30 of the common aquatic photosynthesis productivity models. The model by Eppley et al (1985) is cited as providing the most elegant and straight forward approach to the estimation of algal productivity. In this

model, the estimate of primary production [g C m^{-2} d^{-1}] is simply defined as being directly proportional to the chlorophyll concentration [mg chl m^3] by an empirically determined proportionality constant as shown in Equation 3.1.

$$PP\ [g\ C\ m^{-2}\ d^{-1}] = (chl_o\ [mg\ chl\ m^{-3}])^{1/2} \qquad \text{Eq. (3.1)}$$

Eppley et al (1985) proposed this model in response to newly available satellite imagery from which chlorophyll concentrations could be inferred. A large data set collected during oceanic cruises was used to produce a plot of carbon based primary production versus chlorophyll concentration with the equation of the line of best fit defining the proportionality constant shown in Eq. 3.1. The assessment conducted by Friedrich et al (2009) used for comparison purposes an oceanic ^{14}C productivity data set (n = 1000) available as a supplement to the paper. Of the thirty or so most commonly cited productivity models assessed, the simple relationship of $(chlorophyll\_a)^{1/2}$ outperformed 19 more complicated models in terms of deviations from observed and predicted productivity. Other comparisons discussed by the authors confirmed that variations in model skill were not clearly associated with model complexity or type. Interestingly most models (including that of Eppley et al. 1985) were observed to underestimate variability in primary production; with simple models displaying significantly less bias than models resolving wavelength and depth.

A factor analysis applied to a subset of variables within the ClimPP dataset, Figure 3.4; reveals a high degree of correlation between surface chlorophyll a concentration and depth integrated primary productivity (IPP) and PAR; thus suggesting why the model simply consisting of Chlorophyll_a concentration is often the best predictor of productivity.

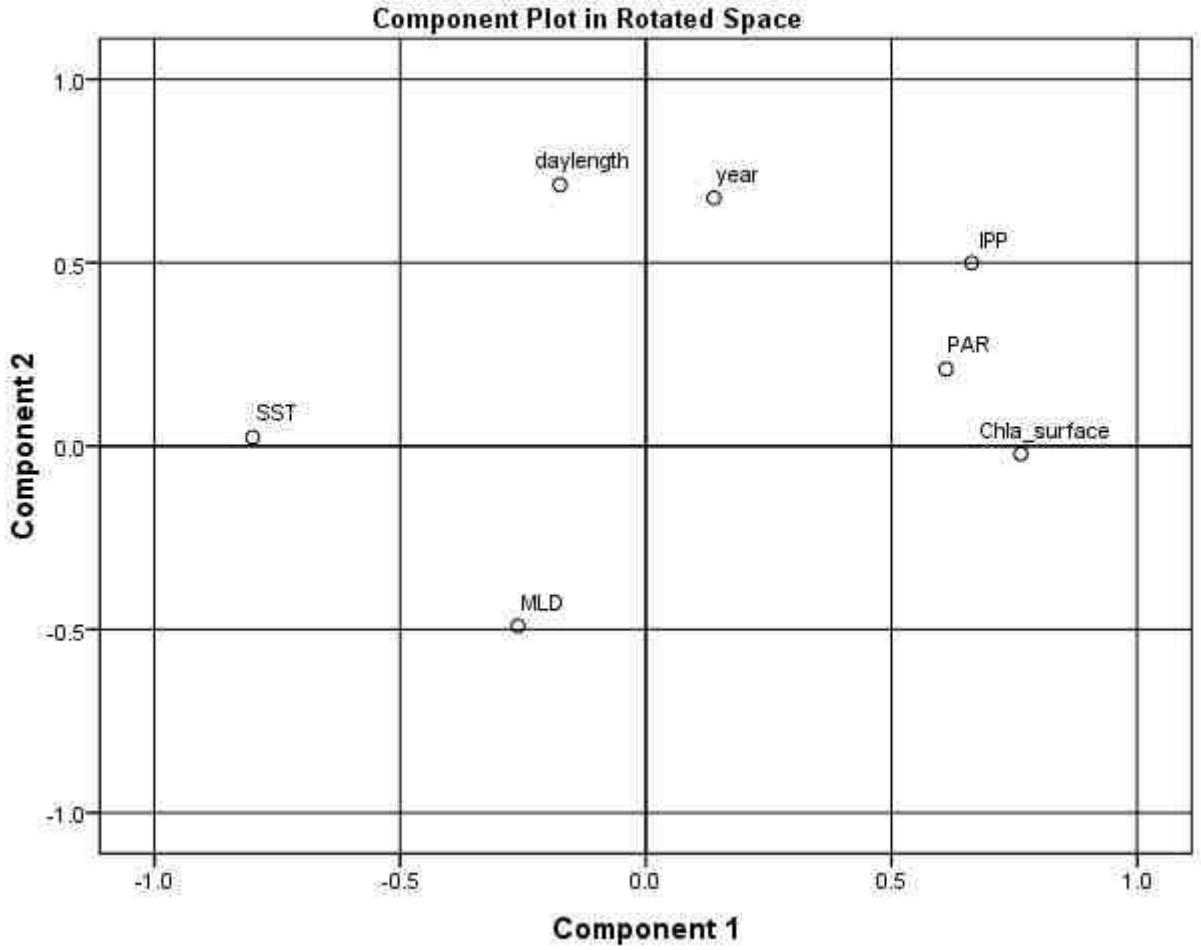

Figure 3-4 Factor Analysis of subset of the ClimPP data set, n = 941. Variables; year, day-length, MLD = mixed-layer depth for sampling location, SST = sea surface temperature, PAR = the photosynthetically active radiation, Chla_surface = surface chlorophyll_*a* concentration, IPP = depth integrated algal productivity to the 1% light level.

This observation reveals the challenges that arise when attempts are made to extrapolate from observations in controlled laboratory conditions to complex field systems. This result may also indicate why simple PI curve metrics such as the initial light limited rate of photosynthesis (alpha), or Pmax, *as normalised to algal biomass* appear to provide useful and consistent insights into photosynthesis in field (and laboratory based) systems. This observation can also be used to highlight the uncertainty inherent in field based measures of productivity and illustrates the need for comparison of productivity measures developed using other methodologies.

3.3. Conclusions and Purpose

Investigations reported in this thesis were aimed at assessing the efficacy of a novel approach for extraction of photosynthesis-irradiance parameters from in-situ online dissolved oxygen data developed during previous research (Fallowfield et al. 2001, Evans et al. 2003) and to make a contribution to an improved understanding of biological processes within waste stabilisation ponds. The in-situ PI approach developed here was considered to require testing and validation in controlled laboratory conditions against data collected using the standard PI determination method prior to use within a large and complex WSP. Results of experiments conducted toward this end were reported in Chapter 5. Field investigations were conducted by means of a series of four, purpose built, online monitoring stations installed at a large maturation waste stabilisation pond treating activated sludge (AS) effluent at Bolivar WWTP (Chapter 6). High temporal resolution online data was analysed to determine in-situ photosynthetic rates obtained to allow comparison against results of Weatherall (2001), and those obtained from a laboratory based algal bioreactor (Chapter 5) and the scientific literature (e.g. Kayombo et al. 2002, Gehring et al. 2010). This work was conducted as a part of an extensive program of research conducted over a period of more than a decade on the Bolivar WSP system in Adelaide, South Australia. Characterising both biotic (Weatherall 2001, Sweeney 2004, Yamamoto 2007, 2010, Short 2010) and non-biotic (Herdianto 2003, Sweeney 2004) variables known to influence pond ecology and effluent quality provided information to improve the scientific understanding of factors that offer promise as pond design and optimisation tools (Oswald 1995, Fallowfield et al. 1992, Mayo and Noike 1994, Sweeney et al. 2003, Shilton and Harrison 2003, Ratchford and Fallowfield 2003, Sweeney et al. 2007, Short et al. 2007, Gehring et al. 2010,

Yamamoto et al. 2010). This is the first reported assessment of photosynthetic oxygen dynamics at Bolivar WSP 1 and was understood at the time of writing to be the only study of its type reported in the WSP literature.

4. MATERIALS AND METHODS

4.1. HRAP Bioreactor

The HRAP bioreactor design was based on the general principles used in standard HRAP systems as described in Cromar (1996), Fallowfield et al. (2001) and Evans et al. (2005); with modifications detailed below. Plan and side view diagrams of the system are shown in Figure 4.1 and 4.2.

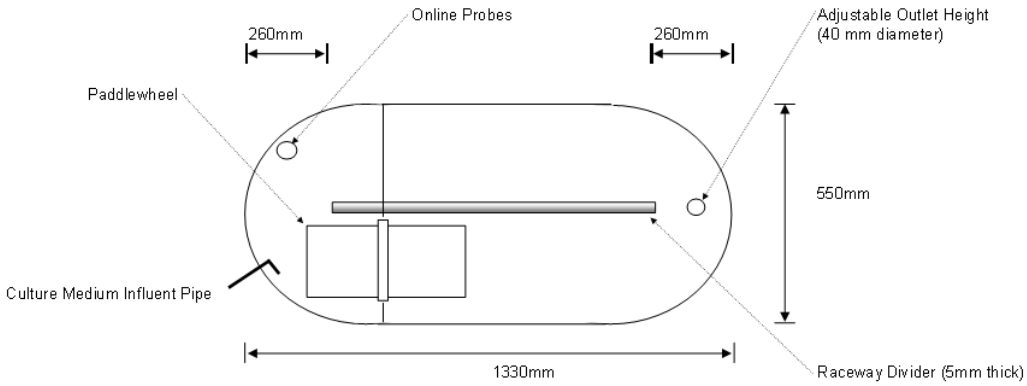

Figure 4-1 HRAP Bioreactor (Plan View).

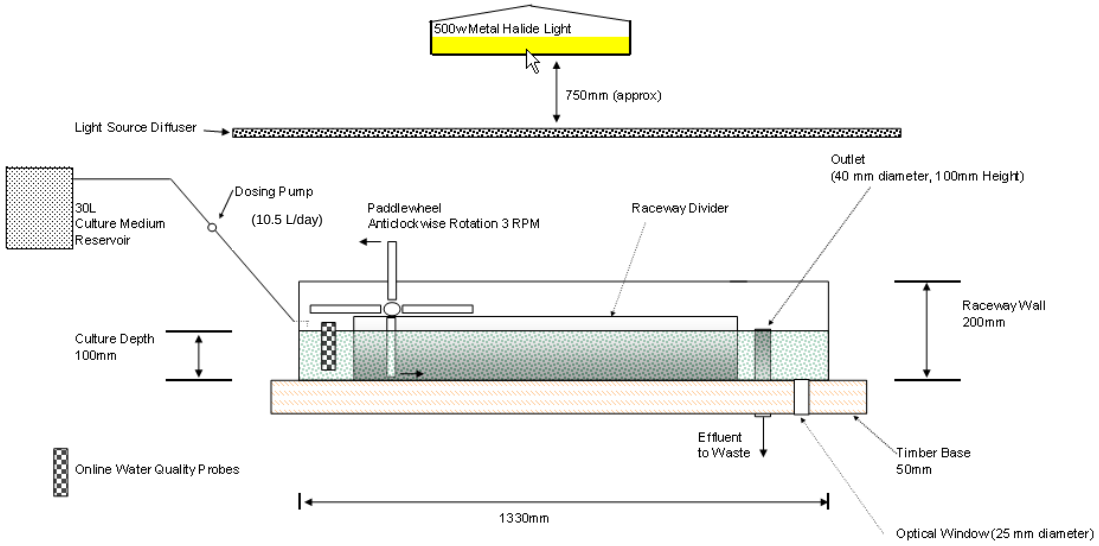

Figure 4-2 HRAP Bioreactor (Side View).

The HRAP bioreactor consisted of a semi-circular raceway constructed using standard Perspex™ of 5mm thickness and glued using the recommended Perspex™ cement. Culture depth within the system was predetermined at 100mm (nominal) by the height of the overflow outlet pipe permanently fixed into the race-way base. The culture was mixed at 3rpm (nominal) by four bladed paddlewheel constructed from acrylic plastic using a 240 volt 'variator' motor (Tubingen MP2, Serial #: 2959, variable speed) connected to a fixed reduction gearbox (SILT Type 130, 3/1 reduction). A peristaltic 'pH dosing pump' (Masterflex, Cole Parmer 7015/20), silicon hose of 18mm ID (nominal) was used to transfer growth medium from a closed (light excluded) 30L storage tank. The information shown in Table 4.1 shows physical dimensions and average operational parameters measured during the experimental trials. The HRAP was fed with modified Woods Hole medium and COD loading rate was varied using different concentrations of sodium acetate solution. A non-axenic starter culture of one species of Chlorophyceae (*Chlorella vulgaris*) was obtained (with permission) from a stock culture obtained and maintained by Dr. Michael Short. This starter culture was initially used to seed the bioreactor. A mixed algal/bacterial culture was then allowed to develop over time with minimal intervention required with the exception of filtering of algal predators (*Daphnia sp*. likely Morella. Dr. M. Short; pers. com.) on occasion by passing the culture through a 100 µm stainless steel screen. Careful cleaning of equipment used in the field (e.g. water quality probes) appeared to prevent re-infection. The bioreactor culture was monitored regularly to ensure it was free of algal predatory zooplankton.

Raceway Height (mm)	200
Raceway Length (mm)	1300
Raceway Area (m^2)	0.73
Culture Depth (mm)	100
Culture Volume (L)	67.5
Influent Addition Rate (L/day)	10.5 (± 0.3)
Retention Time (days)	6.5 (± 0.2)
Re-aeration Coefficient; Kla @ 20°C (day^{-1}) [Atmospheric diffusion from mixing]	39.8
Diffusion Rate @ 20°C (mg/L/hour) [Atmospheric diffusion from mixing]	15.1
Light Source	Metal Halide 400 W
Incident PFD (µmol/m^2/sec)	104.2 (± 2.9)
Culture Medium (0mg/m^2 SCOD)	Modified Woods-Hole Medium (Short 2010) with addition of Sodium Acetate solution.
Culture Medium (100mg/m^2 SCOD)	
Culture Medium (300mg/m^2 SCOD)	

Table 4-1 HRAP Bioreactor Specifications.

Photographs showing the system from different orientations during operation are shown in Plates 4.1 – 4.3.

Plate 4-1. HRAP Bioreactor and Optical Bench.

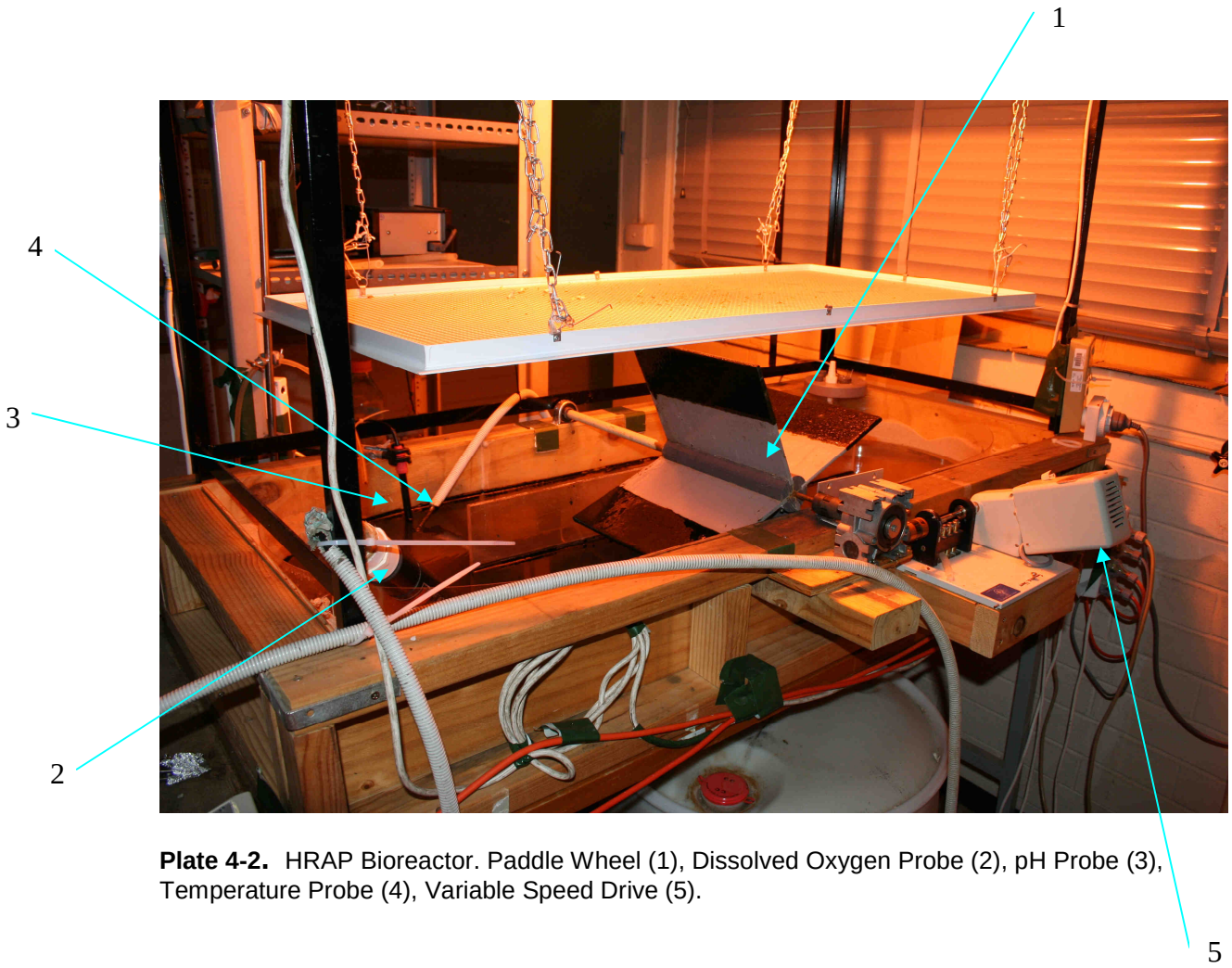

Plate 4-2. HRAP Bioreactor. Paddle Wheel (1), Dissolved Oxygen Probe (2), pH Probe (3), Temperature Probe (4), Variable Speed Drive (5).

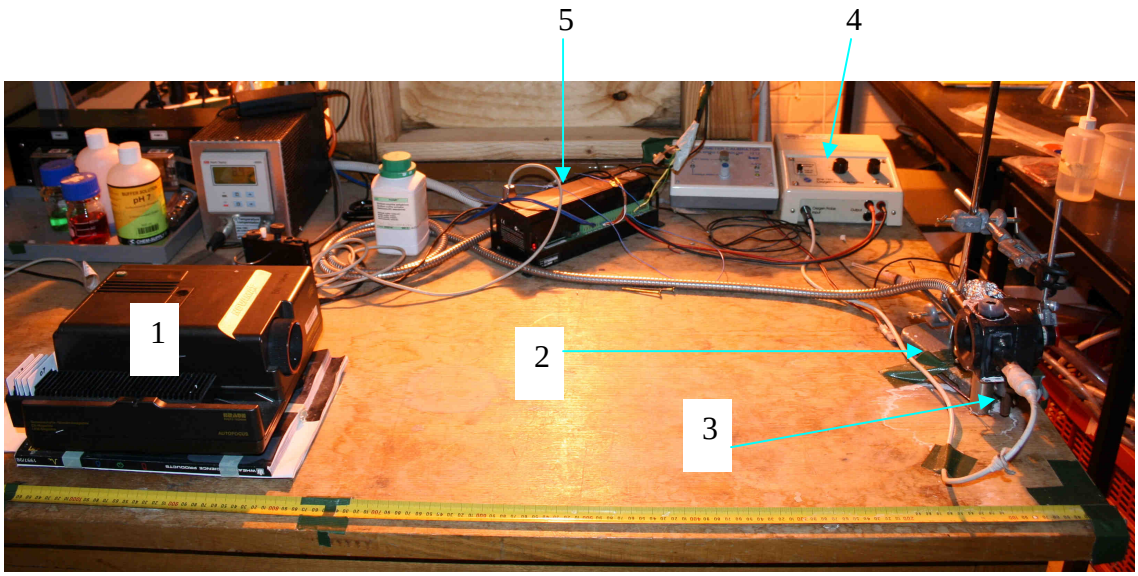

Plate 4-3. HRAP Bioreactor Optical Bench. Projector (1), Algal chamber (2), dissolved oxygen probe (3), dissolved oxygen signal amplifier (4), chamber mixing controller (5), data-logger (6).

Re-aeration

The mini-pond paddlewheel was operated at a speed of 3 rpm in order to achieve a nominal water velocity of 7 cm/s mid-stream (measured using neutral buoyancy float and stop watch). The re-aeration from atmosphere afforded by the paddlewheel mixing was determined in accordance with the methodology described in Fallowfield et al. (2001). This consisted of dissolving a mass of sodium sulphite in fresh mini-pond medium (containing no algae or bacteria) to initially de-oxygenate the media in the HRAP and the logging the increase in dissolved oxygen as a function of time. Estimated re-aeration coefficient and diffusion rate are shown in Table 4.1.

Lighting

A metal halide lamp (Osram HQI 400W/D) with an opaque acrylic filter between the bulb and the surface of the HRAP was powered with a 'HPS400 Agrolamp 420w 240v 2.1A Ballast'. Globes were changed between treatment rounds as a spectroradiometer was not available to check spectral characteristics of used globes. A published emission spectra of the above globe (with a clear acrylic filter) is provided as reference.

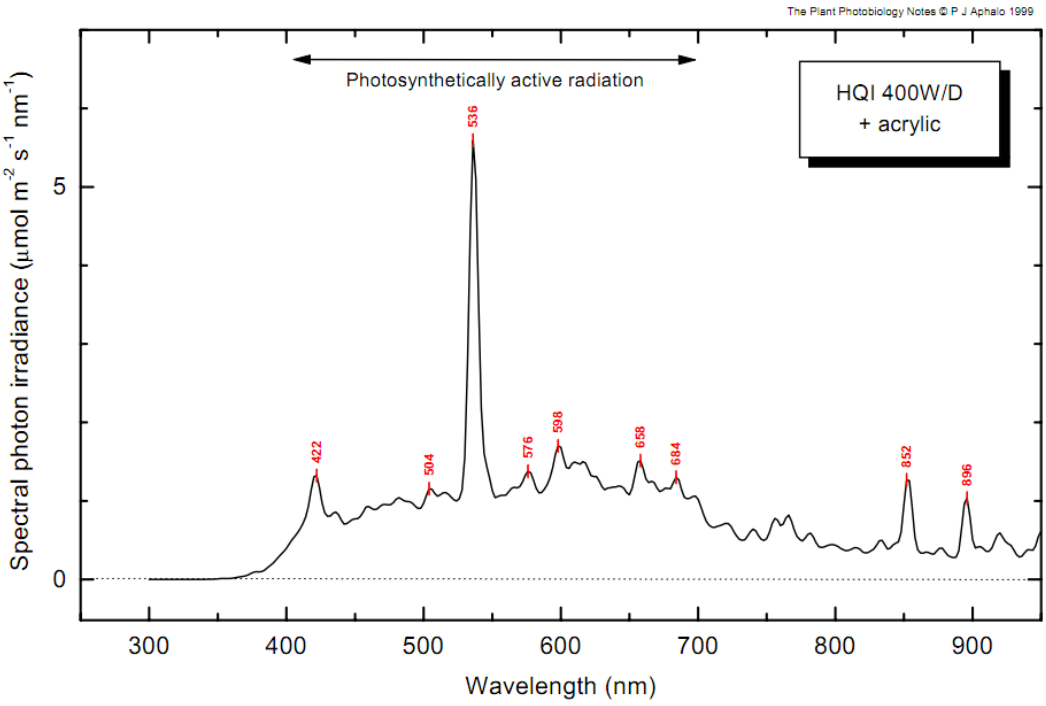

Figure 4-3. Emission spectra of Osram HQI 400W/D metal halide lamp (Aphallo 2011: University of Helsiki; Ecophysiology Group: http://www.mv.helsinki.fi/aphalo/photobio/lamps.html).

Photon Flux Density (PFD; µmol/m^2/sec) incident on the surface and at the specified depths and passing through the culture was measured daily (or as possible) using a Skye™ quantum sensor (SKE-510 400-700nm PAR), attached to a retort stand and lowered through the culture at 5-10mm depth increments. Transmitted light was determined by placing the quantum sensor immediately beneath the bioreactor optical window.

All measurements were taken at the same spatial location adjacent the effluent outlet in the pond for convenience and comparability.

Light attenuation

Light attenuation based on measurements of transmitted light (PAR) was conducted using the methodology detailed in Fallowfield et al. (2001); by use of a portable PAR sensor with repeated measurements taken at a series of depths.

Wet Chemistry

The following analyses were conducted on samples collected from both the Bolivar WSP and the lab based HRAP bioreactor.

Chlorophyll *a* concentration was determined following filtration of a known volume of culture through GF/C (1.2µm nominal pore size) filters. The volume filtered was determined by the nature of the culture, dispersed or floccular material; 100 ml generally provided a sufficient signal to noise ratio. The filters were extracted into acetone (in the dark, 4°C over 24h). The chlorophyll a concentration was calculated using the tri-chromatic equation method described in APHA (1992); 10200H.

Suspended and Volatile Suspended Solids concentration was determined using the methods described in Sections 2540D and 2450E respectively of APHA (1992); a 100ml aliquot was determined by experience to provide a sufficient signal to noise ratio without disrupting culture retention time excessively. Where appropriate the filtrate obtained from these assays was used for determining 'soluble' components of the following chemical parameters.

Carbon (Total/Organic/Inorganic) concentration was determined using a Shimadzu TOC-5000A carbon analyser in accordance with the procedure outlined in the user's manual and in section 5310A of APHA (1992).

Chemical Oxygen Demand (Total/Soluble) concentration was determined in accordance with the closed reflux, colorimetric method outlined in section 5220D of APHA (1992).

Biochemical Oxygen Demand (soluble) concentration was determined using the 5-day BOD test as outlined in section 5210B of APHA (1992) and as described in the WTW OxiTop® system manual without using allylthiourea as a nitrification inhibitor.

Bacterial Protein concentration was determined using the Bradford Protein Assay (Bradford 1977, Zor and Sellinger 1996) using Bovine Serum Albumin (BSA) as a standard. All samples were processed in triplicate as follows. A 9 ml volume of filtered sample (GF/C) was centrifuged at 2500g for 20 mins at 4°C to pelletise the algal portion of the planktonic non-floccular biomass; the supernatant was then centrifuged at a minimum of 5400g for a nominal period of 20 minutes at 4°C to pelletise the planktonic bacterial biomass. After removal of the supernatant the pellet was resuspended in 1 ml of supernatant. The remaining supernatant was used to prepare standards to avoid the impact of dissolved organic compounds on sample transparency. To a 1.5 ml eppendorf™ tube the following was added; 700 µl supernatant, 100 µl of standard or sample and 200 µl of 0.2 M NaOH to lyse the cells. A digestion period of 45 minutes was then followed by dilution of the sample by the additional of distilled water to a final volume of 10 ml. A 5 ml aliquot of Bradford reagent was then added followed by a 20 minutes reaction time to ensure for full colour development. The absorbance of the sample or standard was then measured 595 nm using a Sigma™ 6K15 spectrophotometer.

Online Data

*Dissolved Oxyg*en concentration was determined at a nominal frequency of 5 minutes by online measurement using a Danfoss™ Evita® Oxygen Probe. Probe depth was nominally at 75% culture depth (75 mm from water surface). A

Temperature Technology™ T-TEC Temper 6-3A (4-20mA) data logger was used in conjunction with a Datataker™ DT100 datalogger. Online DO determinations were supplemented and checked using a WTW™ Oxi 330 Nova Analytics Pty Ltd portable field system.

pH was determined using a glass electrode, reference electrode with automatic temperature compensation system (BME 13535 pH controller; ABB Kent Taylor). Stability of the pH calibration was an issue identified at an early stage in the bioreactor operation. Due to resource limitation online pH determination was replaced by daily (nominal) 'grab sample' determinations using a hand held WTW™ pH-320, Nova Analytics Pty Ltd portable field system.

Temperature of the culture was determined using a (TTEC PT100) PT100 temperature probe with 4m cable. Data was logged in parallel with dissolved oxygen using a separate channel on the Datataker™ DT100 datalogger, and was supplemented and checked using the temperature channel from a WTW™ Oxi 330 Nova Analytics Pty Ltd portable field system.

Standard Photosynthesis-Irradiance Determinations

Photosynthesis – Irradiance (PI) measurements were made using the standard PI apparatus and methodology as described in Hobson and Fallowfield (2001) with the exception that oxygen concentration and transmitted light intensity were logged concurrently at a frequency of 2 seconds.

Experimental and Operational Conditions

Each mini-pond experiment was configured in an identical fashion with the exception of areal soluble COD (SCOD) loading per day. A freshly made volume of approximately 40L of the Modified Woods Hole Medium in a cleaned (70% ethanol

rinsed three or more times) reservoir was provided every 4 days operation (or as required to keep the unit operational over the weekend). The medium reservoir was covered with foil to exclude light. Variables that could be directly controlled; retention time, light intensity at mini-pond surface and composition of nutrient medium, with the exception of SCOD (organic carbon), remained unchanged. The mini-pond was not subject to temperature control; the contained culture was subject to diurnal and longer term climatic temperature variations during and between each experimental treatment. Online temperature and dissolved oxygen data were collected throughout each experiment at a schedule of 5 minutes. Photosynthesis irradiance measurements using the standard PI apparatus were undertaken on culture collected at 'dawn' at a frequency of 2 days for the duration of each experimental treatment.

4.2. Murray Bridge HRAP

The Murray Bridge HRAP system is described in detail in Fallowfield et al. 2001. Wet chemistry and online data collection methods detailed in the above reference are also used in this study without modification (unless noted).

4.3. Bolivar WSP

System Characterisation

A description of the Bolivar wastewater treatment plant is provided in Chapter 3 and in detail in the works of Sweeney (2004), Herdianto (2003), Yamamoto (2007) and Short (2010) .

Sampling and Experimental Design

All experiments were conducted in Pond 1 of the Bolivar Wastewater Treatment Plant (WWTP) at locations shown in Figure 4.4. Each location was selected on the

basis of work by Sweeney (2002) to provide locations within the pond that differed in terms of stratification frequency and duration (Chapter 6).

Online Monitoring Stations

Four in total were constructed using materials, tools and advice kindly supplied by the Flinders Medical Centre Biomedical Engineering Section (Plate 4.4). Each station frame was of welded steel construction using 25mm 'angle iron'; each frame was 'hot galv dipped' after removal by brushing and chipping of welding slag for corrosion resistance. A steel powder coated instrument box was then affixed using stainless steel machine screws and washers. Each station was powered by a 12 volt heavy duty fully sealed lead/acid battery clamped into the base of each box and trickle charged during daylight hours by a single attached 75W solar panel with hand crafted bird deterrent. Each station was furnished with Danfoss™ online dissolved oxygen monitoring units and temperature probes kindly provided by Trevor Johns of United Water; each was as described in Section 4.1. The dissolved oxygen probe at each of the four sampling sites site was placed at a depth of 25 cm below water level.

Weather Station

Meteorological data was collected adjacent to Bolivar WSP at a height approximately 3 meters above water level using an Envirodata WM2000 weather station with an auxiliary photosynthetically active radiation (PAR) sensor. The following parameters were measured and recorded automatically at 10 minute intervals;

PAR (mean);

Solar Radiation (mean);

Wind Direction (mean and instantaneous);

Wind Speed (mean and instantaneous)

Thermistor network

The thermistor network developed and deployed by Sweeney (2004) was refurbished and redeployed during the 2003 calendar year. Failed temperature probes were replaced and rusting fixings de-rusted and painted with 'cold-galv' sacrificial coating prior to re-deployment.

Sampling and Downloading Schedule

All online monitoring equipment was set to record data synchronously. Each data-logger was programmed to record data at intervals of 5, 10 or 15 minutes, dependant on the time estimated before exceeding capacity of the memory. All loggers were programmed to cease logging once memory capacity was reached.

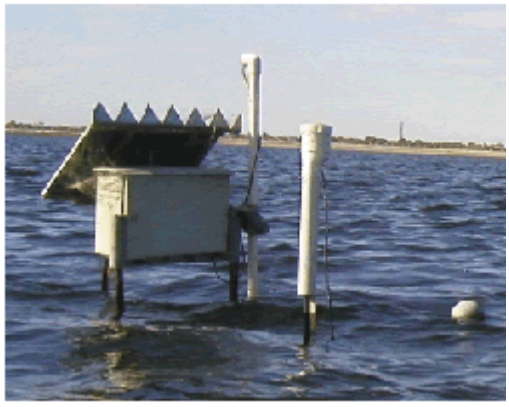

Plate 4.4. Installed handmade online monitoring station showing solar panel and bird deterrent on upper edge. A temperature probe station is located in the foreground. The buoy to the lower right of the image supports the temperature thermistor chain at this location (Location I).

Wet Chemistry

Standard water quality parameters, as listed in Section 4.1 were measured for each sample taken from each of the four locations.

Incident and Transmitted Light

Photon Flux Density (µmol/m^2/sec) incident on the surface and specified depth passing through the 'culture' was measured daily (or as possible) using a Skye™ quantum sensor (SKE-510 400-700nm PAR), attached to clear acrylic tube (25mm diameter) and lowered through the culture at 50 to 250 mm depth increments.

Data Collation and Analysis

Field notes and observations were recorded in dated log books. Data which was manually recorded was transcribed into an electronic format. Online data was downloaded and stored as electronic files (*.txt, *.csv) on a laptop computer. The electronic data files were imported into Microsoft™ Excel® spreadsheet program for analysis. Wet chemistry data was recorded into dated log book and was then transcribed into electronic form using Excel®. Statistical analysis was performed using Microsoft™ Excel®, SPSS™ version 10-17 and Matlab™ versions 2003-2010. Graphical information either in the form of Tables or Figures was compiled using each of the data handling computer programs listed above. All statistical tests of significance were performed at the 5% ($P(\alpha) \leq 0.05$) level.

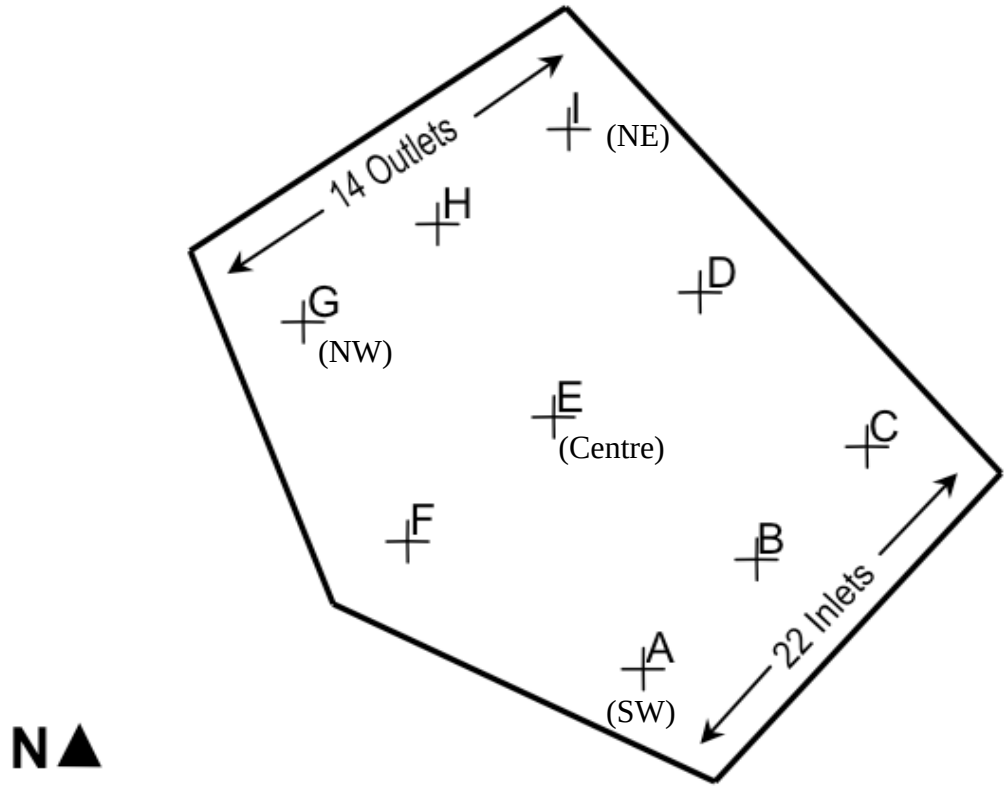

Figure 4.4. Plan diagrammatic view of Bolivar WSP 1. Online monitoring stations were installed at locations G (North-west), I (North-east) E (Centre) and A (South-west. As per Sweeney (2004).

5. HRAP BIOREACTOR

Purpose

A HRAP bioreactor was designed, built and operated in controlled laboratory conditions with aim of allowing comparison of photosynthesis/irradiance curves obtained using a standard laboratory PI apparatus with those calculated from in-pond dissolved oxygen time-series using a modified version of the proposed method of Fallowfield et al. 2001, Evans et al. 2003.

5.1. Introduction

The mass of oxygen produced per unit time from algal photosynthesis is a key parameter used for determining the 'capacity' of an algal-based wastewater treatment process (Chapter 3), i.e. sufficient oxygen must be produced by phytoplankton to meet respiratory requirements of aerobic heterotrophic biomass to stabilise the nutrient load applied to the pond via the addition of wastewater (Oswald 2003, Davies-Colley et al. 2005).

Measurements of oxygen evolution per unit algal biomass conducted at a series of light intensities and corrected for oxygen loss due to algal respiration can provide a precise measure of the relationship between the rate of photosynthesis and light intensity. In actuality, this is the logic underpinning photosynthesis–irradiance determinations (Harris 1984, Reynolds 2006, Falkowski and Raven 2007).

It is, however, important to note that in all but pure (axenic) algal cultures, measurements of respiration rates inferred from measurements of oxygen utilisation rate (OUR) or community respiration rate (CRR) will include respiratory oxygen losses from other micro-organisms (Harris 1984, Kirk 1994). The contribution of other (non-algal) micro-organisms to OUR may, particularly in wastewater environments, be substantial and can be very difficult to accurately and precisely

quantify (Li and Maestrini (1993); see Cromar (1996). As a consequence it is more appropriate to use terms such as OUR or CRR rather than algal respiration unless the potentially large non-photosynthetic bacterial contribution to pond biomass has been characterised (Harris 1984, Kirk 1994, Falkowski and Raven 2007, Sherr and Sherr 2003).

In order to reduce errors in estimates of algal productivity as inferred by measurements of photosynthetic activity, it is desirable to establish the contribution of physical mediators of oxygen flux in the system of interest; i.e. to identify physical sources and sinks of dissolved oxygen and to establish their relative contributions over time. Within the indoor laboratory based HRAP bioreactor the atmosphere provided a source of oxygen via re-aeration, as it does in all HRAP systems in a measurable way, i.e. circulation of culture medium by the paddlewheel disturbed the air–water interface and permitted effective flux (diffusion) of oxygen (and other gasses) to (and from) solution (Chapter 4). This source of DO varies largely as a function of water velocity, pond depth, DO saturation and temperature; and was accounted for by application of the equations presented in Metcalf and Eddy (2004) and as described in Evans et al. 2003. The DO sink provided by diffusion from the liquid phase to the atmosphere upon super-saturation of the culture medium during the photoperiod is poorly documented in the literature at present and is therefore routinely ignored as a sink in models of pond photosynthetic activity. A review of the literature failed to identify publications that explicitly considered this source of error in papers describing pond oxygen budgets. Super-saturation is common in HRAP and WSP systems; in-fact it is more commonly observed than not on cloud free days. One consequence of not incorporating out-gassing of oxygen in estimates of productivity based on PI measurements will be to underestimate, by some proportion, the photosynthetic activity of the algal biomass and therefore

carbon productivity by a proportional amount; a search of the literature revealed no published attempts to incorporate out-gassing due to supersaturation. Quantification of this potential confounder was beyond the scope of this thesis and is considered a worthy topic of future research.

To re-iterate; the purpose of PI measurements is to determine response of algal photosynthesis to changes in light intensity or other variables such as nutrient status, temperature etc. In the field such changes may be manifest on timescales that range from seconds to years; e.g. weather events, the diurnal cycle, the seasonal cycle, climatic variation or changes in wastewater characteristics. It is therefore of interest to understand how PI changes occur in these systems in response to environmental variation as well as factors such as influent concentration; this basic ecological information is likely to be useful for addressing utilitarian questions of pond operation such as determining tolerable loading rates for treatment purposes, or perhaps for more fundamental biological questions relating to the study of algal activity in ecosystems. The measurement of PI using the standard PI apparatus in the field is however often impractical due to the requirement for onsite laboratory facilities; in addition, samples processed in the laboratory may be subject to changes in physiological status due to storage and transport (Harris 1984, Kirk 1994). If samples are grown in the laboratory obvious challenges arise when attempting to translate results of laboratory phyto-physiological investigations to those measured in the field (Harris 1984, Kirk 1994, Short 2010).

Various strategies have been devised to reduce the effects of storage on samples, for example oceanic or large water body PI measurements are frequently conducted in ship board laboratories (Kirk 1994). The use of the ‘light and dark bottle’ in-situ incubation procedure to determine photosynthesis irradiance relationships has been

in use in the field since at least the early 20th Century (Chapter 3). Weatherall (2001) found this method problematic in WSPs as a result of unpredictable variations in incident light intensity and temperature in the field under all but ideal conditions. As a consequence Weatherall (2001) collected samples from the field and assessed them in the laboratory using the standard PI apparatus. A comparison of PI measurements made by Weatherall (2001) on a WSP pond sample using a light and dark bottle experiment and standard PI determination showed that the two methods could produce comparable results. However the standard PI measurement was made on the same sample very soon after collection at a pond-side transportable laboratory thus negating the confounding effects of storage and to some degree transport.

In addition to these difficulties, PI determinations conducted using either method are extremely labor intensive and technically difficult to successfully perform and ideally should be conducted in replicate to provide more reliable results (Hobson and Fallowfield 2003). Alternatives approaches that use more straightforward approaches are therefore considered highly desirable (Kirk 1994).

The HRAP lab-based bioreactor described in this chapter was designed to provide a lab scale, algal based wastewater treatment system, with good control of parameters such as light intensity and temperature; and allow comparisons of PI curves measured using the standard apparatus of Hobson and Fallowfield (2003) with online PI measurements data according to Evans et al (2003).

The HRAP bioreactor was operated with continuous addition of a synthetic sewage medium using sodium acetate as an organic carbon source at a series of three loading rates (Chapter 4). Operation started in photoautotrophic mode with no addition of organic (acetate) carbon substrate to the culture medium; two additional trials followed in series; increasing the organic carbon loading after the completion of each trial. This strategy was adopted to provide a range of typical loadings for a

facultative WSP treating domestic sewage. The series of experiments were designed to allow assessment of oxygen dynamics within the system, and not specifically to address the impact of carbon (as acetate). Synthetic sewage was used as medium as it did not contain pathogenic organisms that would pose OH&S risks to laboratory users (Cromar 1996).

The response of the system was monitored by measurement of standard water chemistry parameters for comparison against larger pilot and full-scale algal based systems. As biological systems are difficult to 'scale down' these water quality treatment parameters were considered useful as 'indicators' of bioreactor operation to try and ensure that unique and general properties of the lab based system responses were identifiable.

Upon achieving a 'steady state' (3 hydraulic retention times) an intensive series of PI measurements were undertaken using the standard PI apparatus. Contemporaneous online data were used to calculate online PI values and used to test the hypothesis that such data could be used in field based PI measurements. The time-series pattern of dissolved oxygen concentration versus time was also qualitatively assessed for each treatment against the pattern observed in the Murray Bridge HRAP system (Fallowfield et al. 2001), again to try and ensure that unique and general properties of the lab-based system responses were identifiable.

5.2. Materials and Methods

More detailed descriptions of the mini-pond construction, operating conditions, monitoring protocols and analysis are provided in Chapter 4.

5.2.1. Experimental Design

A series of three experimental treatments were originally devised with the intention of operating the laboratory based HRAP bioreactor system at COD areal loadings

consistent with Cromar (1996) i.e. nominally 100, 350 and 600 kgCOD/ha/day (acetate as organic carbon source in a synthetic sewage medium). The application of such loading rates, holding other variables constant, would have provided data for direct comparison against the findings of Cromar (1996). These COD loadings were chosen since they are within the normal loading range for a facultative WSP. Upon operation of the HRAP bioreactor it was found that carbon loading in this range (and thus oxygen demand) was too high for the culture to remain aerobic in the HRAP bioreactor; in part due to the high light attenuation afforded by dispersed bacterial biomass that proliferated and the low light intensity achievable at the culture surface. An alternative series of loading rates experiments were therefore devised with reference to an important change in the operational loading of Bolivar WSP that occurred following the installation of the activated sludge (AS) tertiary treatment system in 2000, as reported in Sweeney et al. (2005b). The Bolivar WSP was, following this change, subject to loading of secondary activated sludge effluent, effectively acting as tertiary 'maturation pond' in a WSP series (Sweeney et al. 2005b, Short 2010).

On this basis, nominal areal loading rates falling within the soluble BOD and SCOD areal loading ranges for Bolivar during the period of 2001–2004 were selected in order to provide data comparable with contemporary operation at the plant. This provided benefits in two senses; firstly aerobic conditions were maintained as would be necessary for the proliferation of aerobic heterotrophic bacteria and secondly, online monitoring of dissolved oxygen could occur; allowing oxygen dynamics to be analysed.

Experimental treatment nominal carbon loadings were as follows

Inorganic carbon from atmospheric diffusion (photoautotrophic):

- Treatment 1: 0 mg soluble COD/m^2/day.

Organic carbon source (Synthetic sewage medium containing sodium acetate) at two areal loading rates:

- Treatment 2: 100 mg SCOD/m2/day (1 kg soluble BOD/ha/day[1])
- Treatment 3: 300 mg SCOD/m2/day (3 kg soluble BOD/ha/day[2])

Parameters measured are provided in detail in Chapter 4 but are summarised below for convenience and included;

Chlorophyll *a*: a standard proxy measure of algal biomass.

Dissolved Oxygen: online measurements conducted at a nominal schedule of 5 minutes for production of time series oxygen data and calculation of online PI parameters.

Light Attenuation: measured 3 – 4 times weekly in order to provide data for comparison of changes in light penetration between experimental treatments.

pH: online measurement conducted at a nominal schedule of 5 minutes.

Temperature: online measurements conducted at a nominal schedule of 5 minutes for comparison between treatments and determination of oxygen saturation level and therefore re-aeration due to active mixing by paddlewheel.

[1]

[2] Sodium acetate provided a carbon source for bioreactor without a recalcitrant component, thus the assumption of equivalence (in principle) in terms of loading rates of SCOD and BOD.

Carbon: Inorganic carbon data was collected to identify changes in carbon substrate concentration when comparing photoautotrophic mode and carbon loaded mode of operation.

Bacterial Protein: to identify changes in biomass composition when comparing photoautotrophic mode and carbon loaded mode of operation.

Steady State Conditions: a period of three retention times with nominal equipment status was used as the criterion for definition of steady state (stable) conditions (Metcalf and Eddy 2003).

Photoperiod: 18 hours illumination followed by 6 hours dark period. At the low luminance incident on the bioreactor this light/dark ratio permitted maintanence of aerobic conditions at the highest loading rates, whilst allowing sufficient time for dissolved oxygen concentrations to decline after 'sunset' each day.

5.3. Results and Discussion

5.3.1. Measures of Pond Performance

Summary data showing mean and standard deviation of SCOD and soluble total organic carbon (STOC) areal loading rate, hydraulic retention time, photon flux density (PFD) light intensity at HRAP surface and culture temperature for each experimental treatment are provided in Table 5.1. Pond retention time was calculated based on measurements of mini-pond effluent volume averaged over the time course of each experimental treatment.

Areal loading rates for each treatment were derived from measurements of influent SCOD and STOC concentration and were a function of retention time. The measured Org-C areal loadings (Table 5.1) were close to the ratio expected based on a theoretical value of 48 mg C per 100mg COD for sodium acetate (Standard Methods

1992). Consequently the deviations of measured loading rates from nominal (intended) were considered to be largely the result of errors in measurement of effluent volume. A summary of wastewater quality and biomass parameters assayed during the 'steady state' period for each of the experimental treatments are shown in Table 5.2.

For ease of interpretation summary data showing 'box and whisker plots' (box-plots) of parameters measured during the 'steady state' portion of each trial are provided in Figures 5.1 – 5.5. In each case the horizontal bar represents the median value, the shaded area 'box' shows the inter-quartile range, whilst the 'whiskers' show the absolute range for each data set. Each parameter is displayed separately allowing for comparisons across the three experimental treatments.

Dissolved Oxygen

A significant difference (Table 5.2) in median oxygen concentration was observed between treatments (Figure 5.1). This pattern was in agreement with typical observations of outdoor and pilot scale pond systems that display decreased DO tension in response to increased loading of organic carbon. Such loading provides conditions more suitable for the vigorous growth of aerobic heterotrophic bacteria, and at a given algal productivity, results in decreased DO tension due to increased unit volume respiration (Fallowfield et al. 2001).

Further discussion regarding dissolved oxygen is provided in Section 5.3.2.

Experimental Treatment	Acetate Loading (mgSCOD/m^2/day)	Acetate Loading (mgSTOC/m^2/day)	Rt (days)	PFD (µmol/m^2/sec)	Vertical Attenuation Coefficient (Kd (PAR) m^{-1}	Tc (°C)
0 (Treatment 1) (mgSCOD/m^2/day)	0	0	6.6 (0.36) n = 4	103.2 (2.35) n = 4	21 (n = 4)	18.6 (0.558) N = 10 days
100 (Treatment 2) (mgSCOD/m^2/day)	89 (8.21) n = 4	51.7 (2.42) n = 5	6.3 (0.47) n = 4	106.1 (3.70) n = 5	3.7 (n = 4)	19.7 (0.873) N = 12 days
300 (Treatment 3) (mgSCOD/m^2/day)	324 (20.83) n = 6	189 (10.33) n = 7	6.1 (0.35) n = 6	104.4 (1.54) n = 8	5.6 (n = 6)	20.1 (0.654) N = 23 days

Table 5-1 Arithmetic mean (standard deviation) and sample size, n, for pond SCOD and soluble total organic carbon (STOC) loading and physical parameters. T_c; culture temperature collected over time period specified at 5-minute intervals. Rt = volumetric retention time, PFD = photon flux density.

	DO (mg/L)	T (°C)	pH	SS (mg/L)	VSS (mg/L)	Chl_*a* (mg/L)	Protein (mg/L)	STC (mg/L)	IC (mg/L)	STOC (mg/L)	COD (mg/L)	SCOD (mg/L)
Treatment 1 0 mgSCOD/m^2/day (0 mg SCOD/L/day)	13.5* (2.31) [287]	18.6* (0.55) [287]	10.20* (0.32) [287]	286 (113) [15]	256 (97) [14]	1.36 (0.720) [15]	108* (160) [4]	28* (6) [10]	4.9* (2.2) [10]	23 (5) [10]	379 (105.6) [5]	131 (15.1) [4}
Treatment 2 100 mgSCOD/m^2/day (1.3 mg SCOD/L/day)	10.11* (0.87) [287]	19.7* (0.87) [287]	9.41* (0.13) [287]	198** (50) [11]	189 (66) [8]	0.37** (0.07) [6]	590* (260) [4]	46* (6) [7]	23.4* (3.3) [7]	22 (6) [7]	503 (106) [4]	155 (13.1) [4]
Treatment 3 300 mgSCOD/m^2/day (3.7 mg SCOD/L/day)	8.33* (0.66) [287]	20.1* (0.65) [287]	8.43* (0.30) [287]	304 (82) [7]	220 (52) [7]	1.11 (0.157) [6]	3218* (739) [4]	152* (33) [5]	63.7* (5.8) [5]	89** (37) [5]	1169 (-) [2]	215** (-)^ [2]
P value (5% significance level)	< 0.0001	< 0.0001	< 0.0001	= 0.0003	= 0.057	= 0.0032	= 0.0073	= 0.0001	< 0.0001	= 0.0036	= 0.0387	= 0.0415

Table 5-2 Summary of wastewater quality and biomass parameters collected during the 'steady state' period of each experimental treatment in the final effluent: Arithmetic mean, (standard deviation), [sample size]. *All treatments significantly different with respect to the median of specified parameter (5% significance level, Kruskal-Wallis nonparametric one-way analysis of variance). DO = dissolved oxygen concentration; T = culture medium temperature; SS = suspended solids; VSS = volatile suspended solids; Chl_*a* = chlorophyll_*a* concentration; STC = soluble total carbon (GF/C filtrate); IC = inorganic carbon concentration; STOC = soluble total organic carbon; COD = chemical oxygen demand; SCOD = soluble chemical oxygen demand. Online parameters were derived by averaging across all days of a treatment to produce an 'average day', thus each treatment has a total of 287 data points, each of five minutes duration; the data shown is the average of this data.

**Single treatment significantly different with respect to the median of the specified parameter (5% significance level,) ^Data lost due to analysis equipment failure. Note that arithmetic mean and standard deviation are shown as measures of central tendency and dispersion in order to provide more familiar statistics for the reader. P values are based on comparison of median.

Algal Biomass

Variations in chlorophyll_*a* concentrations between treatments are shown in Figure 5.2. A significant difference (Table 5.2) in median chlorophyll_*a* concentration was observed between treatment 2 and treatments 1 and 3. Visual inspection of Figure 5.2 suggested that this resulted from the relatively low chlorophyll_*a* concentration observed in Treatment 2; supported by statistical comparison of Treatment 1 and 3 chlorophyll_*a* concentrations, which were shown not to be significantly different ($p = 0.5031$, 5% significance level, $n = 15, 11$, Wilcoxon Rank Sum Test). Both of the carbon loaded treatments (Treatments 2 and 3) displayed reduced variation around the median chlorophyll_*a* concentration compared to the photoautotrophic system (Treatment 1). By implication the algal population density was substantially more stable in the non-photoautotrophic, acetate loaded configurations. It was considered likely that reduced light attenuation (Table 5.1.) in the carbon loaded treatments was afforded by the presence of ALBAZOD (Soeder 1984, Chapter 7); i.e. suspended flocculent algal and bacterial biomass. As self shading of the carbon loaded cultures appeared to be reduced in comparison to the photoautotrophic treatment this may have allowed a more stable light climate and therefore less variable algal density to persist. Chlorophyll_*a* concentrations in all treatments were noted to be within the range of data obtained from the Murray Bridge HRAP trials (Fallowfield et al. 2001).

Suspended and Volatile Suspended Solids

The suspended and volatile suspended solids assay (SS and VSS respectively) provides data routinely used in wastewater treatment process assessments. SS results for the three treatments are shown in Figure 5.3. A very similar pattern of variation to that observed for median chlorophyll_*a* was apparent between treatments with respect to median VSS (Table 5.2) and SS (Figure 5.3).

In algal based systems the biomass captured by filtration through 1.2 μm pore size GF/C filter consists of both algal and bacterial components; however previous work by Evans et al. (2005) showed that reaction rates calculated using VSS as a proxy for biomass for high rate algal ponds may be reasonable provided that account was made for the algal component of the biomass. A common empirical process parameter used to characterize AS wastewater treatment process designs and operating conditions is the 'food-to-microorganism (biomass) ratio' (F/M) and is reported in the literature as being in the order of 0.04g substrate per gVSS/day (Metcalf and Eddy 2003) for extended mechanical aeration. This equates to 40mg of substrate loaded per 1000 mg of VSS, or expressed as an F/M ratio of 0.04.

Based on VSS levels observed in the bioreactor, the calculated F/M ratio for Treatment 3 was 0.017. This calculation assumed that the bulk of the bacterial biomass was captured by the VSS assay, and an algal biomass concentration of 100mg/L, based on Chl_a representing 1–2% algal biomass dry weight for green algal species common to WSPs (Reynolds 2006). It follows that a VSS for bacterial heterotrophs in the HRAP bioreactor of approximately half of this value (50mg/L) would result in a F/M of the same order as a standard AS system for Treatment 3. It is the case, however, that AS systems operate at very short retention times, high suspended solids and with no requirement for light penetration they can be very deep as a result AS systems are very much more compact but highly energy intensive due to the requirement for mechanical aeration; than algal based systems.

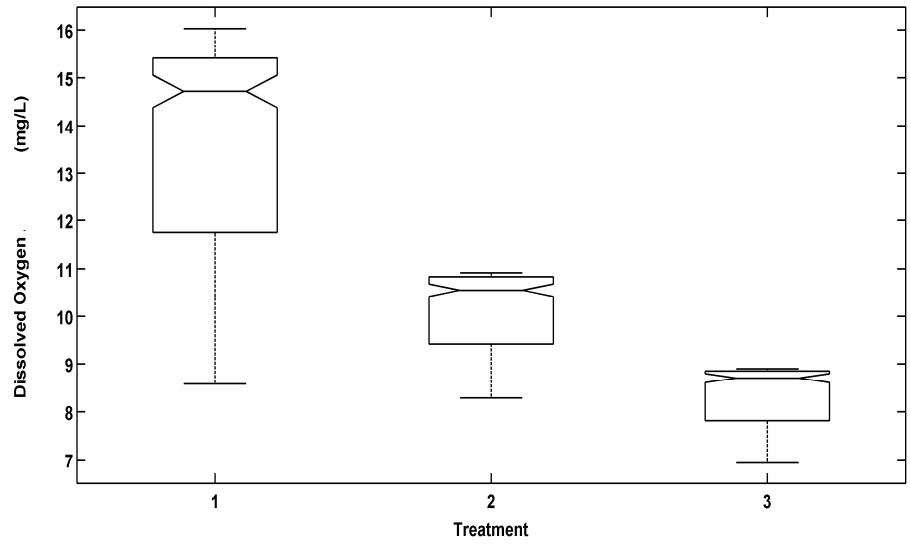

Figure 5-1 Box and Whisker plots of dissolved oxygen for each experimental treatment. n = 287 dissolved oxygen measurements, i.e. across all days of each trial for each 5 minutes period of 24 hours. Treatment 1 = 0mg SCOD/m^2/day Treatment 2 = 100mg SCOD/m^2/day Treatment 3 = 300mg SCOD/m^2/day

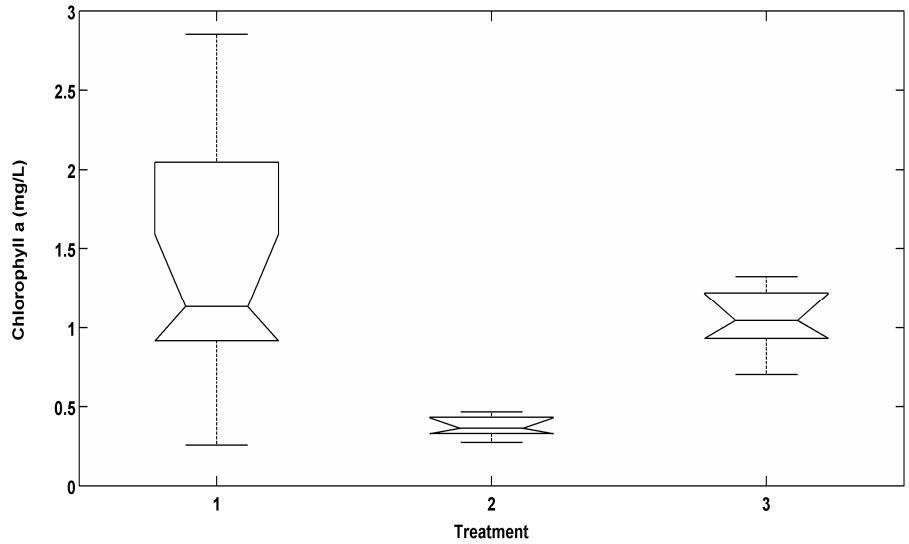

Figure 5-2 Box and Whisker plots of chlorophyll_*a* concentration for each experimental treatment. n = 15, 9 and 11 data points respectively. Treatment 1 = 0mg SCOD/m^2/day Treatment 2 = 100mg SCOD/m^2/day Treatment 3 = 300mg SCOD/m^2/day.

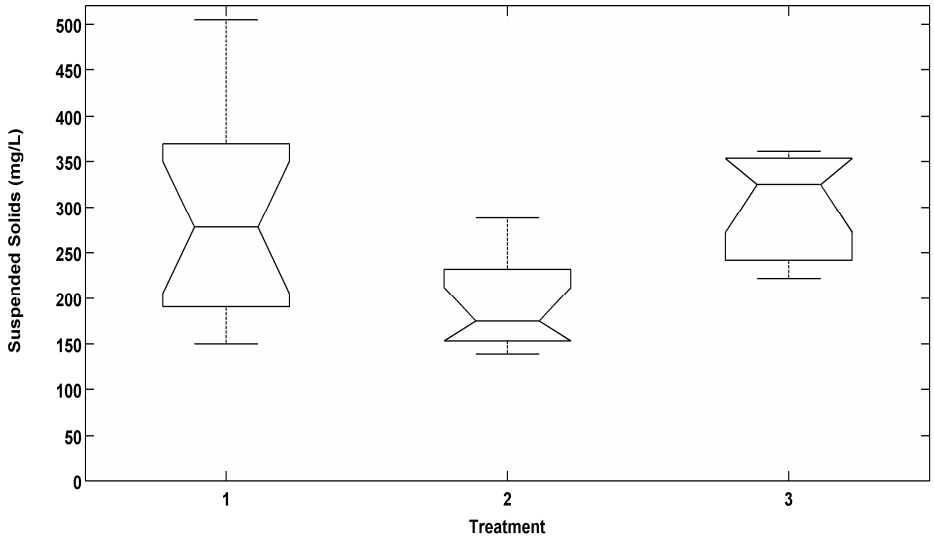

Figure 5-3 Box and Whisker plots of suspended solids for each experimental treatment. n = 15, 11 and 7 data points respectively. Treatment 1 = 0mg SCOD/m^2/day Treatment 2 = 100mg SCOD/m^2/day Treatment 3 = 300mg SCOD/m^2/day.

Bacterial Protein

In order to allow direct comparison between treatments with respect to bacterial biomass, a protein assay was conducted on bioreactor samples subjected to a series of centrifugation stages (Chapter 4) to separate algal and bacterial fractions. Results of this bacterial protein assay are shown in Figure 5.4. A significant difference (Table 5.2) with respect to median protein concentration was observed between treatments. The changes in protein concentration observed between each trial were considered most consistent with the hypothesis that greater loading of SCOD (BOD/DOM) resulted in increased heterotrophic bacterial productivity. This assertion was supported by visual inspection of Plate 5.1 and 5.2, which show scanning electron micrographs (SEM) of mini-pond biomass captured on 0.2 micron filter substrate following filtration through 1.2 micron GFC. Morphology of the organisms visible in the EM was interpreted as heterotrophic bacteria, possibly adhering to polysaccharide fragments (van den Akker pers. com. 2009).

Inorganic Carbon

Bacterial respiration is considered to be the main source of CO_2 for algal photosynthesis in wastewater treatment and many other aquatic systems (Chapter 2 & 3). Results of the IC assay are shown in Figure 5.5. A significant difference (Table 5.2) with respect to median IC concentration was observed between treatments. The changes in IC concentration observed between each trial were consistent with the hypothesis that greater loading of SCOD[3] resulted in increased biomass of heterotrophic bacteria and hence resulted in a greater release of IC into the culture medium. It is noteworthy that the pattern of change with respect to inorganic carbon concentration in Treatments 1, 2 and 3 was not reflected by a consistent pattern of increase in chlorophyll_*a* concentration as may have been expected if algal photosynthesis was carbon limited. It should be noted that addition of the carbon substrate corresponded with the development of ALBAZOD and improved light penetration into the culture in Treatments 2 and 3, thus making direct comparison with the photoautotrophic growth conditions (Treatment 1) more challenging.

Light Attenuation

Measurements of culture light attenuation and visual observations of floc morphology suggested that light penetration was likely to be the major driver of differences in chlorophyll_*a* concentration and by implication algal concentration. In photoautotrophic growth conditions (Treatment 1) flocculent particles were generally very small or not visible to the naked eye and dispersed throughout the culture medium. This corresponded with substantially decreased light penetration through the culture (Table 5.1). In the carbon loading treatments (2 and 3), individual

[3] May be considered functionally equivalent to BOD or DOM in natural ecosystems if DOM is not recalcitrant.

flocculent particles were clearly visible to the naked eye; and in the high carbon loading configuration (Treatment 3) the 'flocs' had the appearance of 'cut grass'; possibly the result of high levels of 'sticky' polysaccharide production by heterotrophic bacteria (van den Akker pers. com. 2005). The presence of flocculent particles resulted in effective light penetration in the carbon loaded treatments.

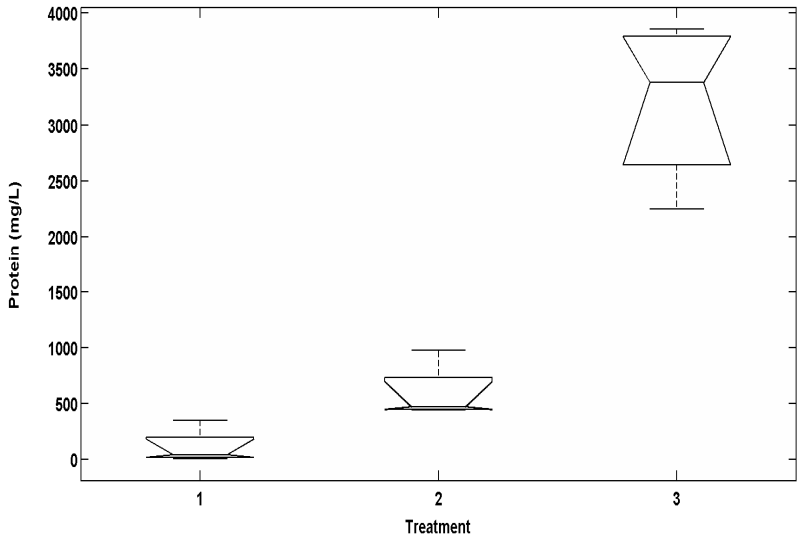

Figure 5-4 Box and Whisker plots of bacterial protein for each experimental treatment. n = 4 data points for each treatment. Treatment 1 = 0mg SCOD/m^2/day Treatment 2 = 100mg SCOD/m^2/day Treatment 3 = 300mg SCOD/m^2/day.

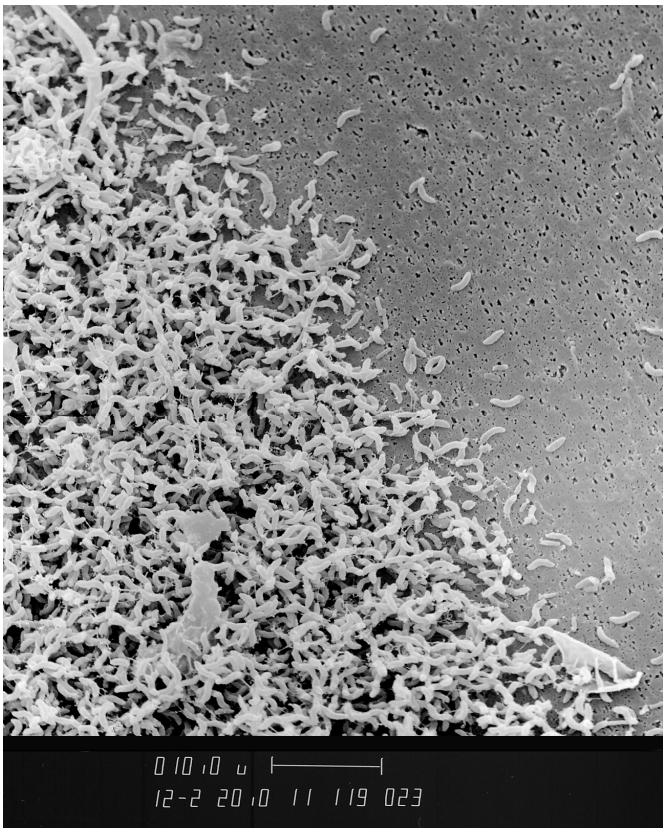

Plate 5-1 Scanning electron micrograph of culture biomass captured by 0.2-micron filter. Treatment 3 = 300 mg SCOD/m^2/day.

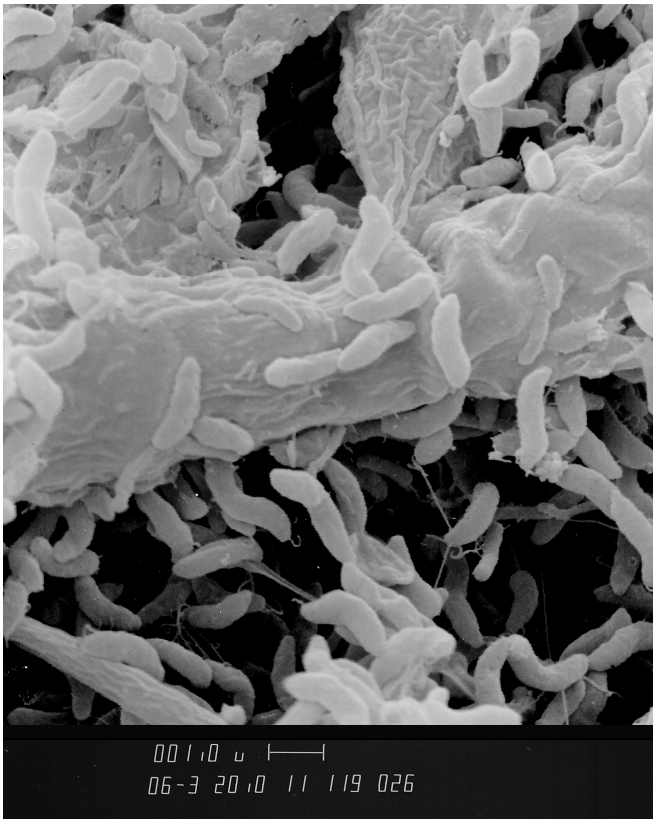

Plate 5-2 Scanning electron micrograph of culture biomass captured by 0.2-micron filter. Treatment 3 = 300 mg SCOD/m^2/day.

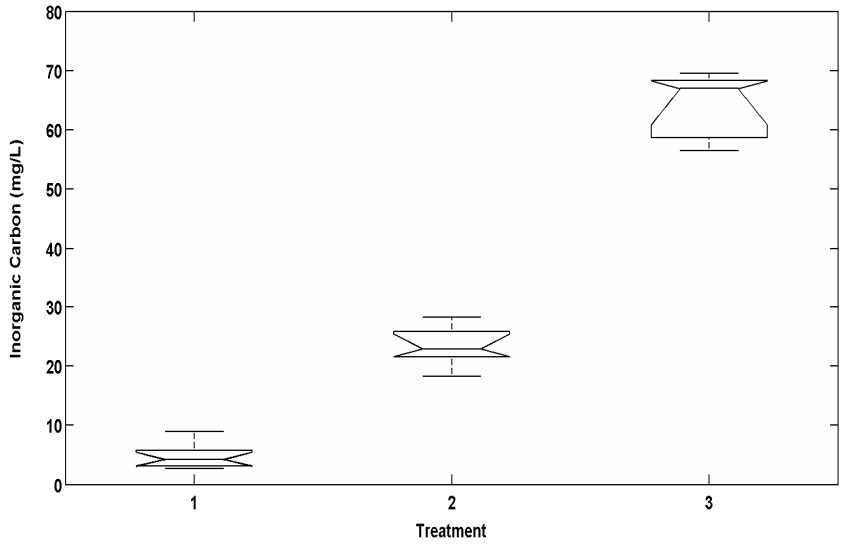

Figure 5-5 Box and Whisker plots of Inorganic Carbon (IC) for each experimental treatment. n = 11, 7 and 6 data points respectively for each treatment. Treatment 1 = 0mg SCOD/m^2/day, Treatment 2 = 100 mg SCOD/m^2/day, Treatment 3 = 300 mg SCOD/m^2/day.

5.3.2. Online Data and PI determinations

Dissolved Oxygen

Scatter-plots showing mean culture temperature and oxygen concentration for the duration of each experimental treatment are provided in Figures 5.6 to 5.8; each plot displays online DO and temperature mean ± 1 standard deviation for each 10 minute increment over the 24 hour 'day' for the full duration of each trial. Each measurement was taken automatically at the same time of the day and each data point on each figure is therefore the average of measurements for that time of day in that trial.

In all treatments the variation in dissolved oxygen concentration during the 24 hour cycle appeared qualitatively consistent with the pattern observed in the Murray Bridge pilot scale HRAP (Fallowfield et al. 2001) and the Bolivar WSP (Chapter 6). That is; dissolved oxygen concentration in the bioreactor increased rapidly following 'dawn' until reaching a plateau; in either a super saturated (Treatment 1 and 2) or close to saturated level (Treatment 3). Following 'sunset' the culture oxygen tension rapidly dropped due to efflux of oxygen from the culture due to mixing and respiratory oxygen requirements; the rate of decrease in oxygen utilisation also stabilised closer to 'dawn' as noted for the Murray Bridge HRAP. Inspection of Figures 5.6 (Photoautotrophic Treatment 1) reveals considerable variation around the average dissolved oxygen concentration in comparison to Treatments 2 and 3, Figure 5.7 and 5.8 respectively; consistent with the pattern of variation within each treatment noted for chlorophyll_*a* concentration. In physical systems, such as an oscillating spring, damping of oscillations can be achieved by application of a force e.g. from a shock absorber. It was considered possible that the decrease in variability observed in DO concentrations (and chlorophyll_a), in the carbon (acetate) loaded

treatments (2 and 3) in comparison to the photoautotrophic treatment reflected an analogous dampening effect; possibly provided by bacterial oxygen utilisation. Whilst this assertion is speculative, such metaphors (or phenomena) are acknowledged as useful tools or models in studies of population dynamics, e.g. May (1974), Nisbet et al. (1997).

Temperature variation

In all treatments variation in temperature followed a similar pattern during the daily cycle; significant differences in the magnitude of pond temperature (Table 5.2) were observed between all treatments. Whilst differences in temperature magnitude between treatments were significant; in absolute terms the variation between treatments was only of the order of 1 to 2 °C. To account for these differences in temperature on the solubility of oxygen in water the PI parameters calculated in following sections used temperature data collected contemporaneously with that of dissolved oxygen as described by Evans et al. (2003).

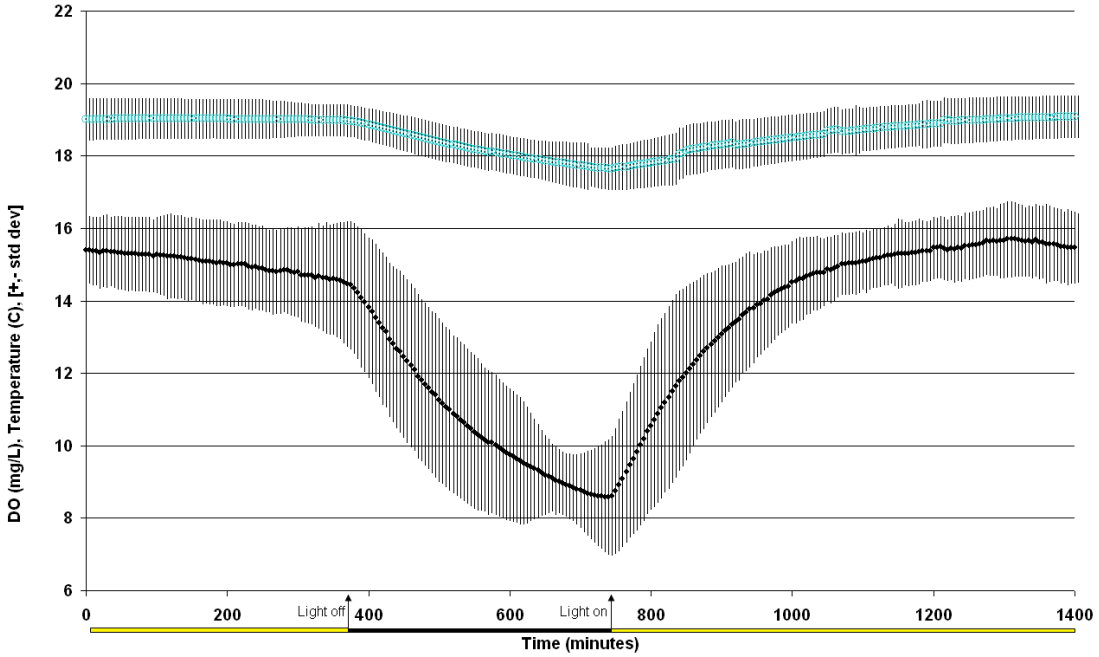

Figure 5-6 Scatter-plots of average temperature (blue dots) and average dissolved oxygen (black dots), ± standard deviation (grey bars) for both data types: N = 10 days, 10 minute logging schedule. Treatment 1 = 0mg SCOD/m^2/day.

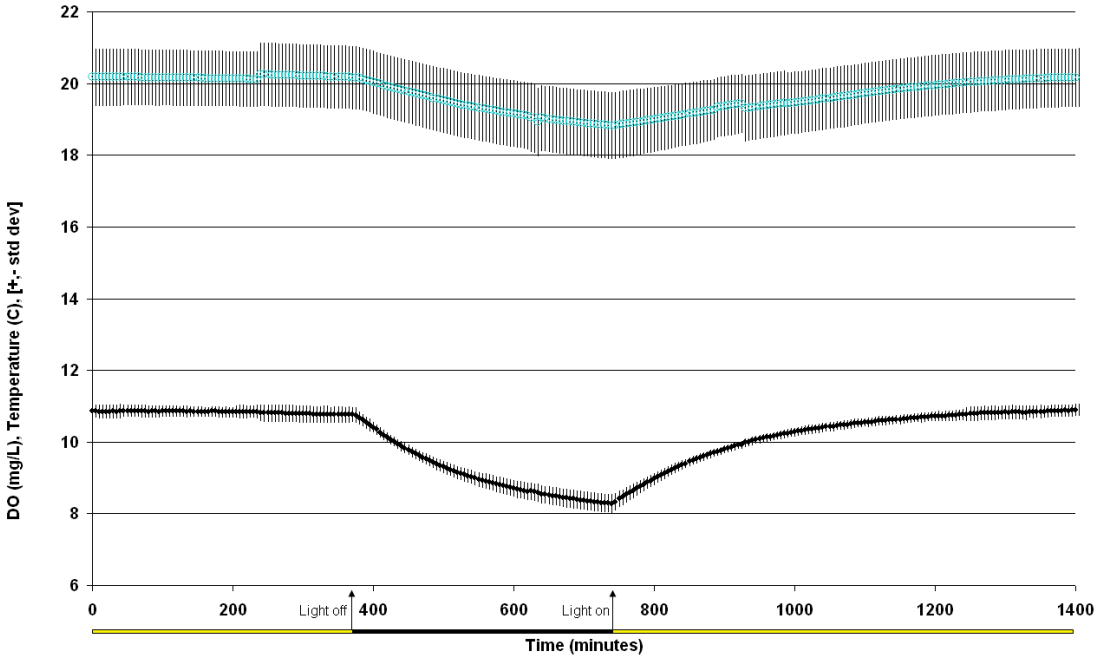

Figure 5-7 Scatter-plots of average temperature (blue dots) and average dissolved oxygen (black dots), ± standard deviation (grey bars) for both data types: N = 12 days, 10 minute logging schedule. Treatment 2 = 100mg SCOD/m^2/day.

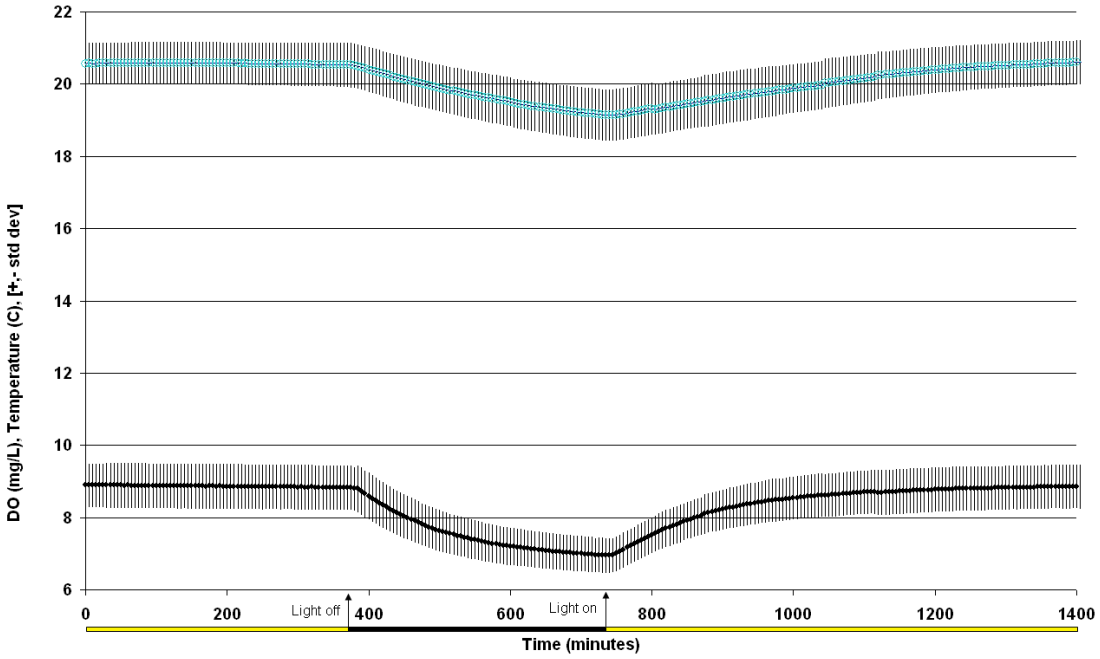

Figure 5-8 Scatter-plots of average temperature (blue dots [top]) and average dissolved oxygen (black dots [bottom]), ± standard deviation (grey bars) for both data types: N = 23 days, 10 minute logging schedule. Treatment 3 = 300mg SCOD/m^2/day.

Oxygen utilization rates (OUR) calculated for each experimental treatment are shown in Table 5.3 (see Evans et al. 2003 for methodology).The parameter OUR/hour was calculated from online dissolved oxygen data and provided a measure of average hourly rate of change in dissolved oxygen concentration during the period closest to dawn (50 minutes prior); corrected for re-aeration due to the pond paddle-wheel surface disturbance (when below saturation). The pattern of variation observed for OUR/hour between treatments was qualitatively consistent with that for chlorophyll_*a* and suspended solids as shown in Figures 5.2 and 5.3; that is a 'U' shape when comparing treatment 1, 2 and 3. It is noteworthy that variation in OUR was substantially greater between treatments than within treatments; this was considered to indicate that loading conditions between treatments differed enough to ensure that the OUR parameter was a distinguishing characteristic or indicator of the pattern of oxygenic flux in the culture medium due to treatment conditions.

As discussed above; the term 'oxygen utilization rate' is often used interchangeably

with community respiration rate in the literature as they have equivalent meanings; i.e. biomass in wastewater loaded HRAP and WSP systems consists overwhelmingly of bacteria and algae and therefore measurements of respiration (via DO concentration) will include contributions from algal and bacterial components in addition to small (presumably) contributions from fungal and/or invertebrate respiration.

In recent decades it has been shown that bacterial non-photosynthetic organisms can be a major or dominant component of the planktonic biomass in pond based wastewater treatment systems with abundance in algal/bacterial composition correlating with factors such as climatic variation and nutrient loading (e.g. Cromar and Fallowfield 1996). In highly productive algal based treatment systems; heterotrophic bacteria can proliferate in the nutrient rich medium and shade the algal cells that produce the oxygen they (bacteria) require for respiratory activity. Heterotrophic bacteria, when respiring, release carbon dioxide into the culture medium; thus providing carbon for using by the enzyme RuBisCO; the enzyme responsible for catalyzing sugar formation in the cell (Chapter 2). In simplistic terms, as the balance of aerobic, anoxic or anaerobic metabolic processes in a pond changes so does the balance between algal/bacterial respiration (oxygen uptake) and algal photosynthesis (oxygen production) changes (Chapter 2 and 3); thus the rationale for determining relative contributions of each of these component processes to reveal the resulting pattern of oxygen dynamics in response to the diurnal cycle and changes in nutrient loading or biomass composition.

As indicated by the above, the processes that operate within such systems are complex; fortunately some important and apparently reasonable simplifying assumptions can be made in photosynthesis/irradiance investigations including that of respiration rates remaining constant (at a given temperature) in the presence or

absence of light (Kirk 1994, Falkowski and Raven 2007, Chapter 3). The OURs presented in Table 5.3 were calculated from online oxygen data gathered in the absence of light immediately before illumination to prevent oxygenic photosynthetic activity masking the signal. Differences in oxygenic production upon illumination were therefore assumed to be dependent entirely upon algal photosynthesis. The corresponding OUR as normalized to chlorophyll_*a* concentrations are shown in Table 5.4. Normalization to chlorophyll_*a* provides a means of comparing these metrics when they are by definition independent with respect to any differences in algal concentration (assuming that photosynthetic pigment concentrations per unit biomass remain relatively constant). It was considered noteworthy that the pattern of variation between treatments revealed in Table 5.4 was largely unchanged by normalization with respect to chlorophyll_*a* despite substantial differences in chlorophyll_*a* concentration. This was considered most likely to indicate the presence of a large respiring non-algal (bacterial) biomass in all treatments.

	OUR/hour (mgO_2/L/h)	Standard Deviation (mgO_2/L/h)	Number of pre-dawn observations (days)
Treatment 1 (0 mgSCOD/m^2/day)	1.77	0.20	10
Treatment 2 (100mgSCOD/m^2/day)	0.19	0.05	12
Treatment 3 (300mgSCOD/m^2/day)	3.8	0.08	23

Table 5-3. Pre dawn oxygen utilization rates; mg dissolved oxygen per litre per hour; Arithmetic mean and standard deviation of the 50 minutes of predawn rate measurements across the full term of each treatment period.

	OUR/hour/Chl_a (mgO_2/mgChl_a/h)	Standard Deviation (mgO_2/ mgChl_a /h)	Number of pre-dawn observations (days)
Treatment 1 (0 mgSCOD/m^2/day)	1.30	0.70	10
Treatment 2 (100mgSCOD/m^2/day)	0.51	0.16	12
Treatment 3 (300mgSCOD/m^2/day)	3.44	0.49	23

Table 5-4. Pre dawn oxygen utilization rate mg dissolved oxygen per unit chlorophyll_*a* per hour; Arithmetic mean and standard deviation of the 50 minutes of predawn rate measurements across the full term of each treatment period.

Gross and Net Photosynthetic Rates

Net photosynthetic rate can be simply defined as the difference (in terms of oxygen) between OUR and gross photosynthetic rate (Falkowski and Raven 2007), i.e. the increase in oxygen production per unit time (due to photosynthesis) corrected for losses due to respiration. Figure 5.9 shows representative online temperature, light and DO data obtained from the Murray Bridge pilot scale HRAP system (Evans et al. 2003). The portion of the DO curve marked 'R' was the pre-dawn change in DO; in this case DO was increasing at a constant rate due to the atmospheric re-aeration

provided by the paddlewheel; OUR was therefore easily calculated as a function of the deviation (due to biomass respiration) from the (known) atmospheric re-aeration rate curve. The portion of the DO curve arrowed ‘P’ showed the post-dawn increase in oxygen concentration per unit time and provided gross photosynthetic rate (GPR) when aeration rate was subtracted to reveal the portion of increase due only to oxygen photosynthesis. It was noted by the authors that a ‘lag’ in terms of time occurred between sunrise and illumination of the pond surface and the subsequent increase in pond DO; due to the fact that only a portion of the pond volume (and biomass) was exposed at the surface at an instant in time and required a period of time for cycling through the light field.

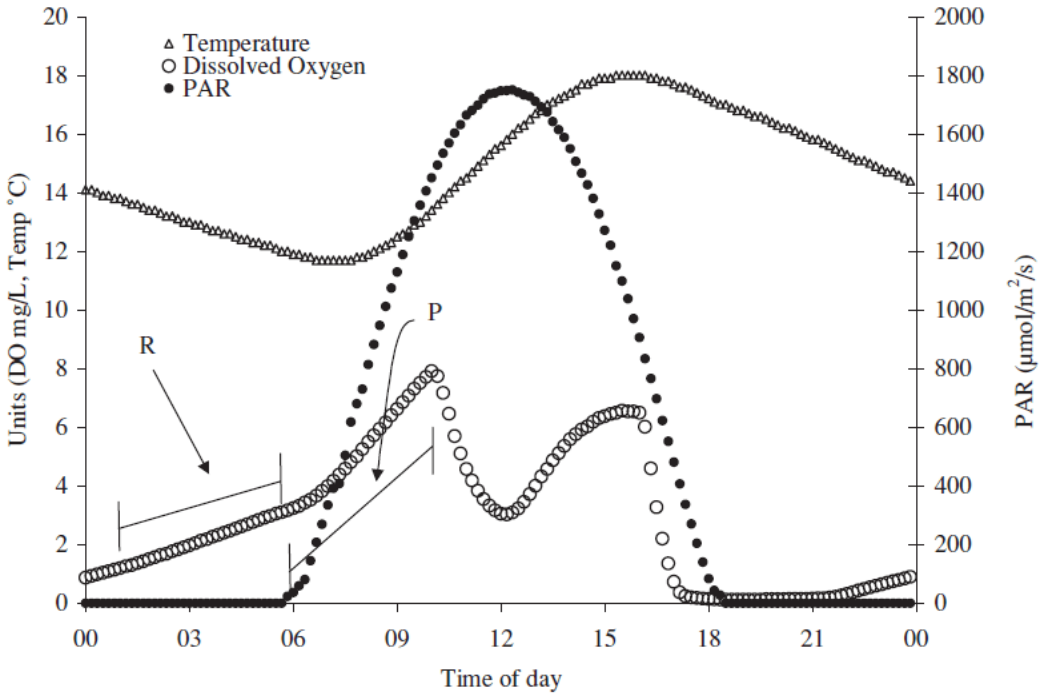

Figure 5-9 Change in dissolved oxygen concentration, photosynthetically active radiation and temperature during a 24-hour period (depth = 0.3m, retention time = 20 days. Murray Bridge HRAP system; from Evans et al. 2003.

These parameters (OUR and GPR) were used to derive net photosynthetic rate (P_{net}) and were then plotted as shown against online measurements of PAR (Figure 5.10). The form of this figure is that of a standard PI curve and it was posited by the authors that such a treatment of online data may provide a means of assessing the relationship between photosynthesis and irradiance in the field with similar fidelity to that obtained through use of the standard PI apparatus. If so the initial light limited rate of photosynthesis (alpha; 'A' in Figure 5.10) and the saturation onset parameter (Ik; 'Ek' in Figure 5.10) could be derived. These derived metrics (Ik and Ek) were not the focus of the research presented below due to the design of the HRAP bioreactor; specifically, light intensity varied as a 'square wave' and this was not analogous to the changes in PFD experienced in outdoor systems.

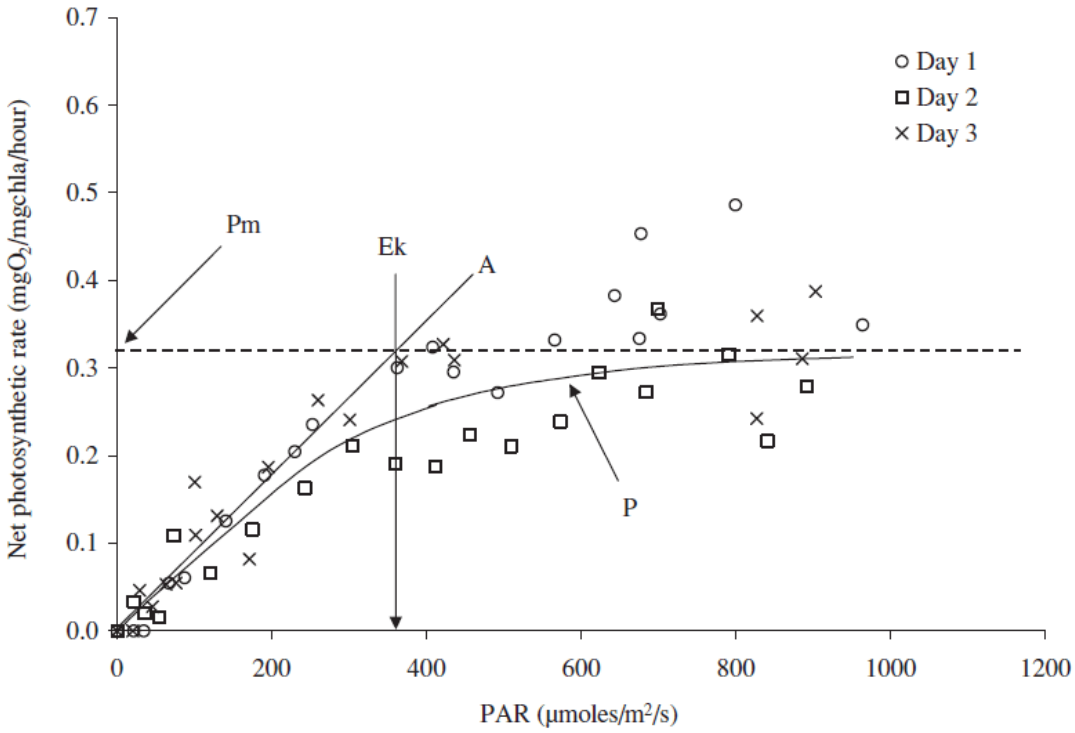

Figure 5-10 Net photosynthetic rate per unit chlorophyll_a (depth = 0.3m, retention time = 20 days. Murray Bridge HRAP system; from Evans et al. 2003.

It was considered, however, straightforward to assess OURs, net and gross photosynthetic rates calculated from online data in comparison to the standard PI

apparatus as these parameters can be calculated as rates per unit time simply based on changes in oxygen production data; this is the main focus of the data analysis presented below. This methodology was also applied to the online data collected from the Bolivar WSP (Chapter 6) as analysis did not rely on understanding the importance (or otherwise) of the observed lag in DO concentrations in these outdoor systems or in principle the constant irradiance obtainable from the laboratory based bioreactor. The extraction of higher dimensional parameters from online DO and irradiance data would therefore be a potentially fruitful area for future research and development of this technique.

The biomass in the lab-based HRAP bioreactor received a constant post dawn PFD (nominal 105µmol/m^2/sec). As a consequence, the rate of dissolved oxygen production per unit chlorophyll_*a* in the lab-based bioreactor could be expected, in principle, to approach a 'steady state' maximum value in terms of net photosynthetic rate during the 'day' (illumination). Figures 5.11-5.13 show the time-series of rate of dissolved oxygen production per unit chlorophyll_*a* for each treatment when corrected for respiratory losses (OUR/hour/Chl_a) and paddlewheel derived oxygen (Online_P_{net})[4]. The photoperiod is shown by the yellow bar whilst the night period is shown by the black bar. Despite the superficially similar time-series of gross oxygen production observed in Figures 5.6–5.8 three distinct patterns are apparent when Online_Pnet rates denoted as NPR in these figures are compared.

[4] Note that correction for paddlewheel derived oxygen was only performed when and if oxygen concentration was below saturation.

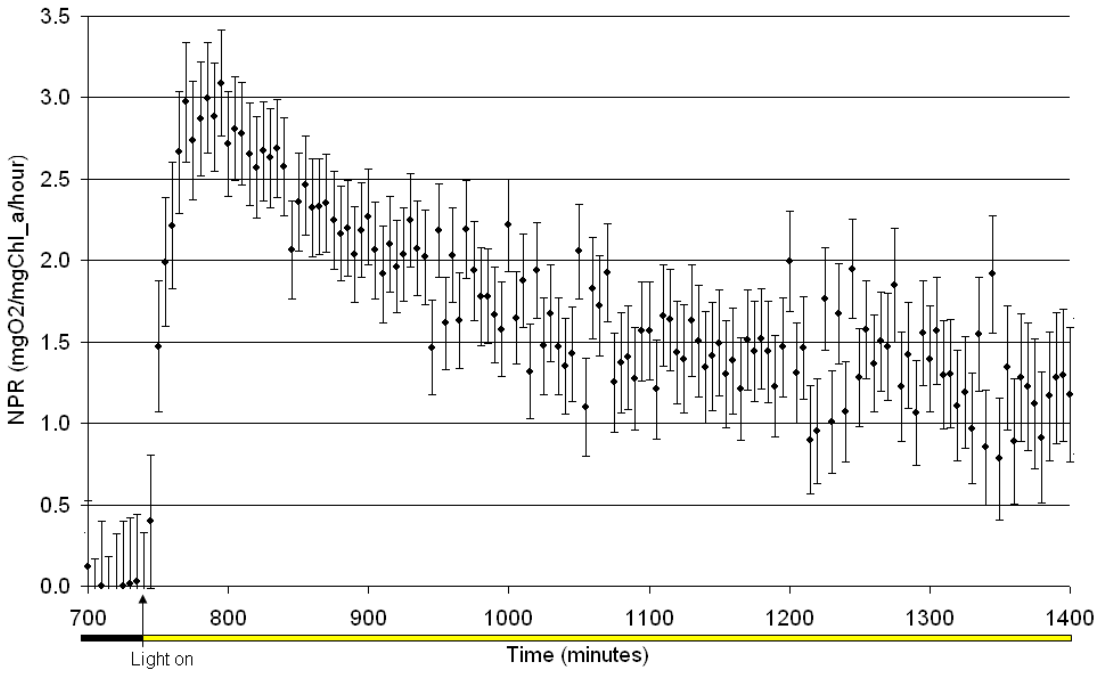

Figure 5-11 Scatter-plot of net photosynthetic rate (NPR, P_{net}) (black dots ± standard deviation (bars) obtained using online data, N = 10 days, 10 minute logging schedule. pH = 10.2 ± 0.32, open culture of *C. vulgaris*.Treatment 1 = 0mg SCOD/m^2/day.

The time-series of Online_P_{net} for the photoautotrophic configuration (Treatment 1) (Figure 5.11; no added carbon); shows a sharp increase in the rate of photosynthesis leading to a maximum value (Online_P_{max}) early in the day; followed by a decline to approximately half of this value. This pattern of change in online Pnet was considered most consistent with carbon dioxide limitation; and this conclusion was supported by the observation that pH of the culture in this treatment was very high (10.2 ± 0.32) which closely corresponded to the pK2 value for bicarbonate to carbonate dissociation (Metcalf and Eddy 2003). It is noteworthy that as oxygenic photosynthesis occurs, hydrogen ions are removed from solution by the algal cells via the cell membrane bound proton pump (Falkowski and Raven 2007) thus increasing the pH of the culture medium and therefore decreasing the availability of free CO2 (carbonic acid in solution). This was considered to provide an explanation for the decline in Online_P_{net} following an initial peak. Interestingly this decline in P_{net} was not observed when using the standard PI apparatus; this was considered to

reflect the comparatively short time periods (≈45 minutes) required for complete PI measurements using the standard PI method; specifically this may imply that CO_2 was not used up (in Treatment 1) within the short period of time required to complete a standard PI measurement.

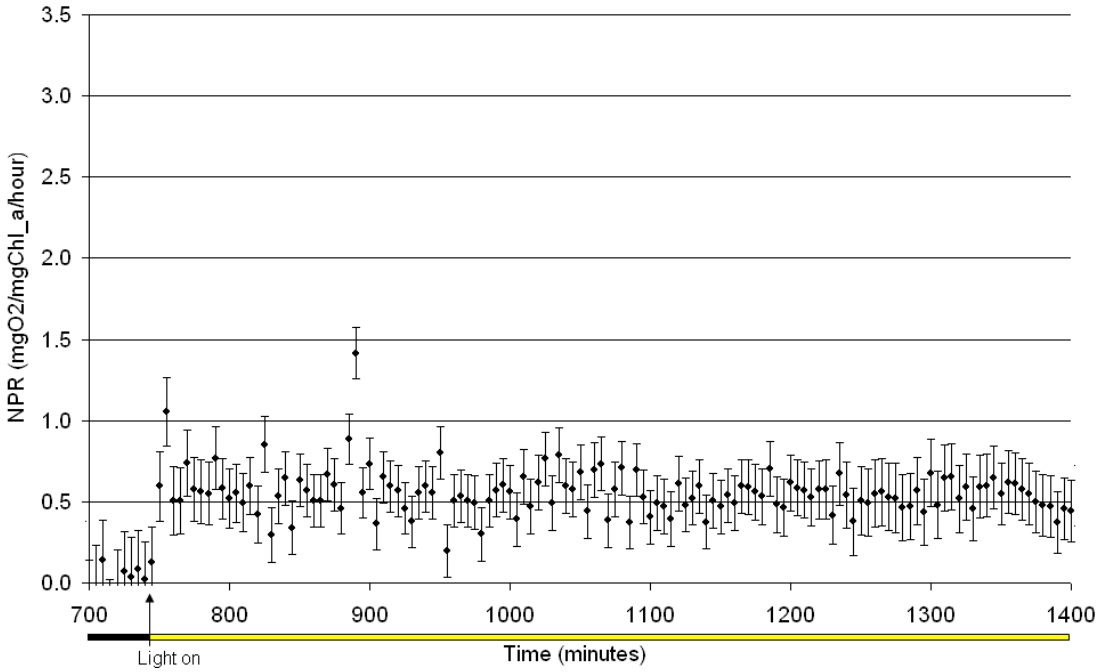

Figure 5-12 Scatter-plot of net photosynthetic rate (NPR, P_{net}) (black dots ± standard deviation (bars) obtained using online data, N = 12 days, 10 minute logging schedule. pH = 9.41 ± 0.13, open culture of *C. vulgaris*. Treatment 2 = 100mg SCOD/m^2/day.

The time-series of Online_P_{net} for the first carbon loaded treatment (Treatment 2; 100mgSCOD/m^2/day) shown in Figure 5.12 displayed an increase in net photosynthetic rate post-illumination which then remained relatively constant during the photoperiod. This result was considered counter intuitive when a comparison with the more strongly carbon loaded treatment (Treatment 3; 300mg SCOD/m2/day) was made (Figure 5.13). That is, the lower carbon loading in Treatment 2 was expected to result in decreased oxygen demand (in comparison) and therefore result in a higher peak rate of net oxygen production; the opposite was observed. However, based on the temporal behaviour of the photoautotrophic treatment; which displayed a pattern variation in Online_P_{net} consistent with CO_2

limitation (high pH $\Rightarrow$ low free CO_2); it was considered reasonable to conclude that the low average Online_Pnet value in Treatment 2 was again reflecting CO_2 limitation (see section below 'Comparison of Standard and Online Photosynthesis Irradiance Metrics').

It should be emphasized that the dissolved oxygen data used to create these figures were unitized to chlorophyll_*a* concentration and respiration; therefore direct comparison can be made without regard to differences in chlorophyll_*a* concentration or respiration between treatments.

The time-series for Treatment 3 (Fig 5.13) displayed a gradual increase in Online_P_{net} during the photoperiod until a maximum value was attained late in the 'day'. The substantial differences in the pattern of Online_P_{net} observed between Treatments 2 and 3 were not considered attributable to light attenuation in the culture (Table 5.1); initially it was considered possible that the differences in Online_P_{net} between these two carbon loading treatments may have resulted from contrasting flocculent particle (floc) morphology and an impact on light climate for the algal cells bound to the floc. This was based on visual observations that Treatment 3 floc's were larger and had an appearance of 'cut grass'; a common characteristic of HRAP biomass (Fallowfield 2010 pers. com.). Confirmation of this assertion would have required careful analysis of floc morphology to determine any impact of floc morphology on 'light-climate' (or other drivers of photosynthesis). An influence of light attenuation was however considered unlikely (between Treatment 2 and 3) upon comparison of Online_P_{net} data against the standard PI measurements which showed that photosynthetic rate in Treatment 2 (Figure 5.14) appeared light saturated. That is; the maximum rate of photosynthesis (P_{max}) measured using the standard PI

apparatus corresponded with the maximal rate Online_P_{max} calculated using the online PI approach. In this case increasing the PFD incident on the culture, a feature of the standard PI measurement approach, did not result in a notable increase in photosynthetic rate.

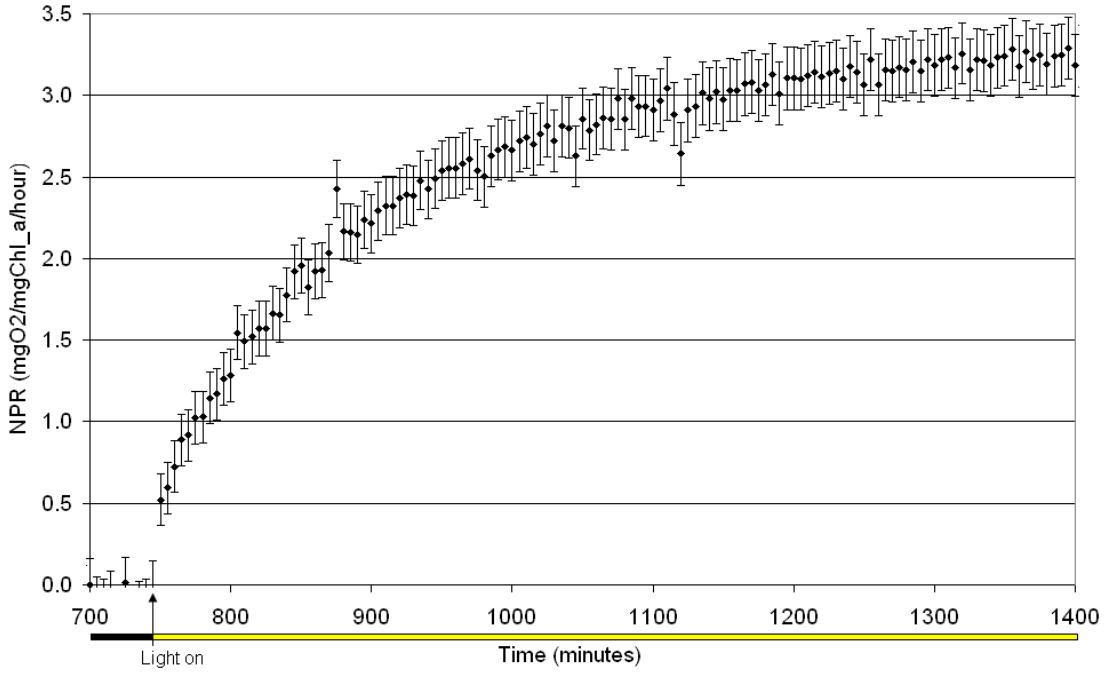

Figure 5-13 Scatter-plot of net photosynthetic rate (NPR, P_{net}) (black dots ± standard deviation (bars) obtained using online data, N = 23 days, 10 minute logging schedule. pH = 8.43 ± 0.3, open culture of *C. vulgaris*. Treatment 3 = 300mg SCOD/m^2/day.

Comparison of Standard and Online Photosynthesis-Irradiance Metrics

Measurements of photosynthesis-irradiance curves using the standard apparatus were conducted at regular intervals during the course of each of the three trials; results are summarised for comparison against standard PI data in Table 5.5. For comparative purposes, Figures 5.14 - 5.16 show PI curves obtained using the standard apparatus and include the Online_P_{max} parameter; maximum average Online_Pnet derived from the online data (overlaid in green). Black circles represent average net photosynthetic rates obtained using the standard PI apparatus as described in Hobson and

Fallowfield (2001) and Chapter 2 and 3; the standard deviation of net photosynthesis at each PFD is shown by the error bars. The equation of Webb et al. (1974) was used to fit the three respective PI curves using a non-linear least squares fit for each replicate (Hobson and Fallowfield 2001). In all cases the intersection of the initial rate of photosynthesis (alpha) and P_{max} specifies I_k, the PFD for saturation onset of the maximum rate of photosynthesis (Kirk 1994) in each treatment. The green circles represent mean Online_P_{max} with the standard deviation around the mean shown by the green error bars. Variations in Online_P_{max} was noted to be substantially less that that observed using the standard PI apparatus; this was considered to reflect the noise inherent in the highly sensitive Clarke electrode used in the standard PI apparatus and also the large sample size available using the very stable but less sensitive online electrode used in the bioreactor. From inspection it is apparent that standard PI measurements when compared against the Online_P_{max} at the same PFD (105 µmol/m2/sec) were, with the exception of Treatment 1; not significantly different from those calculated using online data.

It is important to note that it was considered appropriate to compare the Pnet (standard apparatus) value obtained at a PFD of 105 µmol/m2/sec (rather than Pmax) with the average maximum Online_Pnet obtained using the bioreactor (Online_P_{max}), as incident light intensities above this value could not be obtained using the bioreactor. If bio-reactor incident irradiance was increased to a higher level (not possible due to hardware limitations) photosynthetic rate may be expected to increase up to the Pmax value determined with the standard PI apparatus for each treatment. This would be a useful modification to the equipment for future research.

It was noted that the value of I_k determined from standard PI Treatment 2 was a

mean of 22µmol/m^2/sec, substantially lower than that observed for Treatments 1 and 3; this was considered to reflect the non-standard bi-modal shape of the PI curve in Treatment 2 (Figure 5.15); calculation of Pmax using the equation of Web et. al. (1974) appeared to be biased by this bi-modal shape and possibly falsely indicate a low I_k . As to the presence of a bi-modal shape, a search of the literature revealed no obvious biological explanation apart from random noise; it was considered possible that a larger sample size using the standard method would be required to determine if this pattern was real or an artefact.

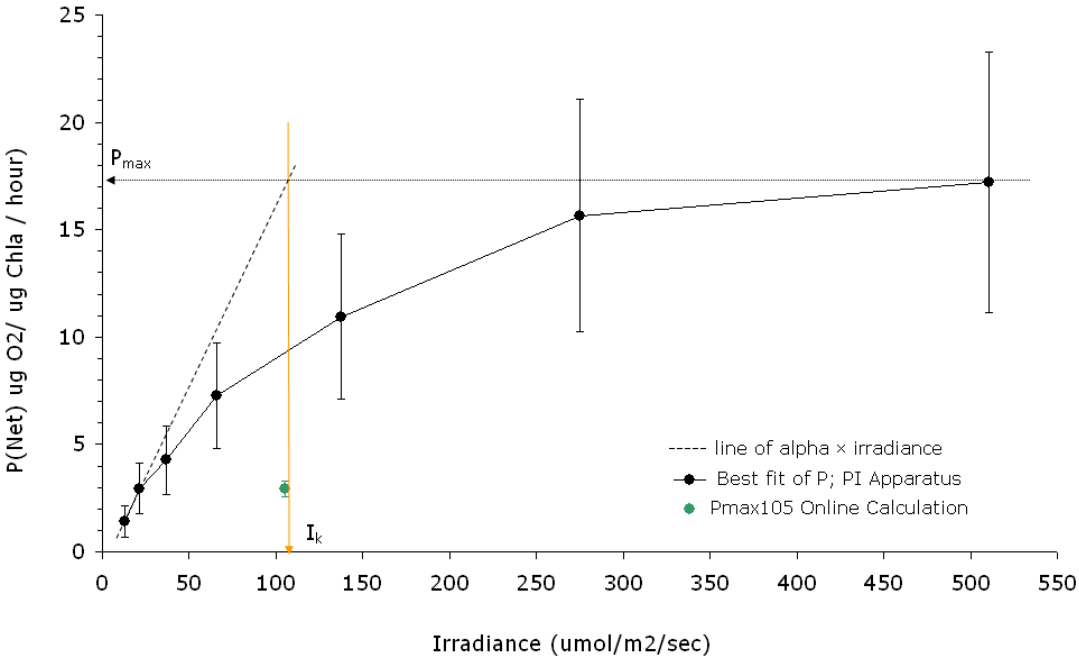

Figure 5-14 Scatter-plot of net photosynthetic rate (P_{net}) (black dots ± standard deviation (bars) obtained using standard PI apparatus, 4 measurements in triplicate and that obtained using online data (Online_P_{max}) (green dot ± standard deviation (green bars), N = 10 days, 10 minute logging schedule. pH = 10.2 ± 0.32, open culture of *C. vulgaris*. Treatment 1 = 0mg SCOD/m^2/day.

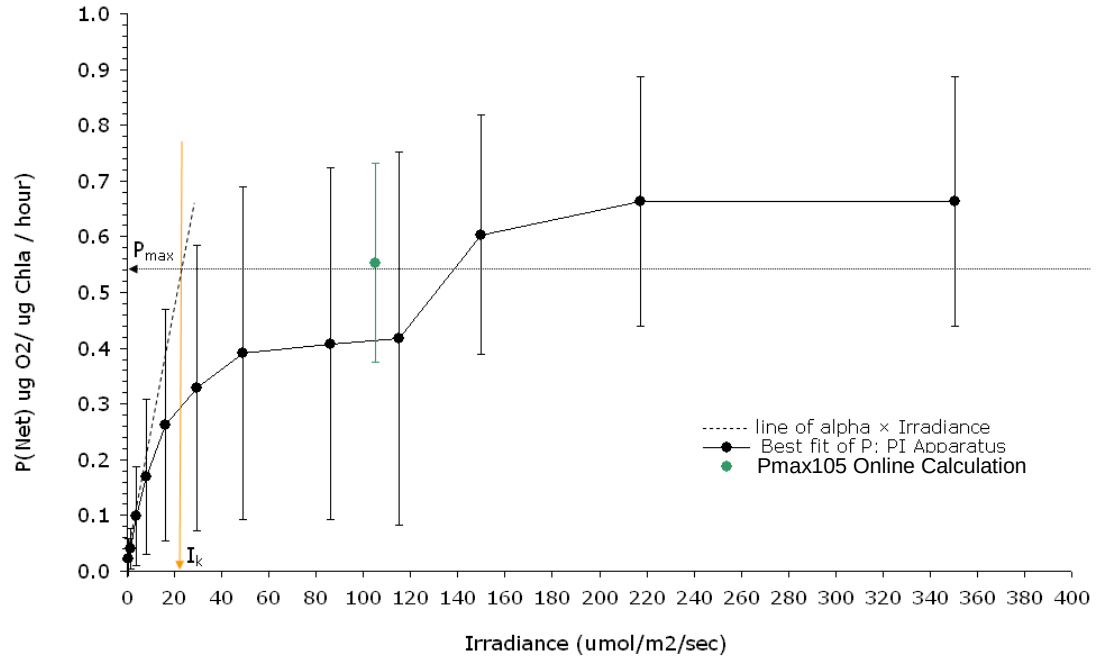

Figure 5-15 Scatter-plot of net photosynthetic rate (P_{net}) (black dots ± standard deviation (bars) obtained using standard PI apparatus, 6 measurements in triplicate and that obtained using online data (Online_P_{max}) (green dot ± standard deviation (green bars), N = 12 days, 10 minute logging schedule. pH = 9.41 ± 0.13, open culture of *C. vulgaris*.Treatment 2 = 100mg SCOD/m2/day.

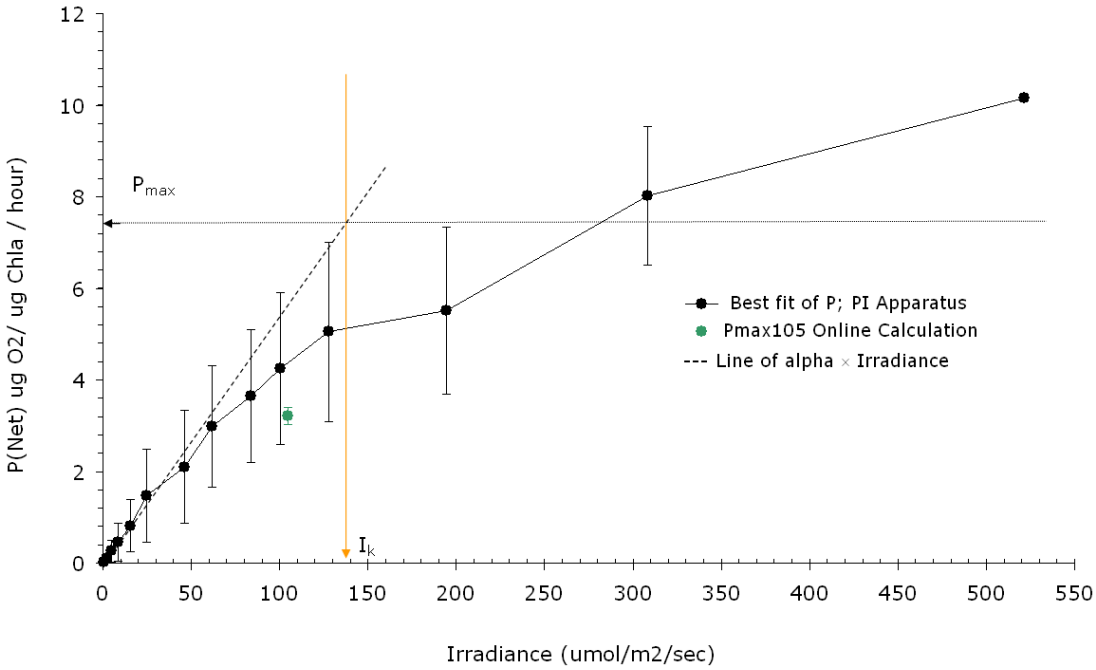

Figure 5-16 Scatter-plot of net photosynthetic rate (P_{net}) (black dots ± standard deviation (bars) obtained using standard PI apparatus, 8 measurements in triplicate and that obtained using online data (Online_P_{max}) (green dot ± standard deviation (green bars), N = 23 days, 10 minute logging schedule. pH = 8.43 ± 0.3, open culture of *C. vulgaris*. Treatment 3 = 300mg SCOD/m2/day.

Data Source		**alpha [µgO_2/µgchl_a/ h]**	**Dark respiration [µgO2/µgchl_a/h**	**P_{max} [µg O_2/µgchl_a/h] (Standard PI)**	**P_{net} [µg O_2/µgchl_a/h] at pond surface PFD =105µmol/m^2/sec (Standard PI) and Online_P_{max}**	**I_k [µmol/m^2/sec]**
Treatment 1	**PI apparatus**	0.16 (0.06) n = 4	1.7 (0.49) n = 4	17.4 (6.14) n = 4	9.5* (3.5) n = 4	109
	Online PI	N/A	1.3 (0.7) n = 10	N/A	2.92* (0.36) n = 10 P < 0.001	N/A
Treatment 2	**PI apparatus**	0.01 (0.008) n = 6	0.16* (0.06) n = 6	0.64 (0.4) n = 6	0.41 (0.22) n = 6	22
	Online PI	N/A	0.50* (0.16) n = 12 P < 0.01	N/A	0.55 (0.18) n = 12	N/A
Treatment 3	**PI apparatus**	0.05 (0.02)	3.0 (3.4) n = 8	7.65 (3.1) n= 8	4.25 (1.7) n = 8	139
	Online PI	N/A	3.44 (0.49) n = 23	N/A	3.22 (0.19) n = 23	N/A

Table 5-5 Summary statistics for standard PI apparatus calculations, arithmetic mean, standard deviation and sample size for HRAP operated at a surface irradiance of 105 µmol/m^2/sec. Alpha: initial rate of photosynthesis, Dark respiration rate: respiration rate immediately prior to illumination of culture. P_{max}: maximum rate of photosynthesis. P_{net} = rate of photosynthesis obtained by interpolation from PI curve obtained using standard apparatus. Online_P_{max} = average maximum of online net photosynthesis. *All treatments significantly different with respect to the median of specified parameter (5% significance level, Kruskal-Wallis nonparametric one-way analysis of variance).

5.4. Conclusions

A laboratory based HRAP bioreactor was designed, built and operated in controlled laboratory conditions. It provided data for comparison of photosynthesis/irradiance curves obtained using a standard laboratory PI apparatus with photosynthetic rates calculated from in-pond dissolved oxygen time-series using a modified version of the method proposed by Evans et al. 2003.

Standard wastewater treatment parameters were measured and compared between treatments and with a pilot scale outdoor system. Results of this comparison indicated that oxygen dynamics and pond chemistry parameters were not unusual for a HRAP system operating under the variety of loading conditions applied.

Online data was used to calculate photosynthesis curves and compared with those determined using the standard PI apparatus. The non-carbon loaded (photoautotrophic) Treatment 1 was included for comparison purposes to provide a 'baseline' condition not subject to loading with carbon (a condition not typically observed in wastewater treatment systems). Oxygen dynamics in this treatment displayed behaviour not inconsistent with carbon limitation; a condition which was inferred from to have potentially impacted upon the first carbon loaded treatment (Treatment 2). It is noted that the experimental design was not intended to address this issue directly and is a possible avenue for future research.

It was concluded that no significant difference existed in terms of the Online_P_{max} at an appropriate comparison PFD of 105 µmol/m^2/sec in the carbon loaded treatments; specifically that the use of online data was sufficient for calculation of net

photosynthesis in carbon loaded conditions; in this case a point on the curve defined by incident PFD. In the photoautotrophic culture (Treatment 1) a poor correlation between the standard PI and the Online_Pnet measurement was observed; the most straight forward explanation for this was considered to be that an improved light climate was present within the standard PI apparatus and that gas exchange may have been improved due to vigorous mixing in the culture vessel.

It is argued that the results presented in this chapter support the assertion that online oxygen, light and temperature data can be used to calculate valid photosynthesis curves. The use of this novel approach if translatable to outdoor systems (Chapter 6) would be extremely useful for assessing pond performance and development of control parameters for managing treatment ponds in response to changes in influent characteristics or season for example.

6. OXYGEN AND TEMPERATURE DYNAMICS BOLIVAR WSP 1

Purpose

A series of four monitoring stations were constructed and installed in the Bolivar WSP 1 and used to monitor dissolved oxygen and temperature at four spatially distinct locations identified by Sweeney (2004) as differing with respect to persistence of stratification. Complete and qualitatively representative data sets from approximately two weeks of online and wet chemistry data in each of February and May 2005 were used for comparison. Regular grab samples were collected during each of these intensive sampling periods from a series of four depths at each location (surface, 25cm, 50 cm and 75 cm below surface); each sample was analysed using standard wastewater quality parameters. Online oxygen and temperature data for each day was collected at each location (nominal depth = 25 cm) and averaged at each location to provide an 'average daily' time series for subsequent calculation of photosynthetic rates, consistent with the methodology presented in Chapter 5. Comparison was made against photosynthetic rate measurements obtained from the Murray Bridge pilot scale HRAP system and laboratory-scale HRAP system. Temperature data from a thermistor chain installed at each location was used to determine the pattern of stratification during the sampling period at each location with the intention of determining if stratification patterns influenced dissolved oxygen concentrations. Online time-series data were combined into surface-plot interpolations of the pond, in the manner of Sweeney (2004) for qualitative comparisons of pond spatial behaviour with respect to these parameters. Sweeney (2004) obtained an intensive series of snapshot samples of DO concentration across Bolivar WSP 1 using a hand-held probe over a 10-day sampling period in summer (February 2000) and winter (August/September 2000), whilst this work was of low

temporal resolution in comparison to that presented below it was considered that the results from the February sampling period were at least directly comparable in terms of season.

6.1. Introduction

Until recently the WSP system at Bolivar was the major nutrient reduction stage of treatment provided to sewage from the north-western suburbs of Adelaide prior to effluent disposal at sea. It was constructed as two parallel series of three shallow WSP ponds, with a combined area of approximately 344 Hectares and a retention time in each treatment train of approximately 32 days; at the time of writing effluent from the system not recycled for agricultural or non-potable use was disposed to sea via a concrete lined outflow channel (to Gulf St Vincent) of approximately 12 kilometres length.

As discussed in Chapter 2, 3 and Chapter 5, the mass of oxygen produced per unit time from algal photosynthesis is a key parameter used for determining 'capacity' of an aerobic algal-based wastewater treatment process, i.e. sufficient oxygen must be produced by phytoplankton to meet respiratory requirements of an aerobic heterotrophic biomass for it to stabilise the nutrient load applied to the pond via the addition of wastewater (Oswald 2003, Davies-Colley et al. 2005).

Measurements of oxygen evolution per unit algal biomass conducted at a series of light intensities and corrected for oxygen loss due to algal respiration can provide a useful measure of net photosynthesis (Harris 1984, Kirk 1994, Reynolds 2006, Falkowski and Raven 2007) and as shown in Chapter 5 can reveal aspects of pond ecology that are not apparent from simple measurements of bulk DO. As revealed with the laboratory-based system described in Chapter 5, estimates of algal productivity as inferred by measurements of photosynthetic activity are more

accurate if contributions to the time-course of DO, be they physical (e.g. atmospheric re-aeration) or biological (e.g. non-oxygenic organisms) are better understood. Within the WSP, as with the Murray Bridge pilot-scale HRAP and indoor laboratory-based HRAP bioreactor, the atmosphere provided a source and sink of oxygen via. As with these other systems, losses from diffusion to the atmosphere are not well addressed in the literature and are ignored for the purposes of this discussion, whilst noting that this is an area requiring further research. The method of determining OUR for the pond biomass adapted for use in Chapter 5 and proposed in Fallowfield et al. (2001) and Evans et al. (2003), was applied with modification due to the fact that a constant mixing (and liquid velocity) induced atmospheric diffusion term was not present. The theoretical impact of wind speed and direction on flow patterns of the WSP was carefully assessed by Sweeney (2004) using computational fluid dynamic (CFD) modelling. Shear stress resulting from wind moving across the water body surface and driving the formation of wind-induced circulatory currents is unambiguously shown in the literature (Kirk 1994). Sweeney (2004) showed that a CFD model of the WSP displayed a 'rapid departure from quasi plug-flow conditions above 3m/s (10.8 km/h) for all wind directions'. It was concluded from this work that flow predicted by the *CFD model* of the pond was unaffected by modelled wind speeds lower than 10.8 km/h. Nevertheless a validation study using in-situ deployment of drogues by Sweeney (2004) revealed "no obvious first-order relationship between wind-speed and pond flow velocity, or wind direction and pond flow direction at any depth". It was noted by the author that hydraulic regime, in contrast to other similar studies, varied in response to *variations* in wind velocity and that the pattern of flow was qualitatively dependant on the previous (flow pattern) equilibrium in the pond.

On the basis of this information it was not considered possible to incorporate an

oxygen diffusion term from the atmosphere into estimates of OUR (Section 6.3.4). It was considered likely that the magnitude of this source of error would correlate positively with wind speed as CFD simulations of pond flow suggested that wind induced circulatory currents would form. Such errors could therefore be particularly significant during strong wind events. Whilst in principle it would seem reasonable to minimise this error by restricting analysis to periods of low wind velocity; the observation by Sweeney (2004) that pattern of flow was dependent on previous equilibrium as well as variations in wind velocity suggested that such an approach would not necessarily provide data with lower errors in oxygen diffusion estimates or be more representative of the true state of the system. Nevertheless, Sweeney et al. (2005) showed that duration of stratification could be predicted with a reasonable level of accuracy using a CFD model when wind velocity was less than 1.5m/s; and provide an indication of the extent of local mixing when inversions break down or form (Sweeney et al. 2005a).

A possible means of quantifying contribution of atmospheric oxygen to the pond in future studies could be by collection of contemporaneous measurements of fluid velocity at a series of depths across the pond for the purpose of calibration and validation of the CFD model and empirical calculations of atmospheric gas transfer. While noting the challenges outlined above, contemporaneous measurements of temperature, light and dissolved oxygen were collected at four locations in the WSP during two periods of 2005 and used to characterise the dynamics of photosynthesis during these periods. The average time-series pattern of dissolved oxygen concentration and temperature versus time were qualitatively and quantitatively assessed against the pattern observed in the Murray Bridge HRAP and laboratory based system to establish if patterns of change in PI in the WSP appeared unique or if more general properties may be common to all three systems.

Detailed descriptions of both the physical and biological aspects of the Bolivar WSP system including not covered in this Thesis are provided in the works of Herdianto (2003), Sweeney (2004), Yamamoto (2007) and Short (2010) and peer reviewed publications by these authors.

6.2. Materials and Methods

In addition to the descriptions below, materials and methods used to assess oxygen dynamics using online data in Bolivar WSP 1 can be found in Chapters 4 and 5.

6.2.1. Sampling and Experimental Design

Sampling locations are shown in Figure 6.1. Each location was selected on the basis of work by Sweeney (2004) to provide spatial coverage across Pond 1 in locations that were known to often differ in terms of stratification frequency and duration and distance from the pond inlets and outlets (Chapter 3). Assessment of pond stratification frequency (Section 6.3.2) showed a qualitatively similar pattern of stratification to that observed by Sweeney (2004). Each of the monitoring stations was furnished with online dissolved oxygen units and output was logged electronically and powered by a solar panel and 12v lead acid battery (Chapter 4). The dissolved oxygen probe at each site was placed at a nominal depth of 25 cm below water level with temperature measured using an online sensor physically attached to the DO probe at each location.

Turbidity and chlorophyll fluorescence were logged using a Scufa™ fluorescence probe at the North Eastern (NE) monitoring location contemporaneously with dissolved oxygen and temperature. Due to technical problems with the Scufa™ calibration this data was considered not to be of sufficient quality to be presented.

Thermistor network

The 15 location thermistor network developed and deployed by Sweeney (2004) was

refurbished, redeployed and maintained during the 2003-2005 calendar years and data collected. For the purposes of conciseness and relevance to the research focus of this Thesis, only data obtained from the thermistor chain locations corresponding to the dissolved oxygen monitoring stations are presented. The additional temperature data files corresponding to other locations would be required to perform CFD of hydraulic conditions in the manner of Sweeney (2004). The design depth of Bolivar WSP 1 was 1.2m. Each thermistor chain was therefore able to extend automatically to cover this depth interval. It was noted however that depth to sediment at the four sampling locations was generally of 1m or less during these sampling periods. Presumably the result of sediment accumulation in the pond due to the extensive activated sludge carryover that was observed during both sampling periods. This was particularly noticeable during the May 05 sampling period when a sludge blanket approximately 25-50cm thick was observed at the inlet portion of the pond and at the SW monitoring station. As such the configuration of the thermistor chains provided the following four nominal intervals from the pond surface to the base of the pond; 10cm below surface (attached to float), 25cm below surface, 50cm below surface and 75cm below surface. This convention was followed in the presentation of data.

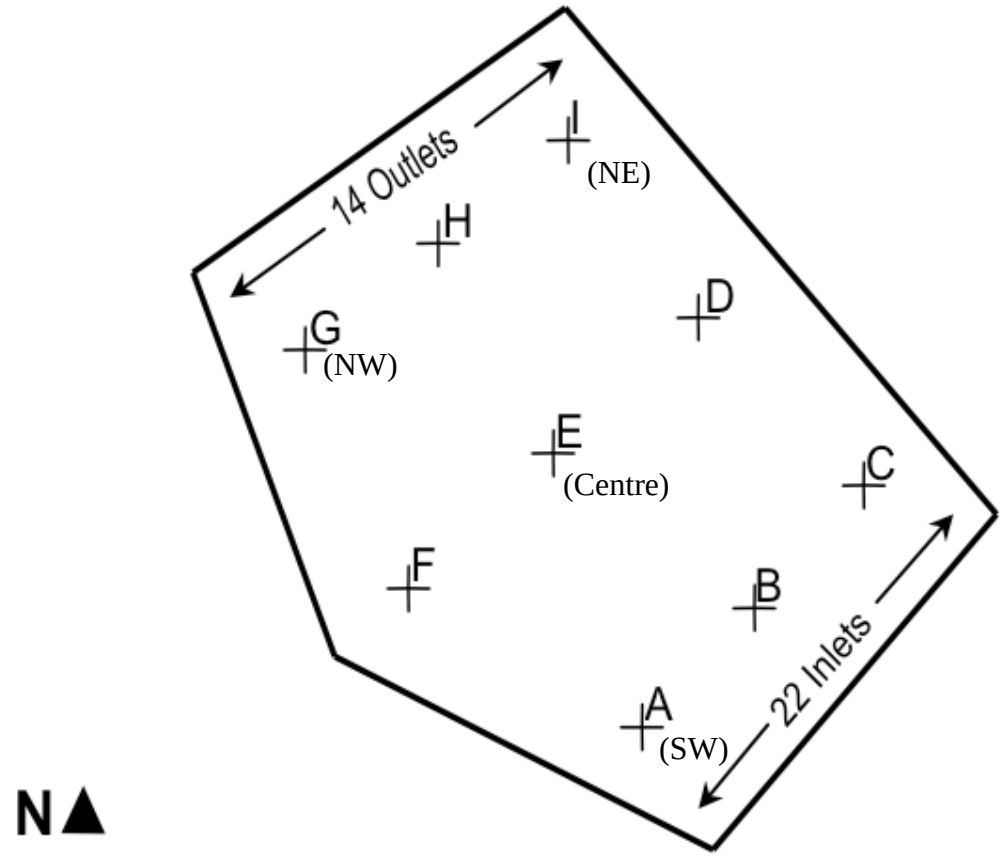

Figure 6-1. Plan diagrammatic view of Bolivar WSP 1. Online monitoring stations were installed at locations G (North West), I (North East) E (Centre) and A (South West). After Sweeney (2004); reproduced from Chapter 4 for convenience.

Sampling and Downloading Schedule

All online monitoring equipment was programmed to record data synchronously. Each data-logger was programmed to record data at intervals of 5, 10 or 15 minutes, dependant on the time estimated before exceeding capacity of the memory. All loggers were programmed to cease logging once memory capacity was reached. Data downloading schedule was nominally set to weekly intervals as this provided opportunity to clean the DO probe heads of accumulated bio-film. Weather conditions were primary in determining actual sampling date due to safety considerations. Loggers typically operated for two weeks before running short of memory; however bio-film growth was generally a problem within a week of

cleaning and in a matter of days during some warmer periods of weather. Observations of bio-film growth on DO probes were noted and checked against a handheld DO probe response to ensure that unbiased data representative of the pond dissolved oxygen at that location was used for analysis. The online DO data collected during the two periods presented in this chapter was considered to be unaffected by bio-fouling due to frequent sampling events (twice per week). It was noteworthy that the summer sampling event reported in Sweeney (2004) was undertaken during February 2001, therefore providing the opportunity to make comparisons at an equivalent time of year (season).

Wet Chemistry

Standard water quality parameters, as listed in Chapter 4 were measured for each sample taken from the specific depth at each of the four locations.

Light Attenuation

PAR ($\mu mol/m^2/sec$) incident on the surface and the nominated depths passing through the culture were measured using a quantum sensor (SKE-510 400-700nm PAR) attached to the outside of an acrylic tube (25mm diameter) and lowered through the culture at 50 to 250 mm depth increments. Measurements were conducted as regularly as conditions allowed.

Online PAR

PAR ($\mu mol/m^2/sec$) within 75cm of the pond surface was measured using a quantum sensor (SKE-510 400-700nm PAR) and logged electronically.

Pond Dissolved Oxygen Dynamics

Online data from each of the four sampling locations was processed according to the methodology detailed in Chapter 5 to produce online-data derived photosynthesis response curves for each location, during the time period of interest (Figures 6.32-6.33).

Surface Plots

Online data from each of the four sampling locations was processed using the macro's and script files detailed in (Appendix A) to produce surface-plots of parameters based on DO and temperature. Wind velocity and PAR data was included adjacent to each surface plot to provide full coverage of online data collected at each time-step.

Sampling Periods

Data from two periods of 2005 were presented, February 16th - 28th and May 1st – 11th inclusive. Both of these data sets differed substantially in terms of water temperature, incident irradiance and pattern of stratification. Whilst the data was obtained in different seasons it was not considered possible to infer seasonal trends based on a data set that did not cover repeated periods of multiple years nor include the winter and spring. Nevertheless the data and analysis presented below allowed a detailed examination of oxygen dynamics in this large WSP large pond, where parameters (light, temperature and chlorophyll_*a*), accepted in the literature as driving photosynthetic activity in algal ponds, differed enough between sampling periods to provide an opportunity to reveal meaningful interactions between them. The advantages of studying a well characterized system in terms of depth, loading rate and retention time are obvious when attempting to reveal ecological relationships in complex biological systems. This was made clear during field work when pond depth was observed to vary across the pond due to sludge accumulation during 2004 and 2005, particularly so at the SW monitoring site during the May sampling period. Variations in the depth to sediment were apparent across the pond in comparison to the work of Sweeney (2004), as such it was initially considered likely that the specific findings regarding hydraulic flow predicted by CFD modeling may have changed in the intervening period and therefore require additional work to

update for direct comparison. Nevertheless, patterns of stratification in the WSP (Section 6.3.2) revealed a substantial degree of concordance in qualitative terms with those reported in work of Sweeney (2004). This suggested that apparent differences in sludge accumulation across the pond were not sufficient to vary large scale patterns of mixing.

6.3. Results and Discussion

6.3.1. Standard Measures of Pond Performance

Summary data showing mean and standard deviation of dissolved oxygen, chlorophyll_*a*, suspended and volatile suspended solids, organic and inorganic carbon and pH for two depths (25cm and 75cm), vertical light attenuation and stratification status at each location for the February and May sampling periods are provided in Tables 6.1 - 6.4. Grab samples (Tables 6.1 and 6.2) were obtained from each sampling location in systematic order; i.e. NE, Centre, SW and then NW. At each sampling location 1L water samples from 25cm and 75cm below surface were obtained within a few minutes of each other, each in triplicate. Parameters such as DO and pH were measured at the two depths in situ immediately before or after water samples were collected. Sampling of the four sites required approximately 2 hours; with sampling planned to begin in the mid-morning (10 – 11am). Logistically it was not always possible to begin at this time; similarly, when sampling at a location, repairs or other requirements could and did delay sampling. It was therefore considered that grab sample data obtained for ‘within sampling location’ depth comparisons could, in principle, be made with more precision than comparisons ‘between sampling location’ due to the time delay between the sampling of separate locations. The data shown in Tables 6.3 and 6.4 was obtained from online monitoring equipment located at the four monitoring station locations during February and May 2005.

Location	Depth (cm)	DO (mg/L)	Chl_a (mg/L)	SS (mg/L)	VSS (mg/L)	TOC (mg/L)	IC (mg/L)	VAC (Kd [PAR] m-1	T [ºC]	pH
I (North East)	25	4.9 (0.73)	0.018 (0.018)	13.3 (3.5)	10.8 (4.8)	21.6 (6.1)	49.0 (1.2)	2.12	24.6 (1.8)	7.6 (0.05)
	75	4.8 (0.57)	0.011 (0.009)	13.8 (5.3)	9.8 (4.1)	19.2 (2.5)	49.1 (0.9)	n=3	23.8 (1.7)	7.7 (0.05)
G (North West)	25	4.9 (0.33)	0.019 (0.023)	12.3 (5.4)	9.0 (3.7)	18.0 (1.8)	47.6 (4.3)	2.14	25.2 (1.2)	7.6 (0.14)
	75	4.8 (0.67)	0.012 (0.013)	13.3 (4.1)	9.5 (3.3)	12.8 (6.5)	50.1 (4.5)	n=3	23.1 (1.5)	7.7 (0.08)
E (Centre)	25	5.1 (0.33)	0.017 (0.009)	9.4 (5.6)	6.8 (3.2)	17.8 (5.2)	50.0 (1.1)	2.20	24.2 (1.4)	7.7 (0.05)
	75	4.9 (0.35)	0.012 (0.009)	12.8 (4.4)	7.9 (3.0)	18.3 (2.4)	49.7 (0.3)	n=3	23.8 (1.2)	7.7 (0.04)
A (South West)	25	4.6 (0.46)	0.012 (0.003)	12.6 (2.7)	9.3 (2.4)	16.3 (2.1)	44.2 (7.4)	2.30	25.2 (1.6)	7.5 (0.21)
	75	4.5 (0.48)	0.014 (0.006)	14.8 (4.0)	11.9 (3.1)	18.8 (5.9)	44.3 (6.9)	n=3	24.7 (1.8)	7.5 (0.22)

Table 6-1 Arithmetic mean (± standard deviation); DO = dissolved oxygen, Chl_a = chlorophyll_*a*, SS = suspended solids, VSS = volatile suspended solids, TOC = total organic carbon, IC = inorganic carbon, VAC = vertical light attenuation coefficient, n = 4 grab samples during period 16th – 28th February 2005.

Location	Depth (cm)	DO (mg/L)	Chl_a (mg/L)	SS (mg/L)	VSS (mg/L)	TOC (mg/L)	IC (mg/L)	VAC (Kd [PAR] m-1	T [ºC]	pH
I (North East)	25	9.6 (1.91)	0.010 (0.009)	12.5 (0.8)	11.3 (5.6)	17.9 (8.5)	29.8 (8.0)	2.31	20.2 (1.0)	8.2 (0.47)
	75	10.0 (1.91)	0.025 (0.011)	33.6 (19.2)	14.4 (5.6)	22.0 (8.0)	27.8 (8.1)	n=4	19.3 (0.3)	8.4 (0.47)
G (North West)	25	12.1 (1.77)	0.278 (0.468)	16.9 (12.0)	15.6 (9.4)	26.2 (9.2)	24.3 (11.7)	2.16	19.8 (1.3)	8.6 (0.27)
	75	13.5 (3.39)	0.058 (0.039)	21.1 (5.9)	11.3 (8.3)	27.3 (12.2)	23.9 (12.2)	n=4	18.9 (0.6)	8.7 (0.34)
E (Centre)	25	12.2 (1.91)	0.010 (0.002)	11.5 (4.0)	9.3 (5.0)	25.8 (8.0)	22.2 (10.1)	2.61	19.9 (1.2)	8.5 (0.23)
	75	11.4 (5.3)	0.532 (0.706)	47.5 (33.2)	23.5 (21.1)	23.0 (6.2)	24.2 (8.3)	n=3	19.0 (1.3)	8.6 (0.14)
A (South West)	25	8.0 (4.81)	0.124 (0.169)	25.0 (25.6)	20.7 (20.4)	21.4 (7.7)	23.0 (11.1)	2.25	21.8 (0.5)	7.3 (0.12)
	75	8.7 (0.64)	0.231 (0.275)	112.4 (124.7)	58.9 (58.5)	23.1 (8.8)	23.0 (11.8)	n=4	20.7 (0.1)	7.5 (0.31)

Table 6-2 Arithmetic mean (± standard deviation);); DO = dissolved oxygen, Chl_a = chlorophyll_*a*, SS = suspended solids, VSS = volatile suspended solids, TOC = total organic carbon, IC = inorganic carbon, VAC = vertical light attenuation coefficient, n = 4 grab samples during period 1st – 11th May 2005.

Biomass

As the standard proxy for algal concentration; chlorophyll_*a* concentrations between locations are shown in Table 6.1 and 6.2. Chlorophyll_*a* concentrations observed during February 2005 at all locations were extremely low by comparison with the findings of Sweeney (2004); approximately 1.5 orders of magnitude lower than would be typical of a facultative WSP. This was reflected in the similarly low concentrations of suspended and volatile suspended solids; which again, were approximately 1.3 orders of magnitude lower than the mean value of 128 mg/L of Sweeney (2004). The measurements undertaken by Sweeney (2004) were completed prior to the change in pre-treatment at the Bolivar WWTP; specifically the incorporation of an activated sludge system prior to release of this treated effluent into the pond system and the conversion of the WSP into a maturation pond. The substantial differences observed between these studies in terms of biomass concentration were likely to reflect changes in influent characteristics following commissioning of the activated sludge plant during 2001. Work reported in Yamamoto (2007) and Yamamoto et al. (2010) was conducted concurrently at Bolivar with the work presented in this Thesis; Yamamoto (2007) placed a series of transparent microcosms at the NW sampling site and 'spiked' the microcosm tubes with either a nitrate/nitrite or ammonia solution (pond water only in control) in order to track the progress of in-situ nitrification potential of the Bolivar WSP. Increases in chlorophyll_*a* concentrations within each microcosm treatment during incubation (21 days) were between approximately 1.5 to 1.8 orders of magnitude in both treatment and control microcosms: but increased in absolute terms only to relatively low levels (40 – 600 µgChl_*a*/L) suggesting that nitrogen limitation was not likely to be responsible for the extremely low in-situ chlorophyll_*a* concentrations observed in the ponds. Other explanations for low phytoplankton

productivity considered were carbon limitation, wind induced mixing, clearance by zooplankton, photoinhibition and sedimentation.

Such low concentrations of chlorophyll_*a* in a WSP can be considered very unusual as a search of the literature did not reveal other examples; this may reflect the unusual wastewater received by Bolivar WSP 1 (but see; von Sperling and Mascarenhas 2005) or more likely the relatively limited extent of research into maturation pond photobiology. Interestingly, recent observations of maturation ponds at Williamstown and Tanunda revealed a similar pattern of low chlorophyll_*a* and minimal light attenuation (N. Buchanan pers. com. 2010).

Changes in biomass concentration observed across the pond during the May 2005 sampling period were substantially more varied in comparison to those observed in February 2005. Chlorophyll_*a* concentrations during the May 2005 sampling period at the NE sampling location were of similar magnitude to those observed in February 2005, this often contrasted strongly with those observed at one or both depths at the other sampling locations. For example, at the NW sampling location (site) the mean chlorophyll_*a* concentration was approximately an order of magnitude higher than the NE site at the 25cm depth in May 2005, this was also the case in comparison to the NE and the SW site.

It was considered noteworthy that median chlorophyll_*a* and suspended solids concentrations varied significantly ($P<0.01$, 5% significance level, Kruskal-Wallis nonparametric one-way analysis of variance) with respect to depth at the NW, Centre and SW sites during May 2005. Differences in chlorophyll_*a* (algal biomass) concentration during May 2005 were not necessarily reflected in a substantial change in suspended solids, e.g. the NW site showed an order of magnitude difference in chlorophyll_a between the 25cm and 75cm depth with an *opposite* trend in suspended solids but not volatile suspended solids. The complexity in these patterns

was considered most likely to reflect variations in hydrodynamic conditions (stratification and possible preferential flow) as inferred by temperature profile variations (Section 6.3.2). It was considered noteworthy that a substantial sludge blanket (approximately 25cm depth) was present at the head of the pond in particular during the May sampling period, apparently due to inefficiency of the sludge clarifiers used in the activated sludge process (pers. com. Site Manager Bolivar 2005) and this was reflected in the high suspended solids/volatile solids observed at the SW monitoring location during May of that year.

Inorganic Carbon

Bacterial respiration is considered to be the main source of CO_2 for algal photosynthesis in wastewater treatment and many other aquatic systems (Chapter 2, 3, 5). Tables 6.1 and 6.2 show the results of the IC assay for WSP samples collected during February and May 2005. A substantial 'draw down' in terms of inorganic carbon was apparent during the May sampling period in comparison to the February sampling period; as was a general increase in pH and DO. These observations were considered consistent with the conclusion that rates of photosynthesis were higher during May. It was considered possible that the combination of relatively low IC during May and high pH at the NE, NW and Centre sampling sites could have limited photosynthesis during periods of the day (Azov 1982); assuming sufficiency with respect to other resources. That is, the relatively high algal biomass concentrations present at some sites during the May sampling period may have, by their photosynthetic activity, raised pH concentrations sufficiently high and drawn down concentrations of carbon substrate (IC) sufficiently low to produce limiting concentrations of this resource during the day. This possibility was supported by results shown in Chapter 5 where a combination of relatively high pH and moderate IC concentration (Treatment 2) were may have limited carbon substrate availability.

Further to this the NE sampling location displayed the least drawdown of IC in February compared to May and displayed the lowest phytoplankton concentration.

Light Attenuation

Measurements of pond vertical attenuation coefficients (VAC) (Table 6.1 – 6.2) were not clearly correlated with differences in chlorophyll_a concentration and by implication algal concentration. Light penetration through the water column was observed to be quite consistent when comparing the February and May sampling periods despite the substantially different chlorophyll_a concentration. This observation was considered likely to have resulted from changes in flocculent particle morphology; with a more floccular (transparent) biomass noted in field observations during the May period (Chapter 5, Section 5.3.1).

Representative examples of light attenuation curves used to calculate VAC were provided as Figures 6.2 and 6.3; and showed light intensity as a function of depth during the February and May 2005 sampling periods respectively. The attenuation function of Kirk (1984) was fitted to each data set (dotted line) and used to calculate VAC. A distinct contrast with respect to light attenuation was noted with respect to the observations of Sweeney (2004) and Weatherall (2001) where extinction of PAR in Bolivar WSP 1 was observed at a depth of typically no more than 30cm. On many occasions during field work in 2004 and 2005 the bottom of the pond was clearly visible to the naked eye. This was later assumed to provide opportunities for algal growth on the sediment during these periods; the extent of contribution of potential microphytobenthos (MPB) to algal productivity was not quantified and is acknowledged as a potential source of error in the calculation of oxygen dynamics. Significant light penetration to the sediment in a WSP can be considered very unusual and a search of the literature did not reveal other examples; as discussed above, recent observations of maturation ponds at Williamstown and Tanunda

showed a similar pattern of low chlorophyll_a and minimal light attenuation (N. Buchanan pers. com. 2010).

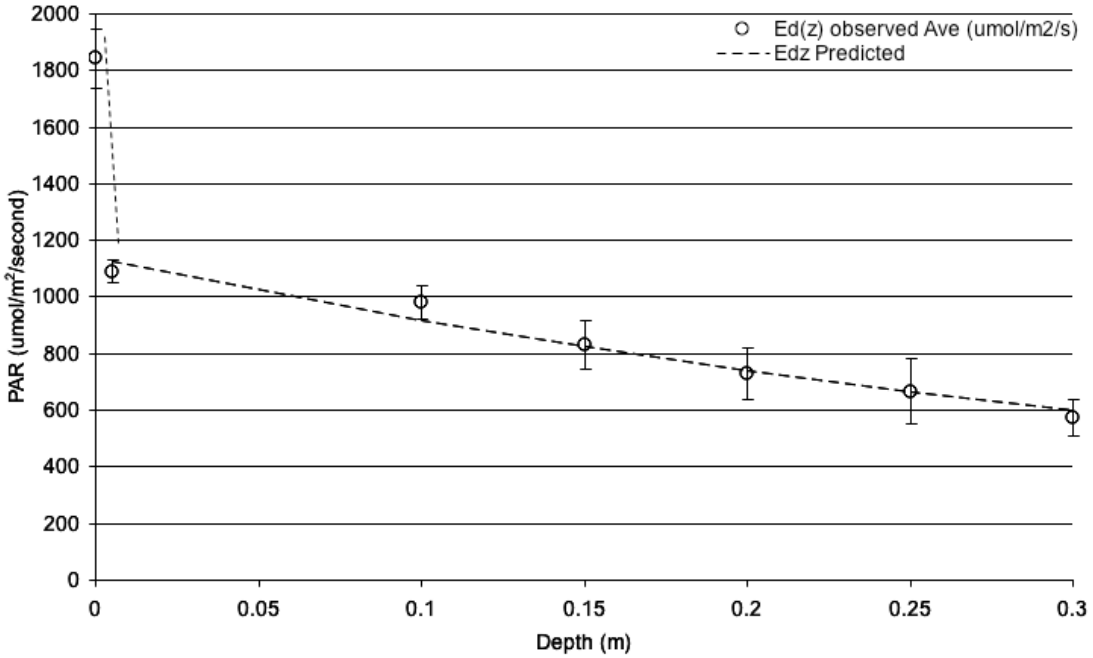

Figure 6-2 Scatter plot of representative data of PAR versus depth for NW (location I) February sampling period, Mean and standard deviation, n=3. Line of best fit (Kirk 84) used to calculate vertical attenuation coefficient (VAC = 2.14). Ed(z) = light intensity at depth z, Chlorophyll_*a* concentration = 0.019 mg/L.

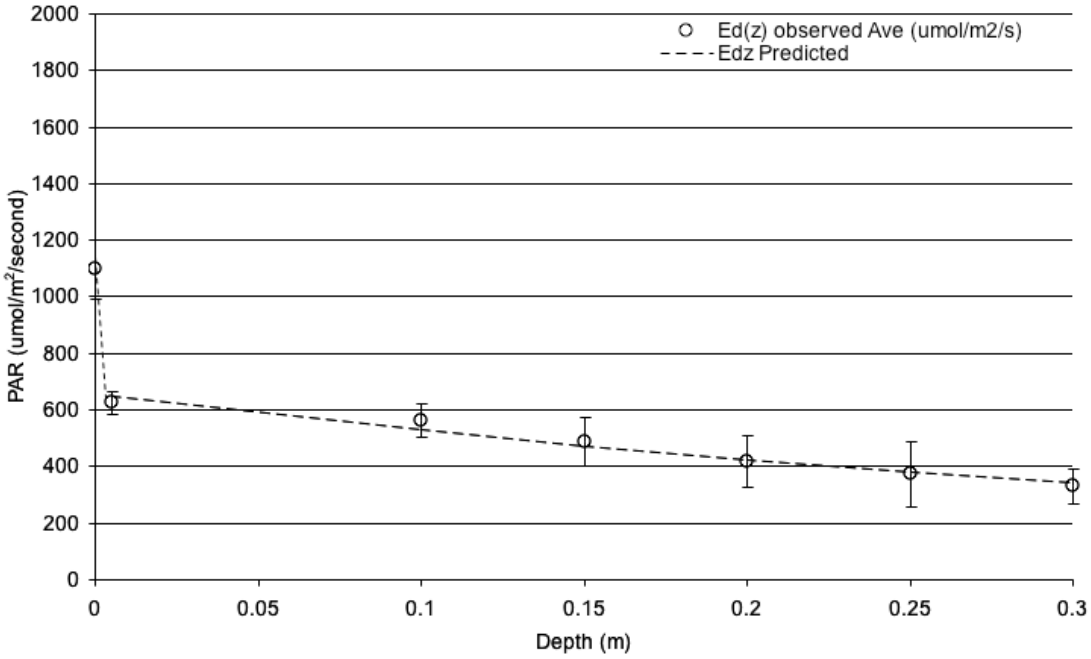

Figure 6-3 Scatter plot of representative data of PAR versus depth for NW (location I) May sampling period, Mean and standard deviation, n=4. Line of best fit (Kirk 84) used to calculate vertical attenuation coefficient (VAC = 2.14). Ed(z) = light intensity at depth z, Chlorophyll_a concentration = 0.278 mg/L.

6.3.2. Factors Associated with Patterns of Change in Pond Temperature and Thermal Stratification

The novel three-dimensional temperature profiling approach of Sweeney (2004) using a series of 'thermistor chains' was applied to assess thermal changes in the pond during each sampling period. Sweeney (2004) collected thermal profiles at 9 locations across the pond during 2001 and 2002, corresponding to the locations shown in Figure 6.1; in addition to individual temperature probes placed in three inlet and three outlet pipes. A description of the thermistor units is provided in Chapter 4 and in detail in Sweeney (2004). A thermistor chain was installed at each of the four monitoring stations to provide data of in-situ thermal gradient for calculation of stratification status and temperature in comparison to dissolved oxygen; with measurements logged at 10 minute intervals. Tables 6.3 and 6.4 show summaries of online data collected during the February and May sampling periods respectively and includes dissolved oxygen concentration, stratification status and

wind velocity. The temperature data shown in Tables 6.1 and 6.2 were collected for confirmation of calibration of the resident thermistor chains but were of low resolution in comparison to that obtained from the thermistor chains and were not included the following discussion.

The criteria for identifying stratification was provided by Sweeney (2004); with a stratification event being indicated by a temperature differential of $-0.6 < x > +0.6$ per meter of pond depth. Sweeney (2004) used a spline fit on this data; presumably to assist in the precise determination of thermal layer depth for the purposes of CFD simulation of hydraulic and thermal conditions. Such precision was considered unnecessary in the context of assessing oxygen dynamics without the benefit of contemporaneous CFD predictions for comparison. As such data from the 25cm nominal depth in the thermistor chain (equivalent depth to online DO probe) was compared by subtraction with the bottom thermistor and normalised to a depth of 1m to provide units identical to those of Sweeney (2004). This provided the quantity 'T25_75' in units of °C/m.

From inspection of Tables 6.3 and 6.4 it is apparent that average stratification across the pond displayed a distinct and contrasting pattern when comparing the February and May sampling periods. Positive stratification events, i.e. temperature gradient per metre > 0.6°C towards the surface, were dominant during the February period with the exception of the NE monitoring location, where thermal gradient conditions were on average iso-thermal. The NW sampling location displayed strongly stratified conditions during the entire 11 day February sampling period, with a mean thermal gradient of 6.5°C/m and a maximum value of 10.8°C/m. The majority of stratification events observed in summer by Sweeney (2004) were of duration less than 10 hours; however some longer term stratification events were observed, especially at the NW and SW sampling site; with both of these sites displaying

stratification events lasting 50 hours or more greater than 30% of the time (Sweeney et al. 2005a). On average the pattern of mean temperature variation at both the 25cm depth and at the bottom of the pond at each location during the February sampling period was considered to be quite small as indicated by the standard deviations calculated from this online data when compared to the observed maxima and minima (Table 6.3). This was considered consistent with the observation that stratification events during this period were of generally long duration during the February sampling period (implying limited mixing).

During the May Sampling period a contrasting pattern of stratification was observed (Table 6.4), with the most frequent stratification events showing an inverse thermocline (warmer at pond bottom), with the NW site displaying isothermal conditions on average; all other locations displayed negative stratification on average. Summary data consisting of 'box and whisker plots' (box-plots) of temperature measured at each monitoring location during the February and May sampling periods are shown in Figures 6.4-6.6. In each case the horizontal bar represents the median value, the shaded area 'box' shows the inter-quartile range, whilst the 'whiskers' show absolute range for each data set. Pond temperature at the 25cm depth in each location is displayed in Figure 6.4, and reveals a substantial difference in median temperature at 25cm depth at all locations between the two sampling periods; with the May median pond temperature being cooler; this was consistent with the contrasting patterns of change in daily temperature between these two sampling periods (Tables 6.3 and 6.4). Variations around the median temperature values were observed to be considerably greater during February compared to the May sampling period at all locations with the exception of the SW sampling site. This difference with respect to the SW sampling site was considered to reflect the proximity of the pond inlets (influent) (Sweeney 2004).

Figure 6.5 and 6.6 shows box plots of temperature at all depths for the February and May sampling periods respectively, with each depth category grouped together. It was considered of note that the median value and variation around this measure of central tendency during February was generally consistent across all sites with the notable exceptions of the NW site where a highly persistent stratification event occurred and the SW site where variation around the median was comparatively low. The observation of a sludge blanket at the SW location was considered to explain this anomaly at the SW site; it was considered likely that the sludge provided insulation from the extremes in temperature observed during this period. A similar observation with respect to the SW site was noted for the May sampling period, where variation around the median at the 75cm depth (pond bottom) was low, again this was considered to reflect the presence of a sludge blanket at this location. Variation at the SW location during May was, however, increased at the shallower depths above this sludge blanket; this was considered likely to reflect the proximity of this site to the warmer influent during the cooler time of year. Whilst the summary data provided in Tables 6.3 and 6.4 and Figures 6.5 and 6.6 was considered to adequately characterise the average pattern of thermocline variation across the pond during these two time periods; a more 'holistic' or big-picture assessment of variation was apparent through inspection of surface plots of data for each 10 minute data logging event.

Location	Depth	DO (mg/L)	T (°C)	Tmax (°C)	Tmin (°C)	TD25_75 (°C/metre)	S (±)	Air Temperature (°C)	Wind Speed (km/h)	Wind Direction (°)
I (North East)	10cm	-	23.2 (2.0)	27.5	18.8	0.2 (0.6) Max = 4.92 Min = -0.2	Iso-thermal	21.5 (4.6) Max = 35.7 Min = 13.5	12.7 (8.3)	170 (95) (Southerly)
	25cm	4.7 (1.4) Max = 8.9 Min = 1.2	23.1 (1.9)	27.5	18.8					
	50cm	-	22.9 (1.8)	27.2	18.7					
	Bottom	-	23.1 (1.4)	27.4	18.8					
G (North West)	10cm	-	23.8 (1.7)	27.6	20.3	6.5 (1.5) Max = 10.8 Min = 4.0	Strongly +ve			
	25cm	5.7 (1.2) Max = 9.8 Min = 2.9	26.3 (1.4)	29.4	23.1					
	50cm	-	23.8 (1.5)	27.1	20.6					
	Bottom	-	23.0 (1.0)	25.1	20.7					
E (Centre)	10cm	-	23.1 (1.8)	27.1	18.8	-0.6 (1.6) Max = 4.4 Min = -3.2	Iso-thermal			
	25cm	4.2 (1.3) Max = 8.0 Min = 0.4	22.9 (1.8)	27.0	18.7					
	50cm	-	22.8 (1.8)	26.5	18.7					
	Bottom	-	23.3 (2.1)	27.1	18.7					
A (South West)	10cm	-	23.2 (2.0)	27.7	18.6	1.8 (3.7) Max = 10.46 Min = -5.3	+ve			
	25cm	4.9 (1.4) Max = 8.6 Min = 1.8	23.4 (1.9)	27.0	18.7					
	50cm	-	22.8 (1.8)	26.6	18.5					
	Bottom	-	22.5 (0.5)	23.1	21.5					

Table 6-3 Arithmetic mean (± standard deviation) and sample size (1712 measurements at 10 minute intervals unless specified); for pond dissolved oxygen concentration (DO), T = temperature, Tmax = maximum temperature recorded, Tmin = minimum temperature recorded, TD25_75 = temperature difference between 25cm depth and bottom (75cm nominal depth), S = stratification status (+ve > 0.6C per metre, -ve < -0.6C per metre), during the period 16th – 28th February 2005.

Location	Depth	DO (mg/L)	T (°C)	Tmax (°C)	Tmin (°C)	TD25_75 (°C/metre)	S (±)	Air Temperature (°C)	Wind Speed (km/h)	Wind Direction (degrees)
I (North East)	10cm	-	16.7 (0.8)	19.0	14.6	-3.6 (0.3) Max = -1.4 Min = -3.9	Strongly -ve	17.8 (4.3) Max = 31.5 Min = 9.4	11 (6)	142 (98) (South Easterly)
	25cm	8.5 (1.7) Max = 12.7 Min = 3.8	16.6 (0.8)	19.0	14.6					
	50cm	-	16.7 (0.7)	18.5	15.0					
	bottom	-	18.4 (0.8)	20.5	16.5					
G (North West)	10cm	-	17.7 (0.8)	19.5	16.0	-0.30 (1.4) Max = 2.8 Min = -3.0	isothermal			
	25cm	8.4 (2.8) n= 1488 Max = 14.2 Min = 0	18.4 (0.8)	20.2	16.7					
	50cm	-	17.8 (0.9)	19.8	16.0					
	bottom	-	18.5 (0.5)	19.6	17.7					
E (Centre)	10cm	-	17.1 (0.9)	19.0	14.9	-2.0 (1.3) Max = 1.5 Min = -4.3	-ve			
	25cm	8.9 (1.7) n = 1515 Max = 13.2 Min = 5.4	16.9 (0.9)	18.8	14.9					
	50cm	-	16.9 (0.9)	18.8	14.9					
	bottom	-	18.0 (0.7)	19.2	16.6					
A (South West)	10cm	-	18.5 (1.3)	22.3	15.6	-0.7 (2.6) Max = 7.1 Min = -7.4	-ve			
	25cm	5.9 (2.4) n = 1506 Max = 13.8 Min = 2.5	19.7 (1.3)	23.7	16.9					
	50cm	-	18.6 (1.1)	21.7	15.9					
	bottom	-	20.1 (0.3)	20.7	19.6					

Table 6-4 Arithmetic mean (± standard deviation) and sample size (1517) measurements at 10 minute intervals unless specified); for pond dissolved oxygen concentration (DO), T = temperature, Tmax = maximum temperature recorded, Tmin = minimum temperature recorded, TD25_75 = temperature difference between 25cm depth and bottom (75cm nominal depth), S = stratification status (+ve > 0.6C per metre, -ve < -0.6C per metre), during the period 1st – 11th May 2005.

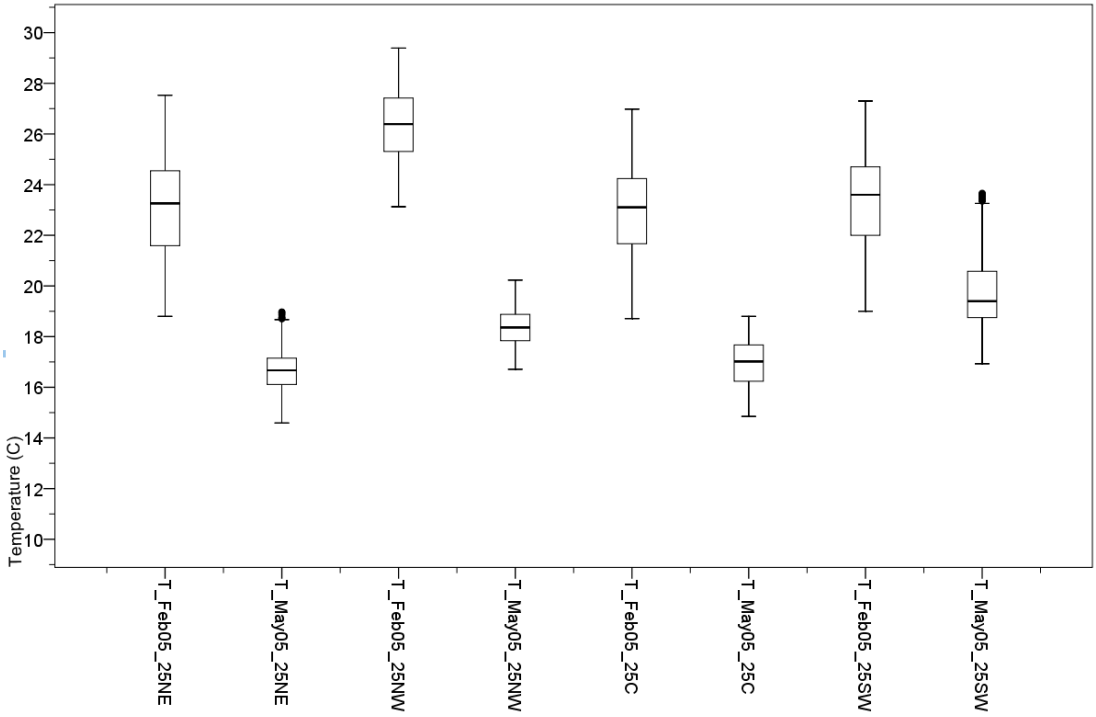

Figure 6-4 Box and Whisker plots of pond temperature for each sampling location at nominal depth of 25cm below the surface, February and May 2005.

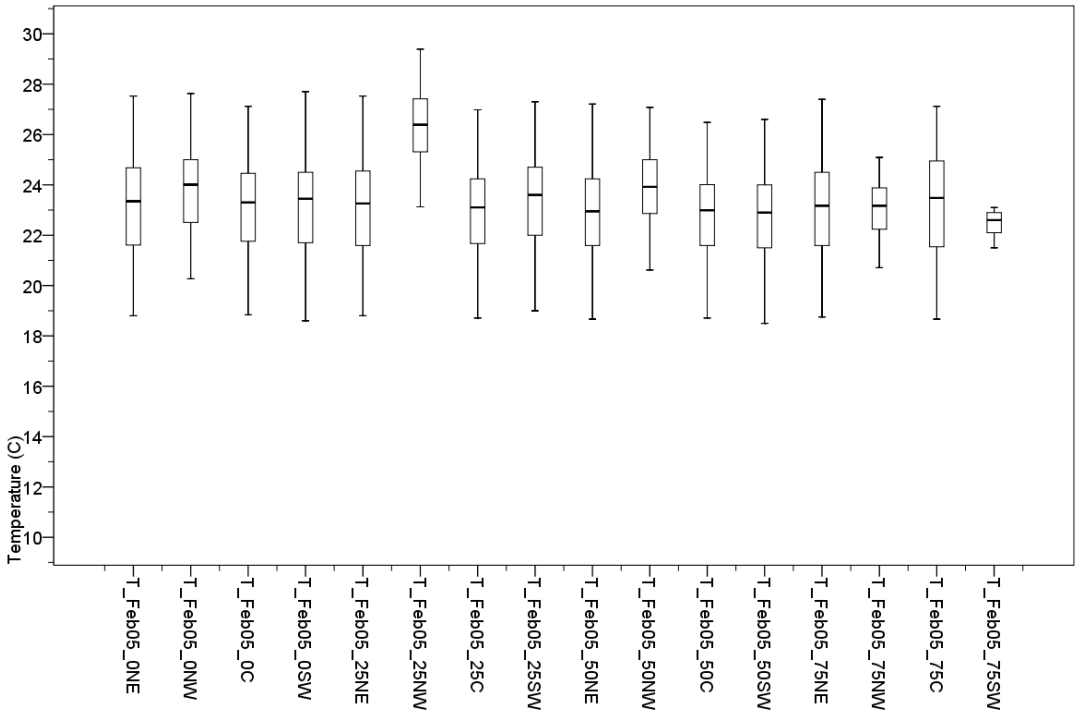

Figure 6-5 Box and Whisker plots of temperature for each location at each depth (0 = 10cm (surface), 25cm nominal, 50cm nominal 75cm nominal depth (bottom). February 2005.

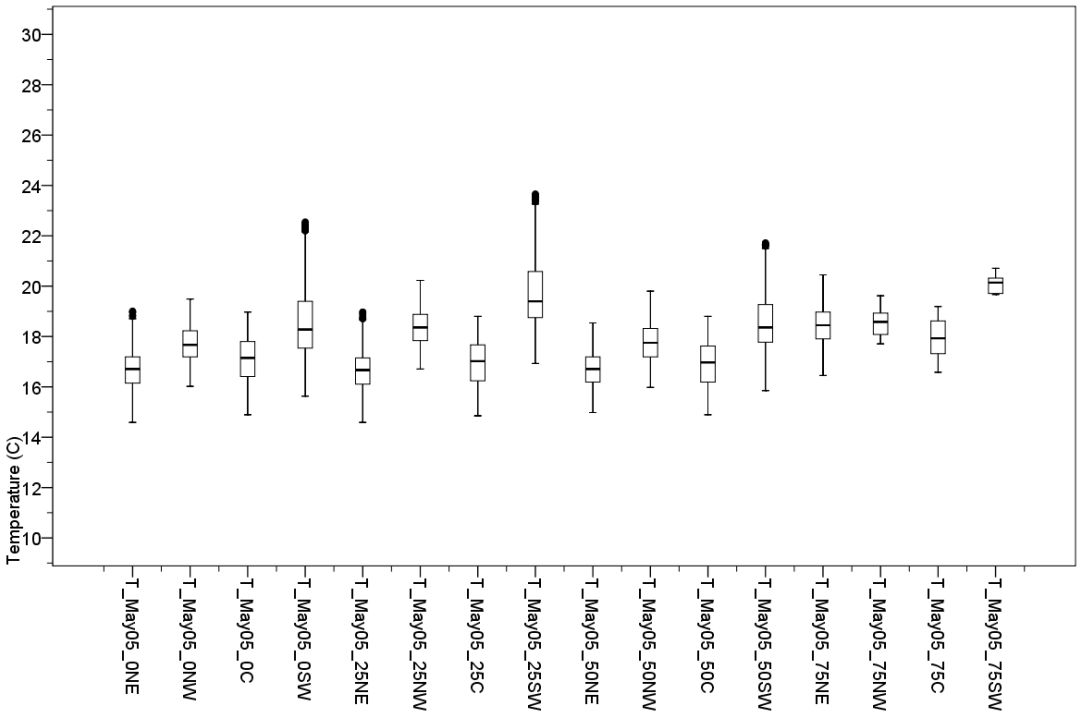

Figure 6-6 Box and Whisker plots of temperature for each location at each depth (0 = 10cm (surface), 25cm nominal, 50cm nominal, 75cm nominal depth (bottom), May 2005.

The surface plotting method of Sweeney (2004) was modified to include dissolved oxygen and PAR data (Appendix A). The surface plots were 'stitched' together in sequence to produce a 2D time series (data movie files) and are provided on the attached optical disk (Appendix B) for viewing of each sampling period. The complete online data set are presented in the 3 movie files for each of the February and May sampling periods.

A. DO (mgDO/L), T ºC (25cm depth), PAR (umol/m^2/s), Wind (km/h)
B. DO, T25_75 stratification (°C/metre), PAR, Wind
C. DO_rate (mgDO/hour), T25_75 stratification (°C/metre), PAR, Wind

An 'average day' data set was then constructed to provide a means of reviewing longer-term patterns of change. This was constructed by taking an average of each 10 minute time-step across all of a sampling period from midnight to midnight. The

resulting data file of 144 average values (10 or 11 days data) at each 10 minute time increment was used to prepare another series of movie files of the form D, E and F for both February and May.

D. DO (mgDO/L), TºC (25cm depth), PAR (umol/m^2/s), Wind (km/h)
E. DO, T25_75 stratification (°C/metre), PAR, Wind
F. DO_rate (mgDO/hour), T25_75 stratification (°C/metre), PAR, Wind

February 2005 Thermal Gradient Surface Plots

Figures 6.7 – 6.10 display an 'average day' frame from each of four periods; midnight, dawn, mid-day and sunset for the February period. In each case an average two-dimensional 'Kriging' least squares model was constructed of temperature data collected over the full period 11 days of sampling at that time of day. The Kriging 2D interpolant across the 'pond' surface was determined by the empirical temperature profile data collected at each of the four monitoring locations; each black line on the surface is an 'iso-therm'; a line of equal temperature. The orange coloured areas of the pond indicated where a vertical thermal profile was predicted to have a higher temperature (> +0.6°C/m) at the 25cm depth from the pond surface than at the bottom of the pond, a positive stratification. White colouring showed isothermal conditions through the depth profile; where the temperature differential between the 25cm depth and bottom of the pond was predicted to be within the range; -0.6°C/m < x <0.6°C/m. The blue colouring showed conditions of negative stratification, where the pond was predicted to have a lower temperature (< -0.6°C/m) at the surface compared to the bottom of the pond. The empirical temperature data was collected at each of the four monitoring locations, identified by

a cross (+). Whilst the spatial resolution of the surface plots in comparison to the investigation of Sweeney (2004) was reduced; the surface plots (6.70 – 6.10) were considered to display a strong qualitative similarity with the findings of the work by Sweeney (2004); particularly with respect to the persistence of stratification at the NW and SW monitoring sites. It was however considered very likely that the use of data with a higher spatial resolution (all 9 sampling locations) would improve the accuracy of predicted temperature at locations between the sites. This was, however, considered unnecessary for the purposes of qualitative comparison of spatial trends of temperature and dissolved oxygen (Section 6.3.3).

At midnight (Figure 6.7) both the NW and SW locations were, on average, positively stratified whilst the Centre and NE sites displayed isothermal conditions. Wind direction was, on average, from the southeast with an average speed of approximately 14km/h. By interpolation provided by the Kriging method, the pond was predicted to display negative stratification in the eastern portion (blue colour); this prediction however would require validation against the higher spatial resolution data set and was considered unreliable. Such limitations of interpolation of surface plots (as for other models of data) are an inherent property of such statistics and are well recognised in the literature.

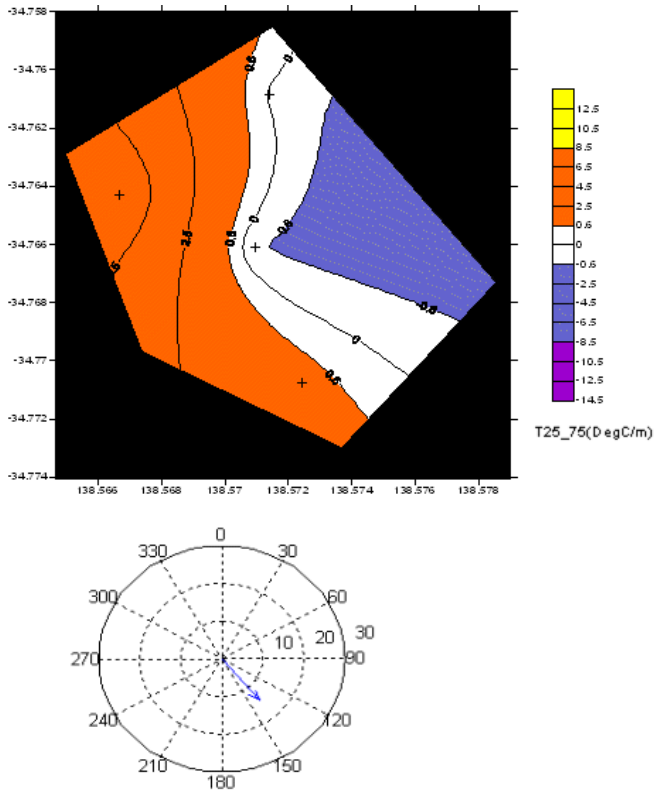

Figure 6-7 Surface plot of thermal gradient; average difference of 25cm nominal depth with temperature at the bottom of thermistor chain. Rose plot of wind velocity; average of 10 days data for Midnight (24:00 – 00:10), 17th – 27th February 2005.

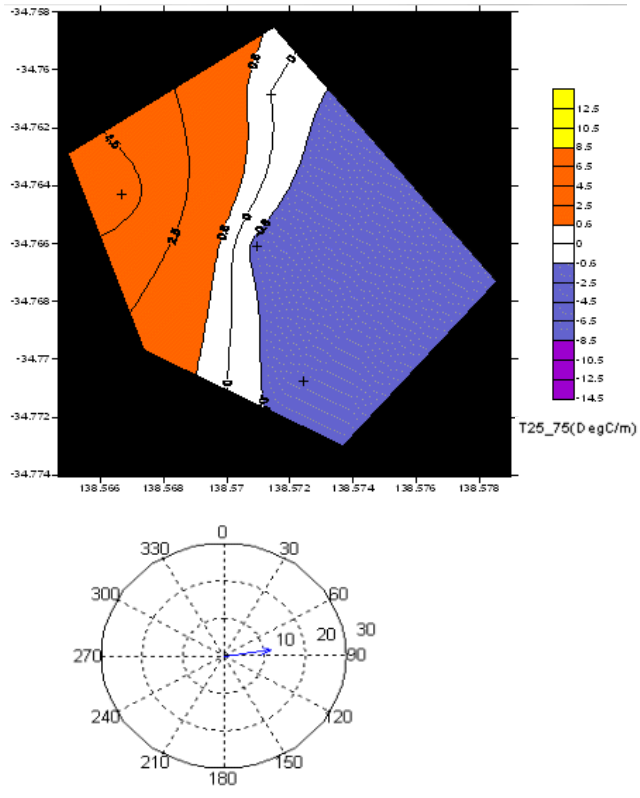

Figure 6-8 Surface plot of thermal gradient; average difference of 25cm nominal depth with temperature at bottom of thermistor chain. Rose plot of wind velocity; average of 10 days data for 10 minute period at Dawn 17th – 27th February 2005.

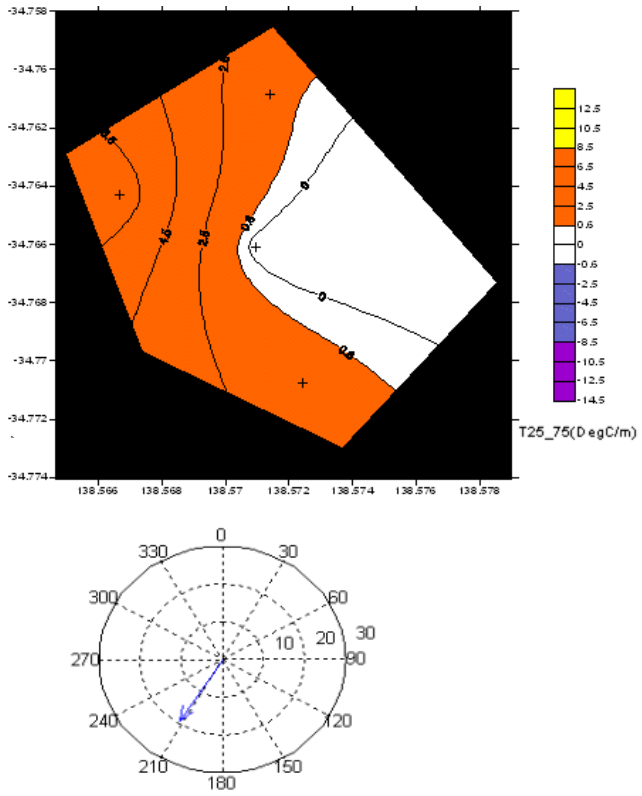

Figure 6-9 Surface plot of thermal gradient; average difference of 25cm nominal depth with temperature at bottom of thermistor chain. Rose plot of wind velocity; average of 10 days data for 10 minute period at Mid-day 17th – 27th February 2005.

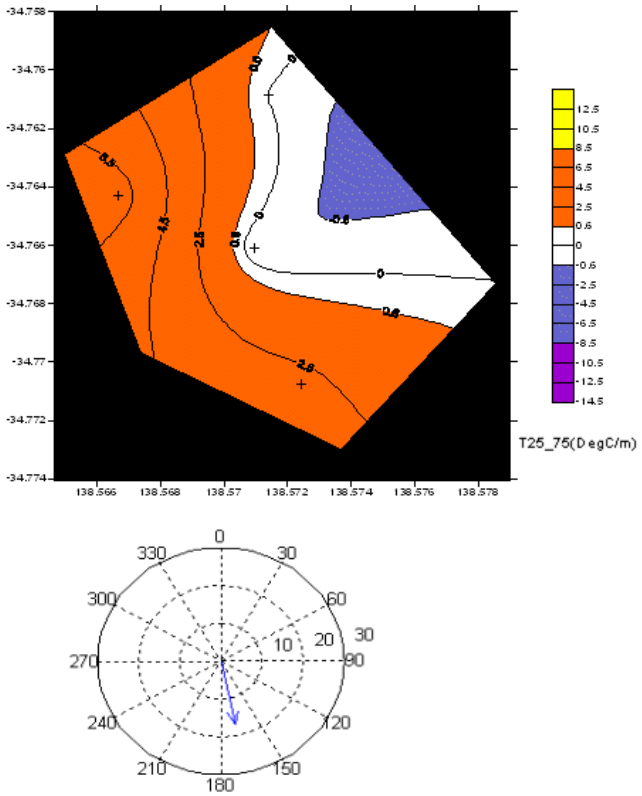

Figure 6-10 Surface plot of thermal gradient; average difference of 25cm nominal depth with temperature at bottom of thermistor chain. Rose plot of wind velocity; average of 10 days data for 10 minute period at Sunset 17th – 27th February 2005.

By dawn (Figure 6.8) a strong positive stratification remained at the NW location but had changed to a negatively stratified condition at the SW and Centre locations, presumably due to efflux of thermal energy from the pond surface during the night. The NE site remained isothermal. Average wind direction at dawn during the February sampling period was from the east with an average speed of approximately 10km/h. By mid-day, on average (Figure 6.9), a positive thermal gradient was present at all monitoring stations with the exception of the centre location, again with the strongest positive thermal gradient being present at the NW site; a result of the heat absorbed into the pond from solar insolation. Average wind direction at mid-day during the February sampling period was from the south south-west with an average speed of 20km/hr (known locally as the summer sea breeze). At sunset, on average (Figure 6.10), a pattern of positive stratification was present at the NW and SW locations with isothermal conditions at the Centre and NE locations. Average wind direction at sunset was from the SSE at a speed of approximately 18 km/h.

May 2005 Thermal Gradient Surface Plots

Figures 6.11 – 6.14 display an 'average day' frame from each of four periods; midnight, dawn, mid-day and sunset for the May period. At midnight, on average (Figure 6.11), the pond, in contrast to the February monitoring period, displayed negative thermal stratification at all monitoring locations, that is, temperature at the bottom of the pond was higher than that at the surface. Average wind direction was similar to that observed during February at midnight, approximately EES with a speed of 10km/h. During the dawn period (Figure 6.12) the pattern of negative stratification across the pond remained unchanged with an average easterly wind direction of approximately 8km/h. By mid-day in May, on average (Figure 6.13), both the NW and SW monitoring stations displayed isothermal conditions, with the

Centre and NE locations maintaining negative stratification. Average wind direction was from approximately WWS at a speed of 13 km/h. By sunset on average (Figure 6.14), a positive thermal stratification had developed at the NW and SW locations, with isothermal conditions in the Centre location, whilst the NE site remained in a condition of strong negative stratification. Average wind direction was from the South, with an average speed of approximately 13km/h.

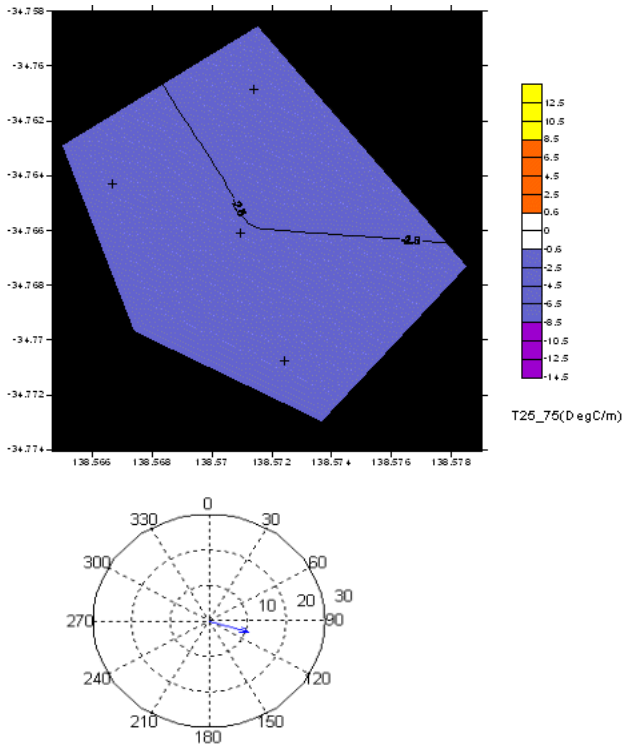

Figure 6-11 Surface plot of thermal gradient; average difference of 25cm nominal depth with temperature at bottom of thermistor chain. Rose plot of wind velocity average of 10 days data for 10 minute period at Midnight (24:00 – 00:10) 1st – 11th May 2005.

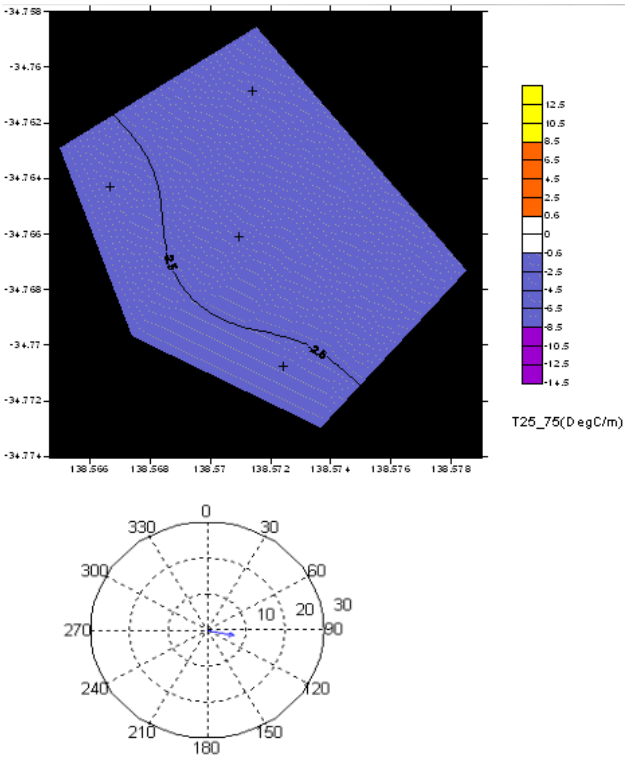

Figure 6-12 Surface plot of thermal gradient; average difference of 25cm nominal depth with temperature at bottom of thermistor chain. Rose plot of wind velocity average of 10 days data for 10 minute period at Dawn 1st – 11th May 2005.

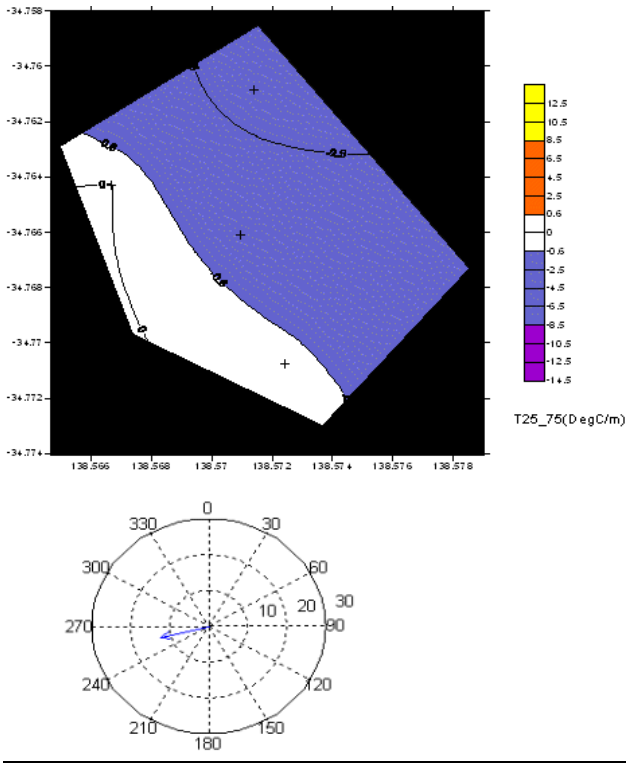

Figure 6-13 Surface plot of thermal gradient; average difference of 25cm nominal depth with temperature at bottom of thermistor chain. Rose plot of wind velocity average of 10 days data for 10 minute period at Mid-day 1st – 11th May 2005.

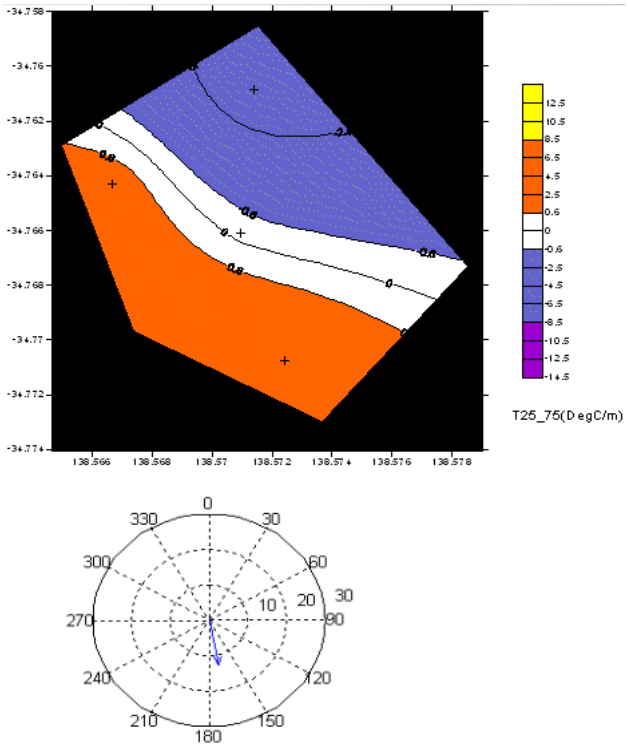

Figure 6-14 Surface plot of thermal gradient; average difference of 25cm nominal depth with temperature at bottom of thermistor chain. Rose plot of wind velocity average of 10 days data for 10 minute period at Sunset 1st – 11th May 2005.

Thermal Gradient Conclusions

The 'average day' summaries presented above for February and May were considered to provide a satisfactory representation of the pattern of average thermal stratification at the four monitoring locations of the pond. Qualitative assessment of the high temporal resolution thermal gradient data (electronic file B) for the February sampling period revealed perhaps a surprising degree of stability in terms of stratification status at the four locations even during periods of strong wind, in apparent contrast to the findings of Sweeney 2004. It was considered possible that this increase in stratification persistence may have resulted from the dramatic decline in planktonic algal chlorophyll_a and suspended solids (turbidity) in the pond following conversion to AS effluent in late 2001 and the substantially higher penetration of light (and heat) into the pond. Sweeney (2004) in an extensive assessment of pond stratification, presented results consistent with the currently

accepted view of pond energy transfer, that higher levels of incident irradiance at the pond surface promoted stratification and that windy conditions forced the hypolimnion deeper or disrupted stratification to induce mixing. The pattern of more persistent positive thermal stratification observed at the NW and SW monitoring stations during both the February and May sampling periods was considered consistent with the findings of Sweeney (2004). It was therefore considered unsurprising that the degree of stratification appeared most strongly associated with insolation; with slow cooling progressing during the evening.

In comparison to the February sampling period, patterns of positive thermal stratification during May were substantially less persistent at all monitoring stations, consistent with the findings of Sweeney et al. (2005 a) (reporting data from 3rd June, 2001).

When positive thermal stratification events were observed during May 2005 they tended to occur at the NW and SW sites most frequently and would then alter state to an iso-thermal configuration (inference of mixing) as insolation declined during the afternoon. The substantially reduced heat transfer into the pond during May (and out at night) due to the lower temperature was considered likely to allow the development of persistent negative thermal stratification gradients, especially at the NE sampling location. The particularly persistent negative stratification event at the NE sampling site during May 2005 may also have been a function of reduced light attenuation (and increased heating at depth during the day and cooling of the surface at night) due to particularly low biomass concentrations at this location. The pattern of stratification at the SW sampling location was considered likely to reflect in part the inflow of relatively warm influent from the pond inlets and the presence of the sludge blankets near the inlets (Sweeney 2004). Whilst the SW site remained very likely to stratify i.e. for approximately 100 hours during May sampling period, the

NE site remained negatively stratified for the entire sampling period (10 days). The contrast with the findings of Sweeney (2004), particularly with respect to persistent negative stratification would require an additional round of CFD modelling and data collection to determine if this was likely to be a function of changes in sludge accumulation patterns and hydraulic flow or biomass induced light attenuation or a combination of both. Interestingly the NE sampling location displayed very low phytoplankton biomass concentrations at both depth increments during both sampling periods. It was considered possible that this characteristic contributed to the consistently higher temperature at depth due to improved penetration of light through the pond. Nevertheless it was not considered possible to separate the relative influence of hydraulic flow and light penetration without CFD modelling and substantially more data collection.

In an attempt to more explicitly reveal the factors associated with the patterns of change in pond temperature and thermal stratification a factor analysis was conducted on the differenced time-series variables T25-75 (Tdiff_1), wind and PAR. These are provided for the February and May 2005 sampling periods as Figures 6.15 and 6.16 respectively (Appendix C). The factor analyses were conducted using a time-series of all online data for these parameters in order to reveal if correlations were apparent amongst these variables and to determine if a pattern of factor and variable association was observed that was consistent with the assertion above that wind velocity was likely to impact strongly upon the pattern of thermal stratification across the pond. A correlation that was not clearly apparent in the qualitative assessments of the 2D time-series data movie files. A factor analysis may allow correlations amongst a number of variables to be summarised as being due to two or more components (Masters 1995). The components 'factored out' are, by definition, independent of each other. If variables aggregate at opposite ends of a component

scale it is an indication that they are inversely correlated with respect to that component. If variables form a group (circled) this is indicative that they may be impacted upon by the component(s) in a similar way. Generally it is considered that a parameter(s) loading on a component scale should be greater than 0.5 to provide confidence that a conclusion regarding a strong

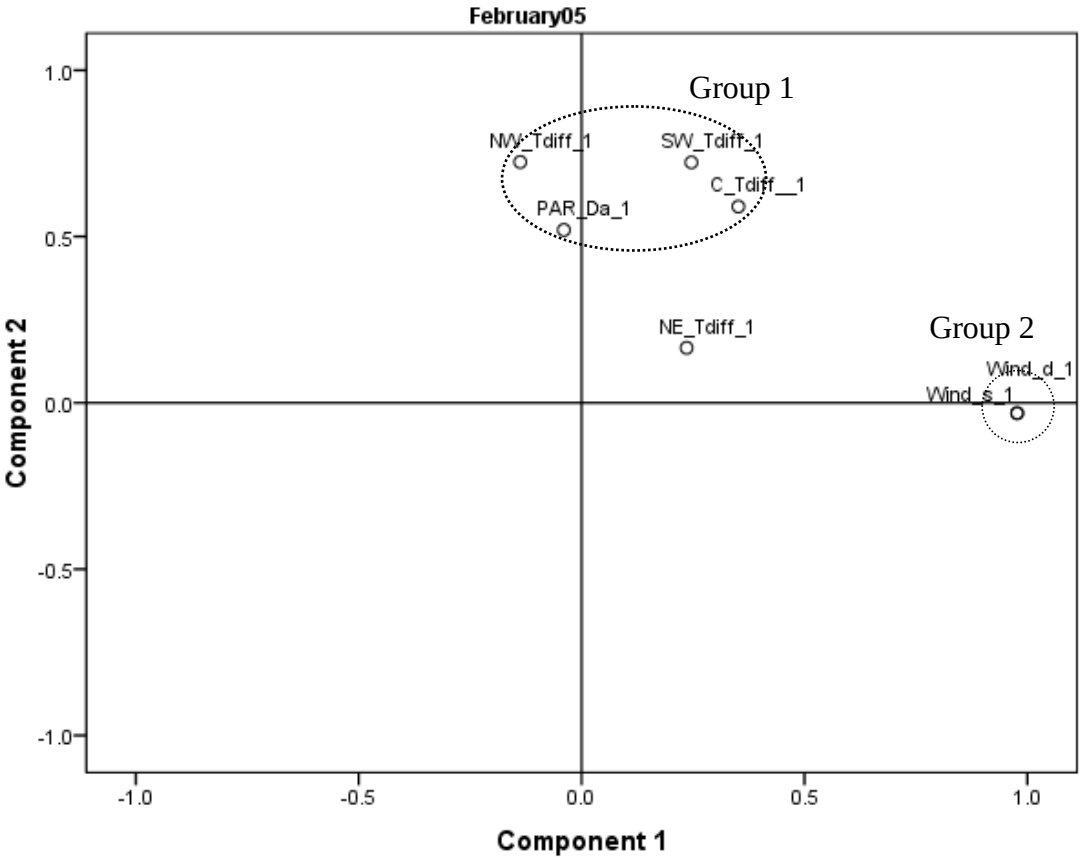

Figure 6-15 Factor analysis of thermal stratification; T25_75 (Tdiff), PAR, wind speed and direction for February 2005 sampling period. Time-series (February 17th – 27th).

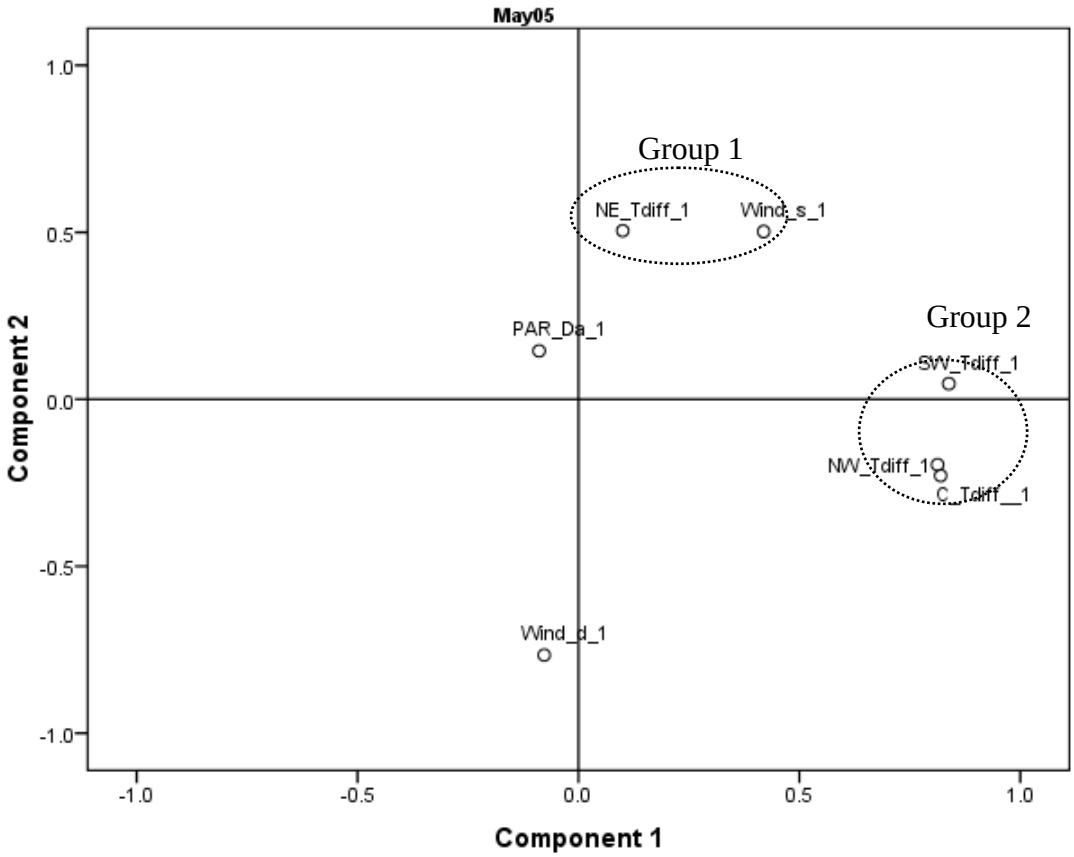

Figure 6-16 Factor analysis of thermal stratification; T25_75 (Tdiff), PAR, wind speed and direction for May 2005 sampling period. Time-series (May 1st – 11th).

association with that factor can be validly drawn (Masters 1995). A factor analysis may provide information concerning the strength of correlations between the parameters assessed but does not provide direct information regarding the cause of these correlations. Therefore, conclusions drawn regarding the identity of 'causal' factors that are presumed to determine the observed correlations remain a matter of judgment and may not be clearly apparent or unambiguously identifiable (Masters 1995). Dotted circles were drawn on each factor analysis to 'contain' variables that appeared to group together (note: not intended to link groups between figures); a component score of 0.5 was used as a delineator to indicate loading of a variable(s) onto a component factor. Full details of the factor analysis are provided in Appendix C. Inspection of Figure 6.15 revealed that thermal stratification during the February 2005 sampling period displayed a strongly positive correlation with PAR at all

sampling locations (Group 1) with the exception of the NE site. The loading of the Group 1 and Group 2 variables on separate component factors indicated that, by definition, stratification status, at these three locations (NW, SW and Centre) was independent of wind velocity during this sampling period. This was not the case with respect to stratification status at the NE sampling location; its loading was approximately equal upon both components, and this was interpreted to indicate that PAR *and* wind velocity were likely to influence stratification status. Whilst wind velocity was not shown to correlate with stratification status during the February sampling period, at all but the NE sampling sites, it was considered likely that hypolimnion depth would vary in response to changes in wind velocity (Sweeney 2004).

Inspection of Figure 6.16 revealed some differences in the pattern of stratification behaviour during the May sampling period in comparison to that observed during February. Specifically, wind speed was loaded almost equally on both components, although slightly less than the 0.5 correlation coefficient criterion on component 1, however the strength of the association with both components was interpreted to suggest that stratification status was likely to be positively correlated with wind speed at all sampling locations. The stratification status at the NE sampling location displayed a strong negative correlation with wind direction, whilst stratification status was by definition independent of wind direction at the other sampling locations. It was considered noteworthy that the wind direction and speed displayed a negative correlation with one another, this was considered to reflect the observation that winds, during the May sampling period, tended to be stronger when arising from the SE.

Conclusions

It was considered that the analysis of the data presented above provided sufficient

information to conclude the following;

- Periods of positive thermal stratification were most persistent during the February sampling period.
  - A positive thermal stratification event occurred for the entire sampling period at the NW sampling location.
  - The persistence of positive thermal stratification events during this period was highest at the NW, Centre and SW sampling locations.
  - The average pattern of thermal stratification observed across the pond during this period was qualitatively consistent with that observed by Sweeney (2004) despite the lower spatial resolution of the data presented.
  - The impact of changes in wind speed on stratification status during this period was considered most likely to result in an increase in hypolimnion depth (by inference) rather than breakdown of stratification at the NW, Centre and SW sampling locations.
  - It was considered possible that the dramatic decline in planktonic algal biomass and suspended solids in late 2001, corresponding with initiation of AS treatment at the head of the pond, may have contributed to the apparently substantial increase in persistence of positive stratification during this February 2005 sampling period compared to that reported in Sweeney (2004).
  - Changes in wind velocity were considered more likely to break down stratification and induce mixing events (by inference) at the NE sampling location.
  - A positive correlation between pond surface irradiance and stratified

conditions was observed at all locations with the exception of the NE sampling site.

  - Negative thermal stratification was more likely to occur at the NE sampling location.

- Periods of negative thermal stratification were most persistent during the May sampling period.
  - Positive thermal stratification events during this period were observed only at the NW, Centre and SW sampling locations.
  - A negative thermal stratification event occurred for this entire sampling period at the NE sampling location.
  - The persistence of positive stratification events during this sampling period was substantially less than that observed during February.
  - The average pattern of thermal stratification observed across the pond during this period was, in general, qualitatively consistent with that observed by Sweeney (2004) with the exception of that observed at the NE sampling location.
  - Thermal stratification status at the NW, Centre and SW sampling locations appeared on average independent from changes in wind direction.
  - Thermal stratification status or the degree of stratification at all sampling locations appeared sensitive to changes in pond surface irradiance.

The apparent concordance of results between qualitative assessment of 2D time-series data movie files (as per Sweeney 2004) and the correlation factor analysis of

the time-series data (conducted after the former) provided confidence that the qualitative analysis approach presented above was a valid means for assessing patterns of pond stratification.

Upon review of the above it was considered noteworthy that the stability of thermal stratification across the NW portion of the pond in particular as observed during the February sampling period, indicated that preferential flow (short circuiting) of the pond influent could have been favoured during this time (Sweeney et al. 2005); whilst noting the spatial resolution of the thermal gradient data was lower than the work of Sweeney (2004).

Retention time of Bolivar WSP 1 was a nominal value of 12 days at the time of sampling, with the system providing a storage 'polishing' and disinfection function prior to filtration and chlorination following passage through Ponds 2 and 3. Sweeney et al. (2005b) noted that it was probable that a 'minimum stratification duration' existed below which short-circuiting is negligible due to local mixing. However, during long periods of positive stratification, retention time may be only a matter of hours in a pond with a mean retention time of 15-20 days (Pedahzur et al.1993). It was therefore considered reasonable to conclude that if patterns of stratification in the subsequent 2 ponds were similar to pond 1 during this period then the extent of disinfection could be compromised (see Sweeney et al. 2003). Whilst chlorine disinfection prior to re-use provided a secondary barrier to human exposure; it would be consistent with the precautionary principle to recommend additional vigilance with respect to chlorination at the final treatment phase during potential periods of significant short circuiting.

6.3.3. Factors Associated with Patterns of Change in Dissolved Oxygen Concentration

Grab Samples

February: A seemingly consistent pattern of dissolved oxygen change with depth was observed based on grab samples (Table 6.1) with a small (non-statistically significant, P>0.1) difference at all of the four sampling locations sampled, with a tendency toward lower average DO concentration at the shallower depth (25cm nominal below surface) compared to the 75cm nominal depth. This observation was contrary to the pattern of oxygen concentration usually observed in a WSP and was considered counterintuitive given that PFD was higher close to the surface due to attenuation throughout the culture. This issue is addressed in detail below.

May: The opposite pattern (also non significant) was generally apparent during the May sampling period, with the exception of the Centre sampling location. This location displayed an apparently consistent higher average DO concentration at the shallower depth (25cm below surface) compared to the 75cm depth.

Neither the May nor February grab sample data revealed strong correlations between dissolved oxygen, chlorophyll_*a* concentration, pH or temperature within a sampling event in contrast to the observations of Sweeney (2004), Sweeney et al. (2007).
It was considered noteworthy that average DO concentration observed during the May 2005 sampling period was, at some locations approximately twice that observed in February 2005. Sweeney (2004) observed the opposite pattern when comparing summer and winter DO concentrations; especially at locations adjacent to the inlets. Field measurements obtained during the winter June-August 2005 sampling period

(data not shown) confirmed this contrast with the findings of Sweeney (2004). It was considered likely that the extremely low chlorophyll_*a* concentrations observed and consistent positive stratification observed during February 2005 were likely to be a factor determining this pattern of variation. Strong diurnal variations in dissolved oxygen concentration, were however, observed within both the February and May sampling events in 2005 (online data), with magnitude appearing to be location specific and sometimes qualitatively dependent on prior wind conditions and mixing (inferred) due to changes in status of thermal stratification (see below).

Online DO and Temperature

As an extension of the novel three-dimensional temperature profiling approach of Sweeney (2004) a series of DO monitoring stations were installed at four locations at a nominal depth below surface of 25cm. It was not possible, due to equipment availability limitations to assess vertical dissolved oxygen gradients using online data. As discussed above Tables 6.3 and 6.4 show summaries of online data collected during the February and May sampling periods respectively and include the parameters dissolved oxygen, stratification status (S) and wind velocity. Inspection of Figure 6.17 shows a 'box and whisker' plot of dissolved oxygen from online oxygen data collected at 10 minute intervals from the 25cm depth at each of the four locations during the periods of February 16^{th}- 28^{th} and May 1^{st} – 11^{th}. A significant difference in median DO within all four locations was observed between the February and May sampling periods ($P<0.001$, 5% significance level, Kruskal-Wallis nonparametric one-way analysis of variance) and was, due to the distinctly contrasting patterns of stratification observed between the sampling periods, considered likely indicate some level of independence of this parameter with respect

to average stratification status. Observations by Sweeney (2004) revealed that average DO concentrations during February 2001 and August/September 2001 were highest in the area closest to the inlets (Sweeney et al. 2007) and with reference to a CFD model of pond hydraulics, likely to result from a pattern of recirculation within the pond.

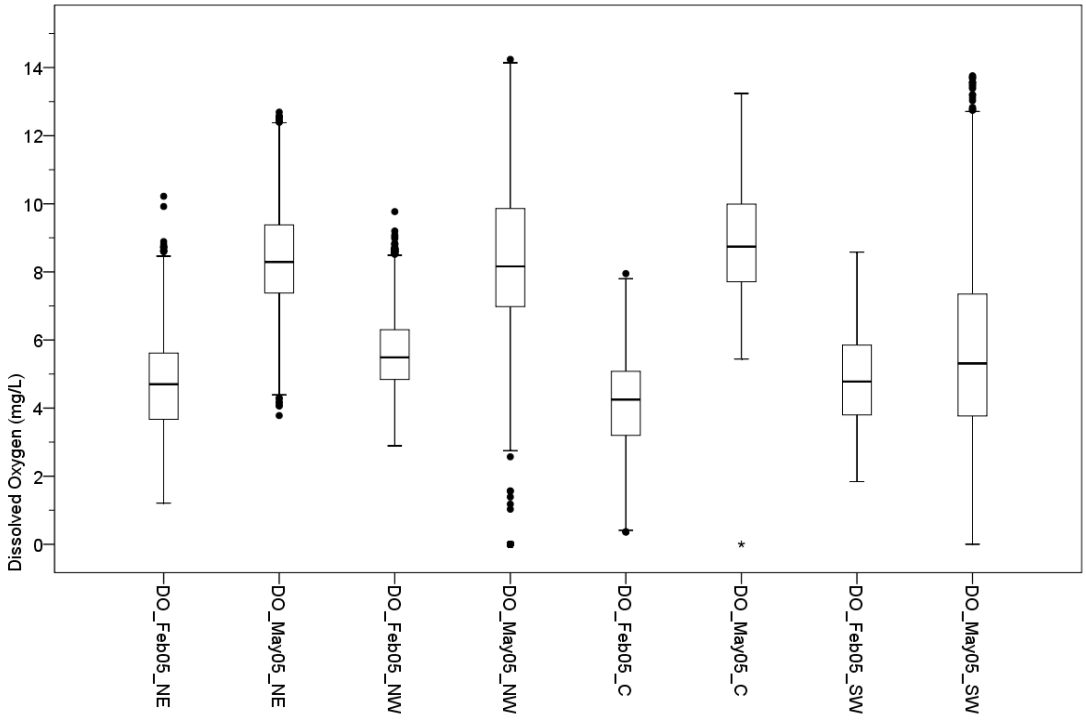

Figure 6-17 Box and Whisker plots of dissolved oxygen for each location and time period displayed to allow comparison of February 16th- 28th and May 1st – 11th sampling periods. Sample sizes shown in Table 6.3 and 6.4.

A generally contrasting pattern during 2005 of central tendency was observed with respect to dissolved oxygen concentration between the February and May sampling periods, Figures 6.18 and 6.19 respectively. During the May 2005 sampling period, median DO concentrations were lower on average at the SW sampling site ($P<0.001$, 5% significance level, Kruskal-Wallis nonparametric one-way analysis of variance) than all other locations. In contrast during the February 2005 sampling period median DO concentrations at the SW monitoring location were not significantly different ($P>0.1$) to those observed at the other sampling locations. Upon reflection,

four possibilities were considered equally plausible when attempting to explain the contrast in DO concentrations with the results of Sweeney (2004).

1. Changes in WSP operation from facultative to maturation (particularly decreased carbon loading and 'reduced' forms of nitrogen) were reflected in changed patterns of algal biomass productivity and resultant oxygenation of the wastewater when comparing the results of Sweeney (2004).
2. Changes in hydraulic flow patterns impacted upon movement and mixing of oxygenated pond water.
3. The availability of higher temporal resolution time-series DO data obtained in this study revealed changes in patterns of pond oxygenation not apparent from data obtained via grab-sampling.
4. A combination of all three.

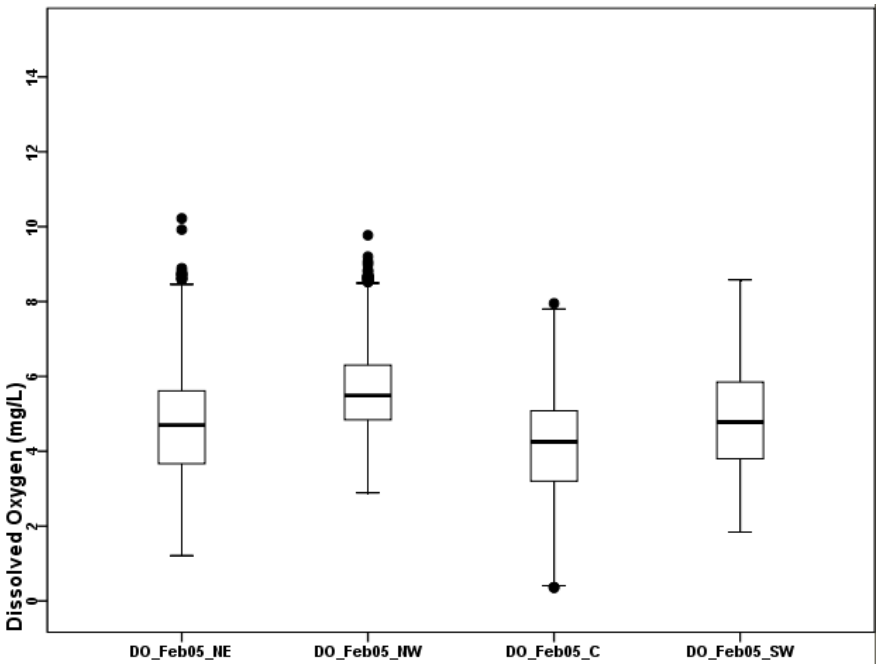

Figure 6-18 Box and Whisker plots of dissolved oxygen for each location during the February sampling period (February 16th- 28th). Sample sizes shown in Table 6.3 and 6.4.

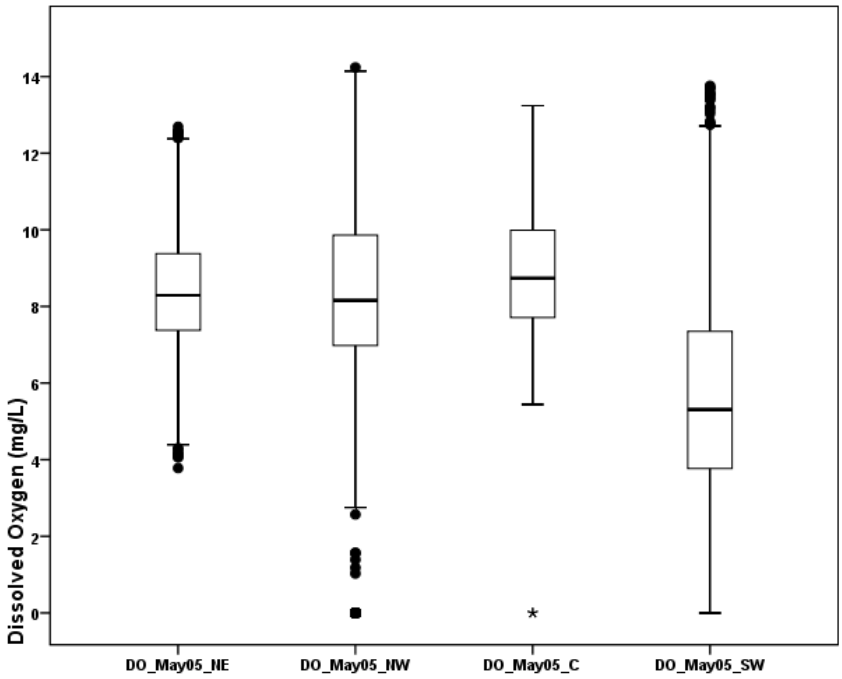

Figure 6-19 Box and Whisker plots of dissolved oxygen for each location during the May 2005 sampling period (May 1st – 11th). Sample sizes shown in Table 6.3 and 6.4.

Whilst the summary data provided in Tables 6.3 and 6.4 and Figures 6.17 - 6.19 was considered to adequately characterize the average pattern of dissolved oxygen variation across the pond during these two time periods; a more 'holistic' or big-picture assessment of variation was apparent through inspection of surface plots of data for each 10 minute data logging event. The surface plotting method of Sweeney (2004) as applied in Section 6.3.2, was modified to include dissolved oxygen and PAR data (Appendix A). The surface plots were 'stitched' together to produce movie files of each time series and are provided (Appendix B) for viewing of each sampling period (Movie Files A, B and C). As discussed in section 6.3.2 an 'average day' data set was constructed to provide a summary of longer term patterns of change and was constructed by taking an average of each 10 minute time-step across all of a sampling period from midnight to midnight. The resulting data file of 144 average values (each of 10 or 11 days data) at each 10 minute time step was used to prepare

another series of movie files of the form D, E and F for both February and May.

February 2005 Dissolved Oxygen and Temperature Surface Plots

Figures 6.20 – 6.23 display an 'average day' frame from each of four periods; midnight, dawn, mid-day and sunset for the February period. In each case a two-dimensional 'kriging' least squares model of dissolved oxygen data collected over the full period of sampling (10 – 11 days) at that time of day was interpolated across the 'pond' surface, as determined by the DO concentration at each of the four monitoring locations; each black line on the surface is an 'iso-DO'; a modelled line of equal DO concentration. The scale of DO ranges from a minimum of 0mg/L (dark green) to a maximum of 16 mg/L (white). The empirical DO data from the four monitoring locations (identified by a cross (+)) was used to fit the DO profile surface. Exactly the same procedure was used to fit corresponding temperature at 25cm depth surface plots (same nominal depth as DO probes); where lines on the surface are 'iso-therms' (lines of equal temperature). The temperature scale ranges from 14°C (dark blue) to 29°C (white). The benefit of using temperature data of the same spatial resolution as DO was clearly apparent when viewing movies of all parameters. Specifically, whilst it would be desirable to have DO data of higher spatial resolution, this was not available and it was found difficult to interpret DO concentration against temperature without a similar spatial distortion. As patterns of thermal stratification were found to be qualitatively similar to those of Sweeney (2004) without data of the highest available spatial resolution (Section 6.3.2), it was considered sufficient in this context, to maintain the same spatial resolution for straightforward qualitative comparison of patterns of DO variation. Patterns of change in spatial DO and temperature gradients were qualitatively assessed by

viewing these surface plots repeatedly in sequence (Sweeney 2004); the following text summarises these qualitative assessments.

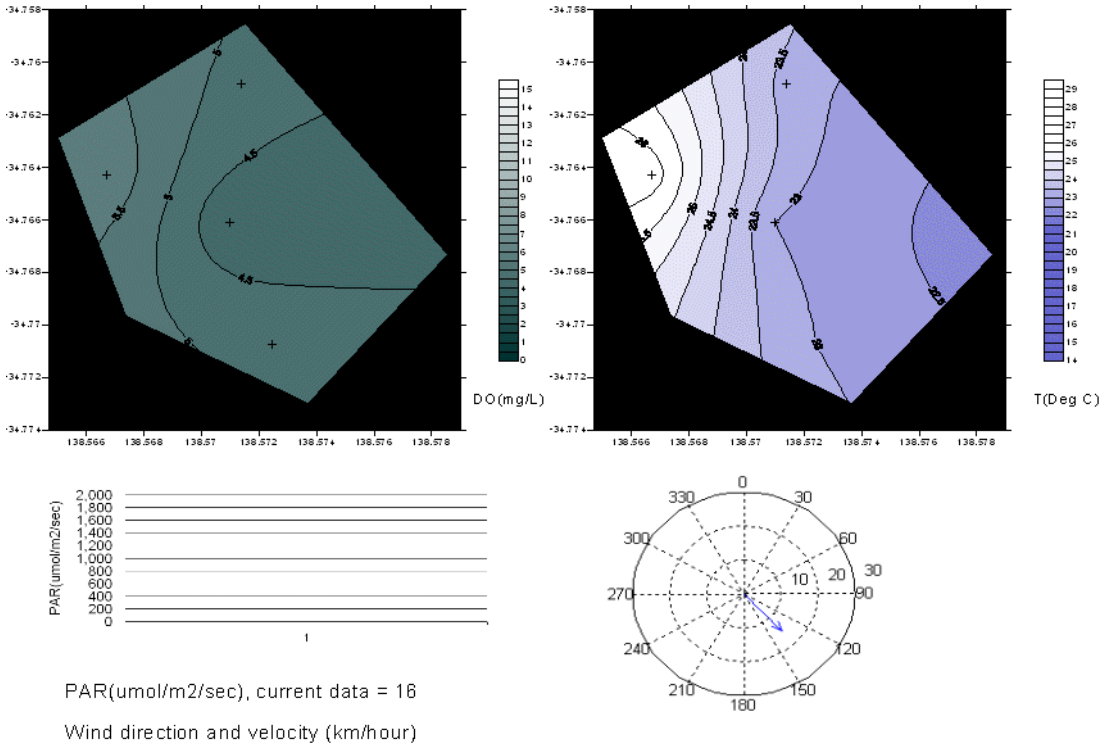

Figure 6-20 Surface plot of average dissolved oxygen, temperature, PAR and wind for February 2005 sampling period. Midnight of 'average day' (February 16th – 28th).

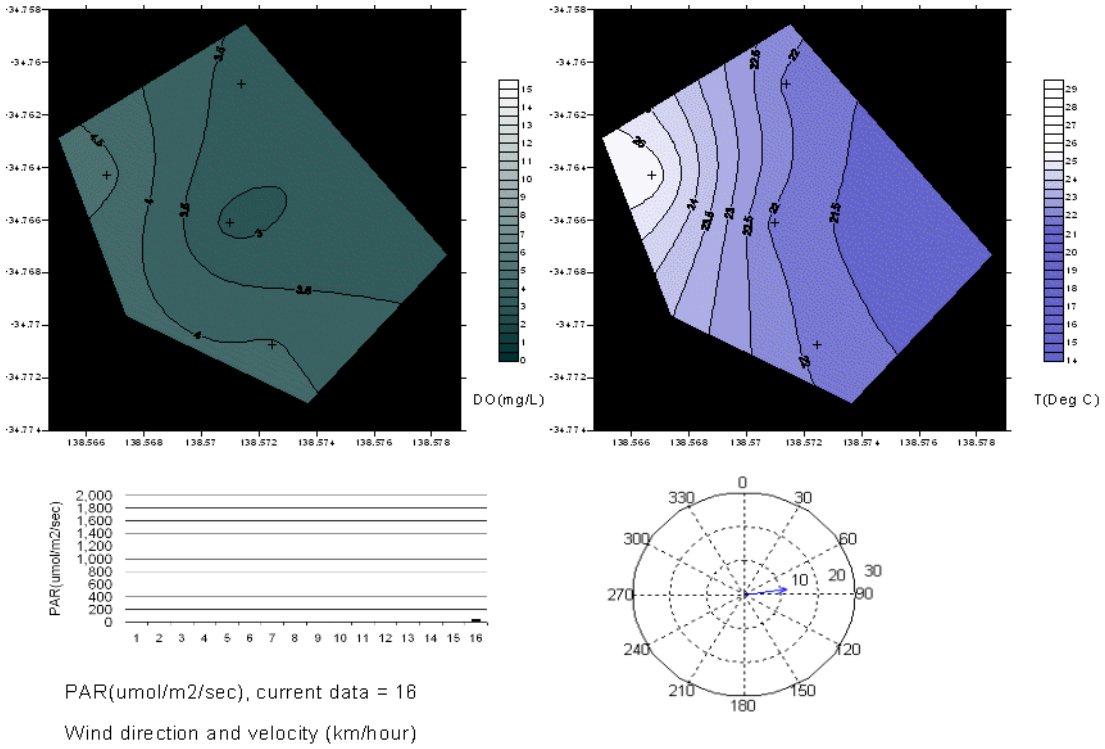

Figure 6-21 Surface plot of average dissolved oxygen, temperature, PAR and wind for February 2005 sampling period. Dawn of 'average day' (February 16th – 28th).

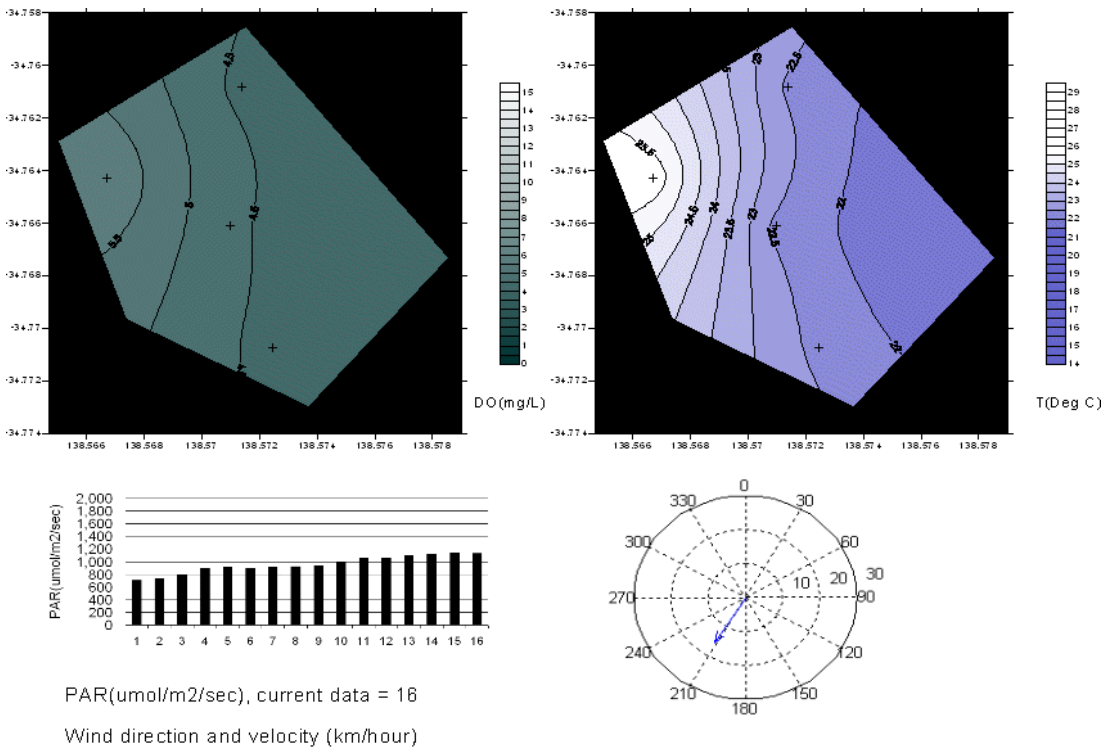

Figure 6-22 Surface plot of average dissolved oxygen, temperature, PAR and wind for February 2005 sampling period. Mid-day of 'average day' (February 16th – 28th).

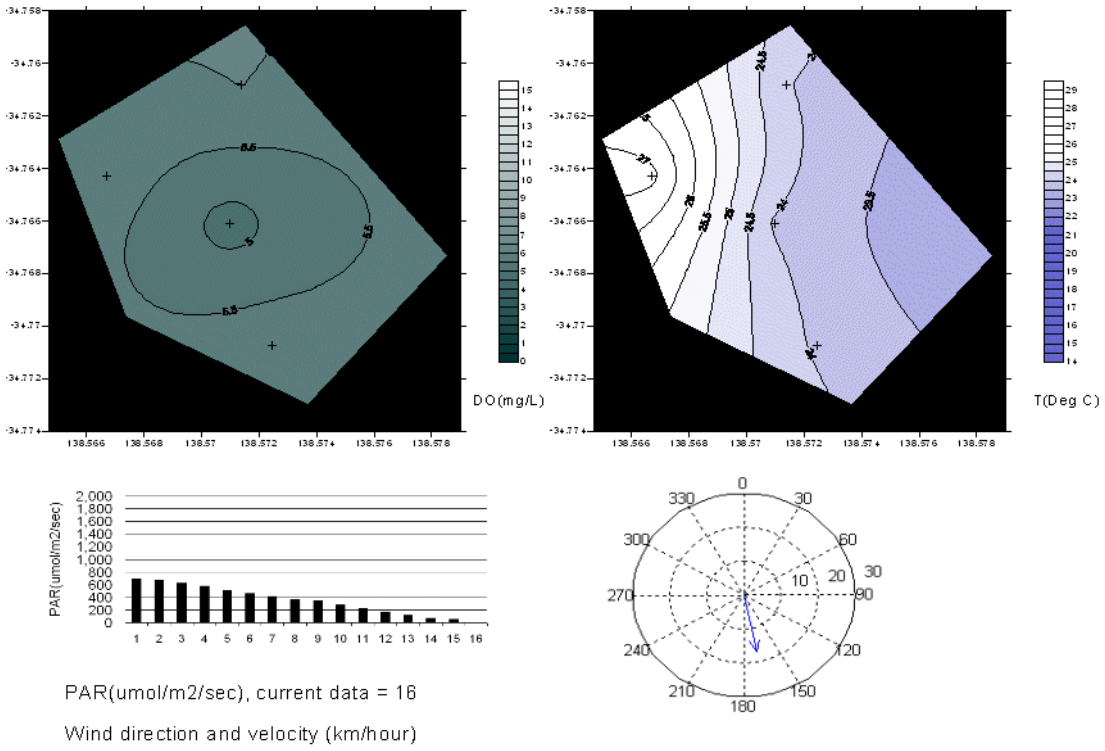

Figure 6-23 Surface plot of average dissolved oxygen, temperature, PAR and wind for February 2005 sampling period. Sunset of 'average day' (February 16th – 28th).

At midnight, on average (Figure 6.20), the Centre sampling location displayed the lowest DO concentration with the SW and NE locations displaying equal DO concentration; DO at the NW site was highest in magnitude. Wind direction was, on average, from the southeast with a mean speed of approximately 14km/h. Temperature at 25cm (nominal depth of DO probes) was approximately equivalent at the SW, Centre and NE sites with a strong positive temperature gradient across the pond at 25cm depth (≈5°C) towards the NW site. By dawn (Figure 6.21) DO concentrations had, on average, declined at all sampling locations by an approximately equivalent amount (1-2mgDO/L) presumably due to respiratory oxygen demand. DO concentrations were approximately equal at the NW and SW sites with the Centre site showing the lowest concentration, being slightly less than that at the NE location. A strong positive temperature gradient (≈ 4°C) remained across the pond at 25cm depth to a maximum magnitude at the NW site, with the other three sites approximately isothermal across the pond (at 25cm depth). Average wind direction at dawn during the February sampling period was from the east with an average speed of approximately 10kp/h. By mid-day, on average (Figure 6.22), DO concentration was again maximal at the NW site and approximately equivalent at the other three sampling locations. The DO gradient across the pond at 25cm depth was approximately 1.5mgDO/L towards the NW sampling location. Average wind direction at mid-day during the February sampling period was from the southwest with a mean speed of approximately 15km/h. At sunset, on average (Figure 6.23), DO concentration was approximately equal at all sampling locations with the exception of the Centre site, which displayed a slightly lower concentration. The pattern of temperature variation at 25cm below the surface across the pond remained consistent during the intervening period with approximately isothermal conditions

across the SW, Centre and NE sites with a positive gradient (≈ 3°C) towards the NW site. Average wind direction at sunset was from the SSE at a speed of approximately 18km/h.

May 2005 Dissolved Oxygen And Temperature Surface Plots

Figures 6.24 – 6.27 display an 'average day' frame from each of four periods; midnight, dawn, mid-day and sunset for the May period. At midnight, on average (Figure 6.24), the pattern of DO concentration at the sampling locations across the pond appeared somewhat similar to that observed during February, with highest magnitude on average at the NW site. A DO concentration gradient of approximately 2.5mgDO/L was apparent from the SW site (adjacent the inlets) towards the outlets. Temperature at the 25cm depth was highest at the SW location with a decrease in temperature towards the northern portion of the pond (away from the inlets); a considerable contrast with respect to the pattern observed for temperature in February 2005 during the midnight time period (Figure 6.20) was apparent. Average wind direction was similar to that observed during February at midnight, approximately EES with a speed of 10km/h. At dawn on average (Figure 6.25), changes in DO concentration at the sampling locations across the pond had decreased rather uniformly, as might be expected from biomass respiratory activity if equivalent biomass concentrations were present. It was the case, however, that biomass concentrations at the NE sampling site were observed to be substantially less than at other sites during May 2005 (Table 6.2). Strong correlations with oxygen draw down or production and measured biomass were not clearly apparent in contrast to the findings of Sweeney (2004). The pattern of temperature variation across the sampling sites during this period remained unchanged; with a slight

cooling on average across the pond with an EES wind direction of speed approximately 8km/h. By mid-day in May, on average (Figure 6.26), both DO concentration and temperature at 25cm depth had retained a very similar pattern of variation across the sampling sites. DO concentration remained highest at the NW sampling location, reducing towards the SW sampling location (adjacent to the inlets), with a gradient in concentration of ≈ 2mgDO/L.

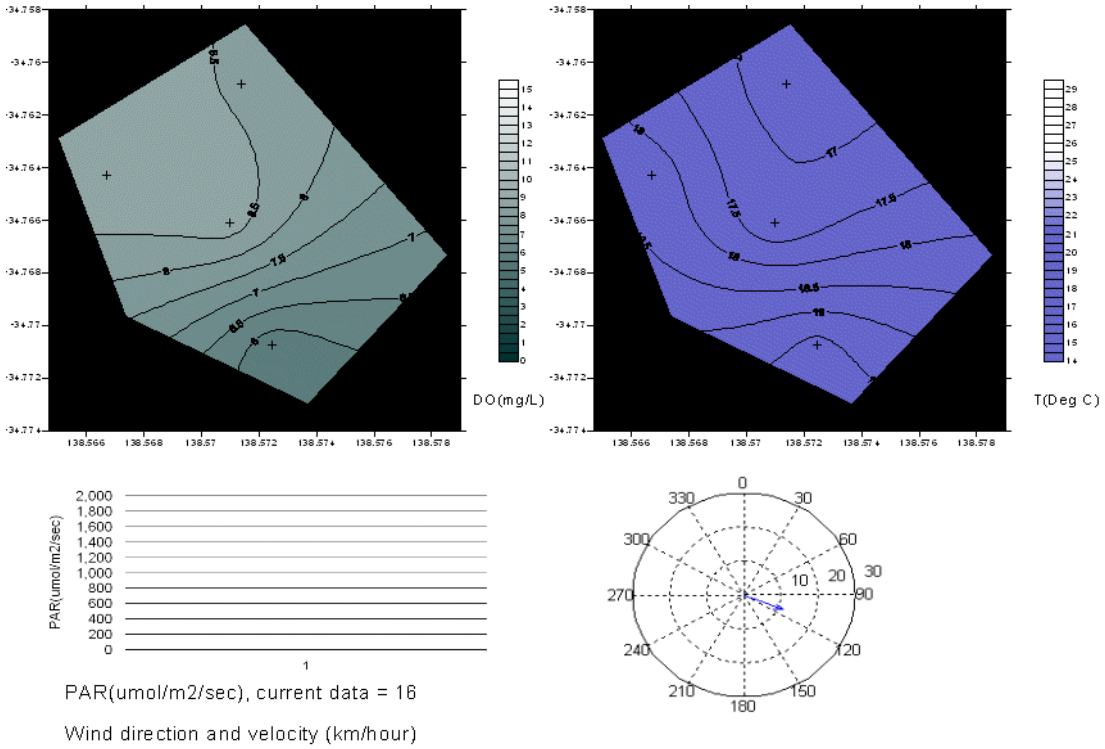

Figure 6-24 Surface plot of average dissolved oxygen, temperature, PAR and wind for May 2005 sampling period. Midnight of 'average day' (May 1st – 11th).

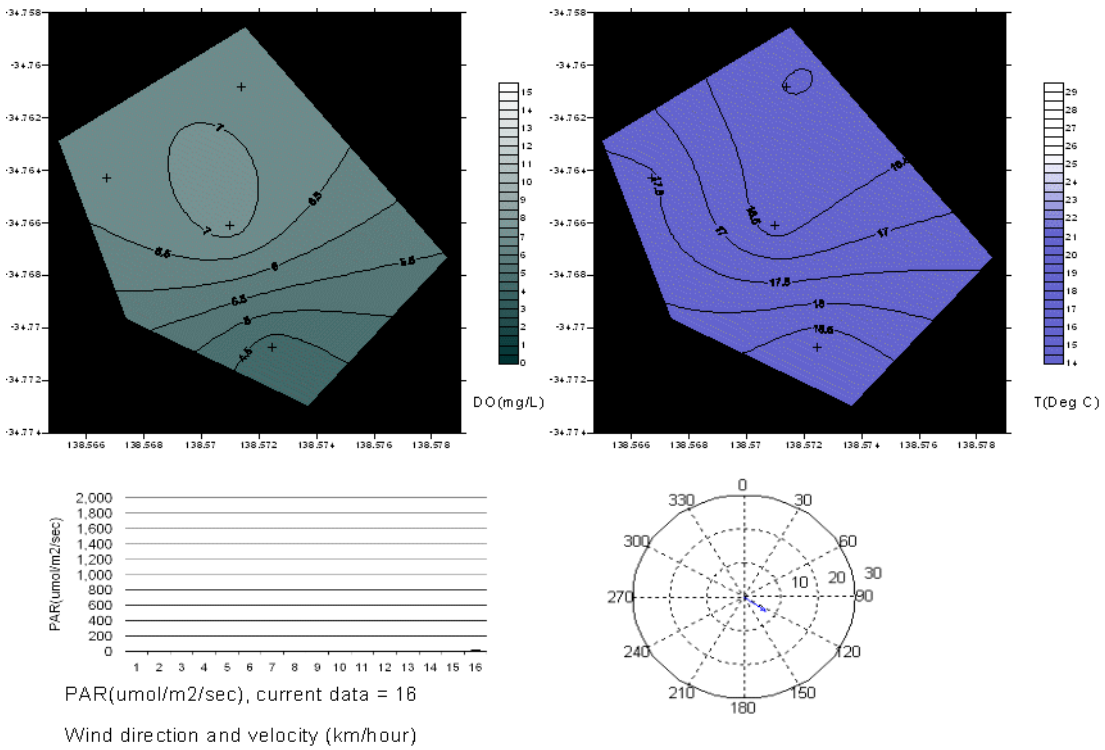

Figure 6-25 Surface plot of average dissolved oxygen, temperature, PAR and wind for May 2005 sampling period. Dawn of 'average day' (May 1st – 11th).

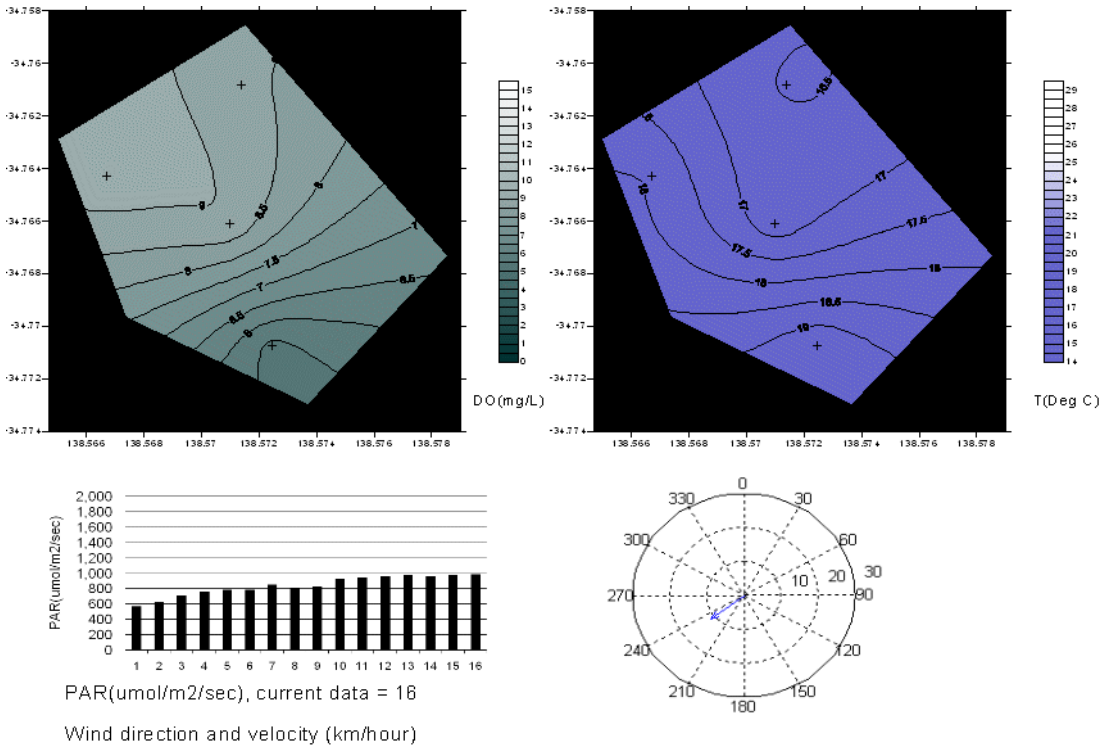

Figure 6-26 Surface plot of average dissolved oxygen, temperature, PAR and wind for May 2005 sampling period. Mid-day of 'average day' (May 1st – 11th).

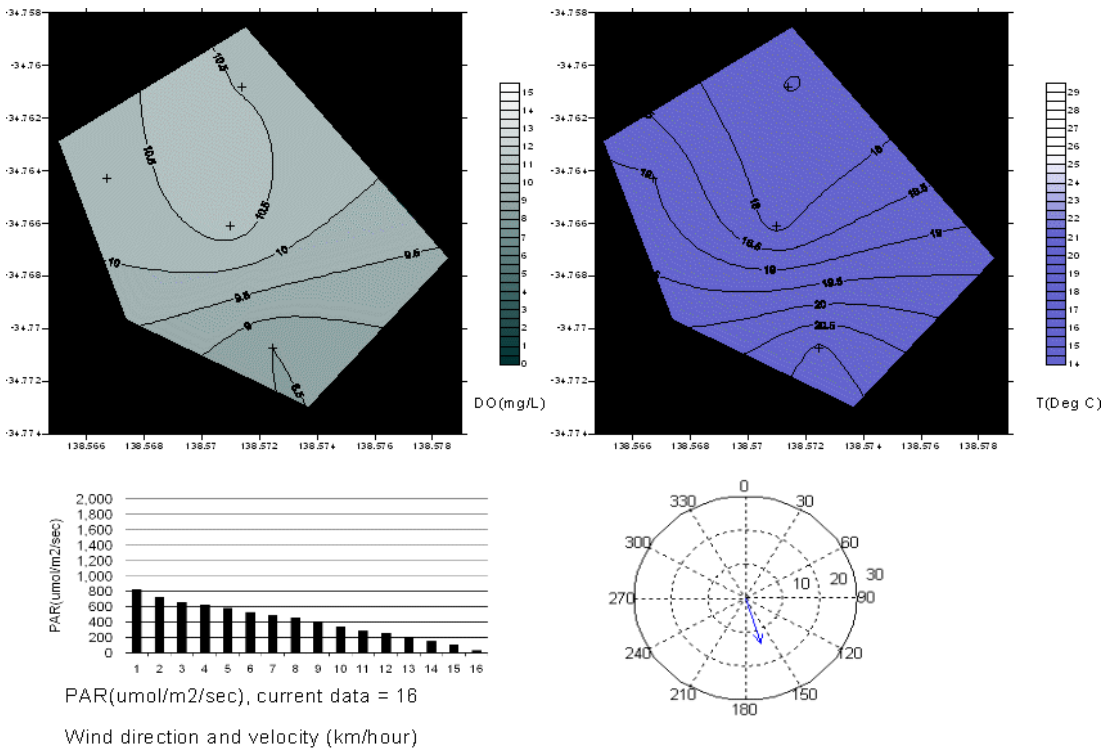

Figure 6-27 Surface plot of average dissolved oxygen, temperature, PAR and wind for May 2005 sampling period. Sunset of 'average day' (May 1st – 11th).

Average wind direction was from approximately WWS at a speed of 13 km/h. By sunset on average (Figure 6.27), DO concentration and temperature had reached close to maximal values, whilst retaining a very similar pattern of variation across all sites. The lowest DO concentration on average was observed at the SW location with a gradient in concentration increasing by approximately 2mg/L towards the northern sampling locations at the 'top' half of the pond. Average wind direction was from the South, with an average speed of approximately 13km/h.

Factors determining Dissolved Oxygen and Temperature Variation

The 'average day' summaries presented above for the February and May sampling periods were considered to provide a satisfactory representation of the qualitative pattern of average change in DO concentration and particularly temperature at the four monitoring locations of the pond: this conclusion was reached after extensive

review of the high resolution time-series ‘A’ movie files. It was considered likely that the consistently higher temperature observed at the NW sampling site should result, all things being equal, in higher rates of photosynthesis at the NW sampling site; this assertion was addressed in the following section (*Rates of Photosynthesis*). Both the February and May sampling periods displayed, similar to the findings of the stratification assessment, an apparently high degree of stability in terms of temperature at the four locations. Nevertheless substantial and rapid changes in the pattern of DO concentration across the pond were often observed and appeared to correspond to strong wind events and sometimes changes in wind direction during both the February and May sampling periods. This appeared to be a characteristic feature of the pattern of DO variation. An exploratory factor analysis (Figures 6.28 – 6.29) was conducted using the complete time series data of DO, PAR and wind velocity in order to reveal correlations amongst these variables and determine if a rational pattern of factor and variable association was observed, consistent with the qualitative observation that wind velocity impacted strongly upon the pattern of DO concentration across the pond. Dotted circles were drawn on each factor analysis to ‘contain’ variables that appeared to group together (within a figure); as in Section 6.3.2 a component score of 0.5 was used as a delineator (Masters 1995).

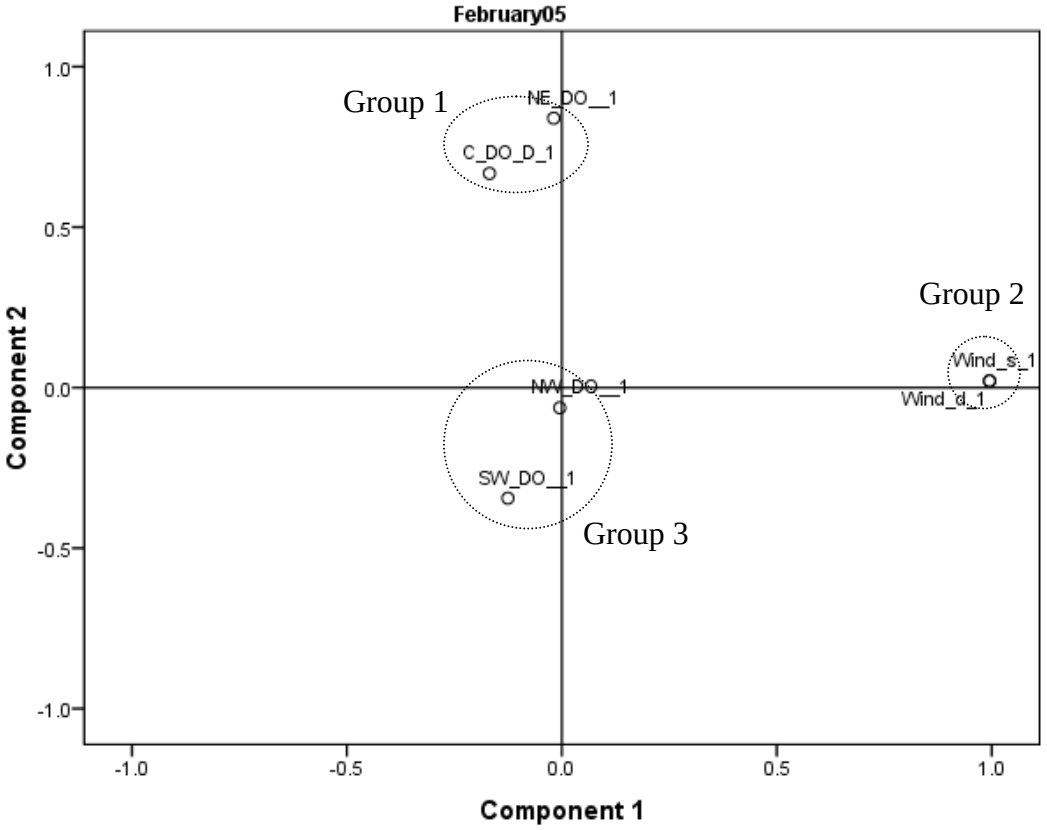

Figure 6-28 Factor analysis of average dissolved oxygen, PAR, wind speed and direction for February 2005 sampling period. Time series all data (February 16th – 28th).

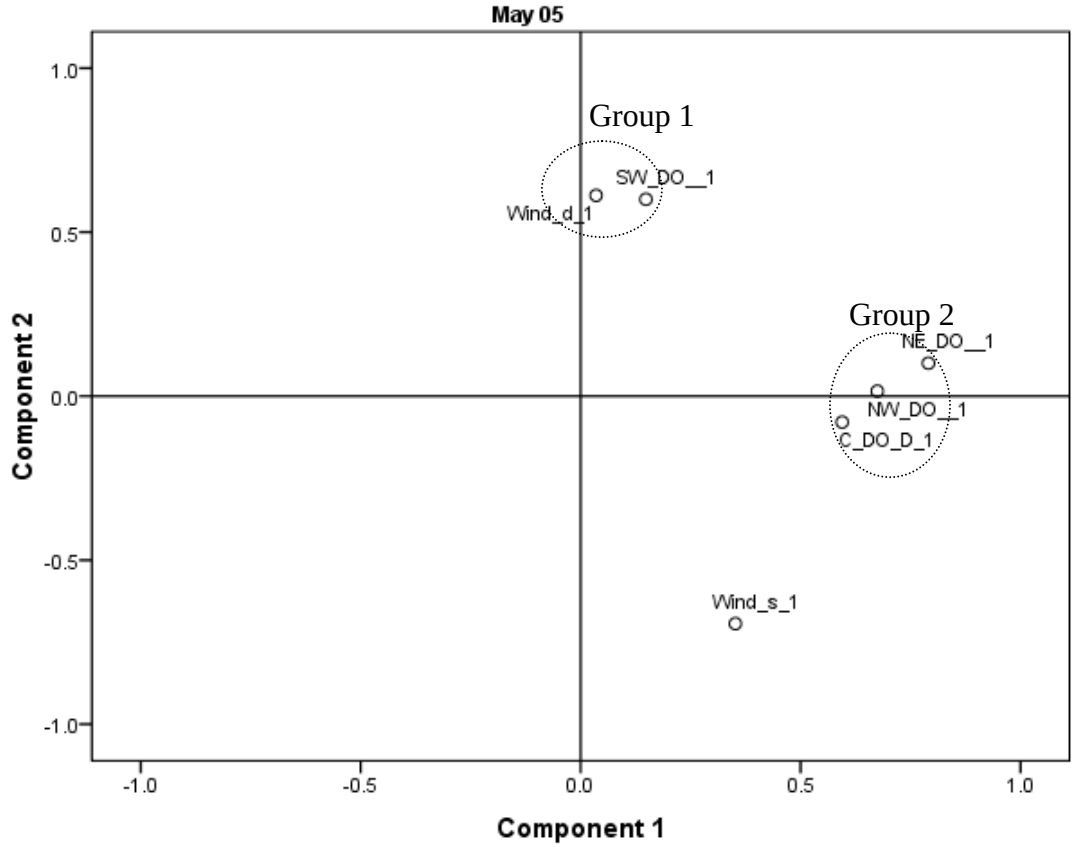

Figure 6-29 Factor analysis of average dissolved oxygen, wind speed and direction for May 2005 sampling period. 'Time series all data (May 1st – 11th).

Inspection of Figure 6.28 revealed that variations in DO concentration at the Centre and NE sampling locations appeared by definition to be independent of wind direction and speed during the February sampling period. The grouping of the NW and SW DO concentration, close to the axis of the two components, indicated that these variables were correlated with casual factor(s) for both components 1 and 2. See Figure 6.29 for a complementary factor analysis for the May sampling period. From inspection a contrasting pattern of correlations was apparent during the May sampling period with wind direction and SW DO forming a grouping loading strongly onto component 2 and by definition independent of the grouping of NE, NW and Centre DO. Thus indicating that during the May sampling period DO concentration at the SW sampling location was positively correlated with wind direction and inversely correlated with wind speed. Wind speed during the May sampling period was inversely correlated with wind direction; this was simply considered indicative that wind speed was consistently stronger (or weaker) from certain directions. Qualitative comparison of factor analysis results from these two time periods suggested that DO concentrations at the NE and Centre sampling locations tended to be resistant to changes in wind velocity. The DO concentration at the SW site tended to be sensitive to changes in wind velocity during both sampling periods. It was considered important to note, however, that correlations identified in a factor analysis, as in all analyses of this type, may be considered indicative of relationships between variables, but by definition cannot be considered unambiguously causal as other variable(s) not included in the analysis may also co-vary. For example the dynamic nature of pond state(s), with respect to hydraulic flow and stratification, was established as a response to changes in wind velocity (Sweeney 2004, Sweeney et al. 2003, 2005a, 2007). CFD models of hydraulic flow

developed by Sweeney (2004) identified wind speed as a variable that, at a range of values, appeared to severely limit accuracy of modelled flow within the system. Attempts to validate the CFD models against empirical data, collected during drogue studies, failed but did confirm the dynamic nature of the system with respect to flow and deviation from theoretical plug flow assumptions. Consequently it was concluded that a lack of knowledge of the 'state' of the system prior to collection of empirical fluid flow data was likely to be a key limitation in terms of testing (in the field) conclusions of fluid flow models (Sweeney 2004). The importance of this finding, with respect to developing a better understanding of the pattern of oxygenation within the pond, may be illustrated with reference to the pattern of oxygenation in the pond reported by Sweeney et al. 2007. These authors concluded that the counter intuitive observations of high DO concentrations at the inlet of the pond were likely to be a consequence of recirculation of oxygen rich water from other areas of the pond. This provides a possible explanation for the observed lack of correspondence between DO and chlorophyll_*a* concentration observed at the NE sampling location during May 2005. That is, despite an order of magnitude difference in chlorophyll_*a* concentration at the NE sampling location, and apparently equivalent light penetration; rates of DO production were similar at all sites (see following section). Inspection of the factor analysis plots of thermal stratification and DO concentration were considered to indicate a degree of similarity with respect to the groupings and correlations of these variables.

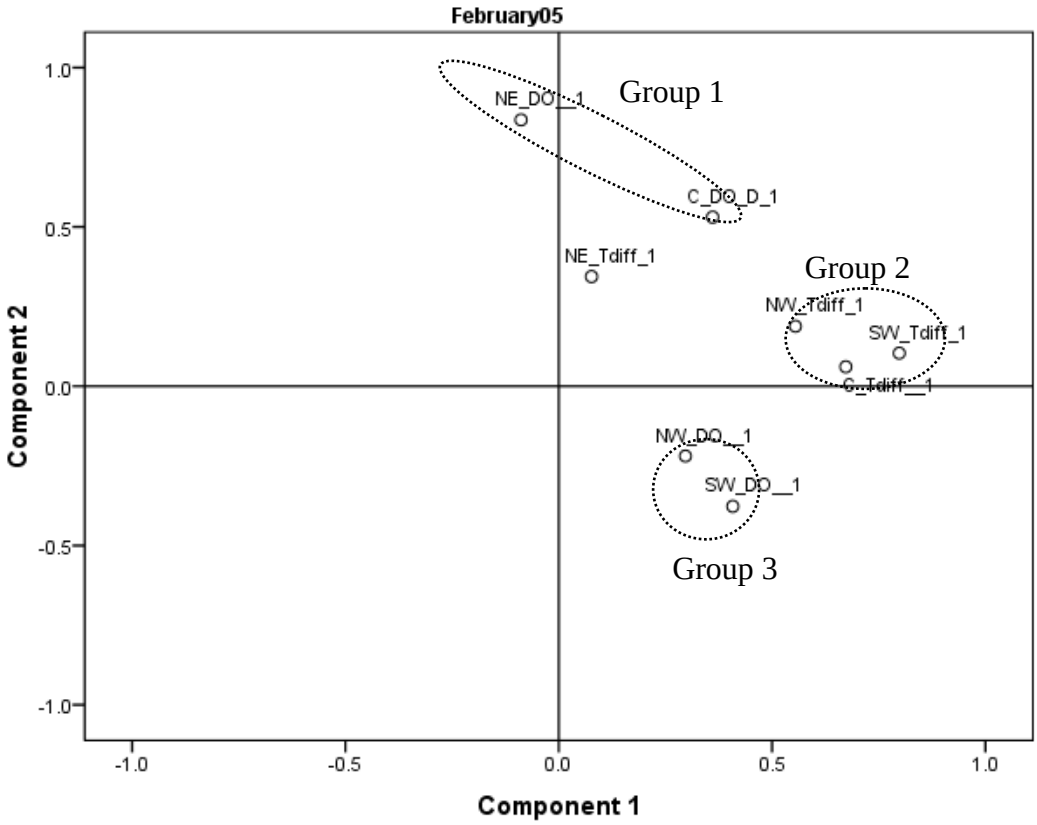

Figure 6-30 Factor analysis of dissolved oxygen concentration DO and stratification status T25_75 (Tdiff_1) for February 2005 sampling period. Time series all data (February 16th – 28th).

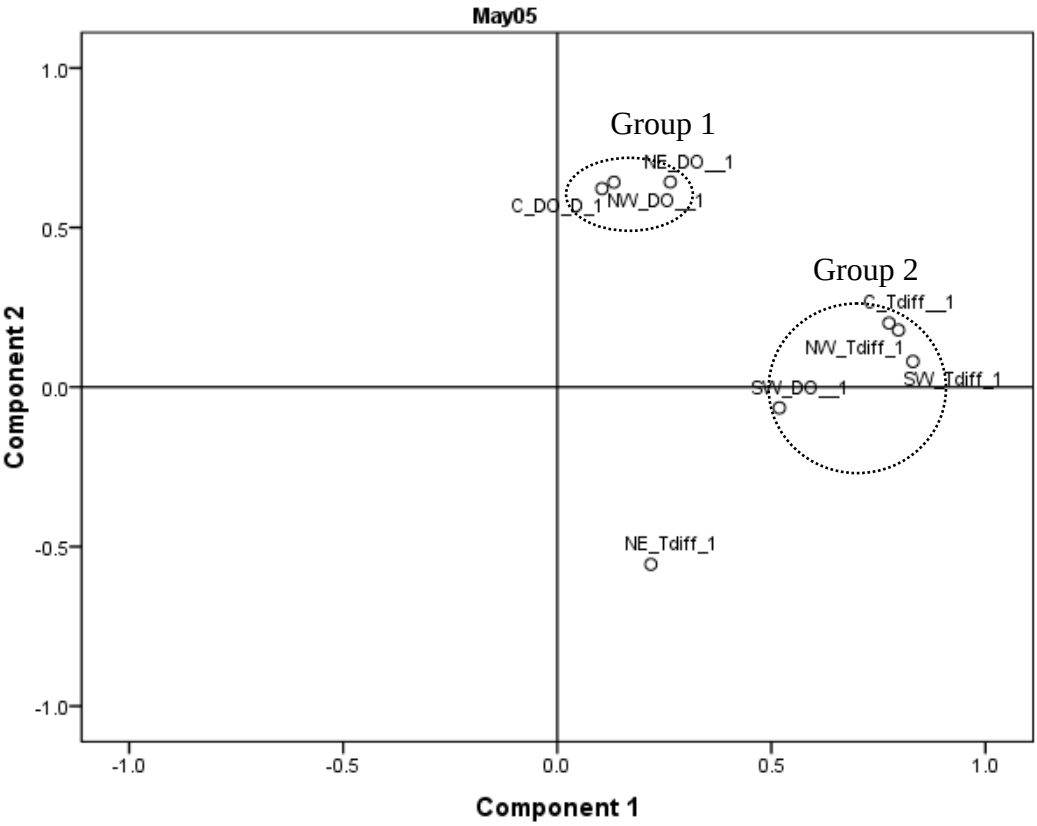

Figure 6-31 Factor analysis of dissolved oxygen concentration DO and stratification status T25_75 (Tdiff_1) May 2005 sampling period. Time series all data (May 1st – 11th).

Figures 6.30-6.31 provide a visual summary of the results of a factor analysis assessing correlations between thermal stratification and DO concentration for the February and May 2005 sampling periods respectively. Inspection of Figure 6.30 indicated that changes in DO concentration at the NE and Centre sampling sites during February varied in a similar fashion, forming a grouping that loaded strongly onto component 2. At the NE sampling location during February DO concentration was positively correlated with stratification status (NE_Tdiff_1), whilst DO concentration at the Centre sampling location tended to be independent of stratification (C_Tdiff_1). Changes in DO concentration at the strongly stratified NW and SW sampling locations varied in a similar fashion to each other (Group 3) and loaded on both components 1 and 2.

Inspection of Figure 6.31 indicated that changes in DO concentration at the NE, NW and Centre sampling sites during May varied in a similar fashion, forming a grouping (Group 1) that loaded strongly onto component 2. At the NE sampling location during May, DO concentration was negatively correlated with stratification status (NE_Tdiff_1), in contrast to the relationship observed during February. DO concentration at the NW and Centre sampling locations tended to be independent of stratification status (NW_Tdiff_1, C_Tdiff_1), whilst DO concentration at the SW sampling site (Group 5) was positively correlated with stratification status at this location and varied independently when compared to DO changes at the other 3 sampling locations.

Conclusions and Implications for Wastewater Treatment

It was considered that the analysis of the data presented above provided sufficient information to conclude the following;

- Average DO concentrations during May 2005 were approximately twice those observed during the February sampling period with the exception of the SW site; where concentrations remained similar. This pattern of pond oxygenation was contrary to that observed by Sweeney (2004) and was considered likely to reflect the extremely low concentrations of chlorophyll_*a* observed at all sites and depths during the February sampling period. Substantially lower influent BOD concentrations as a result of the AS plant upgrade would be expected to result in lower oxygen demand and higher average DO concentrations at all sites (all other factors being equal) due to reduced oxygen demand by heterotrophic bacteria.
- Average DO concentrations during the May sampling period were not clearly related to chlorophyll_*a* or suspended solids concentration. This result was considered somewhat counter intuitive given the observation of strong diurnal variations in DO concentrations and differences in chlorophyll_a of approximately 1 order of magnitude both between and within sites. However, only a small number of grab samples were available for analysis of biomass parameters during the sampling period and variations in these parameter between sampling events may have been substantial. Nevertheless inorganic carbon draw down during the May sampling period was observed to be less substantial at the NE sampling location, an observation that appeared consistent with lower rates of photosynthesis (but see following section).
- Spatial patterns of DO concentration were observed to vary across the pond depending on the time of day within a sampling period. During the

February sampling period all locations displayed, on average, lower DO concentrations in comparison to May; the centre location was generally observed to display the lowest DO concentration during February. The SW sampling location displayed significantly lower DO concentration than other sites during the May sampling period. Qualitative assessment of the 2D time-series data movies revealed frequent substantial and rapid changes in the pattern of DO concentration across the pond in apparent response to strong wind events or changes in wind direction.

- Factor analyses indicated that changes in DO concentration resulting from changes in wind velocity appeared strongly location and season specific.
  - During February, DO concentration at the NE and Centre sampling locations appeared independent of changes in wind velocity. Whilst the other sampling locations (NW and SW sites) appeared sensitive to changes in wind velocity.
  - During May, DO concentration at the SW site displayed a strong positive correlation with wind direction and a strong inverse correlation with wind speed.
- Factor analyses indicated that changes in DO concentration correlated with changes in stratification status appeared strongly location and sampling event specific.
  - During February DO concentration at the NE sampling location was positively correlated with stratification status whilst DO concentration at the Centre sampling location appeared somewhat independent of this variable. Changes in DO concentration, at the strongly stratified NW and SW sampling sites, were both weakly correlated with

stratification status.

- During May DO concentration at the SW sampling site displayed a strong +ve correlation with stratification status whilst DO concentration at the NW and Centre sites tended appeared independent of stratification status. DO concentration at the NE sampling site displayed a strong negative correlation with stratification status.

- That patterns of change in the magnitude of DO concentration appeared to be strongly influenced by location and sampling period (season). It was also considered likely that at a given chlorophyll_a concentration the pattern of DO variation at a location reflected the impact of variables such as wind velocity and stratification status (in addition to PAR).

The conclusions presented above highlight the benefit of collecting DO data at a high temporal resolution. Variations in dissolved oxygen concentrations at the sampling sites were observed on occasion to vary substantially over periods of minutes whilst apparently cyclical variation over the diurnal period was also observed. Substantial differences in the pattern of pond oxygenation were also observed between the February and May sampling periods, this was also considered to highlight the dynamic nature of this system.

Oxygen concentration and algal growth are key variables in determining rates of nutrient conversion reactions; in combination with the findings of Sweeney (2004) that indicated the presence of complex hydrodynamic conditions within the pond dependent on changes in wind velocity, the complex changes in oxygenation activity observed across the pond as detailed above further reveal the complexity of such

systems and the need for extensive online monitoring when one's purpose is to formulate precise (and reasonable) assumptions for use in pond design or operation.

6.3.4. Rates of Photosynthesis

Representative scatter-plots showing mean pond temperature and oxygen concentration for the duration of the May and February sampling period are provided in Figures 6.32 to 6.33, in a manner corresponding to that used to present data in Chapter 5; i.e. each plot was constructed to display online DO and temperature average ± standard deviation for each 10 minute increment over the 24 hour 'day' for the full duration of sampling trial. As discussed in section 6.3.3 each measurement was taken automatically at the same time of the day and each data point on each figure is the average of measurements for that time of day, at a sampling location in that sampling period.

At all sampling locations the variation in dissolved oxygen concentration during the 24 hour cycle appeared qualitatively consistent with the pattern observed in the Murray Bridge pilot scale HRAP (Fallowfield et al. 2001) and the laboratory based bioreactor (Chapter 5). That is; average dissolved oxygen concentration increased following dawn until reaching a maximal level and then declining until reaching a minimum prior to sunrise. The coloured bar at the base of each figure shows the photoperiod (yellow) and night period (black). Inspection of these figures reveals as expected a lag (approximately 1 hour) after sunrise and the consequential increase in DO concentration. The extent of variation, as indicated by the standard deviation bars was generally greater, and less uniform with respect to

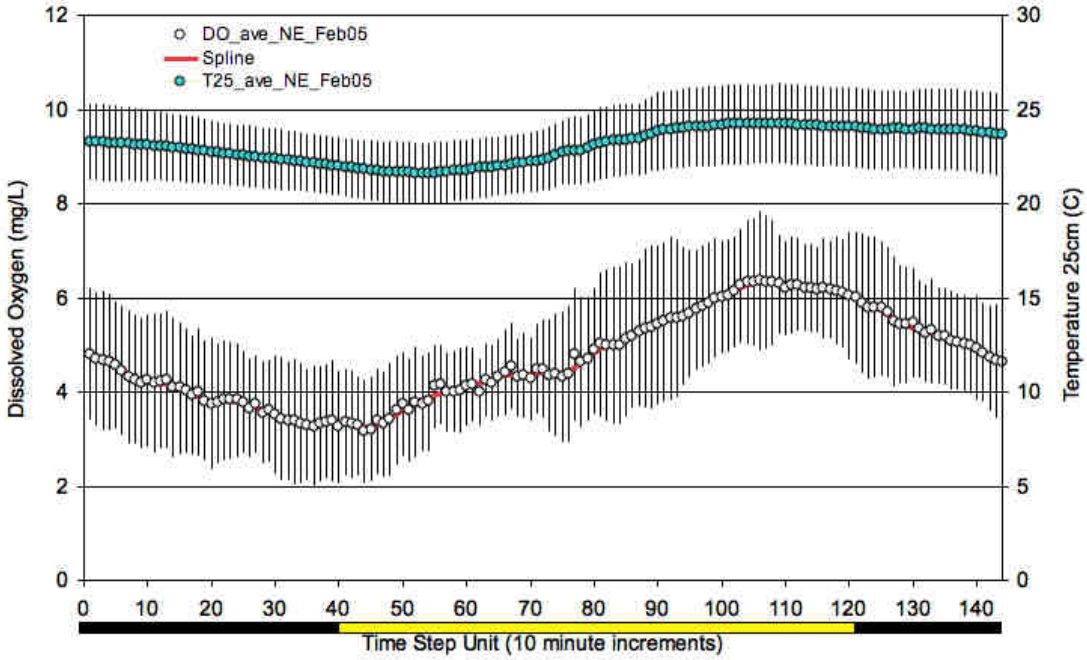

Figure 6-32 Scatter plot DO concentration (mgDO/L), open circles and Temperature (℃), blue circles, ± standard deviation for NE sampling location. February 2005 sampling period. (February 17th – 27th) n = 144, 10 minute increments average of 10 days online data.

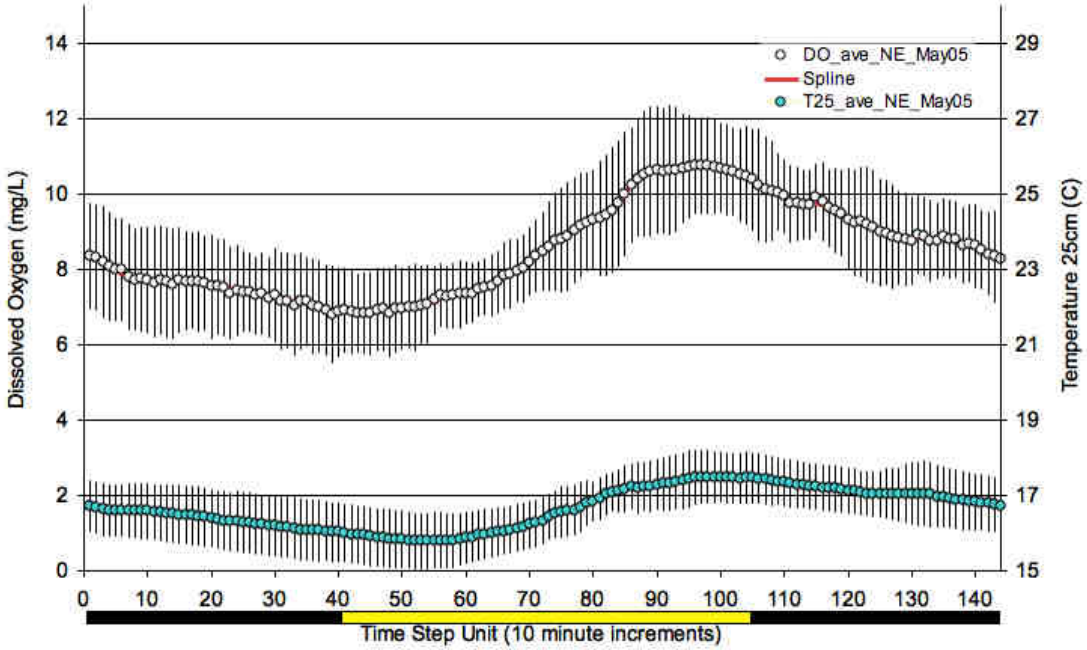

Figure 6-33 Scatter plot DO concentration (mgDO/L), open circles and Temperature (℃), blue circles, ± standard deviation for NE sampling location. May 2005 sampling period. (February 17th – 27th) n = 144, 10 minute increments average of 10 days online data

DO concentration than temperature. This observation was generally consistent with comparisons made at the Murray Bridge HRAP pilot plant and the laboratory based bioreactor.

Gross rates of photosynthesis were determined by measuring the slope of the post dawn increase in DO concentration vs. time and were qualitatively assessed in the fashion used for temperature and dissolved oxygen and described previously. The 'C' series of 2D time-series data movie files revealed that rates of photosynthesis varied in an apparently independent fashion at most sampling locations during both sampling periods. It was assumed that the complementary 'average day' 2D time-series movies would display less variability due to the effect of averaging DO concentrations across the full period of each sampling event; an assessment of the 'F' series movie did not support this assumption. Unexpectedly the extent of variation in instantaneous gross photosynthetic rate from time-step to time-step at a site, in comparison to other sampling locations, appeared unchanged. A box and whisker plot of each time-series was constructed and provided as Figures 6.34 and 6.35. Inspection of these figures and the time-series data used to create them revealed that instantaneous rates of gross photosynthesis varied by up to 3 orders of magnitude within a site and sometimes so between time increments. Figure 6.36 was produced in order to assess variation in instantaneous rates of gross photosynthesis when normalised by chlorophyll_a concentration. Inspection of Figure 6.36 revealed that unrealistic instantaneous rates of gross photosynthesis resulted. It was concluded that attempts to assess rates of instantaneous gross photosynthesis qualitatively were very unlikely to succeed due to the obvious complexity in the patterns of DO instantaneous rate change. The approach detailed in Chapter 5 was therefore used exclusively to determine patterns of change in photosynthetic rates across the pond sampling locations.

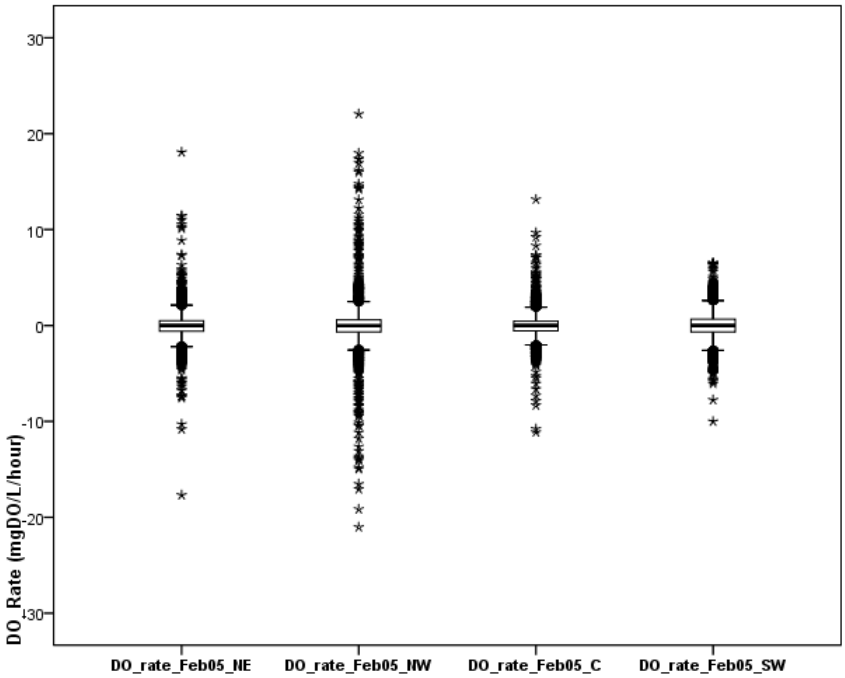

Figure 6-34 Box and whisker plot of gross rate of DO production (mgDO/L/hour), for February 2005 sampling period. (February 17th – 27th) n = 1567, 10 minute increments.

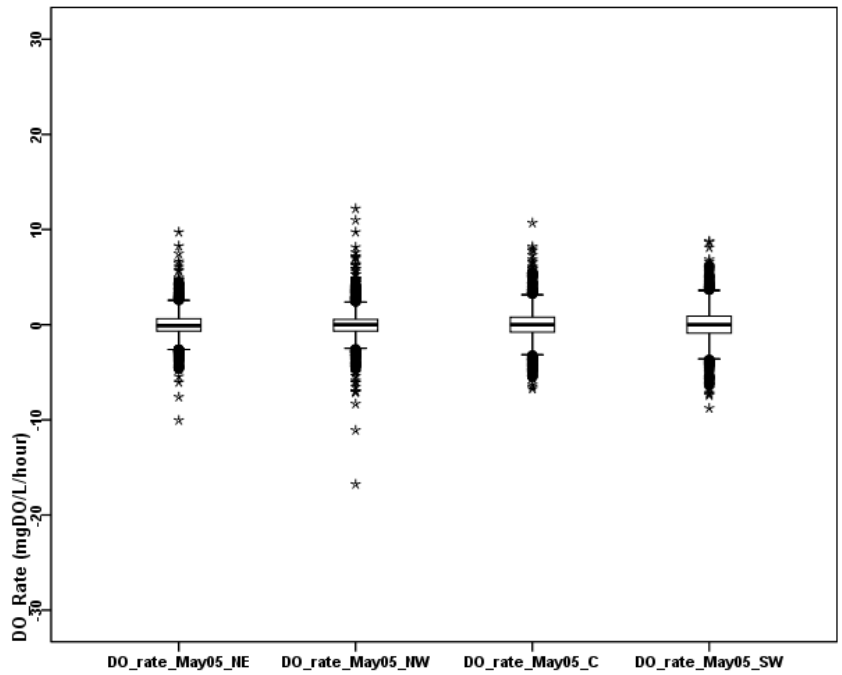

Figure 6-35 Box and whisker plot of gross rate of DO production (mgDO/L/hour), for May 2005 sampling period. (May 1st – 11th). n = 1424, 10 minute increments

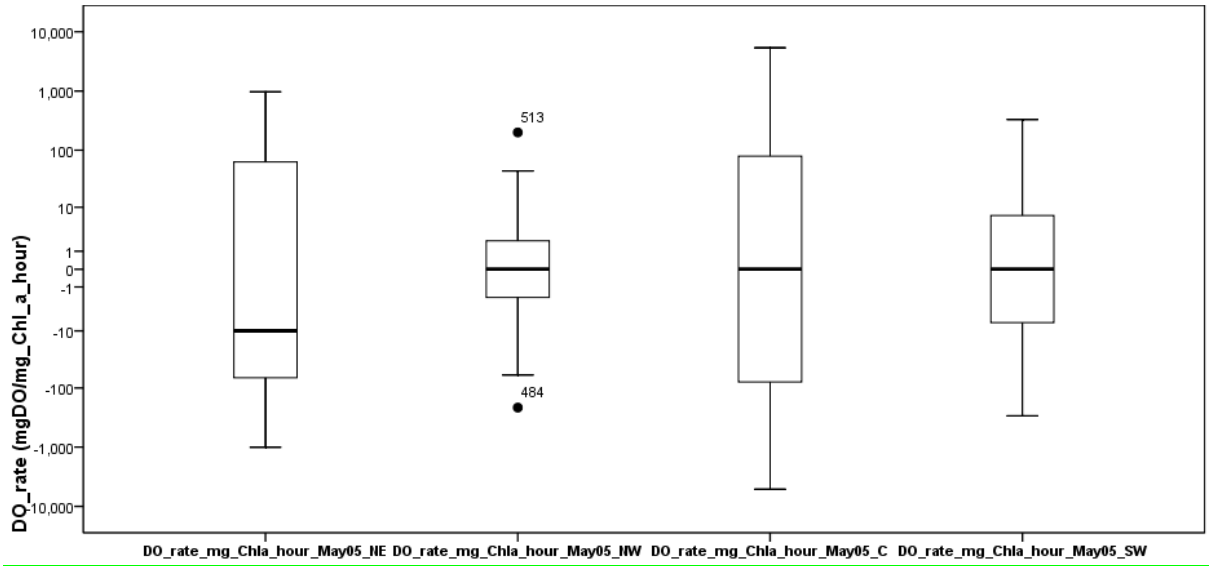

Figure 6-36 Box and whisker plot of gross rate of DO production (mgDO/L/hour/Chl_*a*), for May 2005 sampling period. (May 1st – 11th). n = 1424, 10 minute increments.

Oxygen utilization rates (OUR) calculated for each sampling location during the February and May sampling events are shown in Tables 6.5 and 6.6 (p167-168). The parameter OUR/hour was calculated by linear regression fit of online dissolved oxygen data against time and provided a measure of average hourly rate of change in dissolved oxygen concentration during the period closest to dawn (approximately 1 hour of data at 10 minute intervals); no data was available to allow correction for re-aeration. Figures 6.37-6.38 show representative examples of the pre-dawn and post-dawn changes in oxygen concentration and fit of a least squares regression line. The coefficient of determination (r^2) is defined as the proportion of variance explained by the regression model (Zar 1991). Similarly the corresponding quantity 1- r^2 can be interpreted as the proportion of unexplained variation; the standard deviation of the correlation co-efficient (1- $r^2/\sqrt{(n-1)}$) was therefore used to calculate the standard deviation of OUR/hour for each sampling location and sampling period (Table 6.5). The parameter OUR was normalized by chlorophyll_*a* concentration to produce

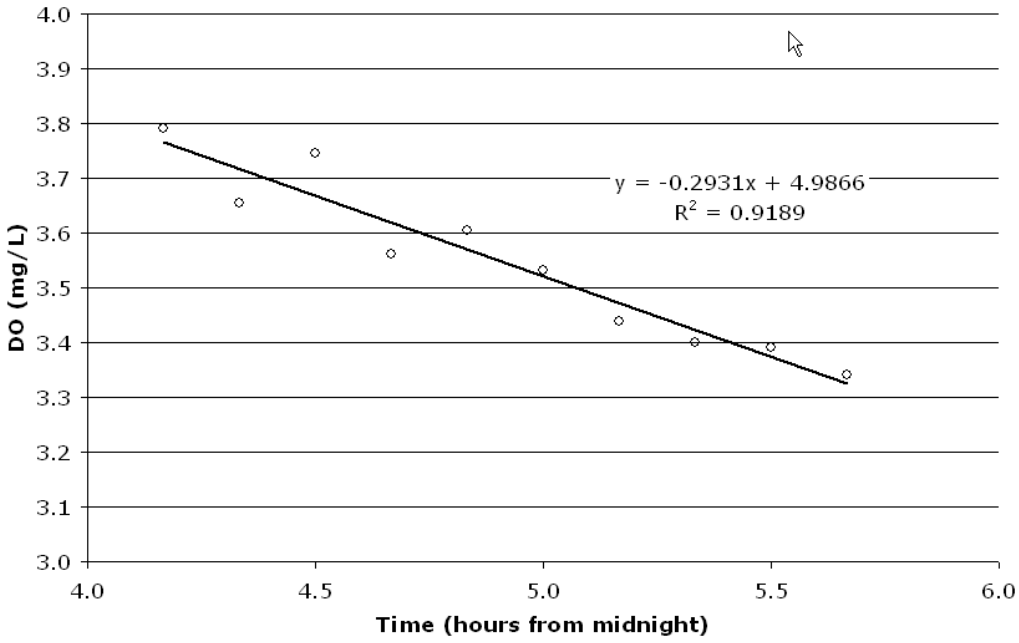

Figure 6-37 Scatter plot of change in DO concentration during the pre-dawn period (mgDO/L/hour), for NE sampling location. February 2005 sampling period (February 17th – 27th) n = 10, 11 days averaged at 10 minute increments.

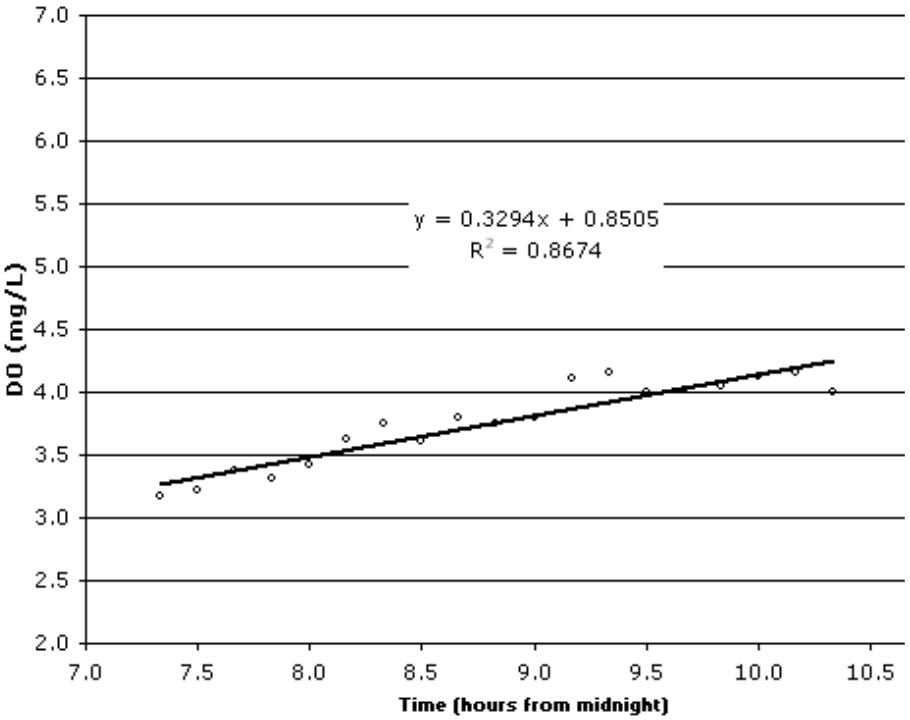

Figure 6-38 Scatter plot of change in DO concentration during the post-dawn period (mgDO/L/hour), for NE sampling location. February 2005 sampling period (February 17th – 27th) n = 14, 11 days averaged data at 10 minute increments.

OUR/hour/Chl_a (Table 6.6); the surrogate measure for algal based respiration rate.

The chlorophyll_*a* concentrations from both depth increments at each site were

averaged in order to account for mixing due to the breakdown of stratification events.

Inspection of Table 6.5 and Figure 6.39 revealed that OUR/hour (community respiration rates) during both February and May 2005 were of similar magnitude to those observed in both the Murray Bridge pilot scale HRAP (Fallowfield et al. 2001) and the laboratory scale HRAP bioreactor (Chapter 5). This was considered to reflect the qualitatively similar patterns of the Bolivar WSP daily 'DO curves' in comparison to those observed in these other systems (Figures 6.32-6.33 and 5.6-5.8). Of note were the high correlation coefficients of OUR/hour observed at all sampling locations indicating that community respiration rates (OUR/hour) may be location specific in some portions of the pond.

For the purposes of spatial comparison, when data OUR/hour for the February and May sampling period were compared (Figure 6.39; open circles and squares respectively); a divergence was noted with respect to the SW sampling site; the site closest to the influent and subject to the presence of a sludge blanket.

When normalized to chlorophyll_a concentration (Table 6.6 and Figure 6.40) the pattern of change across the pond for February remained qualitatively similar with OUR/hour not normalized to chlorophyll_a concentration; probably reflecting the similarity in measured algal biomass concentrations during this period. A substantial difference was however noted in the pattern (and magnitude) of May OUR/hour/chl_a in comparison to February (with the exception of the NE sampling site).

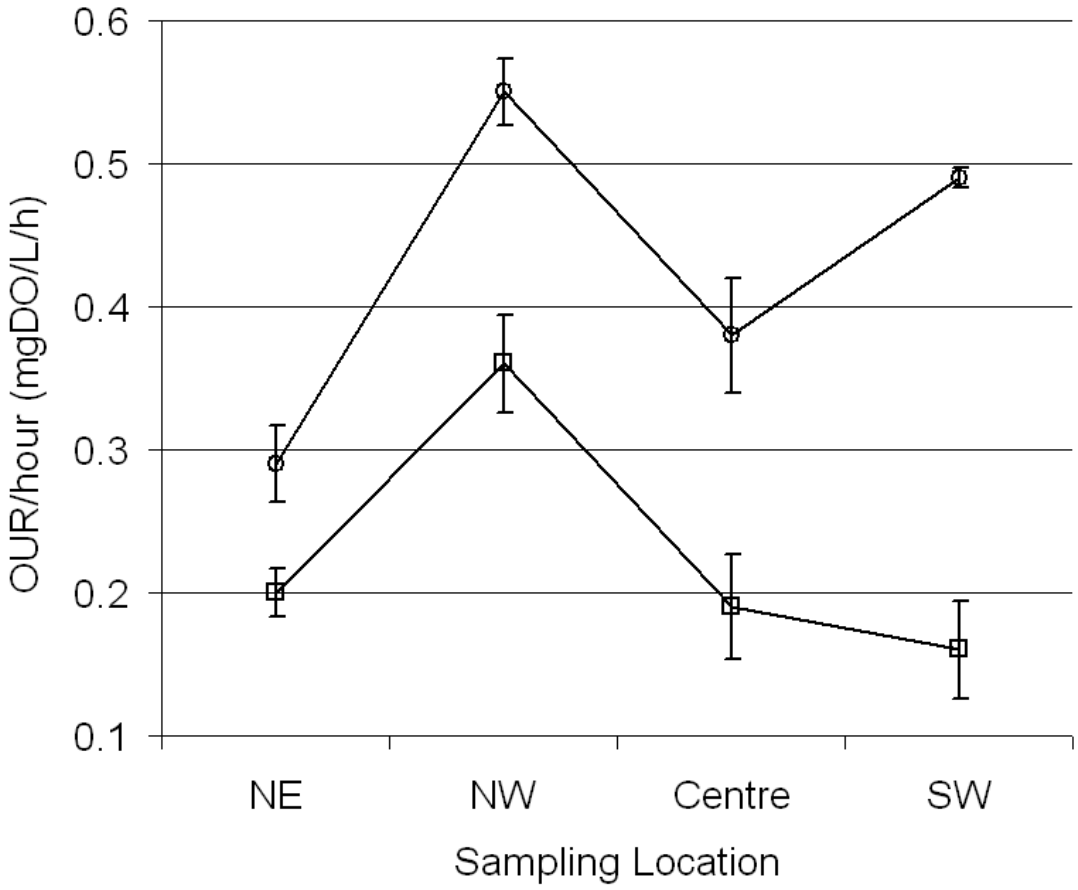

Figure 6-39 Change in OUR/hour (mgDO/L/hour), for all sampling locations. February 2005 (open circles) and May 2005 (squares) sampling periods ± SD. Data from table 6.5.

The magnitude of OUR/hour/Chl_a observed at all sites during the February sampling period was approximately 1.5 orders of magnitude greater than that observed in the Murray Bridge pilot scale HRAP and the laboratory based bioreactor and was considered unrealistically high in comparison to published values; this observation was considered most likely to reflect the impact of sediment respiration (Yamamoto 2010) on oxygen budget calculations of this type; especially when planktonic algal biomass concentrations were low. Inspection of OUR/hour/Chl_a during the May sampling period (Table 6.6 and Figure 6.40) revealed that the NE site (low algal biomass concentration) displayed the highest OUR (normalized to chlorophyll_a); this was considered consistent with the assertion that sediment oxygen demand was somewhat important in locations with minimal plankton

biomass. It was considered noteworthy that chlorophyll_*a* concentrations at the NW, Centre and SW sampling locations were

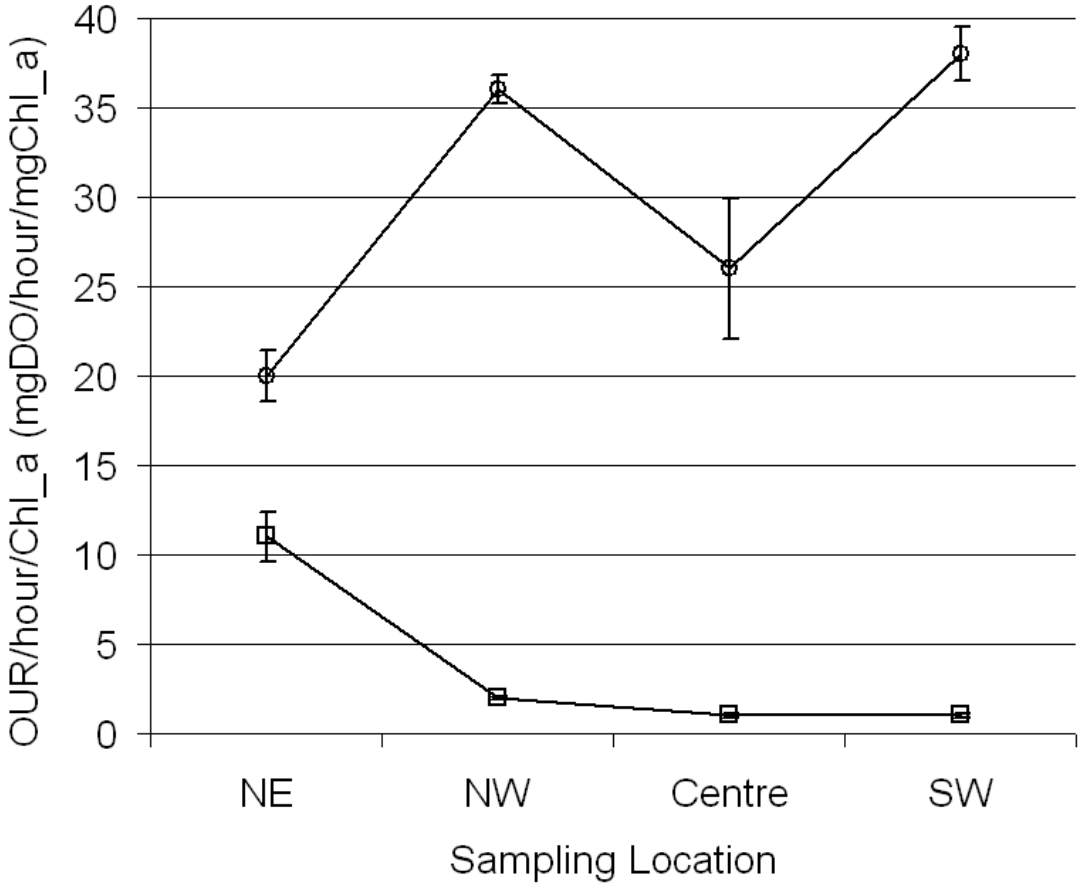

Figure 6-40 Change in OUR/hour/mgChla (mgDO/hour/mgChla), for all sampling locations. February 2005 (open circles) and May 2005 (squares) sampling periods ± SD. Data from Table 6.5.

observed to be at least an order of magnitude higher than the NE site during May 2005 (not the case with respect to suspended solids but see SW site).

As discussed in Chapter 5, some important and apparently reasonable simplifying assumptions can be made in photosynthesis/ irradiance investigations including that of respiration rates remaining constant (at a given temperature) in the presence or absence of light (Kirk 1994, Falkowski and Raven 2007, Chapter 3). The OURs presented in Table 6.5 and 6.6 were calculated from online oxygen data gathered in the absence of light to prevent oxygenic photosynthetic activity masking the signal.

Differences in oxygenic production upon illumination can therefore be assumed to dependent upon algal photosynthesis (whilst noting the absence information regarding atmospheric re-aeration and resulting source of error). The following section assesses photosynthetic rates using the online data presented.

February 2005	**OUR/hour (mgO_2/L/h)**	**SD (mgO_2/L/h)**	**N**	**r^2**
NE sampling location	0.29	0.03	10	0.92
NW	0.55	0.02	10	0.93
Centre	0.38	0.04	10	0.88
SW	0.49	0.01	10	0.98
May 2005				
NE sampling location	0.20	0.02	18	0.93
NW	0.36	0.03	18	0.86
Centre	0.19	0.04	18	0.85
SW	0.16	0.03	18	0.86

Table 6-5 Pre dawn average oxygen utilization rate; mgDO per litre per hour ± sd; May and February sampling period 2005, Based of average (10 -11 days) of DO data from pre-dawn period (n= number of consecutive 10 minute increments used for least squares fit) at each site. Coefficient of determination (r^2) indicates closeness of fit of regression line to empirical data.

February 2005	OUR/hour/Chl_a (mgO_2/h/mgChl_a)	Standard Deviation (mgO_2/h/mgChl_a)
NE sampling location	20	1.4
NW	36	0.8
Centre	26	3.9
SW	38	1.5
May 2005		
NE sampling location	11	1.4
NW	2	0.1
Centre	1	0.1
SW	1	0.15

Table 6-6 Pre dawn oxygen utilization rate normalised to unit chlorophyll_a concentration; May and February sampling period 2005.

Comparison of Gross and Net Photosynthetic Rates

In an analagous fashion to the methodology used to calculate the OUR; online DO data were used to calculate gross photosynthetic rate (GPR); with the exception that post dawn values in the morning were used (Figure 6.38); Chapter 5. That is; the parameter GPR/hour was calculated by linear regression fit of online dissolved oxygen data against time and provided a measure of average hourly rate of change (increase in this case) in dissolved oxygen concentration during the post dawn period. A minimum of approximately 1 hour of data at 10 minute intervals was used for these regressions (Figure 6.38). GPRs for each treatment when expressed both without and with normalization to chlorophyll_a are shown in Table 6.7-6.8 respectively for the February and May 2005 sampling. The corresponding plot of this data Figure 6.41 revealed that the pattern of gross photosynthesis (GPR/hour) (non-normalized to biomass or corrected for community respiration) was in general qualitatively different to that observed for OUR/hour (Figure 6.39) during both these

sampling periods. However, when corrected for planktonic chlorophyll_a concentration (Figure 6.42) a strong degree of similarity in the pattern of change in GPR at the sampling locations was noted for the May sampling period ($r^2 = 0.99$); this was considered to indicate that both community respiration rates and gross photosynthetic rates (OURs and GPRs) during the May sampling period were strongly influenced by planktonic biomass (with the possible exception of the NE location).

When correction was then made for respiration at each of the sampling locations (Tables 6.9-6.10) a substantial degree of consistency was noted in the pattern of net photosynthetic rate (P_{net}) both with and without normalization to biomass (Figures 6.43 and 6.44). This was considered as strong evidence that non-planktonic biomass was of primary importance to OUR and P_{net} during the February sampling period whilst planktonic biomass was of more importance during the May sampling period. This was supported by the observation that NE sampling site during May displayed a similar P_{net} (biomass normalized) when compared to the February data for this site; the NE site displayed consistently low planktonic algal biomass during both sampling periods.

February 2005	GPR/hour (mgO_2/L/h)	SD (mgO_2/L/h)	N	r^2
NE sampling location	0.33	0.03	19	0.87
NW	0.41	0.05	19	0.80
Centre	0.48	0.01	17	0.97
SW	0.31	0.02	14	0.94
May 05				
NE sampling location	0.41	0.02	18	0.93
NW	0.77	0.09	18	0.62
Centre	0.59	0.01	18	0.95
SW	0.38	0.02	14	0.94

Table 6-7 Post dawn average gross photosynthetic rate (not normalised to chlorophyll_a concentration); mgDO per litre per hour ± sd; May and February sampling period 2005, Based of average (10 -11 days) of DO data from pre-dawn period (n= number of consecutive 10 minute increments used for least squares fit) at each site. Coefficient of determination (r^2) indicates closeness of fit of regression line to empirical data.

February 2005	GPR/hour/Chl_a (mgO_2/h/mgChla_a)	SD (mgO_2/h/mgChla_a)
NE sampling location	23	1.5
NW	27	1.9
Centre	33	0.79
SW	24	3.0
May 05		
NE sampling location	12	1.4
NW	2	0.19
Centre	1	0.01
SW	2	0.06

Table 6-8 Post dawn average gross photosynthetic rate (normalised to chlorophyll_a concentration. May and February sampling period 2005

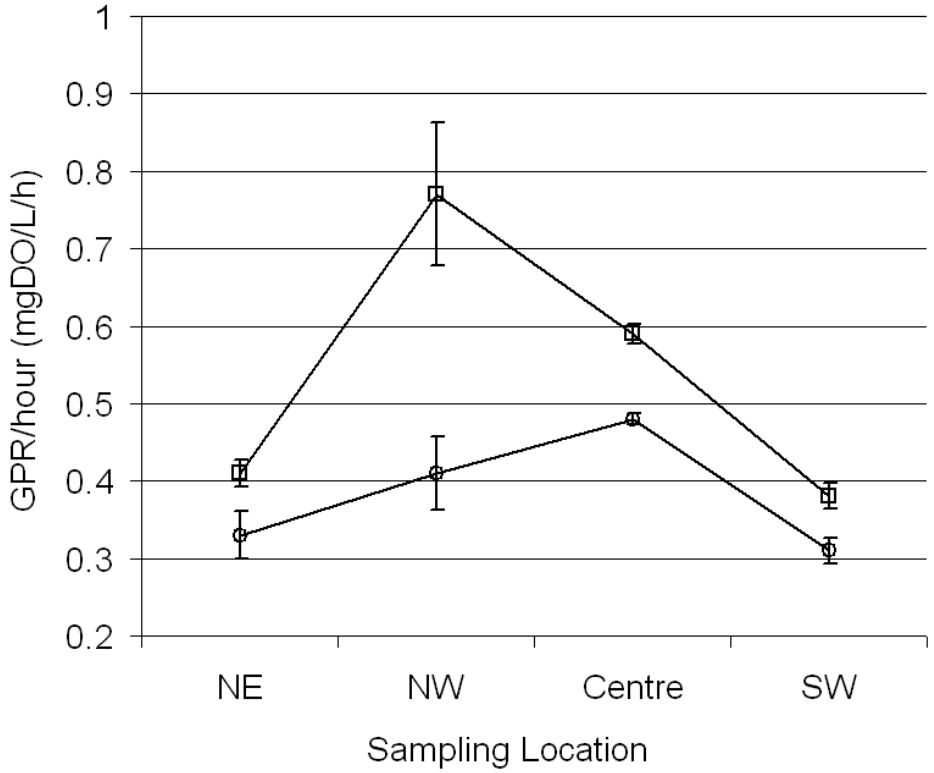

Figure 6-41 change in GPR/hour (mgDO/L/hour), for all sampling locations. February 2005 (open circles) and May 2005 (squares) sampling periods. ± SD. Data from Table 6.7.

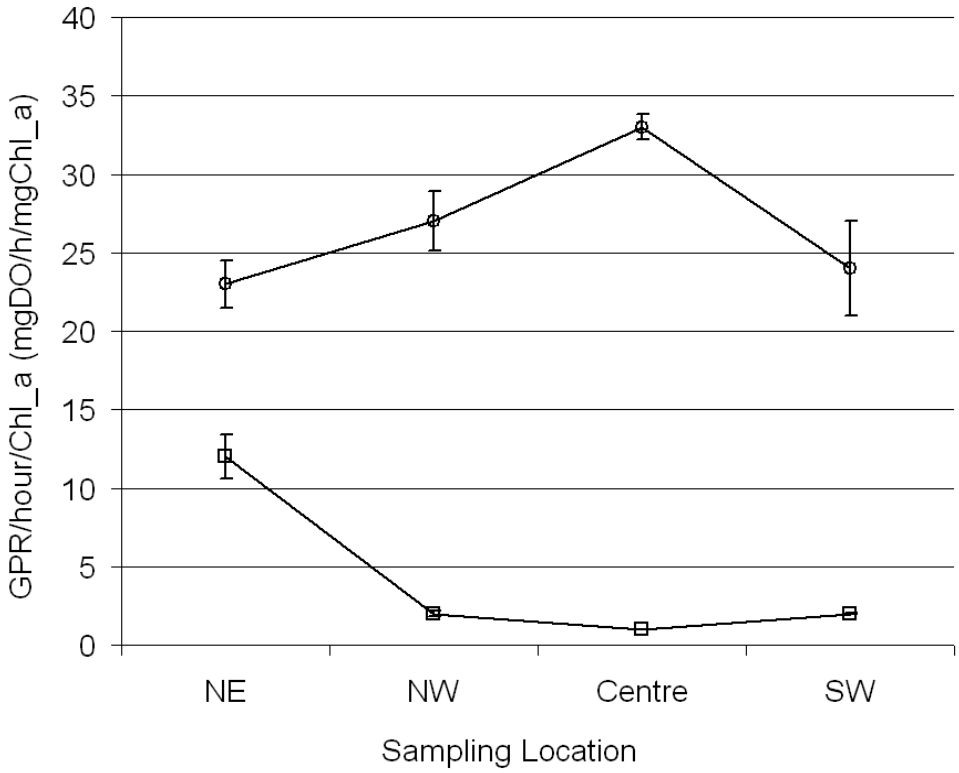

Figure 6-42 change in GPR/hour/Chl_a (mgDO/Chl_a/hour), for all sampling locations. February 2005 (open circles) and May 2005 (squares) sampling periods ± SD. Data from Table 6.8.

February 2005	**P_{net} /hour (mgO2/L/h)**	**Standard Deviation (mgO_2/L/h)**
NE sampling location	0.62	0.04
NW	0.96	0.05
Centre	0.76	0.05
SW	0.80	0.02
May 2005		
NE sampling location	0.41	0.03
NW	0.77	0.10
Centre	0.59	0.07
SW	0.54	0.05

Table 6-9 Post-dawn net photosynthetic rate (not normalised to unit chlorophyll_a concentration); May and February sampling period 2005.

February 2005	**P_{net}/Chl_a/hour (mgO_2/mgChl_a/h)**	**Standard Deviation (mgO_2/mgChl_a /h)**
NE sampling location	43	2.1
NW	62	2.0
Centre	53	4.0
SW	62	3.3
May 2005		
NE sampling location	24	2.0
NW	4.6	0.2
Centre	2.2	0.1
SW	3.0	0.06

Table 6-10 Post-dawn net photosynthetic rate (normalised to unit chlorophyll_a concentration); May and February sampling period 2005.

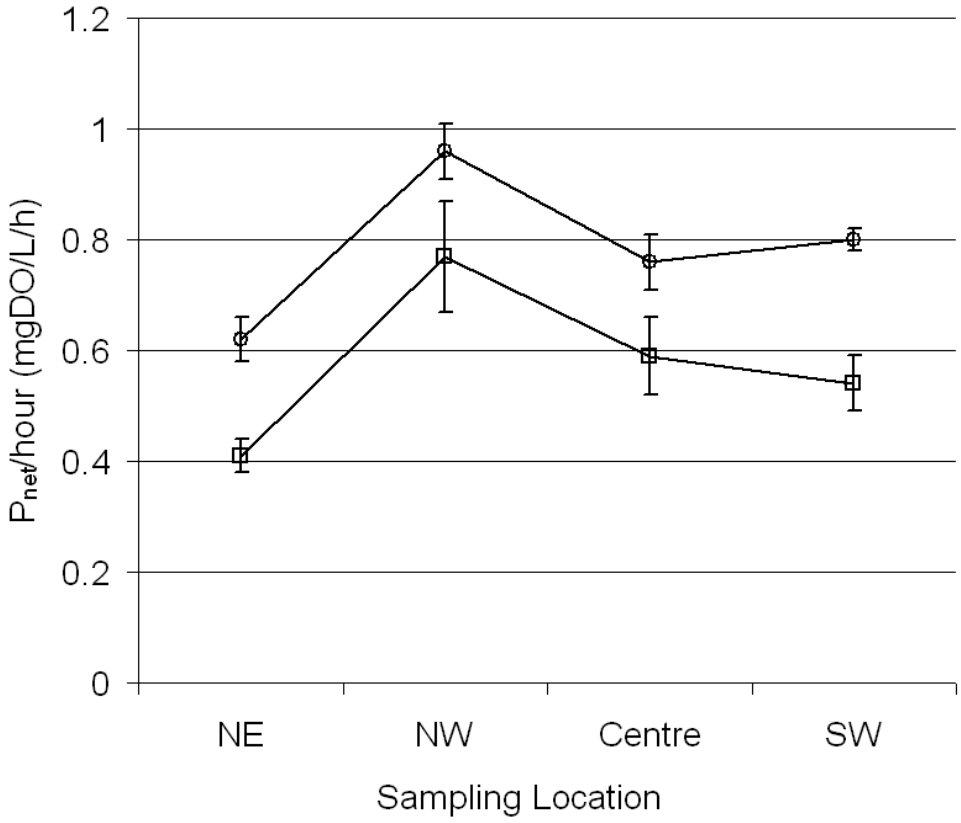

Figure 6-43 Change in P_{net}/hour (mgDO/L/hour), for all sampling locations. February 2005 (open circles) and May 2005 (squares) sampling periods ± SD. Data from Table 6.9.

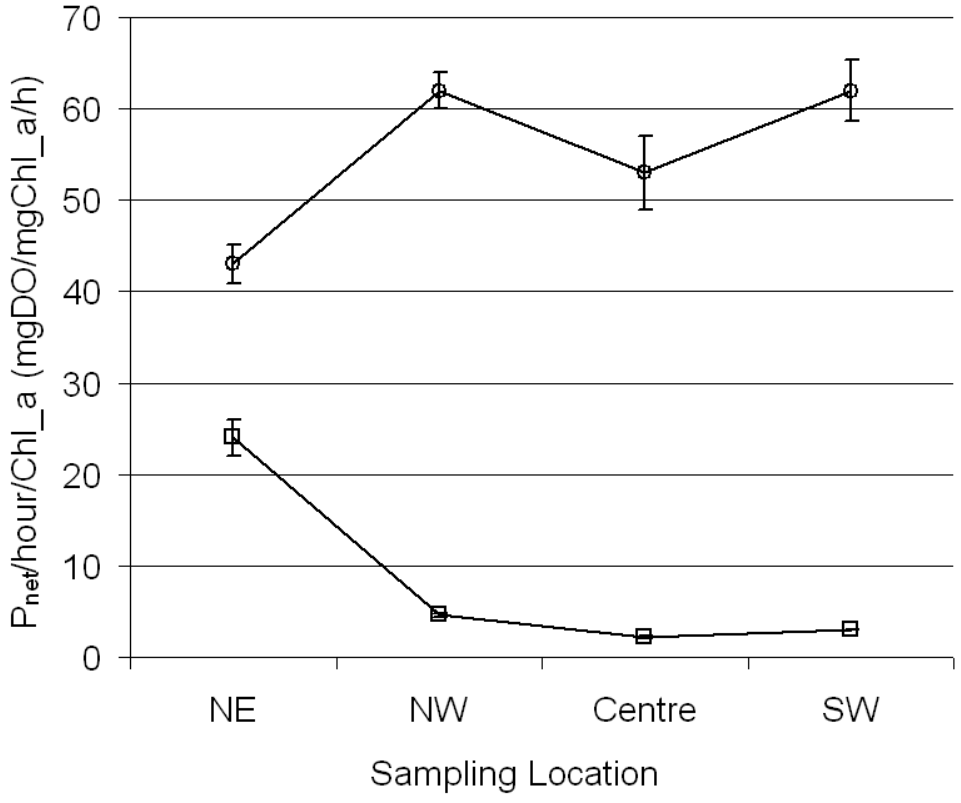

Figure 6-44 Change in P_{net}/hour/Ch_a (mgDO/hour/mgChl_a), for all sampling locations. February 2005 (open circles) and May 2005 (squares) sampling periods ± SD. Data from Table 6.10.

It was considered particularly noteworthy that the magnitude of photosynthetic rates measured during periods of low planktonic biomass; e.g. February 2005 (all sites) and May 2005 (NE site) were unrealistically high, this result was considered to indicate that algal biomass may, due to the minimal light attenuation, be able to accumulate and remain photosynthetically active in association with the sediment.

In order to provide a means of comparing photosynthetic rates calculated using the online data approach with that observed in the literature, the Online_Pnet parameters presented in this chapter were converted to units based on carbon; using the approach of Falkowski 1981, Laws 1991, Falkowski and Raven (2007, p302-303) to calculate phi (ψ) (Figure 6.45) a measure of photosynthetic efficiency. Falkowski and Raven (2007, p352) point out that ψ has the same dimensions as the initial slope of photosynthesis α (Chapter 7) and can be considered a 'light-scaled, depth integrated, assimilation number' (Falkowski 1981). Photosynthesis 'assimilation numbers' or 'quotients' (Section 2.7, p21) provide information about the stoichiometry and energetic efficiency of algal growth (Laws 1991, Reynolds 2006) and can be measured with precision in the laboratory. The typical relationship between oxygen production and carbon assimilation in photosynthesis is revealed with reference to equation 2.1 (p13). Data from laboratory and field studies (Falkowski 1981, Laws 1991, Reynolds 2006, Falkowski and Raven 2007) indicate that conversion of production on an oxygen basis to a carbon basis can be estimated with reasonable confidence by selection a PQ of between 1.0 and 1.4 for new production; that is 1 mole of oxygen produced implies between 1 and 4 moles of CO2 fixed.

$$\Psi = \frac{\int_{t_o}^{tl} \int_{o}^{z_e} P(t,z)dz\,dt}{\int_{o}^{z_e} B(z)dz \cdot \int_{t_o}^{t} I_o(t)dt}$$

Figure 6-45 Total water-column light utilisation index (ψ). P = primary productivity (C/m^3/hr), B = chlorophyll biomass (mgChl_a/m^3), I_o= incident light intensity a surface (400-700nm µmoles/m^2/s), t = time (hours), Ze = depth of the euphotic zone (from Falkowski 1981).

These authors present data showing variations in the light utilization efficiency function ψ, they state was compiled from hundreds of stations in the worlds ocean (Falkowski and Raven 2007 p 353). This data is reproduced in Figure 6.46 and 6.47 and was superimposed against that obtained using the online PI determination method and data from the Murray Bridge HRAP system Pond 1, the laboratory based bioreactor and the Bolivar sampling events. The online oxygen net productivity data from these wastewater systems was converted to carbon based productivity by assuming a PQ of 1.2 ±0.2 units of carbon fixed per unit oxygen produced.

On inspection, two contrasting fits of the online PI data to the oceanic productivity data were apparent. With respect to Figure 6.46 all Bolivar sites during February 2005 and the NE site during May 2005 displayed substantially higher values of photosynthetic efficiency than the oceanic data; this pattern was also noted in the similar (but lower) phi values calculated using PI data obtained for treatments 1 and 3 during the laboratory bioreactor (Chapter 5). Figure 6.47 revealed that data collected during May 2005 at the NW, Centre and SW sampling locations, the Murray Bridge HRAP and laboratory HRAP treatment 2 displayed a more similar pattern of response in comparison to the oceanic productivity data with respect to phi and total daily photon flux. The simplest explanation for the contrasting results

(Bolivar data) was provided by assuming that the majority of the algal biomass present in the system during February was closely associated with the sediment and due to the excellent light penetration was able to contribute substantially to photosynthesis. Thus the elevated phi levels observed were likely to be simply an artifact of this error in biomass sampling. The concordance between phi determined from these algal based treatment systems and the oceanic productivity data are discussed in more detail in Chapter 7.

These results were considered to provide evidence in support of the assertion that online oxygen data can be used to meaningfully assess rates of photosynthesis and develop an improved understanding of algal based treatment systems and perhaps algal based eco-systems more generally. More specifically with respect to design and management of wastewater treatment systems it would appear likely that practical applications of the online PI approach such as monitoring the response of a system to changes in loading or influent quality could be usefully trialed.

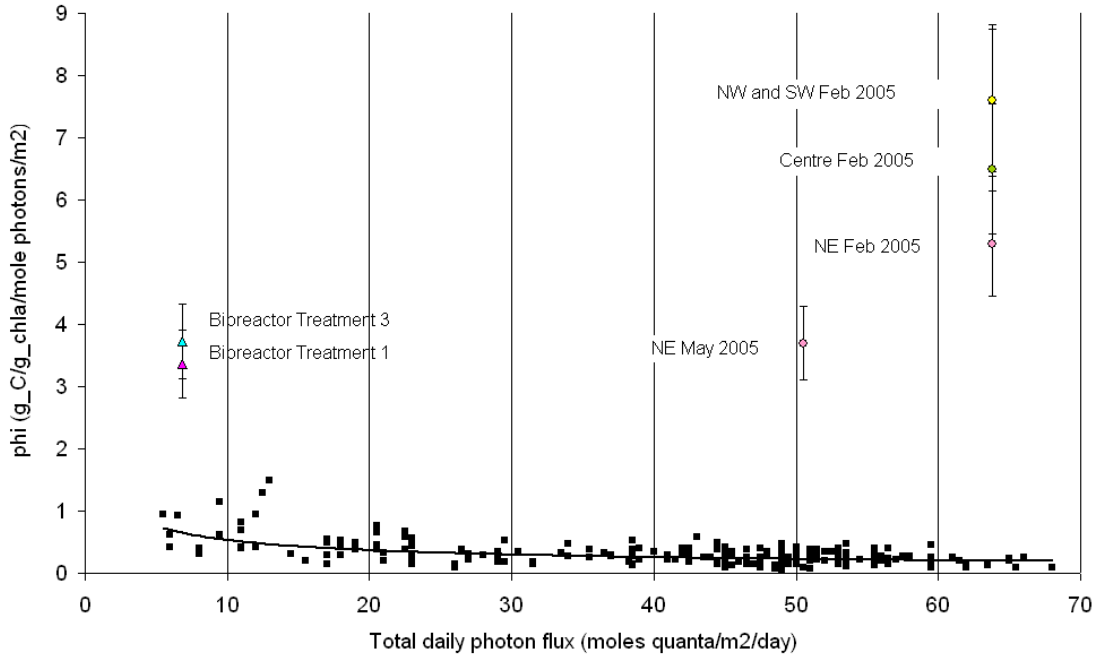

6-46 Pnet/hour February 2005; converted to gC/gChla/mole_photons/m^2 (phi) for all Bolivar sampling locations during and Bioreactor Treatments 1 and 3. Compared to oceanic data collected at hundreds of stations around the world. After Falkowski and Raven (2007).

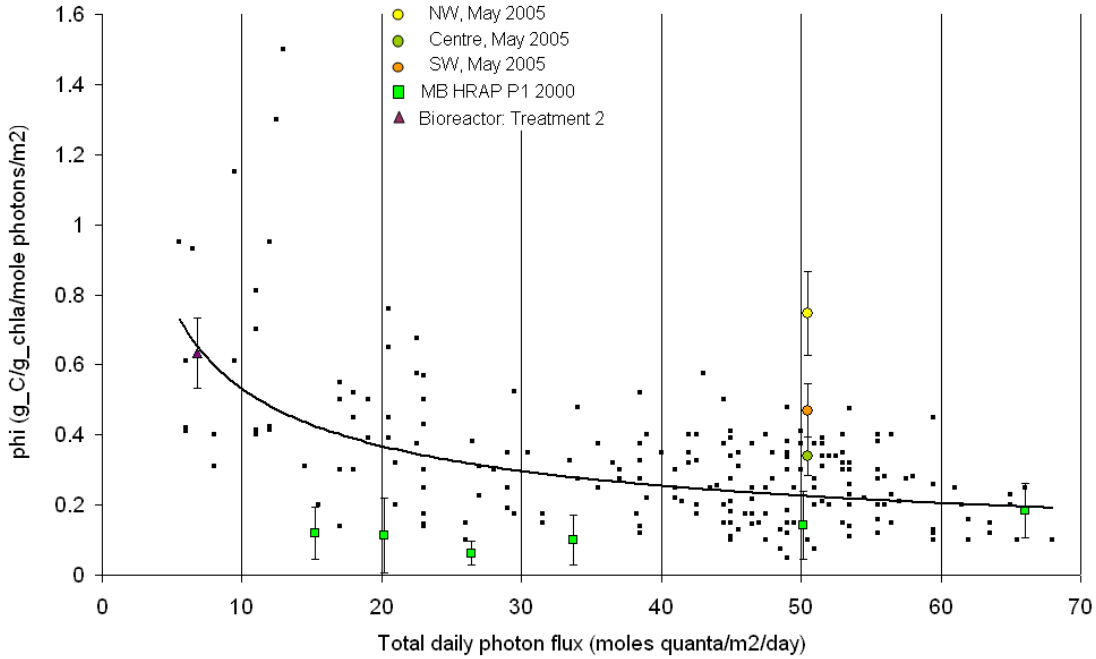

6-47 Pnet/hour May 2005; converted to gC/gChla/mole_photons/m^2 for specified Bolivar sampling locations, Murray Bridge Pond 1 (2000) and Bioreactor Treatment 2. Compared to oceanic data collected at hundreds of stations around the world. After Falkowski and Raven (2007).

6.4. Conclusions

An in-situ online monitoring system consisting of four online dissolved oxygen and temperature monitoring stations was installed at Bolivar WSP 1 with the resulting data used to characterise patterns of DO and temperature variation in parallel with changes in wind velocity during February and May 2005. The novel approach to analysis of photosynthetic rates using online oxygen data (Chapter 5) was trialled and provided a 'window' through which, for the first time, changes in photosynthesis irradiance relationships in response to changes in climate during the seasonal cycle and pond mode (benthic versus planktonic algal dominance) could be clearly established in Bolivar WSP 1. This novel approach appears to provide great promise as a design and management tool for algal based wastewater treatment systems more generally.

The following conclusions were immediately apparent

- Light penetration was greater by approximately and order of magnitude in WSP 1 during this period in comparison to the observations reported in Sweeney (2004).
- Planktonic algal biomass concentrations (chlorophyll_a) at all sampling locations during the February (Summer) sampling period were extremely low in comparison to those observed by Sweeney (2004) and were considered to have resulted from a change in pond influent characteristics after commissioning of the AS treatment system.
- Patterns of thermal stratification in the Bolivar WSP observed during February and May 2005 were qualitatively similar to those observed

by Sweeney (2004).

- Patterns of change in pond oxygenation at the four sampling sites were correlated with temperature and thermal stratification; the impact of wind velocity tended to be greater for the NE and SW sampling sites.
- That short circuiting of flow may have been significant during the February sampling period and that this may have implications for re-use if retention times and disinfection rates are substantially different from design parameters.
- Photosynthetic rates and community respiration rates measured using online data displayed location and time specific patterns of variation that were explicable provided an active benthic algal biomass was assumed. i.e. photosynthetic rates calculated using online data and planktonic biomass concentrations collected during February at all locations and from the NE sampling location during May appeared unreasonably high.

7. DISCUSSION

7.1. Introduction

Investigations reported in this thesis were aimed at assessing the efficacy of a novel approach for extraction of photosynthesis-irradiance parameters from in-situ online dissolved oxygen data reported by Fallowfield et al. (2001) and Evans et al. (2003) and to make a contribution to an improved understanding of biological processes within waste stabilisation ponds. The in-situ PI approach was considered to require testing and initial validation trials in controlled laboratory conditions against data collected using the standard PI determination method (Evans et al. 2003) prior to use within a large and complex WSP. Results of experiments conducted toward this end were reported in Chapter 5. Field investigations were conducted by using a series of four purpose-built online monitoring stations installed at a large maturation waste stabilisation pond treating activated sludge (AS) effluent at Bolivar WWTP. High temporal resolution online data was analysed to determine in-situ photosynthetic rates at Bolivar WSP 1 and compare those obtained from a laboratory based algal bioreactor (Chapter 5) and the scientific literature. This work was conducted as a part of an extensive program of research conducted over a period of more than a decade on the Bolivar WSP system in Adelaide, South Australia. Characterising both the biological and physical nature of these pond systems (Weatherall 2001, Herdianto 2003, Sweeney 2004, Yamamoto 2007, 2010, Short 2010) improves the scientific basis for development and use of pond design and optimisation tools (Oswald 1995, Fallowfield et al. 1992, Mayo and Noike 1994, Sweeney et al. 2003, Shilton and Harrison 2003, Ratchford and Fallowfield 2003, Sweeney et al. 2007, Short et al. 2007, Yamamoto et al. 2010). At the time of writing this is the first reported assessment of photosynthetic oxygen dynamics at Bolivar WSP 1 and was

understood to be the only study of its type reported in the WSP literature.

7.2. Laboratory Based Validation Study

A novel laboratory based HRAP (bioreactor) was designed, built and operated in controlled laboratory conditions to provide data for comparison of photosynthesis/irradiance curves obtained using a standard laboratory PI apparatus with those calculated from in-pond dissolved oxygen time-series using a modified version of the proposed method of Evans et al. 2003 (Chapter 5). Light intensities at the surface of the bioreactor were close to limiting and provided the opportunity to estimate rates of oxygenic production within the notionally linear portion of the photosynthesis-irradiance curve using the standard PI apparatus (Falkowski and raven 2007). In addition to light limited parameters of the PI curve, saturated rates of photosynthesis were also measured by use of the standard PI apparatus. Carbon loading of the system was achieved by use of synthetic sewage medium (Cromar 1996) modified to provide carbon (as acetate) loadings of similar magnitude to those applied to Bolivar WSP 1. Standard water quality treatment parameters were considered to provide satisfactory indicators of bioreactor operation (Cromar 1996, Fallowfield et al 2001, Metcalf and Eddy 2003) for comparison against other algal based systems.

7.2.1. Laboratory Based System Operation

Measurements of culture light attenuation suggested that surface irradiance was close to limiting intensities, this provided conditions suitable for measurement of light limited photosynthetic rates (Section 5.3.2). The presence of flocculent particles in carbon loaded treatments was associated with more effective light penetration into the pond. The pattern of variation in pond chemistry and biological parameter values,

including algal and bacterial biomass, were considered unexceptional for a HRAP system operating under the variety of loading conditions applied. Patterns of change in oxygen concentration in the photoautotrophic treatment were considered to be consistent with carbon limitation; somewhat surprisingly, results from online PI measurements suggested that carbon limitation was potentially a factor in the first carbon loaded heterotrophic treatment (Treatment 2).

Online data collected from the bioreactor was used to calculate net photosynthesis curves and these were compared against those obtained using the standard PI apparatus. No significant difference was observed in terms of net photosynthesis between the two methodologies (in the carbon loaded treatments) at the equivalent light intensity. It was not possible to determine in a straight-forward fashion a means of determining alpha (α) the light-limited rate of photosynthesis using the laboratory based bioreactor system due to square wave nature of the day/night cycle. However, as an extension of the above; the measured values for net photosynthetic rate (per unit chlorophyll_a) were normalised to 'daily' irradiance to calculate 'integrated water-column light utilisation efficiency' (Falkowski 1981, Morel 1991, Laws 1991, presented Chapters 6 & 7). This parameter (ψ) has the same units as the initial slope (α) of the PI curve (Falkowski 1981, Falkowski and Raven 2007) but is generally expressed in units of carbon. For comparative purposes the value of α derived from the standard PI apparatus determinations (on a oxygen basis for simplicity) was compared with that derived by normalizing Online_P_{max} to average irradiance at the surface of the bioreactor (105 µmol/m2/sec). A poor correlation ($r^2 = 0.40$) was generally observed between these parameters across treatments; a within-treatment comparison revealed a relatively good correspondence in terms of α for Treatment 3

(ψ within 40% of α).

It was considered noteworthy that results of ψ (on a carbon basis) were close to the range reported from experimental assessments of algal carbon productivity in light limited cultures (Reynolds 2006, p106) and similar in magnitude to values of reported for oceanic productivity (Falkowski and Raven 2007, p353).

It was concluded that online data and the algorithm developed for analysis were potentially efficacious for calculation of net photosynthesis in carbon loaded conditions in this lab based HRAP system; in this case a point on the PI curve defined by the bioreactor incident light intensity.

The most important limitation of this laboratory-based study was considered to be a lack of a pattern of changing light which prevented a direct comparison of the initial slope of photosynthesis using the two methodologies.

Harris (1999) argued that apparently complex behaviour in aquatic ecosystems may infact result from a small number of fundamental principles that 'impart higher level order and predictability' on a system. If these principles are fundamental then one would expect them to be 'forcing functions' across aquatic ecosystems; one of these he asserts (quite reasonably) is that input of energy (light) and nutrient input controls overall biomass (and by inference productivity) (Chapter 3). In a system such as a WSP with well defined shape, depth and volume and high nutrient levels it would on this basis appear reasonable that measures of photosynthetic rate should be more easily determined (less subject to noise) than those measured in many difficult to

define natural systems. On this basis it was considered that a field trial in a full scale WSP system could in principle provide data for calculation of photosynthesis parameters of somewhat similar quality to that observed in the Murray Bridge HRAP system despite the impact of wind induced mixing, stratification and variable patterns of flow.

7.3. Bolivar WSP

A series of four purpose built online monitoring stations were designed and installed at Bolivar WSP 1 to provide data for a detailed assessment of patterns of thermal stratification, oxygen dynamics and comparison of photosynthetic rates obtained from the laboratory based algal bioreactor and the literature. Comparisons of parameters such as thermal stratification and dissolved oxygen concentration in response to changes in irradiance and wind velocity were made to allow integration and comparison of these findings with those obtained by Herdianto (2003), Sweeney (2004) Yamamoto (2007) and Short (2010).

Planktonic chlorophyll_*a* concentrations and by implication algal biomass concentrations were observed to be extremely low during February 2005 in comparison to observations of Weatherall (2001) and Sweeney (2004). Whilst generally much higher during the May sampling period, biomass concentration displayed a high degree of variability both across the pond and between depths within sites. These observations were confirmed by comparison with contemporaneous algal biomass observations of Yamamoto (2007) and Short (2010). Unpredictable 'boom-bust' cycles in algal plankton and zoo plankton populations were observed during this period by Short (2010); consistent with previous observations of changes in algal population density reported by Sweeney et al.

(2005b). Short (2010) postulated that reduction in influent ammonia concentration following conversion of the system to AS influent to low loading conditions (Sweeney et al. 2005b) provided conditions more suitable for herbivorous zooplankton as ammonia is toxic to zooplankton at elevated pH. It is noteworthy that free ammonia is also toxic to algae and therefore at high pH can limit photosynthesis (Albeliovich 1976); it appears that algae may however regain the ability to photosynthesise when pH and free ammonia concentrations fall as this pattern can occur on a daily basis (Pearson et al. 1987, Fallowfield et al. 2001). It may also be the case that the WSP is at times nitrogen limited (Sweeney et al. 2005b) thus limiting algal growth. The dominant form of nitrogen in the system after the upgrade to AS was nitrate; energy from carbohydrate respiration for reduction to ammonia within the algal cell prior to use in synthesis is required; as such carbon fixation rates per unit oxygen evolved may be 30% higher than when ammonia is used as a nitrogen source (Falkowski and Raven 2007). Results of inorganic carbon concentration, presented in Chapter 6, showed a significant draw-down in inorganic carbon (IC) concentration in WSP 1 during May 2005; the concentrations of IC observed in the WSP during May 2005 were similar to those observed in the laboratory based bioreactor (Treatment 2) where IC was considered likely to be at limiting concentration at the pH range observed. This result was considered to indicate that an additional factor (carbon limitation) may limit algal biomass during some periods; again presumably resulting from the change to very low BOD influent in 2001, thereby limiting available carbon for algae from the activity of heterotrophic bacteria. Recent observations of maturation ponds at Williamstown and Tanunda SA indicate that similarly low planktonic algal biomass concentrations can occur in other systems of this type (N. Buchanan pers. com. 2010).

Low phytoplankton concentrations in the WSP had important consequences for light attenuation within the system; extinction of light within Bolivar WSP prior to commissioning of the activated sludge plant was generally observed within the first 30cm from the surface of the pond (Weatherall 2001, Sweeney 2004 and R. Evans. Pers. Obs). During February 2005 (and at the NE sampling site during May 2005) the bottom of the pond was clearly visible on many occasions with transmitted light available for growth of microphytobenthos (MPB), a phenomenon often seen in shallow clear water bodies such as Port Phillip Bay Victoria (Harris et al 1996) and not identified in the a search of the WSP literature e.g. Curtis et al 1994, Short pers. com. 2011). The presence (inferred) of a significant microphytobenthos during February 2005, and at the NE sampling location during May 2005 was considered likely based on the following observations;

1. Unrealistically high rates of gross and net photosynthesis (based on online PI determinations) observed during February 2005 when normalised to planktonic chlorophyll_*a*.
2. The apparent lack of draw-down of inorganic carbon in the pelagic zone during February 2005 despite high observed rates of photosynthesis; in contrast to observations during May 2005.
3. Consistently low light attenuation and consequently non-light limiting conditions at the bottom of the pond.

The abundant growth of macrophytes and microphytobenthos is well documented in pond systems where sufficient light reaches sediment (Colijn and de Jong 1984, Beardall and Light 1997b, Harris 1996, Fulweiler et al., 2008) but not in WSPs. Recent work by Yamamoto et al. (2010) revealed an important role for sediments in terms of nitrogen cycling in Bolivar WSP 1 and provided evidence that biomass assimilation was likely to dominate nitrogen removal in WSP environments. The microcosm assessment methodology of Yamamoto et al. (2010) included incubation in the dark but did not include measurement of sediment photosynthetic pigment. As such it is hypothesised that during periods of high PFD at the sediment pelagic interface that microphytobenthos may play an important role in nitrogen removal. Sigmon and Cahoon (1997) point out that microphytobenthos (MPB) has been shown to have the capacity to regulate nutrient fluxes across the sediment-water interface via direct uptake in coastal marine environments (Darley et al. 1979, Sundback et al. 1991). In a mesocosm study of intact cores of sediment incubated in a laboratory continuous flow system Sundback et al. 1991 showed that flux of nutrients NH_4^+, NO_3^- and $PO4^{3-}$ out of sediment into the water column was limited by uptake (inferred) from MPB. Other studies e.g. Sunback and Jonsson (1988) show that substantial levels of photosynthetic production are possible in shallow, intertidal, littoral coastal ecosystems. MPB can be important in regulating N cycling in some systems. For example, Rysgaard et al. (1995) showed that benthic micro algae were able to successfully inhibit coupled nitrification–denitrification in the benthos through effective out-competition for substrate NH_4^+-N. Similarly, work by Risgaard-Peterson et al. (2004) suggested that direct competitive interaction takes place between algae and ammonia oxidisers, and that benthic algae can be superior competitors during this interaction because of higher N uptake rates and growth rates

than nitrifying bacteria. This generally results in little or no nitrification in the upper pelagic 'photic' zone but a sharp increase below this zone (Short pers. com. 2011). Benthic primary production has also been shown to alter nutrient fluxes and denitrification by oxygenating surface sediments through photosynthesis and through nutrient assimilation (see Fulweiler et al., 2008). On the basis of the above it was postulated that MPB may drive the productivity of the Bolivar WSP during periods of low phytoplankton and high light penetration; potentially limiting nutrients released from sediment due to anaerobic/anoxic conditions (reducing conditions, e.g. N and IC) the growth of MPB may provide substantial productivity for higher trophic levels (zooplankton) during these periods. Zooplankton feeding on the potentially abundant MPB would be available to clear the pelagic zone thus maintaining transparent conditions suitable for the MPB. It has been shown that MPB can attach to sediment and stabilise sediment particles; reducing the likely hood of re-suspension (Beardall and Light 1997a); anecdotal observations at Bolivar WSP 1 during February 2005 suggested that sediments were surprisingly resistant to turbation during wind events (Chapter 6). This may have simply have reflected the strong degree of stratification in the pond but a similar pattern was generally noted across the pond. See Table 7.1 for a summary of algal biomass concentrations in sediments from a range of shallow aquatic habitats (<20m) (corrected for the presence of pheophytin a breakdown product of chlorophyll_a (Beardall and Light (1997a). These authors cautioned that some of the extremely high oxygenic productivity values shown could in-part reflect variations in the thickness of the sediment sampled; nevertheless mean measurements of gross primary productivity of MPB (Table 7.2) were generally commensurate with these biomass estimates. As might be expected from a shallow, transparent (during February 2005) and nutrient

rich pond; the average gross photosynthetic rates for Bolivar WSP 1 were comparatively high but, importantly; within the observed range shown in the table, suggesting that the calculated rates (based on the online data) were reasonable. Whilst MPB was not the focus of this thesis and can not be considered definitive without data directly assessing sediment biomass; the insights of detailed above could be considered to be an example of the characteristics that the online data and analysis algorithm may reveal about potential mechanisms of wastewater treatment when applied to high resolution online data.

Analysis of patterns of thermal stratification for Bolivar WSP 1 revealed, in general, a high degree of consistency in qualitative terms with the observations of Sweeney (2004); this was despite the lower spatial resolution of the data across the pond. Of note with respect to contrast with earlier work was the apparent resistance of thermal stratification to changes in wind velocity at some pond locations during both sampling periods. For example during the February sampling period the NW sampling location retained a strong positive thermal stratification during the entire 11 day sampling period despite considerable peaks in wind speed during some periods. It was considered most likely that changes in hypolimnion depth resulted during periods of high wind speed at locations displaying persistent thermal stratification (Sweeney 2004). It was noted that net photosynthetic rates (not normalised to Chl_*a*) during February were highest at the two sites (NW and SW) both displaying positive stratification on average. Again, during the May sampling period net photosynthetic rates at the NW sampling site were highest in comparison to the other sites; during this period the NW site was isothermal i.e. did not display stratification. This was considered to indicate that location in the pond may influence photosynthetic rate. In order to test this assertion more research would be required with additional seasonal

data to establish if such patterns change over time or are resilient.

Consistent with the work of Sweeney (2004) the persistence of positive thermal stratification events was greatest at the NW, SW and Centre sampling locations with persistence of positive thermal stratification at these localities being much greater during summer. Negative thermal stratification (colder layer of water at the surface) was displayed at the NE sampling locality during the entire May05 sampling period, changes in stratification status at the other sampling sites were typically cyclic and varied during the diurnal period. It was noted that the NE sampling site displayed consistently low phytoplankton (and excellent light penetration) during the May05 sampling period, consistent with that observed across all sites during the February05 sampling period. It was considered possible that a lack of suspended biomass during February 2005 at all locations (and the NE site during May05) may have contributed to additional radiative cooling or heating dependent upon air temperature (see Kirk 1994) and contributed to the apparently substantial increase in persistence of stratification in comparison to the work of Sweeney (2004). Nevertheless, more research would be required to confirm this assertion.

Investigations of stratification and persistence of the thermocline and CFD modelled hydrodynamic flow of the pond in relationship to irradiance and wind velocity and reported in Sweeney et al. (2003) indicated that preferential flow (short circuiting) of influent may be favoured during long and positive stratification events. Retention time of Bolivar WSP was a nominal value of 12 days at the time of sampling, with the system providing a storage ‘polishing’ and disinfection function prior to filtration and chlorination following passage through Ponds 2 and 3. Sweeney et al. (2003) noted that it was probable that a ‘minimum stratification duration’ existed below

which short circuiting is negligible due to local mixing. However, during long periods of positive stratification, retention time may be only a matter of hours in a pond with a mean retention time of 15-20 days (Pedahzur et al.1993). It was therefore considered reasonable to conclude that if patterns of stratification in the subsequent 2 ponds were similar to Pond 1 that disinfection could be compromised during some periods (see Sweeney et al. 2003). Whilst chlorine disinfection prior to re-use provided a secondary barrier to human exposure and the greater transparency of the pond may assist in UV facilitated disinfection processes; it was considered consistent with the precautionary principle to consider additional vigilance with respect to chlorination at the final treatment phase during potential periods of significant short circuiting.

Results from in-situ (field-based) measurements of photosynthesis are difficult to interpret using the standard PI apparatus if storage or transport of samples is required (Kirk 1994). A review of the WSP literature revealed few attempts to determine photosynthetic rates of WSP ponds using measurements of dissolved oxygen in situ. An exception was that of Kayombo et al. (2002) who assessed diurnal patterns of change in physical-chemical parameters in a small WSP system treating domestic wastewater (sewage) for a population of 5000 people at the University of Dar es Salaam, Tanzania. These authors concluded that diurnal variation of the parameters measured (DO, pH and temperature) followed a cyclic pattern determined by hourly and daily variation of light intensity. A statistically significant relationship was observed by Kayombo et al. (2002) between pH and DO, consistent with algae 'pumping' protons from solution during photosynthesis and increasing pH of the pond water. The paper reported average rates of DO production and utilisation

(based on linear regression) in the individual ponds but lacked sufficient methodological detail to establish what portions of the daily DO 'curve' were used by the authors to generate these parameters; unfortunately no data was presented detailing algal biomass concentrations.

For the sake of the following comparison, it was assumed that the reported DO production and utilisation rates of Kayombo et al. (2002) were obtained in an analogous fashion to that detailed in this thesis; it was not however, possible to compare rates unitised to algal biomass. A summary of the results obtained from the maturation ponds in the series (Kayombo et al. 2002) were provided with the potentially equivalent measures (identical units) obtained by analysis of Bolivar WSP 1 online data as reported in Chapter 6 (Table 7.3). Average oxygen utilisation rate based on 24 hours data and obtained from measurement of effluent DO concentration at the outlets of three maturation ponds by Kayombo et al. (2002), appeared similar in magnitude to that observed at some localities sampled in the Bolivar WSP.

Observations of average DO production rate were in general higher in magnitude in the Bolivar system; however Kayombo et al. (2002) provided no information regarding irradiance or season so quantitative comparison must be appropriately cautious. Net photosynthetic rates were not reported by the Kayombo et al. (2002) and were therefore calculated by addition for the purposes of this comparison and provided in Table 7.3. The net photosynthetic rate was again similar to, but generally lower than, that observed in the Bolivar maturation pond.

A scarcity of published studies in the peer reviewed literature appears to characterise the current state of the science in this area of WSP research; comparison against such a limited data set does not therefore allow for definitive conclusions regarding the

merits or otherwise of either method. Nevertheless the comparison provides a starting point from which future comparisons can be made. Unfortunately the methodology applied by Kayombo et al (2002) in determining OUR and DO production rate was not clearly detailed thus making the comparisons tenuous.

Fortuitously, another study was reported by Weatherell (2001) who attempted to obtain PI curves (with minimal storage of samples) collected from the same series of WSPs at the University of Dar es Salaam, Tanzania. Analysis using the standard PI apparatus in the field was reported to be unsuccessful (Weatherell 2001) due to the lack of a field based laboratory to provide controlled conditions for analysis. A brief study using the light-dark bottle method (e.g. Manning et al. 1938) was trialled but considered to be unsatisfactory. A time series of grab samples were therefore collected in the field and analysed in the laboratory using the standard PI apparatus and provided data from twenty two weekly samples for assessment (Weatherell et al. 2007). For comparative purposes net photosynthetic rates, planktonic biomass and light attenuation results of this work (from maturation ponds) were also summarised in Table 7.4. Whilst potentially confounded by bottle effects the data reported by Weatherell et al. (2003) identified distinct diurnal variations in P_{max} and α; these were attributed to variation in chlorophyll_a concentration.

For comparative purpose, the data collected from Bolivar WSP 1 during May 2005 (shown in bold typeface in Table 7.4) was also considered to reveal a contrast (in comparison to February 2005) in measured photosynthetic rates when concentrations of phytoplankton were significant. Weatherall et al. 2003 observed 'surprisingly' large variations in diurnal column chlorophyll_a concentrations and cautiously attributed this observation to very high growth rates during the day and similarly

high rates of decline overnight. In contrast, very low concentrations of chlorophyll_*a* were consistently observed in the Bolivar maturation pond in 2005. During these periods, and similarly when chlorophyll_a concentrations were higher, variation in light attenuation was low whilst the photosynthetic parameter Pmax displayed little variation within a location on average. Variation however, was considerable between periods (February 2005, May 2005) or between locations (during May 2005; NE location) when average planktonic algal biomass concentrations were substantially different. This was considered to highlight the importance of obtaining data with both high spatial and temporal resolution and display the potential utility of photosynthetic rate determinations in-situ.

The comparisons discussed above are necessarily preliminary due to limited data available in the literature; however it appears to illustrate the potential utility of the in-situ approach to determination of photosynthetic rates. The apparently consistent relationships revealed from analysis of online dissolved oxygen data obtained contemporaneously at multiple sites in a WSP using this novel approach provided confidence that it may be a be useful alternative to that provided by sample storage and analysis using the standard PI approach. Both approaches should provide complementary data. The PI apparatus can unambiguously provide the initial light limited rate of photosynthesis on a per unit PAR basis but appears to enhance light climate due to enhanced mixing within the PI chamber, whilst the 'light history' of the samples is extremely important. The online data approach appears to offer potential as a means of calculating in-situ photosynthetic efficiency (Falkowski 1981, Laws 1991) and if so would avoid the issues arising from sample storage and transport. The apparently similar results for ψ revealed in comparison with the

oceanic productivity database was considered surprising and somewhat remarkable. This observation is considered a useful target for future research in light of the important effort currently underway to understand aquatic photosynthesis and its contribution to global carbon assimilation from atmospheric sources both anthropogenic and non-anthropogenic.

	Sub-tidal Marine n = 62	**Sub-tidal Esturine n = 29**	**Intertidal Marine n = 12**	**Intertidal Esterine/Saltmarsh n = 25**
Minimum ($mg\ chl\_a/m^2$)	0.04	4	0.04	0.23
Maximum	1030	558	500	324
Mean (sd)	107 (185)	98 (119)	82 (137)	57 (76)

Table 7.1. Summary of microphytobenthos biomass from literature, expressed as mg chl_a/m^2 in different environments (n = number of estimates). From Beardall and Light 1997a.

	Sub-tidal Marine n = 14	**Sub-tidal Esterine n = 12**	**Intertidal Marine n = 3**	**Intertidal Esterine/Saltmarsh n = 14**	**Bolivar WSP 1 n = 4**
Minimum ($mgC/m^2/h$)	2.1	10	23	1	84 (SW site)
Maximum	276	178	75	120	131 (Centre site)
Mean (sd)	59(72)	65 (57)	49 (26)	48 (33)	104 (21)

Table 7.2. Summary of microphytobenthos gross primary productivity from literature, expressed as mgC/m^2/h in different environments (n = number of estimates). From Beardall and Light 1997a. Data from Bolivar WSP 1 included for comparison; average of all sites during February 2005: Determined from online PI determinations and conversion of oxygen production (per square meter) to unit carbon production using assimilation number = 1.1 (O_2-CO_2) and division by 3.66 (CO2 to C) (Falkowski 1991, Laws 1991, Raven and Falkowski 2007).

Source	OUR/hour (mgDO/L/h)	GPR/hour (mgDO/L/h)	Pnet/hour (mgDO/L/h)
Kayombo et al. 2002	0.23 (0.04) n = 3 (ponds)	0.18 (0.11) n = 3	0.4 (0.03) n = 3
Bolivar WSP 1 (February 05)			
NE	0.29 (0.03) n = 10	0.33 (0.03) n = 10	0.62 (0.04) n = 10
NW	0.55 (0.02) n = 10	0.41 (0.05) n = 10	0.96 (0.05) n = 10
Centre	0.38 (0.04) n = 10	0.48 (0.01) n = 10	0.76 (0.05) n = 10
SW	0.49 ((0.01) n = 10	0.31 ((0.02) n = 10	0.80 (0.02) n = 10
Bolivar WSP 1 (May 05)			
NE	0.20 (0.02) n = 11	0.41 (0.02) n = 11	0.41 (0.03) n = 11
NW	0.36 (0.03) n = 11	0.77 (0.62) n = 11	0.77 (0.10) n = 11
Centre	0.19 (0.04) n = 11	0.59 (0.95) n = 11	0.59 (0.07) n = 11
SW	0.16 (0.03) n = 11	0.38 (0.94) n = 11	0.54 (0.05) n = 11

Table 7.3. Summary of oxygen utilization, gross and net photosynthetic rates without normalisation to biomass, mean, sd and sample size for maturation WSPs. Kayombo et al. 2002 (n = 1 day of 15 minute interval online DO data, average of 3 maturation ponds). Bolivar WSP, n = 10 or 11 days of 10 minute interval online DO data (Chapter 6).

Source	Pnet/hour/Chl_a (µgDO/µgChl_a/hour)	Planktonic Chlorophyll_a (µg/L)	PAR Attenuation (m^{-1})
Weatherell et al. 2007	**8.54 (3.18) n = 3**	**236 n = 4**	6.98 n = 4
Bolivar WSP 1 (February 05)			
NE	43 (2.1) n = 10	14.5 n = 4	2.12 n = 3
NW	62 (2.0) n = 10	15.5 n = 4	2.14 n = 3
Centre	53 (4.0) n = 10	14.5 n = 4	2.20 n = 3
SW	62 (3.3) n = 10	13 n = 4	2.30 n = 3
Bolivar WSP 1 (May 05)			
NE	24 (2.0) n = 11	17.5 n = 4	2.31 n = 4
NW	**4.6 (0.2) n = 11**	**168 n = 4**	2.16 n = 4
Centre	**2.2 (0.1) n = 11**	**271 n = 4**	2.61 n = 3
SW	**3.0 (0.06) n = 11**	**178 n = 4**	2.25 n = 4

Table 7.4. Summary of biomass normalized photosynthetic rates, mean, sd and sample size for maturation WSP. Weatherell et al. 2007 (n = 3 morning PI assessments using the standard apparatus). Bolivar WSP 1, n = 10 or 11 days of 10 minute online DO data PI determination. Planktonic chlorophyll_a concentration and light attenuation coefficient (Chapter 6).

The research presented above provides for the first time a detailed assessment of oxygen dynamics in a WSP using an in-situ technique using online data. This novel approach allowed for consistent and apparently rational comparison of results from an outdoor HRAP system, a laboratory based HRAP, the largest WSP in the southern hemisphere and the substantive oceanic algal productivity database, which at the time of writing was used as the basis for extant models of global carbon cycling between the ocean and atmosphere.

As such the methodology described when applied to on-line real time data appears to offer significant potential as a pond design and management tool for optimisation of influent loading on a daily, weekly and seasonal basis.

7.4. Further Studies

The 'Argo' Oxygen Program (2007) (http://www.argo.net) presented a 'white paper' that 'justifies and outlines a program to add dissolved oxygen probes to the ARGO 3000 free drifting profiling floats observation system and determine on a global-scale, seasonal and long term variations in sub-surface dissolved oxygen concentrations'. Data sets obtained through this research are provided 'as is' as open source resources for the research community. Studies of algal photosynthesis in systems such as maturation lagoons may provide a unique means of understanding algal activity in difficult to define (physically) systems such as oceans. Factors that can be well defined in WSPs such as nutrient load and retention time may provide unique opportunities for clearly defining (at extremes but in meso-scale outdoor and well definable systems) the action of fundamental driving forces such as light intensity, light attenuation, planktonic vs. bethic algal and bacterial biomass, temperature, turbulent mixing and possibly the impact of toxins (Simon 1998) and pathogens (Lane 2008) on algal productivity and the global carbon cycle.

References

Aalderink, RH and Jovin, J. (1997) Identification of the parameters describing primary production from continuous oxygen signals. Water Science and Technology, vol. 36 (5) pp. 43-51

Albeliovich,A and Azov,Y. (1976) Toxicity of ammonia to algae in sewage oxidation ponds. Applied Environmental Microbiology, vol. 31 (801-806)

Amai, A., Fukushima, T., Matsushige, K., Kim, Y.H. and Choi, K. (2002) Characterization of dissolved organic matter in effluents from wastewater treatment plants. vol. 36 (4), pp. 859-870

Arnold, W and Oppenheimer, JR. (1950) Internal conversion in the photosynthetic mechanism of blue-green algae. The Journal of General Physiology, vol. 33 (4) pp. 423-435

Azov,Y and Goldman, JC. (1982) Free ammonia inhibition of algal photosynthesis in intensive cultures. Applied Environmental Microbiology, vol. 43 (4) pp. 735-739

Beardall, J and Light, B. (1997a) Microphytobenthos in Port Phillip Bay: Distribution and Primary Productivity: Technical Report No.30. pp. 1-68

Beardall, J., Johnson, A. and Raven, J. (1998) Environmental regulation of CO2 concentrating mechanisms in microalgae. Canadian Journal of Botany, vol. 76 (6) pp. 1010-1017

Beardall, J and Light, B. (1997b) Biomass, Productivity and Nutrient Requirements of Microphytobenthos: Technical Report No. 16. CSIRO Institute for Natural Resources and Environment Port Phillip Bay Environmental Study 21st Floor, 625 Little Collins Street Melbourne, Victoria 3000. pp. 1-27

Behrenfeld, J and Falkowski, P.G. (1997) Photosynthetic rates derived from satellite-based chlorophyll concentration. Limnology and Oceanography, vol. 42 (1) pp. 1-20

Behrenfeld, J., Maranon, E., Siegal, D.A and Hooker, S.B. (2002) Photoacclimation and nutrient-based model of light-saturated photosynthesis for quantifying oceanic primary production. Marine Ecology Progress Series, vol. 228 pp. 103-117.

Bender, M., Grande, K., Marra, K.J.J., Williams, P.J.L., Seiburth, J.S., Pilson, L., Hitchcock, G., Orchado, J., Hunt, C., Donaghay, P. and Heinemann, K. (1987). A comparison of four methods for determining planktonic community production. Limnol. Oceanogr. vol. 32 (5) pp. 1085-1098

Benemann, J.R., Weissman, J.C., Koopman, B.L. and Oswald W.J. (1977). Energy production by microbial photosynthesis. Nature, vol. 268 (5615) pp. 19-23

Beran, B. and Kargi, F. (2005) A dynamic mathematical model for wastewater stabilization ponds. Ecological Modelling, vol. 181 (1) pp. 39-57

Bernal, C.B., Vazquez, G., Quintal, I.B. and Bussy, A.L. (2008). Microalgal Dynamics in Batch Reactors for Municipal Wastewater Treatment Containing Dairy Sewage Water. Water, Air, and Soil Pollution, vol. 190 (1-4) pp. 259-270

Berner, T., Dubinksy, Z., Schanz, F., Grobbelaar, J.U., Rai, H, Uehlinger, U. and Falkowski, P.G. (1986) The measurement of primary productivity in a high-rate oxidation pond (HROP). Journal of Plankton Research, vol. 8 (4) pp. 659-672

Boffetta, G. Crisanti, A. Paparella, F. Provenzale, A. and Vulpiani, A. (1998) Slow and fast dynamics in coupled systems: A time series analysis view. Physica D, vol. 116 pp. 12

Bolton, N.F., Cromar, N.J. and Fallowfield, H.J. (2010) A review of the factors affecting sunlight inactivation of micro-organisms in waste stabilisation ponds; preliminary results for enterococci. Water Science and Technology, vol. 34 pp. 141-147

Bonachela, S., Acuna, R. and Casas, J. (2007). Environmental factors and management practices controlling oxygen dynamics in agricultural irrigation ponds in a semiarid Mediterranean region: Implications for pond agricultural functions. Water Research (2007) vol. 41 (6) pp. 1225-1234

Borde, X., Guieysse, B. Delago, O. Munoz, R., Hatti-Kaul, R., Nugier-Chauvin, C., Patin, H. and Mattiasson, B. (2002) Synergistic relationships in algal–bacterial microcosms for the treatment of aromatic pollutants. Bioresource Technology pp. 8

Bradford, M.M. (1976) A rapid and sensitive method for the quantification of microorganisms quantities of protein utilising the principle of protein-dye binding. Analytical Biochemistry, vol. 72 pp. 248-254

Buhr, H.O. and Miller, S.B. (1983) A dynamic model of the high-rate algal-bacterial wastewater treatment pond. Water Research, vol. 17 pp. 29-37

Carmago Valero, M.M. and Mara, D.D. (2007) Nitrogen removal in maturation ponds: tracer experiments with 15N-labelled ammonia. Water Science & Technology vol. 55 (11) pp. 81-85

Carr, M., Friedrichs, M.A., Schmeltz, M. Aita, M, Antoine, D, Arrigi, K.R. Asanuma, I. et al. (2006) A comparison of global estimates of marine primary production from ocean color. Deep-Sea Research II, vol. 53 (741-770) pp. 1-30

Ciavatta, Patres, R., Badetti, C. Ferrari, G and Beck, M. (2008) Estimation of phytoplanktonic production and system respiration from data collected by a real-time monitoring network in the Lagoon of Venice. Ecological Modelling, vol. 212 (1-2) pp. 28-36

Clark, L.C. Jr., Wolf, R., Granger, D. and Taylor, Z. (1953) Continuous recording of blood oxygen tensions by polarography. Journal of Applied Physiology, vol. 6 (3), pp. 189-93

Coates, M.J. and Mondon, J. (2009) Effect of environmental flows on deep, anoxic pools. Ecological Modelling, vol. 220 pp. 1643-1651

Cole, J, Pace, M.L. Carpenter, S.R. and Kitchell, J.F. (2000) Persistence of net heterotrophy in lakes during nutrient addition and food web manipulations. Limnol. Oceanogr., vol. 45 (8) pp. 1718-1730

Colijn, F. and de Jonge, V.N. (1984) Primary production of microphytobenthos in the Ems-Dollard Estuary. Marine Ecology Progress Series, vol. 14 pp. 185-196

Conley, D.J., Paerl, H.W., Howarth, R.W, Boesch, D.F., Setzinger, S.P., Havens, K.E, Lancelot, C. and Likens, G.E. (2009). Controlling Eutrophication:
Nitrogen and Phosphorus. Science, vol. 323 pp. 1014-1015

Cromar, N.J. and Fallowfield, H.J. (2003) Use of image analysis to determine algal and bacterial biomass in a high rate algal pond following Percoll® fractionation. Water Science and Technology, vol. 48 (2) pp. 53-60

Cromar, N.J. and Fallowfield, H.J. (1992) Separation of components of the biomass from high rate algal ponds using Percoll R density gradient centrifugation. The Journal of Applied Phycology vol. 4 pp. 157-163

Cromar, N.J. and Fallowfield, H.J. and Martin, N.J. (1996) Influence of environmental parameters on biomass production and nutrient removal in a high rate algal pond operated by continuous culture. Water Science and Technology vol. 34 (11) pp. 133-140

Cromar, N.J. (1994) Composition of biomass and computer modelling of high rate algal ponds. PhD thesis, Napier University.

Cullen, J.J. (1990) On Models of Growth and Photosynthesis in Phytoplankton. Deep-Sea Research, vol. 37 pp. 667-683

Curtis, T.P. Marra, D.D., Dixo, N.G.H. and Silva, S.A. (1994) Light penetration in waste stabilisation ponds. Water Research, vol. 28 (5) pp. 1031-1038

Danger, M., Leflaive, J, Oumarou, C. Ten-Hage, L. and Lacroix, G. (2007a) Control of phytoplankton-bacteria interactions by stoichiometric constraints. Oikos, vol. 116 (7) pp. 1079-1086

Danger, M., Oumarou, C. Benest, D. and Lacroix, G (2007b) Bacteria can control stoichiometry and nutrient limitation of phytoplankton. Functional Ecology, vol. 21 (2) pp. 202-210

Darley, W.M., Ohman, H.J. and Wimpee, B.B. (1979) Utilization of dis- solved organic carbon by natural populations of epiben- thic salt marsh diatoms. J. Journal of Phycology, vol. 15 pp. 1-15

Davies-Colley, R.J., Craggs, R.J., Park, J. and Nagels, J.W. (2005) Optical characteristics of waste stabilization ponds - recommendations for monitoring. Water Science and Technology, vol. 51(12) pp. 153-161

Davis, R.J. and Koop, K. (2006) Eutrophication in Australian Rivers, Reservoirs and Estuaries – A Southern Hemisphere Perspective on the Science and its Implications. Hydrobiologia, vol. 559 (1) pp. 23-76

Dhiab, R.B., Ouada, H.B. Bousetta, H., Frank, F. Elabed, A and Brouers, M. (2007) Growth, fluorescence, photosynthetic O2 production and pigment content of salt adapted cultures of Arthrospira (spirulina) platensis. Journal of Applied Phycology vol. 19 pp. 293-301

Dorsch, MM, Scragg, R.K.R, McMichael, A.J, Baghurst, P.A and Dyer, K.F (1984) Congenital malformations and maternal drinking waer supply in rural South Australia: A case control study. American Journal of Epidemiology, vol. 119 (4) pp. 473-486

Duarte, M.D. and Prairie, Y.T. (2005) Prevalence of Heterotrophy and Atmospheric CO2 Emissions from Aquatic Ecosystems. Ecosystems, vol. 8 (7) pp. 862-870

Dubinsky, Z. Falkowski, P.G. Post, A.F., Hes, U.M.V (1987) A system for measuring phytoplankton photosynthesis in a defined light field with an oxygen electrode. Journal of Plankton Research, vol. 9 (4) pp. 607-612

Dugan, G.L., Glueke, C.G. and Oswald, W.J. (1972) Recycling system for poultry wastes. J. WPCF, vol. 44 (3) pp. 432-440

Edwards, R.W. Duffield, A.N. and Marshall, E.J. (1978) Estimates of community metabolism of drainage channels from oxygen distribution. Proc. EWRS 5th Syrup. on Aquatic Weeds, pp. 295-302

El Ouarghi, H. Boumansour, B.E. Dufayt, O. Hamouri, B.E. and Vassel, J.L. (2000) Hydrodynamics and oxygen balance in a high-rate algal pond. Water Science & Technology, vol. 42 (10) pp. 349-356

Ellis, R.J. (1979) The most abundant protein in the world. TIBS, November, pp. 241-244

Emerson, R. and Lewis, C.M. (1942) The photosynthetic efficiency of pycocyanin in chroococcus and the problem of carotenoid participation participation in photosynthesis. The Journal of General Physiology, vol. 25 (4) pp. 579-595

Emerson, R. and Green, L. (1934) Manometric Measurements of photosynthesis in the marine alga Gigartina. The Journal of General Physiology, vol. 17 (6) pp. 817-842

Eppley, R., Steward, E. Abbott, M. and Heyman,U. (1985) Estimating ocean primary production from satellite chlorophyll: introduction to regional differences and

statistics for the southern California Bight. Journal of Plankton Research, vol. pp. 57-70

Eppley, R.W. (1980) Estimating phytoplankton growth rates in the central oligotrophic oceans . Brookhaven Symposium Biology, vol. 31 pp. 230-242

Eriksen, N.T., Riisgard, F.K., Gunther, W.S. and Iversen, J.L.L. (2007) On-line estimation of O2 production, CO2 uptake, and growth kinetics of microalgal cultures in a gas-tight photobioreactor. Journal of Applied Phycology, vol. 19 pp. 14

Evans, R.A., Cromar, N.J. and Fallowfield, H.J. (2005) Performance of a pilot-scale high rate algal pond system treating abattoir wastewater in rural South Australia: nitrification and denitrification. Water Science and Technology, vol. 51 (12)

Evans, R.A., Fallowfield, H.J. and Cromar, N.J. (2003) Characterisation of oxygen dynamics within a high-rate algal pond system used to treat abattoir wastewater. Water Science and Technology, vol. 48 (2) pp. 61-68

Falkowski, P.G. (1981) Light-shade adaptation and assimilation numbers. Journal of Plankton Research, vol. 3 (2) pp. 203-216

Falkowski, P.G. (1994) Light utilization and photoinhibition of photosynthesis in marine phytoplankton. U.S. Department of Energy, DE-AC02-76CH00016. (1994) pp. 1-55

Falkowski, P.G. and Raven, J.A. (2007) Aquatic Photosynthesis- Second Edition. Aquatic Photosynthesis, Princeton University Press, Princeton and Oxford, pp. 464

Fallowfield, H.J. Mesple, F. Martin, N.J. Casellas, C. and Bontoux, J. (1992) Validation of computer models for high rate algal pond operation for wastewater treatment using data from Mediterranean and Scottish pilot scale systems: implications for management in coastal regions. Water Science and Technology, vol. 25 (12) pp. 215-224

Fallowfield, H.J., Cromar, N.J. and Evans, R.A. (2001). The use of highrate algal ponds in the treatment of abattoir wastes. Final report for Meat and Livestock Australia, RPDA 501. pp. 256.

Fallowfield, H.J., Cromar, N.J. and Evison, L.M. (1996). Coliform die-off rate constants in a high rate algal pond and the effect of operational and environmental variable. Water Science and Technology, vol. 34 (11) pp. 141-147

Fallowfield, H.J. and Garret, M.K. (1983) Algal Biomass From Farm Waste. (1983) U.K. Department of Energy and The Department of Agriculture. pp. 1-187

Fee, E.J. (1990) Computer programs for calculating in situ phytoplankton photosynthesis. Can. Tech. Rep. Fish. Aquatic Sci. vol. 1740 pp. 1-27

Feller, U., Anders, I. and Mae, T. (2008) Rubiscolytics: fate of Rubisco after its enzymatic function in a cell is terminated. Journal of Experimental Botany, vol. 59 (7) pp. 1615-1624

Fisher, S.G. and Carpenter, S.R. (1976) Ecosystem and macrophyte primary production of the Fort River, Massachussetts. Hydrobiologia, vol. 47 pp. 175-187

Fox, D.R., Bately, G.E., Blackburn, D., Bone, Y. Bryars, S. Cheshire, A, Collings, G, Fairweather, P.P., Fallowfiled, H.J, Harris, G. Henderson, B, Kampf, J. Mayar, S, Pattiaratchi, C, Petrusevics, P., Townsend, M, Westphalen, G. and Wilkinson, J. (2007) ACWS Final Report, vol 1. CSIRO pp. 1-68

French, C.S. and Rabideua, G.S. (1945) The quantum yield of oxygen production by chloroplasts suspended in solutions containing ferric oxalate. The Journal of General Physiology, vol. 28 (4) pp. 329-342

Friedrichs, M., Carr, M.E., Barber, R.T., Scardi, M, Antoine, D., et al. (2009) Assessing the uncertainties of model estimates of primary productivity in the tropical Pacific Ocean. Journal of Marine Systems, vol. 76 (1-2) pp. 113-133

Fulweiler, R.W., Nixon, S.W., Buckley, B.A. and Granger, S.L. (2008) Net Sediment N2 Fluxes in a Coastal Marine System—Experimental Manipulations and a Conceptual Model. Ecosystems, vol. 11 pp. 1168-1180

Fyfe, J. Smalley, J. Hagare, D. and Sivakumar, M. (2007) Physical and hydrodynamic characteristics of a dairy shed waste stabilisation pond system. Water Science & Technology, vol. 55 (11) pp. 11-20

Fyfe, J., Sivakumar, M., Hagare, D. and Jenkins, A. (2007) Dynamic variation of supernatant quality in a dairy shed waste stabilisation pond system. Water Science & Technology, vol. 55 (11) pp. 245

Gavis, J. and Ferguson, J.F. (1975) Kinetics of carbon dioxide uptake by phytoplankton at high pH. Limnol. Oceanogr. vol. 20 (2) pp. 211-221

Gehring, T., Silva, J.D., Kehl, O., Castilos Jr., Costa, R.H.R, Uhlenhut, F., Alex, J., Horn, A.H. and Wichern, M. (2010) Modelling waste stabilisation ponds with an extended version of ASM3. Water Science and Technology vol. 61 (3) pp. 713 - 720

Geider, R.J. and Osborne, B.A. (1992) Algal Photosynthesis. Chapman & Hall, New York.

Genty, B., Briantais, J.M. and Baker, M.R. (1989) The relationship between the quantum yield of photosynthetic electron transport and quenching of chlorophyll fluorescence. Biochim. Biophys. Acta, vol. 1990 pp. 87-92

Gerritsen, V.B. (2003) The plant kingdom's sloth. Protein Spotlight (38) pp. 1-2

Giordano, M. Beardall, J. and Raven, J.A (2005) CO2 Concentrating mechanisms in algae: Mechanisms, Environmental Modulation, and Evolution. Annu. Rev. Plant. Biol. vol. 56 pp. 35

Gloyna, E.F. (1971) World Health Organization Monograph Series No. 60 Waste Stabilization Ponds. WHO. pp. 1-174

Godos, I.D., Blanco, S., Garcia-Encina, P.A. Becares E. and Munoz, R. (2009) Long-term operation of high rate algal ponds for the bioremediation of piggery wastewaters at high loading rates. Bioresource Technology, vol. 100 (19) pp. 4332-4339

Goldman, J.C. (1979) Outdoor algal mass cultures—II. Photosynthetic yield limitations. Water Research, vol. 13 pp. 119-137

Government of South Australia (a) (2009) Water reuse project on track for Adelaide's south. Media Release pp. 1-2

Government of South Australia (b) (2006). Strategic Infrastructure Plan for South Australia Regional Overview. pp. 1-105

Government of South Australia (c) (1966) Report of the Committee Of Enquiry into the Utilization Of Effluent From Bolivar Sewage Treatment Works. Hodgson et al. (1966)

Graham , J.M. Lembi, C.A., Adrian, H.L. and Spencer, D.F. (1995) Physiological responses to temperature and irradiance in SPIROGYRA (ZYGNEMATALES, CHAROPHYCEAEA). J. Phycol. vol. 31 pp. 11

Grobbelaar, J.U. (2000) Physiological and technological considerations for optimising mass algal cultures. Journal of Applied Phycology, vol. 12 pp. 6

Grobbelaar, J.U. (2007) Photosynthetic characteristics of Spirulina platensis grown in commercial-scale open outdoor raceway ponds: what do the organisms tell us?. Journal of Applied Phycology, vol. 19 pp. 8

Grobbelaar, J.U. (2010) Microalgal biomass production: challenges and realities. Photosynthesis Research, vol. 106 pp. 135-144

Grobbelaar, J.U. (1989) Do light/dark cycles of medium frequency enhance phytoplankton productivity? Journal of Applied Phycology, vol. 1 pp. 333-340

Grobbelaar, J.U. Nedbal, L. and Tichy, V. (1996) Influence of high frequency light/dark fluctuations on photosynthetic characteristics of microalgae photoacclimated to different light intensities and implications for mass algal cultivation. Journal of Applied Phycology, vol. 8 pp. 335-343

Gruber, N., Doney, S.C, Emerson, S.R. Gilbert, D., Kobayashi, T., Kortzinger, A., Johnson, G.C., Johnson, K.S. Riser, S.C and Ulloa, O. (2007) The Argo-Oxygen Program (White Paper), pp. 60

Govindjee, B.J. Sixty-three years since Kautsky: chlorophyll a fluorescence. (1995) Australian Journal of Plant Physiology, vol. 22, pp. 131-160

Halsey, K.H. Milligan, A.J. and Behrenfeld, M.J. (2010) Physiological optimization underlies growth rate-independent chlorophyll-specific gross and net primary production. Photosynthesis Research, vol. 103 (2), pp. 125-137

Hancke, K., Kancke, T.B., Olsen, L.M., Johnsen, G. and Glud, R.N (2008) Temperature effects on microalgal photosynthesis-light responses measured by O2 production, Pulse-Amplitude_Modulated Fluorescence, and C14 assimilation. Journal of Phycology, vol. 44 (2) pp. 501-514

Harris, G.P. (1984) Phytoplankton productivity and growth measurements: past, present and future. Journal of Plankton Research, vol. 6 (219-235)

Harris, G.P. (1996) Port Phillip Bay Environmental Study, CSIRO pp. 1-39

Harris, G. (1999) This is not the end of limnology (or of science): the world may well be a lot simpler than we think. Freshwater Biology, vol. 42, pp. 689-706

Hartig, P., Grobbelaar, J.U., Soeder, C.J. and Groeneweg, J. (1988) On the mass culture of microalgae: Aeral Density as an Important factor for achieving maximal productivity. Biomass, vol. 15 pp. 11

Haxo, F.T. and Blinks, L.R. (1950) Photosynthetic action spectra of marine algae. The Journal of General Physiology, vol. pp. 1-34

Herdianto, R. (2003) The design of geometry to improve algal removal of waste stabilisation ponds. Masters Thesis, Flinders University, Department of Environmental Health, School of Medicine.

Hobson, P. and Fallowfield, H.J. (2001) Effect of salinity on photosynthetic activity of Nodularia spumigena. Journal of Applied Phycology, vol. 13 (6) pp. 493-499

Hobson, P. and Fallowfield, H.J. (2003) Effect of irradiance, temperature and salinity on growth and toxin production by Nodularia spumigena. Hydrobiologia, vol. 493 pp. 7-15

Hornberger, G.M., Kelly, M.G. and Eller, R.M. (1976) The relationship between light and photosynthetic rate in a river community and implications for water quality modelling. Water Resources Research, vol. 12, pp. 723-730

Horton, P., Ruban, A.V. and Walters, R.G. (1994) Regulation of Light Harvesting in Green Plants: Indication by nonphotochemical quenching of chlorophyll fluorescence. Plant Physiology, vol. 106, pp. 415-420

Huisman, J., Matthijs, H.C.P., Visser, P.M., Blake, H., Sigon, C.A.M., Passarge, J., Weissing, F.J. and Mur, L.R. (2002) Principles of the light-limited chemostat: Theory and ecological applications, Antoni van Leeuwenhoek, vol. 81 pp. 117-133

Jacob, T., Wagner, H., Stehfest, K, and Willheim, C., (2007) A complete energy balance from photons to new biomass reveals a light- and nutrient-dependent variability in the metabolic costs of carbon assimilation. Journal of Experimental Botany, vol. 58 (8) pp. 2101-2112

Jolliff, J.K., Kindle, J.C., Shulman, I., Penta, B., Friedrichs, M.A.M, Helber, R. and Arnone, R.A. (2009) Summary diagrams for coupled hydrodynamic-ecosystem model skill assessment. Journal of Marine Systems, vol. 76 (1-2) pp. 64-82

Kaiblinger, C., Gresberger, S., Teubner, K. and Dokulil, M.Y. (2007) Photosynthetic efficiency as a function of thermal stratification and phytoplankton size structure in an oligotrophic alpine lake. Hydrobiologia, vol. 578 pp. 29-36

Karlsson, J., Ask, J, Jansson, M., (2008) Winter respiration of allochthonous and autochthonous organic carbon in a subarctic clear-water lake. Limnol. Oceanogr., vol. 53 (3) pp. 948-954

Katsoyiannis, A., and Samara, C. (2007) The fate of dissolved organic carbon (DOC) in the wastewater treatment process and its importance in the removal of wastewater contaminants. Env. Sci. Pollut. Res. Vol. 14, 284-292

Kayombo, S.A. Mbwette, T.S., Mayo, A.Y. Katima, J.H. Jorgensen, S. (2002) Diurnal cycles of variation of physical–chemical parameters in waste stabilization ponds. Ecological Engineering, vol. 18 pp. 287-291

Kelly, M.G., Hornberger, G.M. and Cosby, B.J. (1974) Continuous automated measurement of rates of photosynthesis and respiration in an undisturbed river community. Limnology and Oceanography, vol. 19 (2) pp. 305-312

Kirk, J.T.O. (2003) The vertical attenuation of irradiance as a function of the optical properties of the water. Limnol. Oceanogr., vol. 48 (1) pp. 9-17

Kirk, J.T.O. Light and Photosynthesis in Aquatic Ecosystems, 2nd Edition, Cambridge University Press. (1994)

Klug, J.L. (2005) Bacterial response to dissolved organic matter affects resource availability for algae. Canadian Journal of Fisheries and Aquatic Sciences, vol. 62 (2) pp. 472-481

Kromkamp, J.C. and Forster, R.M. (2003) The use of variable fluoresence measurements in aquatic ecosystems: differences between multiple and single turnover measuring protocols and suggested terminology. Eur. J. Phycol., vol. 38 pp. 11

Kroon, B.M. and Dijkman, N.A (1996) Photosystem II quantum yields, off-line measured P/I parameters and carbohydrate dynamics in Chlorella vulgaris grown under a fluctuating light regime and its application for optimizing mass cultures. journal of Applied Phycology, vol. 8 pp. 313-324

Kroon, B.M., Kettelaars,H., Fallowfield, H.j. and Mur, L.R. (1989) Modelling microalgal productivity in a High Rate Algal Pond based on wavelength dependent optical properties. journal of Applied Phycology, vol. 1 pp. 247-256

Kroon, B.M. and Thoms. S. (2006) From electron to biomass: A mechanistic model to describe phytoplankton photosynthesis and steady state growth rates. Journal of Phycology, vol. 42 (3) pp. 593-609

Kruskopf, M. and Flynn, K. (2006) Chlorophyll content and fluorescence responses cannot be used to gauge reliably phytoplankton biomass, nutrient status or growth rate. New Phytologist, vol. 169 (3) pp. 525-536

Lane, N. (2008) Origins of Death. Nature, vol.453, pp. 582-585

Laws, E.A. (1991) Photosynthetic quotients, new production and net community production in the open ocean. Deep Sea Research Part I: Oceanographic Research Papers, vol. 38 (1) pp. 143-167

Lee, C. (1999) Calculation of light penetration depth in photobioreactors. Biotechnology and Bioprocess Engineering, vol. 4 (1) pp. 1-3

Li, W.K.W and Maestrini, S. (1993) Measurement of Primary Production from the Molecular to the Global Scale. Copenhagen, ICES.

Lindeman, R.L. (1942) The Trophic Dynamic Aspect of Ecology. Ecology, vol. 23 (4) pp. 399-477

Lopez-Arcilla, A.L. Molla, S., Colleta, M.C., Guerriero, M.C. and Carlos, M. (2004) et al. Ecosystem metabolism in a Mediterranean shallow lake (Laguna de Santa Olalla, Donana National Park, SW Spain). Wetlands, vol. 24 pp. 848-858

Loreau, M. (2001) Microbial diversity, producer-decomposer interactions and ecosystem processes-a theoretical model. Proceedings of the Royal Society of London, Series B., vol. 268 (1464) pp. 303-309

Lorenz, E.N. (1963) Deterministic Nonperiodic Flow. Journal of Atmospheric Sciences, vol. 20 pp. 130 - 141

Lorenz, E.N. (1989) Computation Chaos - A prelude to computational instability. Physica D, vol. 299-317 pp. 1-19

Lynch, D.R., McGillicuddy, J.R. and Francisco, E (2009) Skill assessment for coupled biological/physical models of marine systems. Journal of Marine Systems vol. 76 (1-2) pp. 1-3

Manning, W.M., Stauffer, J.F., Duggar, M. and Daniels, F. (1938) Quantum Effliciency of Photosynthesis in Chlorella. J. Am. Chem. Soc., vol. 60 (2) pp. 266-274

Manning, W.M. Juday, C. and Wolf, M. (1938) Photosynthesis in Chlorella. Quantum Efficiency and Rate Measurements in Sunlight. J. Am. Chem. Soc., vol. 60 (2) pp. 274-278

Markager, S. and Sand-Jensen, K. (1989) Patterns of Night-time Respiration in a Dense Phytoplankton Community Under a Natural Light Regime. Journal of Ecology, vol. 77 (1) pp. 49-61

Marshall, E.J.P. (1981) The ecology of a land drainage channel; Oxygen balance. Water Research, vol. 15 pp. 1075-1085

Mashauri, D.A. and Kayombo, S. (2001) The application of the two coupled models for water quality management: facultative pond cum constructed wetland models. 2nd WARFSA/WaterNet Symposium: Integrated Water Resources Management: Theory, Practice, Cases; Cape Town, 30-31 October, 2001, pp. 12

Masters, T. (1995) Neural, Novel and Hybrid Algorithms for Time Series Prediction. John Wiley and Sons, Inc., Brisbane.

May, R. (1974) BiologicalPopulationswithNonoverlappingGenerations:
prising, in view of the general engineering precept that excessively long time Stable Points, Stable Cycles, and Chaos. Science, vol. 186 pp. 645-647

Mayo, A.W. and Noike, T. (1994) Response of Mixed Cultures of Chlorella Vulgaris and Heterotrophic Bacteria to Variation in pH. Water Science & Technology, vol. 30 (8) pp. 285-294

Mazzocchi, F. (2008) Complexity in biology. Exceeding the limits of reductionism and determinism using complexity theory. EMBO reports, vol. 9 (1) pp. 10-14

Mclntire, C.D., Garrison, R.L. Phinney, H.K. and Warren, C.E. (1964) Primary production in laboratory streams. Technical Paper No, 1677, Oregon Agricultural Experiment Station. pp. 11

Meneses, C.G.R., Saraiva, L.B., Melo, J.L.S. and Pearson, H.W. (2005) Variations in BOD, algal biomass and organic matter biodegradation constants in a wind-mixed tropical facultative waste stabilization pond. Water Science and Technology, vol. 51 (12) pp. 183-190

Metcalf and Eddy, Inc, (2003) In: Tchbabglous, G., Burton, F.L. and Stensel, H.D. (Eds), Wastewater Engineering: Treatment and Reuse, 4th ed., McGraw-Hill, New York.

Mihalyfalvy, E., Johnston, H.T., Garret, M.K., Fallowfield, H.J. and Cromar, N.J. (1998) Improved mixing of high rate algal ponds. Water Research, vol. 32 (4) pp. 1334-1337

Moran, M.A. and Hodson, R.E. (1990) Bacterial production on humic and nonhumic components of dissolved organic carbon. Limnol. Oceanogr., vol. 35 (8) pp. 1744-1756

Morel, A. and Smith, R.C. (1974) Relation between total quanta and total energy for aquatic photosynthesis. Limnology and Oceanography, vol. 19 (4) pp. 591-600

Morel, A. (1991) Light and marine photosynthesis: a spectral model with geochemical and climatological implications. Progress in Oceanography, vol. 26 pp. 263-306

Morris, E.P. and Kromkamp, J.C. (2003) Influence of temperature on the relationship between oxygen- and fluorescence-based estimates of Potosynthetic parameters in a marine benthic diatom (Cylindrotheca closterium). Eur. J. Phycol., vol. 38 (2)

Morris, J.G. Jr. (1999) Harmful algal blooms- An Emerging Public Health Problem with possible links to human stress on the environment. Annual Review of Energy and the Environment, vol. 24 pp. 26

Mouget, J., Dakhama, C., Lavoie, M.C., and de la Noue, J., (1995) Algal growth enhancement by bacteria: Is consumption of photosynthetic oxygen involved? FEMS Microbiology Ecology, vol. 18 (1) pp. 3-5

Mukherjee, B., Mukherjee, D, and Nivedita, M. (2007) The transfer rates of inorganic carbon and budgetary analysis in a simulated aquatic system. Ecological Modelling, vol. 204 (3-4) pp. 279-288

Mukherjee, B., Mukherjee, D, Prasad, A. and Novedita, M. (2008) Modelling carbon and nutrient cycling in a simulated pond system at Ranchi. Ecological Modelling, vol. 213 (3-4) pp. 437-448

Mukherjee, B. Pandeya, P.N. and Singhb, S.N. (2002) Mathematical modelling and system analysis of inorganic carbon in the aquatic environment. Ecological Modelling vol. 152 pp. 129-143

Munoz, R. and Guiysse, B. (2006) Algal-bacterial processes for the treatment of hazardous contaminants- A review. Water Research, vol. 40 pp. 17

Myers, J. and Cramer, M. (1948) Metabolic conditions in chlorella. The Journal of General Physiology, vol. 32 (1) pp. 103-110

Neale, P.J. and Marra, J. (1985) Short-term variation of Pmax under natural irradiance conditions: a model and its implications. Marine Ecology Progress Series, vol. 26 pp. 113-124

Nisbet, R.M., Diehl, S., Wilson, W.G., Cooper, S.D., Donaldson, D.D. and Kratz, K. (1997) Primary-Productivity Gradients and Short-term Population Dynamics in Open Systems. Ecological Monographs, vol. 67 (4) pp. 19

Odum, H.T. (1956) Primary Production in Flowing Waters. Limnology and Oceanography, vol. 1 (2) pp. 102-117

Oron, G., Shelef, G., Levi, A., Meydan, A. and Azov, Y (1979) Algae/Bacteria Ratio in High-Rate Ponds Used for Waste Treatment. Applied and Environmental Microbiology, vol. 38 (4) pp. 570-576

Oswald, W.J. (1995) Ponds in the Twenty-First Century. Water Science & Technology, vol. 31 (12) pp. 1-8

Oswald, W.J. and Gotaas, H.B (1955) Photosynthesis in Sewage Treatment. American Society of Civil Engineers; Transactions, N. 686. pp. 1-33

Oswald, W.J. (2003) My sixty years in applied phycology. Journal of Applied Phycology, vol. 15 pp. 99-106

Oswald, W.J., Golueke, C.G. and Horning, D.O. (1965) Closed Ecological Systems. Journal of the Sanitary Engineering Division, Proceedings of the American Society of Civil Engineers, vol. SA 4 pp. 23-46

Oswald, W.J., Gotaas, H.B., Ludwig, H.F. Lynch, V. (1953) Algae Symbiosis in Oxidation Ponds. Sewage and Industrial Wastes, vol. 25 (1) pp. 26-37

Patterson, C. and Curtis, T. (2005) Physical and chemical environments. In Shilton, A. Ed. Pond Treatment Technology, pp. 49-65

Pearson, H.W., Mara, D.D. and Bartone, C.R. (1987) Guidelines for the minimum evaluation of the performance of full-scale waste stabilization pond systems. Water Research, vol. 21 (9) pp. 9

Pearson, H. (2005) Microbiology of waste stabilisation ponds. In Shilton, A. Ed. Pond Treatment Technology, pp. 14-48

Pedahzur, R., Nasser, A., Dor, I., Fattal, B. and Shuval, H. (1993) The effect of baffle installation on the performance of a single-cell stabilisation pond. Water Science and Technology, vol. 27 (7-8) pp. 45-52

Perner-Nochta, I. and Posten, C. (2007) Simulations of light intensity variation in photobioreactors. Journal of Biotechnology, vol. 131 (3) pp. 276-285

Platt, T., Gallegos, C.L. and Harris, W.G. (1980) Photoinhibition of phytoplankton in natural assemblages of Marine Phytoplankton. Journal of Marine research, vol. 38 pp. 687-701

Platt, T. and Gallegos, C.L. (1980) Modelling primary production. Primary Production in the Sea: Falkowski,P.G. Ed., pp. 339-362

Portielje, R., Kersting, K. and Lijklema, L. (1996) Primary production estimation from continuous oxygen measurements in relation to external nutrient input. Water Research, vol. 30 (3) pp. 625-643

Ratchford, I.A.J. & Fallowfield, H.J**.** (1992) The effect of culture wavelength on light enhanced dark respiration. British Phycological Journal. 27 pp. 98.

Ratchford, I.A.J. and Fallowfield, H.J. (2003) The effect of light-dark cycles of medium frequency on photosynthesis by Chlorella vulgarisand the implications for waste stabilisation pond design and performance. Water Science and Technology, vol. 48 (2) pp. 69-74

Raven, J.A. and Larkum, A.W.D (2009) Contributions of anoxygenic and oxygenic phototrophy and chemolithotrophy to carbon and oxygen fluxes in aquatic environments. Aquatic Microbial Ecology, vol. 56 pp. 177-192

Raven, J.A. and Beardall, J. (2006) Chlorophyll fluorescence and ecophysiology-seeing red? New Phytologist, vol. 169 (3) pp. 449-451

Raven, J.A. and Larkum, A.W.D. (2007) Are there ecological implications for the proposed energetic restrictions on photosynthetic oxygen evolution at high oxygen concentrations? Photosynthesis Research, vol. 94 pp. 12

Reynolds, C.S. (2006) The Ecology of Phytoplankton. Cambridge University Press, Melbourne.

Richmond, A. (2004) Principles for attaining maximal microalgal productivity in photobioreactors- an overview. Hydrobiologia, vol. 512 pp. 33-37

Risgaard-Petersen, N., Nicolaisen, M.H. Revsbech, N.P. and Lomstein, B.A. (2004) Competition between Ammonia-Oxidizing Bacteria and Benthic Microalgae. Applied and Environmental Microbiology, vol. 70 (9) pp. 5528-5537

Robson, B.J. and Mitchell, B.D. (2010) Metastability in a river subject to multiple disturbances may constrain restoration options. Marine and Freshwater Research, vol. 61 pp. 778-785

Rysgaard, S., Bondo-Christensen, P. and Nielsen, L.P. (1995) Seasonal variation in nitrification and denitrification in estuarine sediment colonized by benthic microalgae and bioturbating infauna. Marine Ecology Progress Series, vol. 126 pp. 111-121

Ryther, J.H. and Yentsch, C.S. (1958) Primary production of continental shelf waters off New York. Limnology and Oceanography, vol. 3 pp. 327-335

Sargent, M.C. (1940) Effect of Light Intensity on the Development of the Photosynthetic Mechanism. Plant Physiology, vol. 15 pp. 275-279

Sheil, C. (2000) Water's Fall (Running the risks with economic rationalism). Pluto Press Annandale NSW, Australia, pp. 205

Sherr, B. and Sherr, E. (2003) Community respiration/production and bacterial activity in the upper water column of the central Arctic Ocean. Deep Sea Research Part I: Oceanographic Research Papers, vol. 50 (4) pp. 529-542

Shilton, A., Ed. (2005) Pond Treatment Technology. IWA Publishing, London, pp. 479

Shilton, A and Harrison, J. (2003) Guidelines for the hydraulic design of Waste Stabilisation Ponds. Massey University, pp. 1-78

Short, M.D., Cromar, N.J., Nixon, J.B. and Fallowfield, H.J. (2007) Relative performance of duckweed ponds and rock filtration as advanced in-pond wastewater treatment processes for upgrading waste stabilisation pond effluent: a pilot study. Water Science & Technology, vol. 55 (11) pp. 111-119

Short, M. (2010) Advanced techniques for the upgrading of waste stabilisation pond effluent- rock filtration; duckweed; and attached-growth media. Ph.DThesis. pp. 732

Sigmon, D.E. and Cahoon, L.B. (1997) Comparative effects of benthic microalgae and phytoplankton on dissolved silica fluxes. Aquatic Microbial Ecology, vol. 13 pp. 275-284

Silva-Aciares, F.R. and Riquelme, C.E. (2008). Comparisons of the growth of six diatom species between two configuratioins of photobioreactors. Aquacultural Engineering, vol. 38 pp. 10

Simon, D., Helliwell, S. and Robards, K. (1998) Pesticide toxicity endpoints in aquatic ecosystems. Journal of Aquatic Ecosystem Stress and Recovery, vol. 6 pp. 159-177

Smith, E.L. (1936) Photosynthesis in Relation to Light and Carbon Dioxide Smith. Proceedings of the National Academy of Sciences of the United States of America vol. 22 pp. 504-511

Smith, B.M., Ross, C.C. and Walsh. J. (2004) Food-Processing Wastes. Water Environment Research, vol. 76 (6) pp. 1589-1651

Soeder, C.J. (1984). Aquatic bioconversion of effluents in ponds. In: Animals as Waste Converters (E.H. Ketelaars and S.B. Iwewa Eds.) Pudoc, Wageningen, Netherlands, pp. 130-136

Staehr, P.A., Eaite, A.M. and Markager, S. (2009) Effects of sewage water on bio-optical properties and primary production of coastal systems in West Australia. Hydrobiologia, vol. 620, pp. 1-15

Steeman Nielsen, E. (1956) The use of radioactive carbon for measuring organic production in the sea. J. Cons. Int. Exp. Mer., vol. 18 pp. 117-140

Stow, C.A., Jason. J., McGillicuddy Jr., D.J., Doney, S.C., Allen, J.I., Friedrichs, M.A.M., Rose, K.A. and Wallhead, P. (2009) Skill assessment for coupled biological/physical models of marine systems. Journal of Marine Systems, vol. 76 (1-2) pp. 4-15

Sundback, K., Enoksson, V., Graneli, W. and Pettersson, K. (1991) Influence of sublittoral microphytobenthos on the oxygen and nutrient flux between sediment and water: a laboratory continuous-flow study. Marine Ecology Progress Series, vol. 74 pp. 263-279

Sukenik, A., Beardall, J., Kromkamp, J.C. et al. (2009) Photosynthetic performance of outdoor Nannochloropsis mass cultures under a wide range of environmental conditions. Aqutic Microbial Ecology, vol. 56, pp. 297-308

Sweeney, D.G., Cromar, N.J., Nixon, J.B., Ta, C.T. and Fallowfield, H.J. (2003) The spatial significance of water quality indicators in waste stabilization ponds – limitations of residence time distribution analysis in predicting treatment efficiency. Water Science and Technology, vol. 48 (2) pp. 211-218

Sweeney, D.G., Nixon, J.B., Cromar, N.J. and Fallowfield, H.J. (2007) Temporal and spatial variation of physical, biological, and chemical parameters in a large waste stabilisation pond, and the implications for WSP modelling. Water Science & Technology, vol. 55 (11) pp. 1

Sweeney, D.G., Nixon, J.B., Cromar, N.J. and Fallowfield, H.J. (2005a) Profiling and modelling of thermal changes in a large waste stabilisation pond. Water Science and Technology, vol. 51 (12) pp. 163-172

Sweeney, D.G. (2004) Integrating biological and hydraulic aspects of waste stabilisation pond design. Ph.D. Thesis. Flinders University, School of Medicine.

Sweeney, D.G., O'Brien, M.J., Cromar, N.J. and Fallowfield, H.J. (2005b) Changes in waste stabilisation pond performance resulting from the retrofit of activated sludge treatment upstream - part II – management and operating issues. Water Science and Technology, vol. 51 (12) pp. 17-22

Talling, J.F. (1957) The phytoplankton population as a compound photosynthetic system. Scripps Institution of Oceanography, La Tolla, California, pp. 133-149

Talling, J.F. (1956) Photosynthetic characteristics of some freshwater plankton diatoms in relation to underwater radiation. Scripps Institution of Oceanography, La Tolla, California. pp. 29-50

Thyssen, N. and Kelly, M.G. (1985) Water-air exchange of carbon dioxide and oxygen in a river: measurement and comparison of rates. Arch. Hydrobiol. vol. 105 (219-228)

Uehlinger, U., Konig, C. and Reichert, P. (2000) Variability of photosynthesis-irradiance curves and ecosystem respiration in a small river. Freshwater Biology, vol. 44 pp. 493-507

Vahalato, A.V., Salonen, K., Munster, U., Jarvinen, M. and Wetzel, R.G. (2003) Photochemical transformation of allochthonous organic matter provides bioavailable nutrients in a humic lake. Arch. Hydrobiol. vol. 156 (3) pp. 287-314

Veenstra, S. Al-Nozaily, F.A. and Alaerts, G.J. (1995) Purple non-sulfur bacteria and their influence on waste stabilisation pond performance in the Yemen Republic. Water Science and Technology, vol. 31 (12) pp. 141-149

Vincent, W.F., Neale, P.J. and Richerson, P.J. (1984) Photoinhibition: Algal responses to bright light during diel stratification and mixing in a tropical alpine lake. J. Phycol. vol. 20 pp. 12

Vollenweider, R.A. (1974) Manual on Methods for Measuring Primary Production in Aquatic Environment IBP Handbook No. 12. Blackwell Scientific, Oxford.

Von Sperling, M. and Mascarenhas, L.C.A.M. (2005) Performance of very shallow ponds treating effluents from UASB reactors. Water Science and Technology, vol. 51 (12) pp. 83-90

Nixon, S.W. (1998) Enriching the Sea to Death. Scientific American, The Oceans, pp. 49-53.

Nixon, S.W. (1995) Coastal marine eutrophication- a definition-social causes and future concerns. Ophelia (1995) vol. 41 pp. 199-219

Weatherell, C.A. Elliot, D.J. Fallowfield, H.J. and Curtis, T.P. (2003) Variable photosynthetic characteristics in waste stabilisation ponds. Water Science and Technology, vol. 48 (2) pp. 219-226

Weatherell, C.A. (2001) Predicting Algal Concentration in Waste Stabilisation Ponds. Ph.D Thesis, Flinders University, School of Medicine.

Webb, W.L., Newton, M. and Starr, M. (1974) Carbon dioxide exchange of Alnus rubra: a mathematical model. Oecologia, vol. 17 pp. 281-291

Weber, T.S. and Deutsch, C. (2010) Ocean nutrient ratios governed by plankton biogeography. Nature, vol. 467 (7315) pp. 550-554

Westphalen, G., Collings, G., Wear, R., Fernanades, M., Bryars, S. and Chesire, A. (2005) ACWS Technical Report 2 Sea Grass Adelaide. pp. 1-73

Werner, J., Quellet, J., Cheng, C., Ju, Y. and Law, D.R. (2010) Pulp and paper mill effluents induce distinct gene expression changes linked to androgenic and estrogenic responses in the fathead minnow. Environmental Toxicology and Chemistry, vol. 29 (2) pp. 460-439

Yamamoto, A., Short, M.D., van den Akker, B. Cromar, N.J. and Fallowfield, H.J. (2010). Nitrification potential in waste stabilisation ponds: comparison of a secondary and tertiary pond system. Water Science and Technology, vol. 61 (3), pp. 781-788

Yamamoto, A. Nitrification potential in waste stabilisation ponds. Masters Thesis, Flnders University, School of Medicine. (2007).

Zarr, J.R. (1984) Biostatistical Analysis. Prentice-Hall, Englewood- Cliffs, NY, pp. 718.

Zhen-Gang, J., Kang-Ren, J. and Thomas, J. (2007) Three-dimensional water quality and SAV modelling of a large shallow lake. Journal of Great lakes Research, vol. 33 (1), p. 28-45

Zohary, T., Padisak, J, and Naselli-Flores, L. (2010) Phytoplankton in the physical environment: beyond nutrients, at the end, there is some light. Hydrobiologia, vol. 639 pp. 261-269

Zor, T. and Sellinger, Z. Linearization of the Bradford Protein Assay Increases its Sensitivity. Analytical Biochemistry, vol. (236), pp. 302-308

Appendix A

Excel Macros and Matlab Scripts for preparation of data for use in Surfer (Surface Plots)

```
' Excel Macro: ‘bolivar’

Sub bolivar()
Path = "C:\Program Files\Golden Software\Surfer8\Bolivar\"

' bolivar Macro copies data from May05 alldata.xls (four columns of DO or
temperature data) to template file for surfer use.
' Macro recorded 10/2/2007 by richard evans; at the moment it just saves the files
into my docs, is not perfect but works.
' The template needs to be selected at C2 and saved as the name below.
    For i = 1 To 144
    ActiveCell.Range("A1:E1").Select
    Selection.Copy
    Workbooks.Open Filename:= _
        "C:\Program Files\Golden Software\Surfer8\Bolivar\Feb05 data
production\Surfer xls DO\Bolivar data for surfer template"

    ActiveCell.Offset(0, 0).Range("A1").Select
    ActiveSheet.Paste
    ActiveCell.Offset(0, 1).Range("A1").Select
    Application.CutCopyMode = False
    Selection.Cut Destination:=ActiveCell.Offset(1, -1).Range("A1")
    ActiveCell.Offset(0, 1).Range("A1").Select
    Selection.Cut Destination:=ActiveCell.Offset(2, -2).Range("A1")
    ActiveCell.Offset(0, 1).Range("A1").Select
    Selection.Cut Destination:=ActiveCell.Offset(3, -3).Range("A1")
    ActiveCell.Offset(0, 1).Range("A1").Select
    ThisFile = ActiveCell.Value
    ActiveWorkbook.SaveAs Filename:=ThisFile
    ActiveWorkbook.Close
    ActiveCell.Offset(1, 0).Select
    Next i
End Sub
```

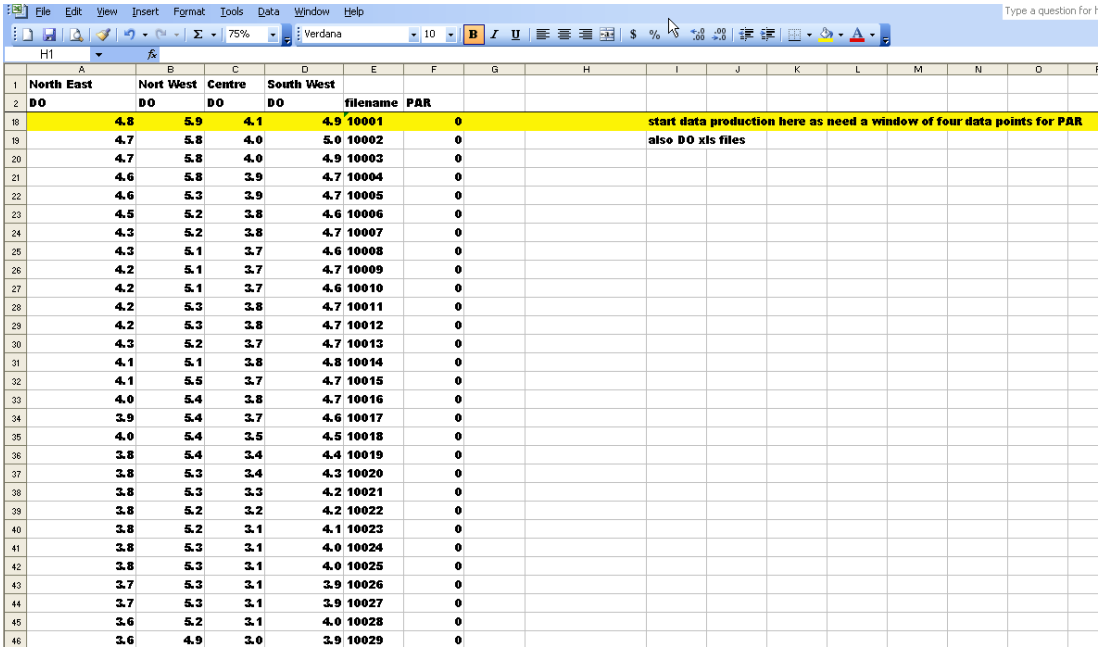

	A	B	C	D	E	F	G	H	I	J	K	L	M	N	O
1	North East	Nort West	Centre	South West											
2	DO	DO	DO	DO	filename	PAR									
18	4.8	5.9	4.1	4.9	10001	0			start data production here as need a window of four data points for PAR						
19	4.7	5.8	4.0	5.0	10002	0			also DO xls files						
20	4.7	5.8	4.0	4.9	10003	0									
21	4.6	5.8	3.9	4.7	10004	0									
22	4.6	5.3	3.9	4.7	10005	0									
23	4.5	5.2	3.8	4.6	10006	0									
24	4.3	5.2	3.8	4.7	10007	0									
25	4.3	5.1	3.7	4.6	10008	0									
26	4.2	5.1	3.7	4.7	10009	0									
27	4.2	5.1	3.7	4.6	10010	0									
28	4.2	5.3	3.8	4.7	10011	0									
29	4.2	5.3	3.8	4.7	10012	0									
30	4.3	5.2	3.7	4.7	10013	0									
31	4.1	5.1	3.8	4.8	10014	0									
32	4.1	5.5	3.7	4.7	10015	0									
33	4.0	5.4	3.8	4.7	10016	0									
34	3.9	5.4	3.7	4.6	10017	0									
35	4.0	5.4	3.5	4.5	10018	0									
36	3.8	5.4	3.4	4.4	10019	0									
37	3.8	5.3	3.4	4.3	10020	0									
38	3.8	5.3	3.3	4.2	10021	0									
39	3.8	5.2	3.2	4.2	10022	0									
40	3.8	5.2	3.1	4.1	10023	0									
41	3.8	5.3	3.1	4.0	10024	0									
42	3.8	5.3	3.1	4.0	10025	0									
43	3.7	5.3	3.1	3.9	10026	0									
44	3.7	5.3	3.1	3.9	10027	0									
45	3.6	5.2	3.1	4.0	10028	0									
46	3.6	4.9	3.0	3.9	10029	0									

Figure A-1. Example spreadsheet structure for dissolved oxygen; file name and incident light (PAR) online data.

Excel Macro: ‘wind’

```
' Sub wind()
Path = "C:\Program Files\Golden Software\Surfer8\Bolivar\"

' bolivar Macro copies data from Feb05 alldata. xls (two columns of wind data and the filename) to template file for Matlab and then surfer use.
' Macro recorded 17/3/2007 and 25/11/10 by richard evans, it saves the files my documents (most often!).
' The template needs to be selected at A1 and saved as the name below.
    For i = 3 To 22
    ActiveCell.Range("A1:C1").Select
    Selection.Copy
    Workbooks.Open Filename:= _
        "C:\Program Files\Golden Software\Surfer8\Bolivar\Feb05 data production\Surfer xls DO\Bolivar wind template.xls"
    ActiveCell.Offset(0, 0).Range("A1").Select
    ActiveSheet.Paste
    ActiveCell.Offset(0, 2).Range("A1").Select
    ThisFile = ActiveCell.Value
    ActiveWorkbook.SaveAs Filename:=ThisFile
    ActiveWorkbook.Close
    ActiveCell.Offset(1, 0).Select
    Next i
End Sub
```

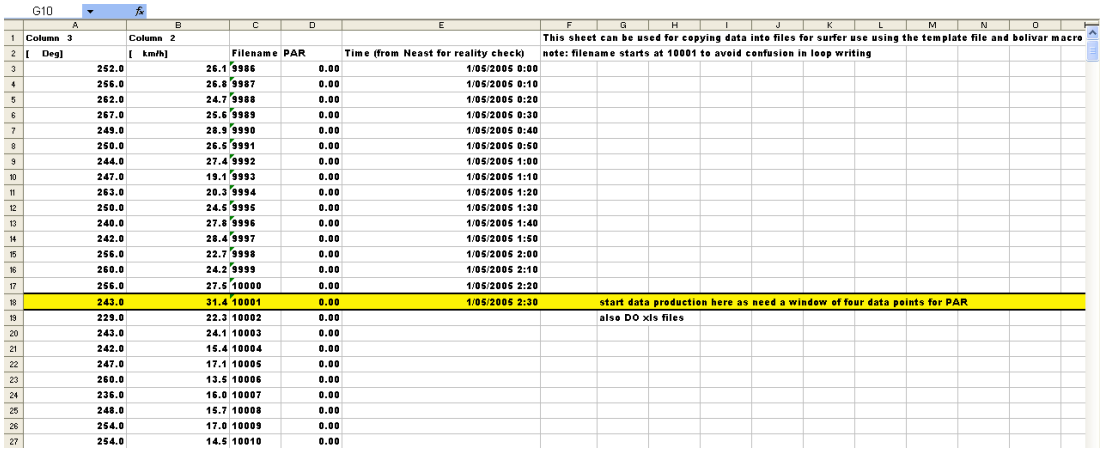

	A	B	C	D	E	F
1	Column 3	Column 2				This sheet can be used for copying data into files for surfer use using the template file and bolivar macro
2	[Deg]	[km/h]	Filename	PAR	Time (from Neast for reality check)	note: filename starts at 10001 to avoid confusion in loop writing
3	252.0	26.1	9986	0.00	1/05/2005 0:00	
4	256.0	26.8	9987	0.00	1/05/2005 0:10	
5	262.0	24.7	9988	0.00	1/05/2005 0:20	
6	267.0	25.6	9989	0.00	1/05/2005 0:30	
7	249.0	28.9	9990	0.00	1/05/2005 0:40	
8	250.0	26.5	9991	0.00	1/05/2005 0:50	
9	244.0	27.4	9992	0.00	1/05/2005 1:00	
10	247.0	19.1	9993	0.00	1/05/2005 1:10	
11	263.0	20.3	9994	0.00	1/05/2005 1:20	
12	250.0	24.5	9995	0.00	1/05/2005 1:30	
13	240.0	27.8	9996	0.00	1/05/2005 1:40	
14	242.0	28.4	9997	0.00	1/05/2005 1:50	
15	256.0	22.7	9998	0.00	1/05/2005 2:00	
16	260.0	24.2	9999	0.00	1/05/2005 2:10	
17	256.0	27.5	10000	0.00	1/05/2005 2:20	
18	243.0	31.4	10001	0.00	1/05/2005 2:30	start data production here as need a window of four data points for PAR
19	229.0	22.3	10002	0.00		also DO xls files
20	243.0	24.1	10003	0.00		
21	242.0	15.4	10004	0.00		
22	247.0	17.1	10005	0.00		
23	260.0	13.5	10006	0.00		
24	236.0	16.0	10007	0.00		
25	248.0	15.7	10008	0.00		
26	254.0	17.0	10009	0.00		
27	254.0	14.5	10010	0.00		

Figure A-2. Example spreadsheet structure for dissolved oxygen; file name and incident light (PAR) online data.

```
Sub PAR()
   For i = 1 To 144
   Dim FilterName As Object
   Dim fruitbun As ChartObject
   Dim myrange As Range
   Dim gifname As String
   Path = "C:\Program Files\Golden Software\Surfer8\Bolivar\"
   ActiveCell.Select
   gifname = ActiveCell.Value
   ActiveCell.Offset(-15, 1).Range("A1:A16").Select
   Set myrange = Selection
   Application.CutCopyMode = False
   Charts.Add
   ActiveChart.ApplyCustomType ChartType:=xlUserDefined,
TypeName:="PAR_Feb"
   ActiveChart.SetSourceData Source:=myrange
   ActiveChart.Location Where:=xlLocationAsObject,
Name:="DO_Ave_day_10min"
   ActiveSheet.ChartObjects(1).Select
   Set fruitbun = ActiveChart.Parent
   ActiveChart.Export Filename:="C:\Program Files\Golden
Software\Surfer8\Bolivar\" + gifname + ".gif", FilterName:="GIF"
   ActiveWindow.Visible = False
   Selection.Delete
   ActiveCell.Offset(16, -1).Range("A1").Select
   Next i
   'Macro recorded 19/2/2007 by richard evans
   'Active cell is start of column (filename column), eg. in column E and PAR in
column F
   'At moment produces a 16 row window for chart, all movements are relative to the
original active cell.
   'Remember to change the sheet name above to get it to work.
End Sub
```

Matlab script file ‘wind’

```
% wind m-file
% uses the excel files produced by excel macro ‘wind’
windfile=10004:11568;
 for john = windfile %specifies files to process
    excelfilename = mat2str(john); %changes number to string
    windir=xlsread(excelfilename,'A2:A6'); %opens excel file copies
wind direction data and names it (based on wind template)
    windspeed=xlsread(excelfilename,'B2:B6');%opens excel file
copies windspeed data and names it
    rad_windir=windir*pi/180; %converts direction data to radians
for cartesian conversion
    [x,y]=pol2cart(rad_windir,windspeed); %prepares data for compass
plot

    max_lim=30;
    minlim=0;

    x_fake=[0 max_lim 0 -max_lim];
    y_fake=[max_lim 0 -max_lim 0];

    h_fake=compass(x_fake,y_fake);
    hold on;
    h=compass(x,y);
    set(h_fake,'Visible','off')

    %h=compass(x,y);
    view([90,-90])
    X = getframe(gcf);
    imwrite(X.cdata,excelfilename,'tiff','Resolution',600)
    clf
  % to make it work with white background open the figure 1 template
and
  % then run, works nicely!
end
    close all
```

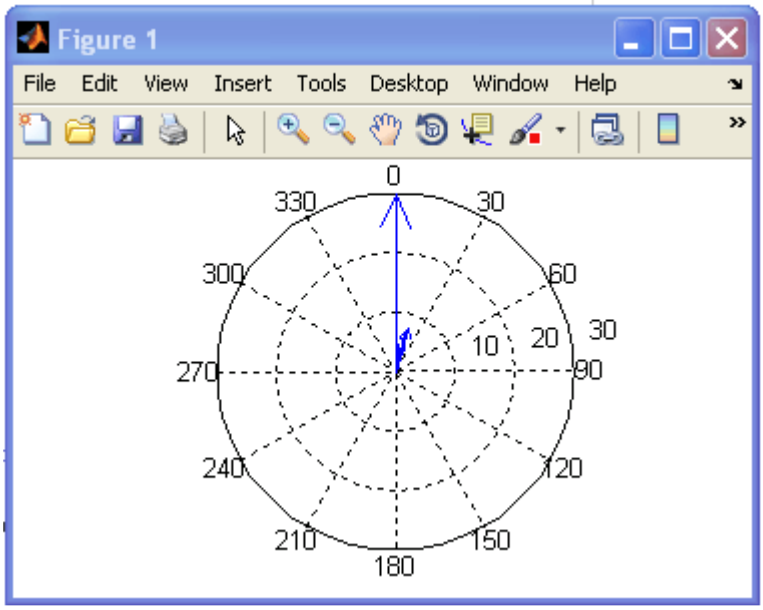

Figure A-3. Matlab Wind rose template file required for Matlab script.

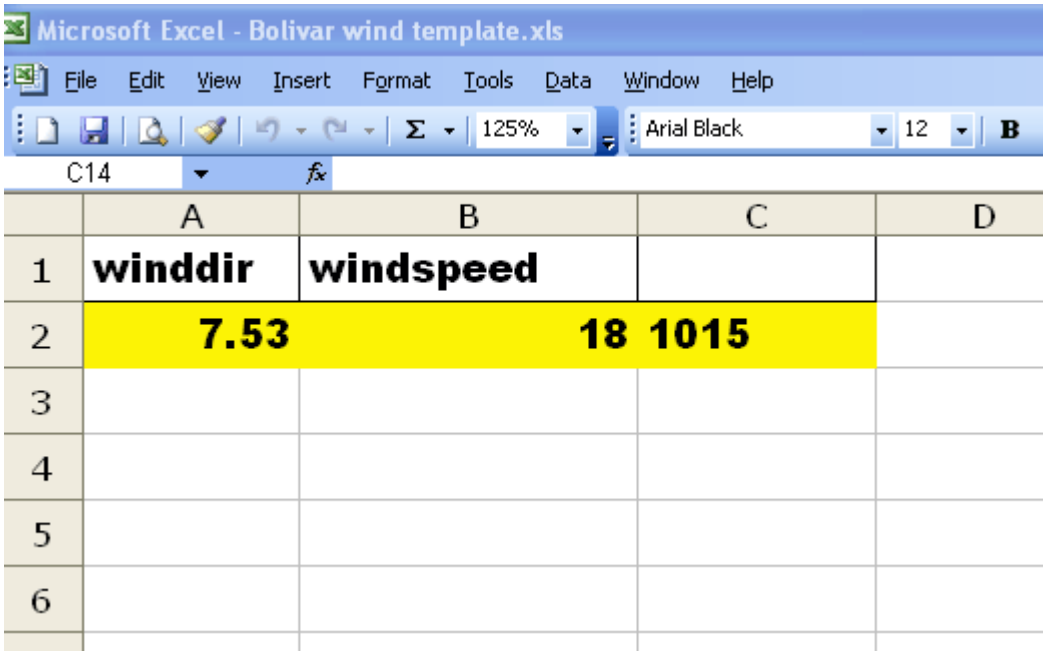

Figure A-4. Wind data file structure required for Matlab script.

Surfer Macro Script for production of surface plots.

Variations provided for context.

```
Sub Main
        ' Macro written by R. Evans 2007 (modified from Dave Sweeney 2001)
'=============================================================
================
' Create the surfer object.
Set SurferApp = CreateObject("Surfer.Application")

'Make surfer visible,
SurferApp.Visible=False

'Get Surfer's startup directory
path = "C:\Program Files\Golden Software\Surfer8\Bolivar\production
templates\working\"

'Loop for each file
For John = 10001 To 11568
        Paul=Str$(John)
        George = LTrim$(Paul)
        Ringo= SurferApp.Path + "\Bolivar\production templates\working\" +
George + ".xls"

'grids the data and saves grid file
retValue = SurferApp.GridData(DataFile:=Ringo, _
        XMin:=138.56467523134, XMax:=138.579, YMin:=-34.774039098664,
YMax:=-34.758, _
```

```
        xCol:=1, yCol:=2, zCol:=3, Algorithm:=srfKriging, Outgrid:= Ringo +
".grd")

Next

End Sub
```

Next Example

```
Sub Main
        ' Macro written by R. Evans 2007 (modified from Dave Sweeney 2001)
'============================================================
===============
' Create the surfer object.
Set SurferApp = CreateObject("Surfer.Application")

'Make surfer visible,
SurferApp.Visible = False
SurferApp.Width = 800
SurferApp.Height = 600

'Get Surfer's startup directory
Path1 = SurferApp.Path + "\Bolivar\data\"

'Loop for each file
For John = 10805 To 11568

        Paul = Str$(John)
        George = LTrim$(Paul)
   Ringo = SurferApp.Path + "\Bolivar\data\Feb05\do and light cubic splined
Feb05\DO and PAR surface plots\DO_Rate_excel\" + George + ".xls"
        Yoko=  SurferApp.Path + "\Bolivar\data\Feb05\temp cubic splined
Feb05\temp surface plots\T25_75_excel\" + George + ".xls"

Set plotdoc1 = SurferApp.Documents.Add
Set plotwin1 = plotdoc1.Windows(1)
plotwin1.Activate
Set shapes1 = plotdoc1.Shapes
'AppActivate "Surfer "
'plotdoc1.PageSetup.Orientation = srfLandscape

'Creates a contour map and assigns the map coordinate system to the variable named
"MapFrame"
Set mapframe1 = shapes1.AddContourMap(GridFileName:=SurferApp.Path _
        + "\Bolivar\data\Feb05\do and light cubic splined Feb05\DO and PAR
surface plots\DO_Rate_grid\" + George + ".xls" + ".grd")

'Declares Levels an object
```

```
Set ContourMap1 = mapframe1.Overlays(1)

'Assigns the Levels collection to the variable named "ContourLevels" good ok up to
here
Set ContourLevels1 = ContourMap1.Levels

'Uses the Levels collection to assign contour intervals.
ContourLevels1.LoadFile(SurferApp.Path + "\Bolivar\production
templates\working\DO_Rate_Level.lvl")

'Fill the contour map levels
ContourMap1.FillContours = True

'Creates a base map and assigns the map coordinate system to the variable named
"MapFrame" Good it works!
Set mapframe2 = Shapes1.AddBaseMap(ImportFileName:=SurferApp.Path
+"\Bolivar\production templates\working\Bolivar blank.bln")

'Base map line properties
Set BaseMap1 = mapframe2.Overlays(1)
BaseMap1.Fill.Pattern = "Solid"

'Creates a post map and assigns the map coordinate system to the variable named
"MapFrame" puts crosses on Good it works!
Set mapframe3 = Shapes1.AddPostMap(DataFileName:=Ringo)

Set PostMap1 = mapframe3.Overlays(1)

' Retrieve the parent PlotDocument object

Set plotdoc1 = mapframe1.Parent

' Clear all selections and then select the MapFrame objects
plotdoc1.Selection.DeselectAll

'Select the maps
mapframe1.Selected = True
mapframe2.Selected = True
mapframe3.Selected = True

' Overlay the selected maps
plotdoc1.Selection.OverlayMaps

'Move DO plot to Top LHS
plotdoc1.Selection.Top=29
plotdoc1.Selection.Left=0

'Shows Colout scale
ContourMap1.ShowColorScale = True
```

```
plotdoc1.Selection.DeselectAll


'Now Temperature

'Creates a contour map and assigns the map coordinate system to the variable named
"MapFrame"
Set MapFrame4 = Shapes1.AddContourMap(GridFileName:=SurferApp.Path _
        + "\Bolivar\data\Feb05\temp cubic splined Feb05\temp surface
plots\T25_75_grid\" + George + ".xls" + ".grd")

'Declares Levels an Object
Set ContourMap2 = MapFrame4.Overlays(1)

'Assigns the Levels collection to the variable named "ContourLevels"
Set ContourLevels2 = ContourMap2.Levels

'Uses the Levels collection to assign contour intervals.
ContourLevels2.LoadFile(SurferApp.Path + "\Bolivar\production
templates\working\Bolivar level Feb T25_75.lvl")

'create color map scale
Set ContourMap2 = MapFrame4.Overlays(1)
'ContourMap2.ShowColorScale = True

'Fill the contour map levels
ContourMap2.FillContours = True

'Creates a base map and assigns the map coordinate system to the variable named
"MapFrame" Good it works!
Set MapFrame5 = Shapes1.AddBaseMap(ImportFileName:=SurferApp.Path
+"\Bolivar\production templates\working\Bolivar blank.bln")

'Base map line properties
Set BaseMap2 = MapFrame5.Overlays(1)
BaseMap2.Fill.Pattern = "Solid"

'Creates a post map and assigns the map coordinate system to the variable named
"MapFrame" puts crosses on: will only work when two seperate plots
Set MapFrame6 = Shapes1.AddPostMap(DataFileName:=Yoko)

Set PostMap2 = MapFrame6.Overlays(1)

' Retrieve the parent PlotDocument object

Set plotdoc1 = mapframe4.Parent

' Clear all selections and then select the MapFrame objects
plotdoc1.Selection.DeselectAll
```

```
'Select the maps
mapframe4.Selected = True
mapframe5.Selected = True
mapframe6.Selected = True

' Overlay the selected maps
plotdoc1.Selection.OverlayMaps

'Move Temperature plot to Top RHS
plotdoc1.Selection.Top=29
plotdoc1.Selection.Left=18

'Shows Colout scale
ContourMap2.ShowColorScale = True

plotdoc1.Selection.DeselectAll

'Now text for

'Creates a text string and assigns it to the variable named "Text3"
Set Text1 = Shapes1.AddText(x:=15.2, y:=15, Text:="DO_rate(mg/L/hour)")
Text1.Font.Size = 13

'Creates a text string and assigns it to the variable named "Text3"
Set Text2 = Shapes1.AddText(x:=34, y:=15, Text:="Tdiff(DegC/m)")
Text2.Font.Size = 13

'imports gif image
Set parplot = plotdoc1.Import(SurferApp.Path + "\Bolivar\data\Feb05\do and light
cubic splined Feb05\gifs of PAR\" + George + ".gif")

'moves image
parplot.Left=1
parplot.Top=12

'Creates a text string and assigns it to the variable named "Text3"
Set Text3 = Shapes1.AddText(x:=2, y:=4.5, Text:="PAR(umol/m2/sec), current data
= 16")
Text3.Font.Size = 20

'Creates a text string and assigns it to the variable named "Text4"
Set Text4 = Shapes1.AddText(x:=2, y:=1, Text:="Feb05 10 Minute Increments 17/2
00:00 to 27/2 24:00")
Text4.Font.Size = 20

'imports tif image
Set Windplot = plotdoc1.Import(SurferApp.Path + "\Bolivar\data\Feb05\wind\" +
George + ".tif")

'moves image
```

```
Windplot.Left=16.5
Windplot.Top=12

'Creates a text string and assigns it to the variable named "Text5"
Set Text5 = Shapes1.AddText(x:=2, y:=3, Text:="Wind direction and velocity
(km/hour)")
Text5.Font.Size = 20

'exports whole lot as a gif; ‘but do not overlook the importance of copper’:
N.Mascuri pers. com. 2011.
plotdoc1.Export(FileName:=SurferApp.Path + "\Bolivar\production
templates\working\" + George + ".gif",
Options:="Height=625,ColorDepth=24,HDPI=60")

Next

End Sub
```

Next Example

```
Sub Main
        ' Macro written by R. Evans 2007 (modified from Dave Sweeney 2001)
'=============================================================
===============
' Create the surfer object.
Set SurferApp = CreateObject("Surfer.Application")

'Make surfer visible,
SurferApp.Visible = False
SurferApp.Width = 800
SurferApp.Height = 600

'Get Surfer's startup directory
Path1 = SurferApp.Path + "\Bolivar\data\"

'Loop for each file
For John = 10801 To 11568

        Paul = Str$(John)
        George = LTrim$(Paul)
   Ringo = SurferApp.Path + "\Bolivar\data\Feb05\do and light cubic splined
Feb05\DO and PAR surface plots\excel files\" + George + ".xls"
        Yoko=  SurferApp.Path + "\Bolivar\data\Feb05\temp cubic splined
Feb05\temp surface plots\T25_75_excel\" + George + ".xls"

Set plotdoc1 = SurferApp.Documents.Add
Set plotwin1 = plotdoc1.Windows(1)
```

```
plotwin1.Activate
Set shapes1 = plotdoc1.Shapes
'AppActivate "Surfer "
'plotdoc1.PageSetup.Orientation = srfLandscape

'Creates a contour map and assigns the map coordinate system to the variable named
"MapFrame"
Set mapframe1 = shapes1.AddContourMap(GridFileName:=SurferApp.Path _
        + "\Bolivar\data\Feb05\do and light cubic splined Feb05\DO and PAR
surface plots\grid files\" + George + ".xls" + ".grd")

'Declares Levels an object
Set ContourMap1 = mapframe1.Overlays(1)

'Assigns the Levels collection to the variable named "ContourLevels" good ok up to
here
Set ContourLevels1 = ContourMap1.Levels

'Uses the Levels collection to assign contour intervals.
ContourLevels1.LoadFile(SurferApp.Path + "\Bolivar\production
templates\working\Bolivar level.lvl")

'Fill the contour map levels
ContourMap1.FillContours = True

'Creates a base map and assigns the map coordinate system to the variable named
"MapFrame" Good it works!
Set mapframe2 = Shapes1.AddBaseMap(ImportFileName:=SurferApp.Path
+"\Bolivar\production templates\working\Bolivar blank.bln")

'Base map line properties
Set BaseMap1 = mapframe2.Overlays(1)
BaseMap1.Fill.Pattern = "Solid"

'Creates a post map and assigns the map coordinate system to the variable named
"MapFrame" puts crosses on Good it works!
Set mapframe3 = Shapes1.AddPostMap(DataFileName:=Ringo)

Set PostMap1 = mapframe3.Overlays(1)

' Retrieve the parent PlotDocument object

Set plotdoc1 = mapframe1.Parent

' Clear all selections and then select the MapFrame objects
plotdoc1.Selection.DeselectAll

'Select the maps
mapframe1.Selected = True
mapframe2.Selected = True
```

```
mapframe3.Selected = True

' Overlay the selected maps
plotdoc1.Selection.OverlayMaps

'Move DO plot to Top LHS
plotdoc1.Selection.Top=29
plotdoc1.Selection.Left=0

'Shows Colout scale
ContourMap1.ShowColorScale = True

plotdoc1.Selection.DeselectAll


'Now Temperature

'Creates a contour map and assigns the map coordinate system to the variable named
"MapFrame"
Set MapFrame4 = Shapes1.AddContourMap(GridFileName:=SurferApp.Path _
        + "\Bolivar\data\Feb05\temp cubic splined Feb05\temp surface
plots\T25_75_grid\" + George + ".xls" + ".grd")

'Declares Levels an Object
Set ContourMap2 = MapFrame4.Overlays(1)

'Assigns the Levels collection to the variable named "ContourLevels"
Set ContourLevels2 = ContourMap2.Levels

'Uses the Levels collection to assign contour intervals.
ContourLevels2.LoadFile(SurferApp.Path + "\Bolivar\production
templates\working\Bolivar level Feb T25_75.lvl")

'create color map scale
Set ContourMap2 = MapFrame4.Overlays(1)
'ContourMap2.ShowColorScale = True

'Fill the contour map levels
ContourMap2.FillContours = True

'Creates a base map and assigns the map coordinate system to the variable named
"MapFrame" Good it works!
Set MapFrame5 = Shapes1.AddBaseMap(ImportFileName:=SurferApp.Path
+"\Bolivar\production templates\working\Bolivar blank.bln")

'Base map line properties
Set BaseMap2 = MapFrame5.Overlays(1)
BaseMap2.Fill.Pattern = "Solid"
```

```
'Creates a post map and assigns the map coordinate system to the variable named
"MapFrame" puts crosses on: will only work when two seperate plots
Set MapFrame6 = Shapes1.AddPostMap(DataFileName:=Yoko)

Set PostMap2 = MapFrame6.Overlays(1)

' Retrieve the parent PlotDocument object

Set plotdoc1 = mapframe4.Parent

' Clear all selections and then select the MapFrame objects
plotdoc1.Selection.DeselectAll

'Select the maps
mapframe4.Selected = True
mapframe5.Selected = True
mapframe6.Selected = True

' Overlay the selected maps
plotdoc1.Selection.OverlayMaps

'Move Temperature plot to Top RHS
plotdoc1.Selection.Top=29
plotdoc1.Selection.Left=18

'Shows Colout scale
ContourMap2.ShowColorScale = True

plotdoc1.Selection.DeselectAll

'Now text for

'Creates a text string and assigns it to the variable named "Text3"
Set Text1 = Shapes1.AddText(x:=15.2, y:=15, Text:="DO(mg/L)")
Text1.Font.Size = 13

'Creates a text string and assigns it to the variable named "Text3"
Set Text2 = Shapes1.AddText(x:=34, y:=15, Text:="Tdiff(Deg C)")
Text2.Font.Size = 13

'imports gif image
Set parplot = plotdoc1.Import(SurferApp.Path + "\Bolivar\data\Feb05\do and light
cubic splined Feb05\gifs of PAR\" + George + ".gif")

'moves image
parplot.Left=1
parplot.Top=12

'Creates a text string and assigns it to the variable named "Text3"
```

```
Set Text3 = Shapes1.AddText(x:=2, y:=4.5, Text:="PAR(umol/m2/sec), current data
= 16")
Text3.Font.Size = 20

'Creates a text string and assigns it to the variable named "Text4"
Set Text4 = Shapes1.AddText(x:=2, y:=1, Text:="Feb05 10 Minute intervals 17/2
00:00 to 27/2 24:00")
Text4.Font.Size = 20

'imports tif image
Set Windplot = plotdoc1.Import(SurferApp.Path + "\Bolivar\data\Feb05\wind\" +
George + ".tif")

'moves image
Windplot.Left=16.5
Windplot.Top=12

'Creates a text string and assigns it to the variable named "Text5"
Set Text5 = Shapes1.AddText(x:=2, y:=3, Text:="Wind direction and velocity
(km/hour)")
Text5.Font.Size = 20

'exports whole lot as a gif
plotdoc1.Export(FileName:=SurferApp.Path + "\Bolivar\production
templates\working\" + George + ".gif",
Options:="Height=625,ColorDepth=24,HDPI=60")

Next

End Sub
```

Next Example

```
Sub Main
        ' Macro written by R. Evans 2007 (modified from Dave Sweeney 2001)
'=============================================================
===============
' Create the surfer object.
Set SurferApp = CreateObject("Surfer.Application")

'Make surfer visible,
SurferApp.Visible = False
SurferApp.Width = 800
SurferApp.Height = 600

'Get Surfer's startup directory
Path1 = SurferApp.Path + "\Bolivar\data\"
```

```
'Loop for each file
For John = 10801 To 11425

        Paul = Str$(John)
        George = LTrim$(Paul)
   Ringo = SurferApp.Path + "\Bolivar\data\May05\do and light cubic splined
May05\DO_Rate\excel files\" + George + ".xls"
        Yoko=  SurferApp.Path + "\Bolivar\data\May05\temp cubic splined
May05\temp surface plots\T25_75_excel\" + George + ".xls"

Set plotdoc1 = SurferApp.Documents.Add
Set plotwin1 = plotdoc1.Windows(1)
plotwin1.Activate
Set shapes1 = plotdoc1.Shapes
'AppActivate "Surfer "
'plotdoc1.PageSetup.Orientation = srfLandscape

'Creates a contour map and assigns the map coordinate system to the variable named
"MapFrame"
Set mapframe1 = shapes1.AddContourMap(GridFileName:=SurferApp.Path _
        + "\Bolivar\data\May05\do and light cubic splined May05\DO_Rate\grid
files\" + George + ".xls" + ".grd")

'Declares Levels an object
Set ContourMap1 = mapframe1.Overlays(1)

'Assigns the Levels collection to the variable named "ContourLevels" good ok up to
here
Set ContourLevels1 = ContourMap1.Levels

'Uses the Levels collection to assign contour intervals.
ContourLevels1.LoadFile(SurferApp.Path + "\Bolivar\production
templates\working\DO_Rate_level.lvl")

'Fill the contour map levels
ContourMap1.FillContours = True

'Creates a base map and assigns the map coordinate system to the variable named
"MapFrame" Good it works!
Set mapframe2 = Shapes1.AddBaseMap(ImportFileName:=SurferApp.Path
+"\Bolivar\production templates\working\Bolivar blank.bln")

'Base map line properties
Set BaseMap1 = mapframe2.Overlays(1)
BaseMap1.Fill.Pattern = "Solid"

'Creates a post map and assigns the map coordinate system to the variable named
"MapFrame" puts crosses on Good it works!
Set mapframe3 = Shapes1.AddPostMap(DataFileName:=Ringo)
```

```
Set PostMap1 = mapframe3.Overlays(1)

' Retrieve the parent PlotDocument object

Set plotdoc1 = mapframe1.Parent

' Clear all selections and then select the MapFrame objects
plotdoc1.Selection.DeselectAll

'Select the maps
mapframe1.Selected = True
mapframe2.Selected = True
mapframe3.Selected = True

' Overlay the selected maps
plotdoc1.Selection.OverlayMaps

'Move DO plot to Top LHS
plotdoc1.Selection.Top=29
plotdoc1.Selection.Left=0

'Shows Colout scale
ContourMap1.ShowColorScale = True

plotdoc1.Selection.DeselectAll


'Now Temperature

'Creates a contour map and assigns the map coordinate system to the variable named
"MapFrame"
Set MapFrame4 = Shapes1.AddContourMap(GridFileName:=SurferApp.Path _
        + "\Bolivar\data\May05\temp cubic splined May05\temp surface
plots\T25_75_grid\" + George + ".xls" + ".grd")

'Declares Levels an Object
Set ContourMap2 = MapFrame4.Overlays(1)

'Assigns the Levels collection to the variable named "ContourLevels"
Set ContourLevels2 = ContourMap2.Levels

'Uses the Levels collection to assign contour intervals.
ContourLevels2.LoadFile(SurferApp.Path + "\Bolivar\production
templates\working\Bolivar level Feb T25_75.lvl")

'create color map scale
Set ContourMap2 = MapFrame4.Overlays(1)
'ContourMap2.ShowColorScale = True
```

```
'Fill the contour map levels
ContourMap2.FillContours = True

'Creates a base map and assigns the map coordinate system to the variable named
"MapFrame" Good it works!
Set MapFrame5 = Shapes1.AddBaseMap(ImportFileName:=SurferApp.Path
+"\Bolivar\production templates\working\Bolivar blank.bln")

'Base map line properties
Set BaseMap2 = MapFrame5.Overlays(1)
BaseMap2.Fill.Pattern = "Solid"

'Creates a post map and assigns the map coordinate system to the variable named
"MapFrame" puts crosses on: will only work when two seperate plots
Set MapFrame6 = Shapes1.AddPostMap(DataFileName:=Yoko)

Set PostMap2 = MapFrame6.Overlays(1)

' Retrieve the parent PlotDocument object

Set plotdoc1 = mapframe4.Parent

' Clear all selections and then select the MapFrame objects
plotdoc1.Selection.DeselectAll

'Select the maps
mapframe4.Selected = True
mapframe5.Selected = True
mapframe6.Selected = True

' Overlay the selected maps
plotdoc1.Selection.OverlayMaps

'Move Temperature plot to Top RHS
plotdoc1.Selection.Top=29
plotdoc1.Selection.Left=18

'Shows Colout scale
ContourMap2.ShowColorScale = True

plotdoc1.Selection.DeselectAll

'Now text for

'Creates a text string and assigns it to the variable named "Text3"
Set Text1 = Shapes1.AddText(x:=15.2, y:=15, Text:="DO_rate(mg/L/hour)")
Text1.Font.Size = 13

'Creates a text string and assigns it to the variable named "Text3"
Set Text2 = Shapes1.AddText(x:=34, y:=15, Text:="T25_75(DegC/m)")
```

```
Text2.Font.Size = 13

'imports gif image
Set parplot = plotdoc1.Import(SurferApp.Path + "\Bolivar\data\May05\do and light
cubic splined May05\gifs of PAR\" + George + ".gif")

'moves image
parplot.Left=1
parplot.Top=13

'Creates a text string and assigns it to the variable named "Text3"
Set Text3 = Shapes1.AddText(x:=2, y:=4.5, Text:="PAR(umol/m2/sec), current data
= 16")
Text3.Font.Size = 20

'Creates a text string and assigns it to the variable named "Text4"
Set Text4 = Shapes1.AddText(x:=2, y:=1, Text:="May05 10 minute intervals 1/5
00:00 to 11/5 24:00")
Text4.Font.Size = 20

'imports tif image
Set Windplot = plotdoc1.Import(SurferApp.Path + "\Bolivar\data\May05\wind\" +
George + ".tif")

'moves image
Windplot.Left=16.5
Windplot.Top=12

'Creates a text string and assigns it to the variable named "Text5"
Set Text5 = Shapes1.AddText(x:=2, y:=3, Text:="Wind direction and velocity
(km/hour)")
Text5.Font.Size = 20

'exports whole lot as a gif
plotdoc1.Export(FileName:=SurferApp.Path + "\Bolivar\production
templates\working\" + George + ".gif",
Options:="Height=625,ColorDepth=24,HDPI=60")

Next
End Sub
```

End Appendix A

Appendix B

Electronic Files

The Table below provides a listing of names and sizes of the 'data movie' files referred to in Chapter 6. These files are provided as a 'zip' archive for download with the Thesis.

The 'zip' file archive is named '03_Appendix_B_Electronic_Files.zip'

Series	Filename	Size
A	Feb05_DO_T_PAR_Wind.mov	148 Mb
	May05_DO_T_PAR_Wind.mov	132 Mb
B	Feb05_DO_T25_75_PAR_Wind.mov	129 Mb
	May05_DO_T25_75_PAR_Wind.mov	118 Mb
C	Feb05_DO_rate_T25_75_PAR_Wind.mov	114 Mb
	May05_DO_rate_T25_75_PAR_Wind.mov	93 Mb
D	Feb05_Ave_DAY_DO_T_PAR_Wind.mov	6.6 Mb
	May05_Ave_Day_DO_T_PAR_Wind.mov	6.1 Mb
E	Feb05_Ave_Day_DO_T25_75_PAR_Wind.mov	5.4 Mb
	May05_Ave_Day_DO_T25_75_PAR_Wind.mov	5.7 Mb
F	Feb05_Ave_Day_DO_Rate_T25_75_PAR_Wind.mov	4.6 Mb
	May05_Ave_Day_DO_Rate_T25_75_PAR_Wind.mov	4.4 Mb

Appendix C

Factor Analysis Output Files (SPSS V17_2010 update)

Output for Chapter 6 Figure 6.15

```
FACTOR   /VARIABLES PAR_Da_1 NE_Tdiff_1 NW_Tdiff_1 C_Tdiff__1 SW_Tdiff_1
Wind_d_1 Wind_s_1   /MISSING LISTWISE   /ANALYSIS PAR_Da_1 NE_Tdiff_1
NW_Tdiff_1 C_Tdiff__1 SW_Tdiff_1 Wind_d_1 Wind_s_1   /PRINT UNIVARIATE INITIAL
EXTRACTION ROTATION   /PLOT ROTATION   /CRITERIA FACTORS(2) ITERATE(25)
/EXTRACTION PC   /CRITERIA ITERATE(25)   /ROTATION VARIMAX
/METHOD=CORRELATION.
```

Factor Analysis

Notes

	Output Created	30-Mar-2011 22:05:34
	Comments	
Input	Data	C:\Complete\Chapter 6 Bolivar\spss\Feb05_aligned.sav
	Active Dataset	DataSet2
	Filter	<none>
	Weight	<none>
	Split File	<none>
	N of Rows in Working Data File	144
Missing Value Handling	Definition of Missing	MISSING=EXCLUDE: User-defined missing values are treated as missing.
	Cases Used	LISTWISE: Statistics are based on cases with no missing values for any variable used.

	Syntax	FACTOR /VARIABLES PAR_Da_1 NE_Tdiff_1 NW_Tdiff_1 C_Tdiff__1 SW_Tdiff_1 Wind_d_1 Wind_s_1 /MISSING LISTWISE /ANALYSIS PAR_Da_1 NE_Tdiff_1 NW_Tdiff_1 C_Tdiff__1 SW_Tdiff_1 Wind_d_1 Wind_s_1 /PRINT UNIVARIATE INITIAL EXTRACTION ROTATION /PLOT ROTATION /CRITERIA FACTORS(2) ITERATE(25) /EXTRACTION PC /CRITERIA ITERATE(25) /ROTATION VARIMAX /METHOD=CORRELATION.
Resources	Processor Time	0:00:00.266
	Elapsed Time	0:00:00.266
	Maximum Memory Required	7204 (7.035K) bytes

[DataSet2] C:\Complete\Chapter 6 Bolivar\spss\Feb05_aligned.sav

Descriptive Statistics

	Mean	Std. Deviation	Analysis N
DIFF(PAR_Day11,1)	.0000	32.83360	143
DIFF(NE_T25_75,1)	.0000	.09038	143
DIFF(NW_T25_75,1)	.0007	.08349	143
DIFF(C_T25_75,1)	.0021	.07068	143
DIFF(SW_T25_75,1)	.0070	.10254	143
DIFF(Wind_dir_Day11,1)	.0343	1.91602	143
DIFF(Wind_dir_Day11,1)	.0343	1.91602	143

Communalities

	Initial	Extraction
DIFF(PAR_Day11,1)	1.000	.272
DIFF(NE_T25_75,1)	1.000	.083
DIFF(NW_T25_75,1)	1.000	.543
DIFF(C_T25_75,1)	1.000	.472
DIFF(SW_T25_75,1)	1.000	.583
DIFF(Wind_dir_Day11,1)	1.000	.955

Descriptive Statistics

	Mean	Std. Deviation	Analysis N
DIFF(PAR_Day11,1)	.0000	32.83360	143
DIFF(NE_T25_75,1)	.0000	.09038	143
DIFF(NW_T25_75,1)	.0007	.08349	143
DIFF(C_T25_75,1)	.0021	.07068	143
DIFF(SW_T25_75,1)	.0070	.10254	143
DIFF(Wind_dir_Day11,1)	.0343	1.91602	143
DIFF(Wind_dir_Day11,1)	1.000	.955	

Extraction Method: Principal Component Analysis.

Total Variance Explained

Component	Initial Eigenvalues		
	Total	% of Variance	Cumulative %
1	2.271	32.448	
2	1.591	22.732	
3	1.065	15.218	70.398
4	.940	13.424	83.822
5	.709	10.134	93.956
6	.423	6.044	100.000
7	1.901E-16	2.715E-15	100.000

Extraction Method: Principal Component Analysis.

Total Variance Explained

Component	Initial Eigenvalues	Extraction Sums of Squared Loadings		
	Cumulative %	Total	% of Variance	Cumulative %
1	32.448	2.271	32.448	32.448
2	55.180	1.591	22.732	55.180

Extraction Method: Principal Component Analysis.

Total Variance Explained

Component	Rotation Sums of Squared Loadings		
	Total	% of Variance	Cumulative %
1	2.169	30.987	30.987
2	1.694	24.193	55.180

Extraction Method: Principal Component Analysis.

Component Matrix[a]

	Component	
	1	2
DIFF(PAR_Day11,1)	.165	.494
DIFF(NE_T25_75,1)	.281	.061
DIFF(NW_T25_75,1)	.154	.721
DIFF(C_T25_75,1)	.553	.407
DIFF(SW_T25_75,1)	.507	.571
DIFF(Wind_dir_Day11,1)	.888	-.408
DIFF(Wind_dir_Day11,1)	.888	-.408

Extraction Method: Principal Component Analysis.

a. 2 components extracted.

Rotated Component Matrix[a]

	Component	
	1	2
DIFF(PAR_Day11,1)	-.040	.520
DIFF(NE_T25_75,1)	.236	.165
DIFF(NW_T25_75,1)	-.138	.724
DIFF(C_T25_75,1)	.352	.590
DIFF(SW_T25_75,1)	.246	.723
DIFF(Wind_dir_Day11,1)	.977	-.031
DIFF(Wind_dir_Day11,1)	.977	-.031

Extraction Method: Principal Component Analysis.

Rotation Method: Varimax with Kaiser Normalization.

a. Rotation converged in 3 iterations.

Component Transformation Matrix

Component	1	2
1	.922	.388
2	-.388	.922

Extraction Method: Principal Component Analysis.

Rotation Method: Varimax with Kaiser Normalization.

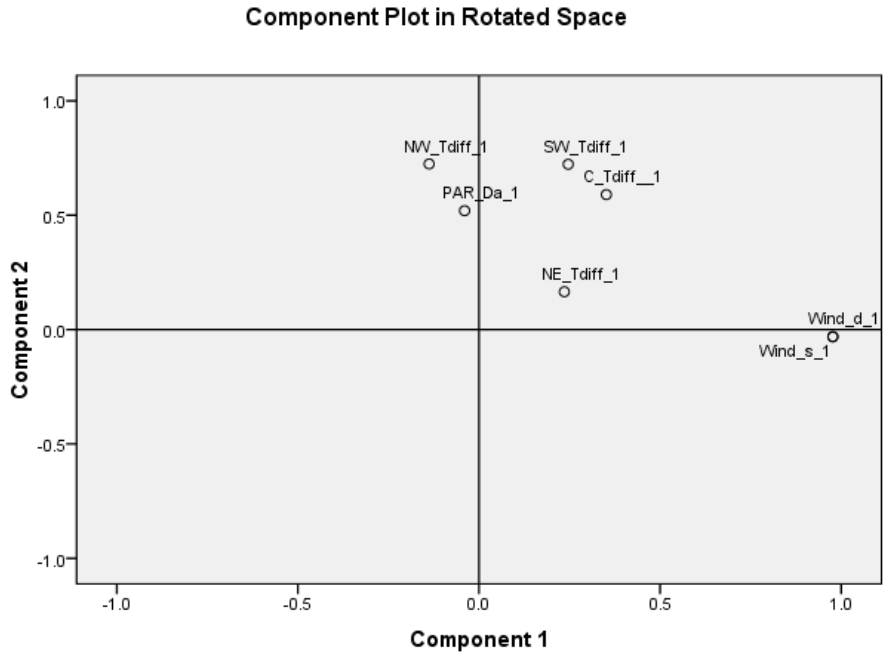

Output for Chapter 6 Figure 6.16

```
FACTOR   /VARIABLES Wind_s_1 Wind_d_1 NE_Tdiff_1 NW_Tdiff_1 C_Tdiff__1
SW_Tdiff_1 PAR_Da_1   /MISSING LISTWISE   /ANALYSIS Wind_s_1 Wind_d_1
NE_Tdiff_1 NW_Tdiff_1 C_Tdiff__1 SW_Tdiff_1 PAR_Da_1   /PRINT UNIVARIATE INITIAL
EXTRACTION   /PLOT ROTATION   /CRITERIA FACTORS(2) ITERATE(25)
/EXTRACTION PC   /ROTATION NOROTATE   /METHOD=CORRELATION.
```

Factor Analysis

Notes		
	Output Created	30-Mar-2011 22:10:27
	Comments	
Input	Data	C:\Complete\Chapter 6 Bolivar\spss\May05_aligned.sav
	Active Dataset	DataSet3
	Filter	<none>
	Weight	<none>
	Split File	<none>
	N of Rows in Working Data File	144
Missing Value Handling	Definition of Missing	MISSING=EXCLUDE: User-defined missing values are treated as missing.

	Cases Used	LISTWISE: Statistics are based on cases with no missing values for any variable used.
	Syntax	FACTOR /VARIABLES Wind_s_1 Wind_d_1 NE_Tdiff_1 NW_Tdiff_1 C_Tdiff__1 SW_Tdiff_1 PAR_Da_1 /MISSING LISTWISE /ANALYSIS Wind_s_1 Wind_d_1 NE_Tdiff_1 NW_Tdiff_1 C_Tdiff__1 SW_Tdiff_1 PAR_Da_1 /PRINT UNIVARIATE INITIAL EXTRACTION /PLOT ROTATION /CRITERIA FACTORS(2) ITERATE(25) /EXTRACTION PC /ROTATION NOROTATE /METHOD=CORRELATION.
Resources	Processor Time	0:00:00.234
	Elapsed Time	0:00:00.281
	Maximum Memory Required	7204 (7.035K) bytes

[DataSet3] C:\Complete\Chapter 6 Bolivar\spss\May05_aligned.sav

Descriptive Statistics

	Mean	Std. Deviation	Analysis N
DIFF(Wind_speed_Day10,1)	-.0133	1.26859	143
DIFF(Wind_dir_Day10,1)	.3776	53.63174	143
DIFF(NE_T25_75,1)	.0000	.06608	143
DIFF(NW_T25_75,1)	.0014	.07410	143
DIFF(C_T25_75,1)	.0007	.07645	143
DIFF(SW_T25_75,1)	.0014	.10614	143
DIFF(PAR_Day10,1)	.0000	25.88980	143

Communalities

	Initial	Extraction
DIFF(Wind_speed_Day10,1)	1.000	.428
DIFF(Wind_dir_Day10,1)	1.000	.593
DIFF(NE_T25_75,1)	1.000	.265

Descriptive Statistics

	Mean	Std. Deviation	Analysis N
DIFF(Wind_speed_Day10,1)	-.0133	1.26859	143
DIFF(Wind_dir_Day10,1)	.3776	53.63174	143
DIFF(NE_T25_75,1)	.0000	.06608	143
DIFF(NW_T25_75,1)	.0014	.07410	143
DIFF(C_T25_75,1)	.0007	.07645	143
DIFF(SW_T25_75,1)	.0014	.10614	143
DIFF(NW_T25_75,1)	1.000	.699	
DIFF(C_T25_75,1)	1.000	.724	
DIFF(SW_T25_75,1)	1.000	.705	
DIFF(PAR_Day10,1)	1.000	.029	

Extraction Method: Principal Component Analysis.

Total Variance Explained

Component	Initial Eigenvalues		
	Total	% of Variance	Cumulative %
1	2.235	31.928	
2	1.208	17.257	
3	1.085	15.495	64.681
4	.949	13.563	78.244
5	.740	10.574	88.818
6	.421	6.019	94.837
7	.361	5.163	100.000

Extraction Method: Principal Component Analysis.

Total Variance Explained

Component	Initial Eigenvalues	Extraction Sums of Squared Loadings		
	Cumulative %	Total	% of Variance	Cumulative %
1	31.928	2.235	31.928	31.928
2	49.186	1.208	17.257	49.186

Extraction Method: Principal Component Analysis.

Component Matrix[a]

	Component	
	1	2
DIFF(Wind_speed_Day10,1)	.419	.502
DIFF(Wind_dir_Day10,1)	-.078	-.766
DIFF(NE_T25_75,1)	.100	.505
DIFF(NW_T25_75,1)	.813	-.196
DIFF(C_T25_75,1)	.820	-.229
DIFF(SW_T25_75,1)	.838	.047
DIFF(PAR_Day10,1)	-.089	.145

Extraction Method: Principal Component Analysis.

a. 2 components extracted.

Component Plot

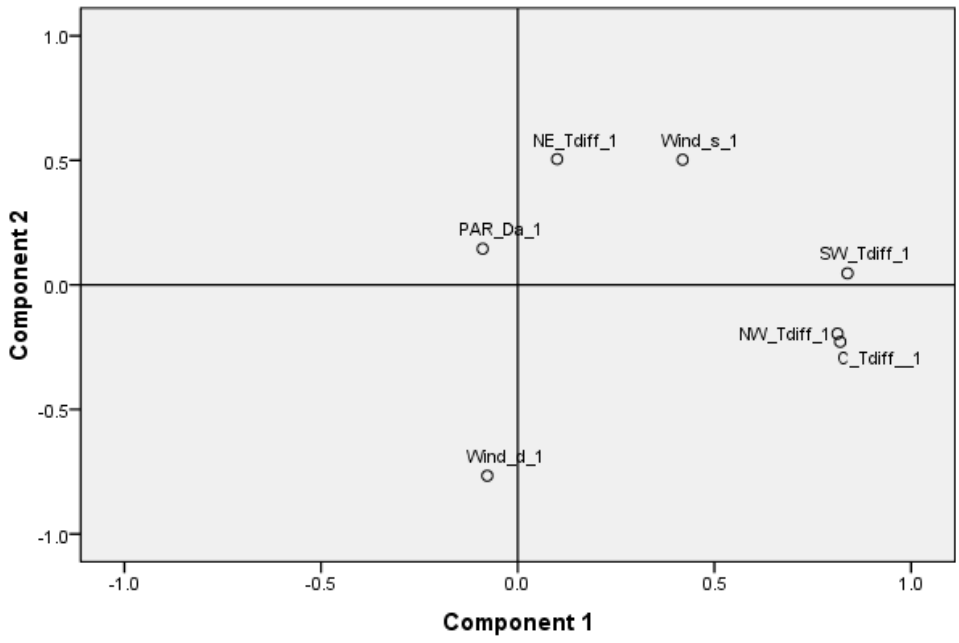

Output for Chapter 6 Figure 6.28

```
FACTOR   /VARIABLES Wind_s_1 C_DO_D_1 SW_DO__1 Wind_d_1 NE_DO__1
NW_DO__1   /MISSING LISTWISE   /ANALYSIS Wind_s_1 C_DO_D_1 SW_DO__1
Wind_d_1 NE_DO__1 NW_DO__1   /PRINT UNIVARIATE INITIAL EXTRACTION
ROTATION   /PLOT ROTATION   /CRITERIA FACTORS(2) ITERATE(25)   /EXTRACTION
PC   /CRITERIA ITERATE(25)   /ROTATION VARIMAX   /METHOD=CORRELATION.
```

Factor Analysis

Notes

	Output Created	30-Mar-2011 22:13:26
	Comments	
Input	Data	C:\Complete\Chapter 6 Bolivar\spss\Feb05_aligned.sav
	Active Dataset	DataSet2
	Filter	<none>
	Weight	<none>
	Split File	<none>
	N of Rows in Working Data File	144
Missing Value Handling	Definition of Missing	MISSING=EXCLUDE: User-defined missing values are treated as missing.
	Cases Used	LISTWISE: Statistics are based on cases with no missing values for any variable used.

	Syntax	FACTOR /VARIABLES Wind_s_1 C_DO_D_1 SW_DO__1 Wind_d_1 NE_DO__1 NW_DO__1 /MISSING LISTWISE /ANALYSIS Wind_s_1 C_DO_D_1 SW_DO__1 Wind_d_1 NE_DO__1 NW_DO__1 /PRINT UNIVARIATE INITIAL EXTRACTION ROTATION /PLOT ROTATION /CRITERIA FACTORS(2) ITERATE(25) /EXTRACTION PC /CRITERIA ITERATE(25) /ROTATION VARIMAX /METHOD=CORRELATION.
Resources	Processor Time	0:00:00.266
	Elapsed Time	0:00:00.282
	Maximum Memory Required	5544 (5.414K) bytes

[DataSet2] C:\Complete\Chapter 6 Bolivar\spss\Feb05_aligned.sav

Descriptive Statistics

	Mean	Std. Deviation	Analysis N
DIFF(Wind_dir_Day11,1)	.0343	1.91602	143
DIFF(C_DO_Day11,1)	-.0021	.22390	143
DIFF(SW_DO_Day11,1)	-.0129	.22835	143
DIFF(Wind_dir_Day11,1)	.0343	1.91602	143
DIFF(NE_DO_Day11,1)	-.0183	.34915	143
DIFF(NW_DO_Day11,1)	-.0146	.77271	143

Communalities

	Initial	Extraction
DIFF(Wind_dir_Day11,1)	1.000	.990
DIFF(C_DO_Day11,1)	1.000	.474
DIFF(SW_DO_Day11,1)	1.000	.134
DIFF(Wind_dir_Day11,1)	1.000	.990
DIFF(NE_DO_Day11,1)	1.000	.705
DIFF(NW_DO_Day11,1)	1.000	.004

Descriptive Statistics

	Mean	Std. Deviation	Analysis N
DIFF(Wind_dir_Day11,1)	.0343	1.91602	143
DIFF(C_DO_Day11,1)	-.0021	.22390	143
DIFF(SW_DO_Day11,1)	-.0129	.22835	143
DIFF(Wind_dir_Day11,1)	.0343	1.91602	143
DIFF(NE_DO_Day11,1)	-.0183	.34915	143

Extraction Method: Principal Component Analysis.

Total Variance Explained

Component	Initial Eigenvalues		
	Total	% of Variance	Cumulative %
1	2.027	33.776	
2	1.271	21.184	
3	1.167	19.449	74.409
4	.939	15.649	90.058
5	.596	9.942	100.000
6	-1.891E-16	-3.152E-15	100.000

Extraction Method: Principal Component Analysis.

Total Variance Explained

Component	Initial Eigenvalues	Extraction Sums of Squared Loadings		
	Cumulative %	Total	% of Variance	Cumulative %
1	33.776	2.027	33.776	33.776
2	54.960	1.271	21.184	54.960

Extraction Method: Principal Component Analysis.

Total Variance Explained

Component	Rotation Sums of Squared Loadings		
	Total	% of Variance	Cumulative %
1	2.024	33.735	33.735
2	1.274	21.225	54.960

Extraction Method: Principal Component Analysis.

Descriptive Statistics

	Mean	Std. Deviation	Analysis N
DIFF(Wind_dir_Day11,1)	.0343	1.91602	143
DIFF(C_DO_Day11,1)	-.0021	.22390	143
DIFF(SW_DO_Day11,1)	-.0129	.22835	143
DIFF(Wind_dir_Day11,1)	.0343	1.91602	143
DIFF(NE_DO_Day11,1)	-.0183	.34915	143

Component Matrix[a]

	Component	
	1	2
DIFF(Wind_dir_Day11,1)	.992	.078
DIFF(C_DO_Day11,1)	-.206	.657
DIFF(SW_DO_Day11,1)	-.106	-.351
DIFF(Wind_dir_Day11,1)	.992	.078
DIFF(NE_DO_Day11,1)	-.067	.837
DIFF(NW_DO_Day11,1)	-.001	-.063

Extraction Method: Principal Component Analysis.

a. 2 components extracted.

Rotated Component Matrix[a]

	Component	
	1	2
DIFF(Wind_dir_Day11,1)	.995	.021
DIFF(C_DO_Day11,1)	-.168	.667
DIFF(SW_DO_Day11,1)	-.126	-.344
DIFF(Wind_dir_Day11,1)	.995	.021
DIFF(NE_DO_Day11,1)	-.019	.839
DIFF(NW_DO_Day11,1)	-.005	-.063

Extraction Method: Principal Component Analysis.

Rotation Method: Varimax with Kaiser Normalization.

a. Rotation converged in 3 iterations.

Descriptive Statistics

	Mean	Std. Deviation	Analysis N
DIFF(Wind_dir_Day11,1)	.0343	1.91602	143
DIFF(C_DO_Day11,1)	-.0021	.22390	143
DIFF(SW_DO_Day11,1)	-.0129	.22835	143
DIFF(Wind_dir_Day11,1)	.0343	1.91602	143
DIFF(NE_DO_Day11,1)	-.0183	.34915	143

Component Transformation Matrix

Component	1	2
1	.998	-.057
2	.057	.998

Extraction Method: Principal Component Analysis.

Rotation Method: Varimax with Kaiser Normalization.

Component Plot in Rotated Space

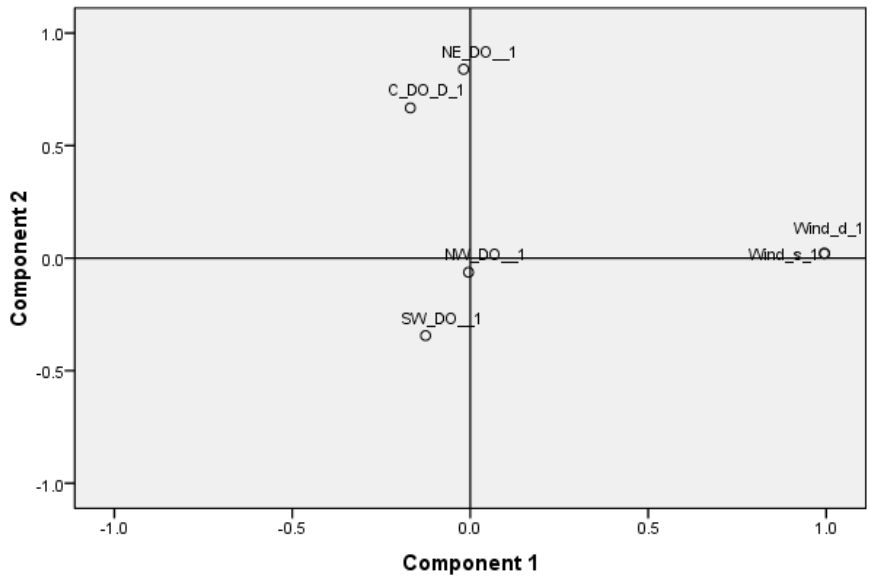

Output for Chapter 6 Figure 6.29

FACTOR /VARIABLES Wind_s_1 Wind_d_1 NE_DO__1 NW_DO__1 C_DO_D_1 SW_DO__1 /MISSING LISTWISE /ANALYSIS Wind_s_1 Wind_d_1 NE_DO__1 NW_DO__1 C_DO_D_1 SW_DO__1 /PRINT UNIVARIATE INITIAL EXTRACTION ROTATION /PLOT ROTATION /CRITERIA FACTORS(2) ITERATE(25) /EXTRACTION PC /CRITERIA ITERATE(25) /ROTATION VARIMAX /METHOD=CORRELATION.

Factor Analysis

Notes

	Output Created	30-Mar-2011 22:15:35
	Comments	
Input	Data	C:\Complete\Chapter 6 Bolivar\spss\May05_aligned.sav
	Active Dataset	DataSet3
	Filter	<none>
	Weight	<none>
	Split File	<none>
	N of Rows in Working Data File	144
Missing Value Handling	Definition of Missing	MISSING=EXCLUDE: User-defined missing values are treated as missing.
	Cases Used	LISTWISE: Statistics are based on cases with no missing values for any variable used.

	Syntax	FACTOR /VARIABLES Wind_s_1 Wind_d_1 NE_DO__1 NW_DO__1 C_DO_D_1 SW_DO__1 /MISSING LISTWISE /ANALYSIS Wind_s_1 Wind_d_1 NE_DO__1 NW_DO__1 C_DO_D_1 SW_DO__1 /PRINT UNIVARIATE INITIAL EXTRACTION ROTATION /PLOT ROTATION /CRITERIA FACTORS(2) ITERATE(25) /EXTRACTION PC /CRITERIA ITERATE(25) /ROTATION VARIMAX /METHOD=CORRELATION.
Resources	Processor Time	0:00:00.297
	Elapsed Time	0:00:00.282
	Maximum Memory Required	5544 (5.414K) bytes

[DataSet3] C:\Complete\Chapter 6 Bolivar\spss\May05_aligned.sav

Descriptive Statistics

	Mean	Std. Deviation	Analysis N
DIFF(Wind_speed_Day10,1)	-.0133	1.26859	143
DIFF(Wind_dir_Day10,1)	.3776	53.63174	143
DIFF(NE_DO_Day10,1)	-.0116	.23952	143
DIFF(NW_DO_Day10,1)	-.0043	.28203	143
DIFF(C_DO_Day10,1)	.0066	.41257	143
DIFF(SW_DO_Day10,1)	.0121	.20589	143

Communalities

	Initial	Extraction
DIFF(Wind_speed_Day10,1)	1.000	.605
DIFF(Wind_dir_Day10,1)	1.000	.376
DIFF(NE_DO_Day10,1)	1.000	.635
DIFF(NW_DO_Day10,1)	1.000	.455
DIFF(C_DO_Day10,1)	1.000	.360
DIFF(SW_DO_Day10,1)	1.000	.382

Descriptive Statistics

	Mean	Std. Deviation	Analysis N
DIFF(Wind_speed_Day10,1)	-.0133	1.26859	143
DIFF(Wind_dir_Day10,1)	.3776	53.63174	143
DIFF(NE_DO_Day10,1)	-.0116	.23952	143
DIFF(NW_DO_Day10,1)	-.0043	.28203	143
DIFF(C_DO_Day10,1)	.0066	.41257	143

Extraction Method: Principal Component Analysis.

Total Variance Explained

Component	Initial Eigenvalues		
	Total	% of Variance	Cumulative %
1	1.603	26.709	
2	1.210	20.165	
3	.992	16.530	63.403
4	.872	14.541	77.944
5	.713	11.891	89.835
6	.610	10.165	100.000

Extraction Method: Principal Component Analysis.

Total Variance Explained

Component	Initial Eigenvalues	Extraction Sums of Squared Loadings		
	Cumulative %	Total	% of Variance	Cumulative %
1	26.709	1.603	26.709	26.709
2	46.874	1.210	20.165	46.874

Extraction Method: Principal Component Analysis.

Total Variance Explained

Component	Rotation Sums of Squared Loadings		
	Total	% of Variance	Cumulative %
1	1.580	26.337	26.337
2	1.232	20.536	46.874

Extraction Method: Principal Component Analysis.

Component Matrix[a]

	Component	
	1	2
DIFF(Wind_speed_Day10,1)	.507	-.590
DIFF(Wind_dir_Day10,1)	-.112	.603
DIFF(NE_DO_Day10,1)	.744	.286
DIFF(NW_DO_Day10,1)	.651	.176
DIFF(C_DO_Day10,1)	.596	.065
DIFF(SW_DO_Day10,1)	.001	.618

Extraction Method: Principal Component Analysis.

a. 2 components extracted.

Rotated Component Matrix[a]

	Component	
	1	2
DIFF(Wind_speed_Day10,1)	.352	-.694
DIFF(Wind_dir_Day10,1)	.035	.612
DIFF(NE_DO_Day10,1)	.791	.100
DIFF(NW_DO_Day10,1)	.674	.015
DIFF(C_DO_Day10,1)	.595	-.079
DIFF(SW_DO_Day10,1)	.148	.600

Extraction Method: Principal Component Analysis.

Rotation Method: Varimax with Kaiser Normalization.

a. Rotation converged in 3 iterations.

Component Transformation Matrix

Component	1	2
1	.971	-.238
2	.238	.971

Extraction Method: Principal Component Analysis.

Rotation Method: Varimax with Kaiser Normalization.

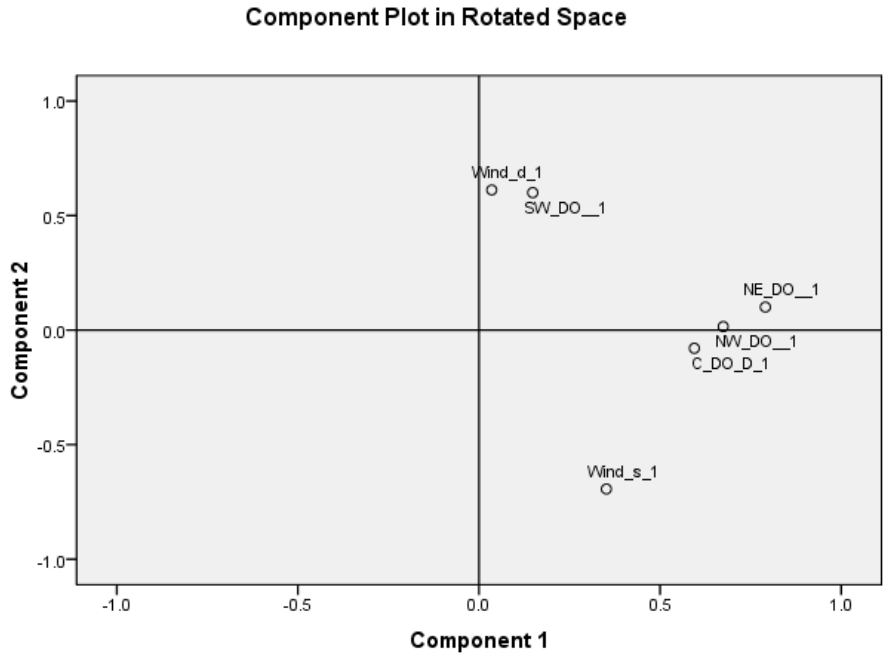

Output for Chapter 6 Figure 6.30

FACTOR /VARIABLES C_DO_D_1 SW_DO__1 NE_DO__1 NW_DO__1 NE_Tdiff_1 NW_Tdiff_1 C_Tdiff__1 SW_Tdiff_1 /MISSING LISTWISE /ANALYSIS C_DO_D_1 SW_DO__1 NE_DO__1 NW_DO__1 NE_Tdiff_1 NW_Tdiff_1 C_Tdiff__1 SW_Tdiff_1 /PRINT UNIVARIATE INITIAL EXTRACTION ROTATION /PLOT ROTATION /CRITERIA FACTORS(2) ITERATE(25) /EXTRACTION PC /CRITERIA ITERATE(25) /ROTATION VARIMAX /METHOD=CORRELATION.

Factor Analysis

Notes

	Output Created	30-Mar-2011 22:17:34
	Comments	
Input	Data	C:\Complete\Chapter 6 Bolivar\spss\Feb05_aligned.sav
	Active Dataset	DataSet2
	Filter	<none>
	Weight	<none>
	Split File	<none>
	N of Rows in Working Data File	144
Missing Value Handling	Definition of Missing	MISSING=EXCLUDE: User-defined missing values are treated as missing.

	Cases Used	LISTWISE: Statistics are based on cases with no missing values for any variable used.
	Syntax	FACTOR /VARIABLES C_DO_D_1 SW_DO__1 NE_DO__1 NW_DO__1 NE_Tdiff_1 NW_Tdiff_1 C_Tdiff__1 SW_Tdiff_1 /MISSING LISTWISE /ANALYSIS C_DO_D_1 SW_DO__1 NE_DO__1 NW_DO__1 NE_Tdiff_1 NW_Tdiff_1 C_Tdiff__1 SW_Tdiff_1 /PRINT UNIVARIATE INITIAL EXTRACTION ROTATION /PLOT ROTATION /CRITERIA FACTORS(2) ITERATE(25) /EXTRACTION PC /CRITERIA ITERATE(25) /ROTATION VARIMAX /METHOD=CORRELATION.
Resources	Processor Time	0:00:00.265
	Elapsed Time	0:00:00.265
	Maximum Memory Required	9080 (8.867K) bytes

[DataSet2] C:\Complete\Chapter 6 Bolivar\spss\Feb05_aligned.sav

Descriptive Statistics

	Mean	Std. Deviation	Analysis N
DIFF(C_DO_Day11,1)	-.0021	.22390	143
DIFF(SW_DO_Day11,1)	-.0129	.22835	143
DIFF(NE_DO_Day11,1)	-.0183	.34915	143
DIFF(NW_DO_Day11,1)	-.0146	.77271	143
DIFF(NE_T25_75,1)	.0000	.09038	143
DIFF(NW_T25_75,1)	.0007	.08349	143
DIFF(C_T25_75,1)	.0021	.07068	143
DIFF(SW_T25_75,1)	.0070	.10254	143

Communalities

	Initial	Extraction
DIFF(C_DO_Day11,1)	1.000	.412
DIFF(SW_DO_Day11,1)	1.000	.309
DIFF(NE_DO_Day11,1)	1.000	.706
DIFF(NW_DO_Day11,1)	1.000	.136
DIFF(NE_T25_75,1)	1.000	.124
DIFF(NW_T25_75,1)	1.000	.343
DIFF(C_T25_75,1)	1.000	.456
DIFF(SW_T25_75,1)	1.000	.647

Extraction Method: Principal Component Analysis.

Total Variance Explained

Component	Initial Eigenvalues		
	Total	% of Variance	Cumulative %
1	1.842	23.019	
2	1.292	16.150	
3	1.097	13.717	52.886
4	1.026	12.825	65.712
5	.917	11.468	77.179
6	.815	10.185	87.364
7	.600	7.495	94.860
8	.411	5.140	100.000

Extraction Method: Principal Component Analysis.

Total Variance Explained

Component	Initial Eigenvalues	Extraction Sums of Squared Loadings		
	Cumulative %	Total	% of Variance	Cumulative %
1	23.019	1.842	23.019	23.019
2	39.170	1.292	16.150	39.170

Extraction Method: Principal Component Analysis.

Total Variance Explained

Component	Rotation Sums of Squared Loadings		
	Total	% of Variance	Cumulative %
1	1.795	22.437	22.437
2	1.339	16.733	39.170

Extraction Method: Principal Component Analysis.

Component Matrix[a]

	Component	
	1	2
DIFF(C_DO_Day11,1)	.499	.403
DIFF(SW_DO_Day11,1)	.280	-.480
DIFF(NE_DO_Day11,1)	.159	.825
DIFF(NW_DO_Day11,1)	.220	-.296
DIFF(NE_T25_75,1)	.174	.307
DIFF(NW_T25_75,1)	.585	.018
DIFF(C_T25_75,1)	.661	-.138
DIFF(SW_T25_75,1)	.794	-.133

Extraction Method: Principal Component Analysis.

a. 2 components extracted.

Rotated Component Matrix[a]

	Component	
	1	2
DIFF(C_DO_Day11,1)	.361	.531
DIFF(SW_DO_Day11,1)	.408	-.377
DIFF(NE_DO_Day11,1)	-.088	.836
DIFF(NW_DO_Day11,1)	.297	-.219
DIFF(NE_T25_75,1)	.077	.344
DIFF(NW_T25_75,1)	.555	.188
DIFF(C_T25_75,1)	.673	.061
DIFF(SW_T25_75,1)	.798	.104

Extraction Method: Principal Component Analysis.

Rotation Method: Varimax with Kaiser Normalization.

a. Rotation converged in 3 iterations.

Component Transformation Matrix

Component	1	2
1	.957	.291
2	-.291	.957

Extraction Method: Principal Component Analysis.

Rotation Method: Varimax with Kaiser Normalization.

Component Plot in Rotated Space

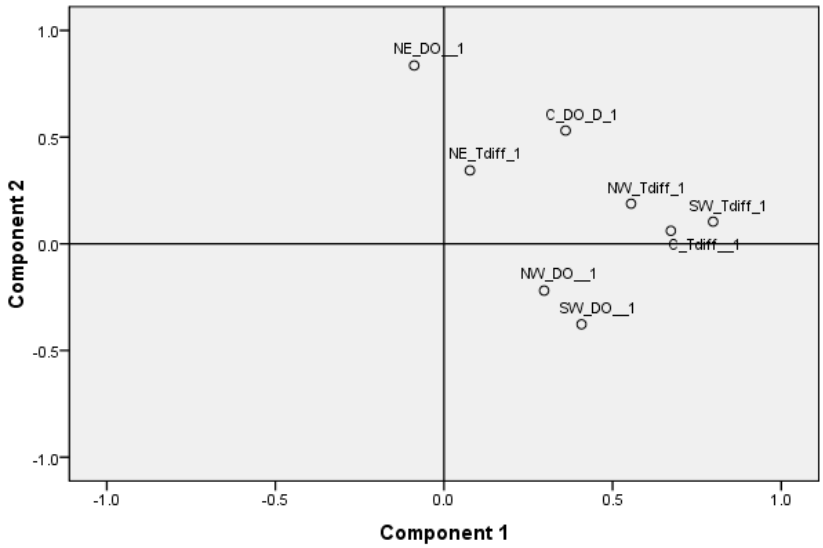

Output for Chapter 6 Figure 6.31

FACTOR /VARIABLES NE_DO__1 NW_DO__1 C_DO_D_1 SW_DO__1 NE_Tdiff_1 NW_Tdiff_1 C_Tdiff__1 SW_Tdiff_1 /MISSING LISTWISE /ANALYSIS NE_DO__1 NW_DO__1 C_DO_D_1 SW_DO__1 NE_Tdiff_1 NW_Tdiff_1 C_Tdiff__1 SW_Tdiff_1 /PRINT UNIVARIATE INITIAL EXTRACTION ROTATION /PLOT ROTATION /CRITERIA FACTORS(2) ITERATE(25) /EXTRACTION PC /CRITERIA ITERATE(25) /ROTATION VARIMAX /METHOD=CORRELATION.

Factor Analysis

Notes

	Output Created	30-Mar-2011 22:19:13
	Comments	
Input	Data	C:\Complete\Chapter 6 Bolivar\spss\May05_aligned.sav
	Active Dataset	DataSet3
	Filter	<none>
	Weight	<none>
	Split File	<none>
	N of Rows in Working Data File	144
Missing Value Handling	Definition of Missing	MISSING=EXCLUDE: User-defined missing values are treated as missing.
	Cases Used	LISTWISE: Statistics are based on cases with no missing values for any variable used.

	Syntax	FACTOR /VARIABLES NE_DO__1 NW_DO__1 C_DO_D_1 SW_DO__1 NE_Tdiff_1 NW_Tdiff_1 C_Tdiff__1 SW_Tdiff_1 /MISSING LISTWISE /ANALYSIS NE_DO__1 NW_DO__1 C_DO_D_1 SW_DO__1 NE_Tdiff_1 NW_Tdiff_1 C_Tdiff__1 SW_Tdiff_1 /PRINT UNIVARIATE INITIAL EXTRACTION ROTATION /PLOT ROTATION /CRITERIA FACTORS(2) ITERATE(25) /EXTRACTION PC /CRITERIA ITERATE(25) /ROTATION VARIMAX /METHOD=CORRELATION.
Resources	Processor Time	0:00:00.250
	Elapsed Time	0:00:00.250
	Maximum Memory Required	9080 (8.867K) bytes

[DataSet3] C:\Complete\Chapter 6 Bolivar\spss\May05_aligned.sav

Descriptive Statistics

	Mean	Std. Deviation	Analysis N
DIFF(NE_DO_Day10,1)	-.0116	.23952	143
DIFF(NW_DO_Day10,1)	-.0043	.28203	143
DIFF(C_DO_Day10,1)	.0066	.41257	143
DIFF(SW_DO_Day10,1)	.0121	.20589	143
DIFF(NE_T25_75,1)	.0000	.06608	143
DIFF(NW_T25_75,1)	.0014	.07410	143
DIFF(C_T25_75,1)	.0007	.07645	143
DIFF(SW_T25_75,1)	.0014	.10614	143

Communalities

	Initial	Extraction
DIFF(NE_DO_Day10,1)	1.000	.482
DIFF(NW_DO_Day10,1)	1.000	.430
DIFF(C_DO_Day10,1)	1.000	.398
DIFF(SW_DO_Day10,1)	1.000	.273
DIFF(NE_T25_75,1)	1.000	.357
DIFF(NW_T25_75,1)	1.000	.667
DIFF(C_T25_75,1)	1.000	.641
DIFF(SW_T25_75,1)	1.000	.696

Extraction Method: Principal Component Analysis.

Total Variance Explained

Component	Initial Eigenvalues		
	Total	% of Variance	Cumulative %
1	2.615	32.692	
2	1.327	16.594	
3	1.024	12.796	62.082
4	.885	11.061	73.143
5	.720	8.995	82.138
6	.606	7.570	89.708
7	.444	5.555	95.263
8	.379	4.737	100.000

Extraction Method: Principal Component Analysis.

Total Variance Explained

Component	Initial Eigenvalues	Extraction Sums of Squared Loadings		
	Cumulative %	Total	% of Variance	Cumulative %
1	32.692	2.615	32.692	32.692
2	49.285	1.327	16.594	49.285

Extraction Method: Principal Component Analysis.

Total Variance Explained

Component	Rotation Sums of Squared Loadings		
	Total	% of Variance	Cumulative %
1	2.340	29.247	29.247
2	1.603	20.038	49.285

Communalities

	Initial	Extraction
DIFF(NE_DO_Day10,1)	1.000	.482
DIFF(NW_DO_Day10,1)	1.000	.430
DIFF(C_DO_Day10,1)	1.000	.398
DIFF(SW_DO_Day10,1)	1.000	.273
DIFF(NE_T25_75,1)	1.000	.357
DIFF(NW_T25_75,1)	1.000	.667
DIFF(C_T25_75,1)	1.000	.641
DIFF(SW_T25_75,1)	1.000	.696

Extraction Method: Principal Component Analysis.

Component Matrix[a]

	Component	
	1	2
DIFF(NE_DO_Day10,1)	.531	-.448
DIFF(NW_DO_Day10,1)	.414	-.508
DIFF(C_DO_Day10,1)	.380	-.503
DIFF(SW_DO_Day10,1)	.430	.298
DIFF(NE_T25_75,1)	-.063	.594
DIFF(NW_T25_75,1)	.789	.210
DIFF(C_T25_75,1)	.780	.181
DIFF(SW_T25_75,1)	.773	.313

Extraction Method: Principal Component Analysis.

a. 2 components extracted.

Rotated Component Matrix[a]

	Component	
	1	2
DIFF(NE_DO_Day10,1)	.264	.642
DIFF(NW_DO_Day10,1)	.132	.642
DIFF(C_DO_Day10,1)	.104	.622
DIFF(SW_DO_Day10,1)	.519	-.065
DIFF(NE_T25_75,1)	.219	-.556
DIFF(NW_T25_75,1)	.797	.178
DIFF(C_T25_75,1)	.775	.201
DIFF(SW_T25_75,1)	.831	.080

Communalities

	Initial	Extraction
DIFF(NE_DO_Day10,1)	1.000	.482
DIFF(NW_DO_Day10,1)	1.000	.430
DIFF(C_DO_Day10,1)	1.000	.398
DIFF(SW_DO_Day10,1)	1.000	.273
DIFF(NE_T25_75,1)	1.000	.357
DIFF(NW_T25_75,1)	1.000	.667
DIFF(C_T25_75,1)	1.000	.641
DIFF(SW_T25_75,1)	1.000	.696

Extraction Method: Principal Component Analysis.

Rotation Method: Varimax with Kaiser Normalization.

a. Rotation converged in 3 iterations.

Component Transformation Matrix

Component	1	2
1	.887	.463
2	.463	-.887

Extraction Method: Principal Component Analysis.

Rotation Method: Varimax with Kaiser Normalization.

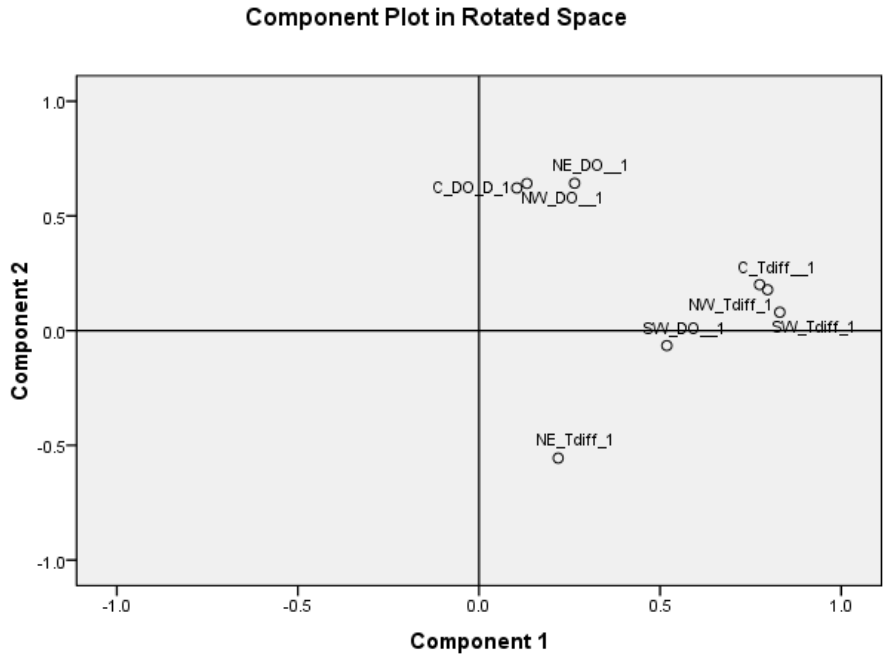

End Appendix C